Physics of Precision Experiments with Z's

F. Jegerlehner *
Paul Scherrer Institute, CH-5232 Villigen PSI, Switzerland

June 3, 1991

*to appear in "Progress in Particle and Nuclear Physics", ed. A. Fässler, Pergamon Press, Oxford U. K.

Physics of Precision Experiments with Z's

F. JEGERLEHNER

Paul Scherrer Institute, CH-5232 Villigen PSI, Switzerland

ABSTRACT

We review the status of precision tests of the electroweak Standard Model. Radiative corrections play an important role for the interpretation of precision measurements and provide a window for the observation of *new physics*. Implications of recent results from LEP and hadron colliders are discussed. So far the agreement between experimental data and standard model predictions is almost perfect. In order to establish possible deviations from the Standard Model we have to wait for the next step in accuracy. This will be achieved during this year with about 10^6 Z's per experiment.

KEYWORDS

Electroweak interactions, intermediate vector bosons, e^+e^- annihilation at the Z resonance, asymmetries, radiative corrections , heavy top effects, extensions of the Standard Model.

TABLE OF CONTENTS

TABLE OF CONTENTS

1. INTRODUCTION

The large electron positron collider LEP at CERN is the world's best "microscope" having a resolution $\lambda = hc/E_{c.m.} = 1.2$ GeV$/E_{c.m.}$(GeV) $\times 10^{-15}$ m $\simeq 1.3 \times 10^{-15}$ cm at the Z peak. This allows us to probe nature at the vector boson mass scale and the hope is to find signals of new structure beyond the Standard Model of electroweak interactions. Since a temperature of 1°K is equivalent to 8.6×10^{-5} eV, LEP events correspond to mini fireballs at a temperature of 6×10^{14} °K a state which presumably existed in the early era of the radiation-dominated universe about 10^{-19} seconds after the big bang. This means that up to this time in the expansion of the universe photons, gluons etc. were so energetic that they could materialize into fermion-antifermion pairs which were energetic enough to produce Z and W bosons in annihilation.

The luminosity L, now at $\simeq 7.0 \times 10^{30}$ cm^{-1} sec^{-1} is expected to reach about $\simeq 1.6 \times 10^{31}$ cm^{-1} sec^{-1} in the future and leads to huge rates of resonant Z boson production making possible very precise tests of weak neutral current transitions at high energies. The large cross-section at the Z-peak, $\sigma^{f\bar{f}}_{peak} \simeq 1.45\,(1.95)\ nb$ for $f = e, \mu, \tau$ and $30.08\,(40.65)\ nb$ for hadrons, (in brackets, the value without QED corrections) gives easily the production of 1 million Z's per year at LEP1. The cross-section is enhanced relative to the pure QED process by a factor $(M_Z/\Gamma_Z)^2 \simeq 10^3$ or about 150 for leptons and 750 for hadrons.

Precision experiments will be possible mainly during the first phase (LEP1) when LEP is running with center of mass (c.m.) energies up to about 110 GeV. In a second stage (LEP2) when energies up to about 200 GeV can be reached the rates will be lower by more than two orders of magnitude.

After one year of operation the four LEP experiments Aleph, Delphi, L3 and Opal have collected more than 700 000 Z's [1]. The weak gauge bosons (intermediate vector bosons), the charged W$^{\pm}$ and the neutral Z, were discovered at CERN in 1983 by the UA1 and UA2 collaborations [2]. The CDF collaboration at FNAL collects vector boson data since 1988 [3]. The data samples collected in hadron colliders experiments are [4]: 112 Z'and 323 W's (UA1), 162 Z's and 1676 W's (UA2) and 272 Z's and 1722 W's (CDF), identified by their leptonic decays.

The basic processes investigated at LEP1/SLC are fermion pair production $e^+e^- \to f\bar{f}(f \neq e)$ and Bhabha scattering $e^+e^- \to e^+e^-$. At LEP2 W-pair production $e^+e^- \to W^+W^-$ will be the main process. Radiative corrections play a crucial role in the interpretation of electroweak precision measurements. We will concentrate on discussing radiative corrections for LEP1/SLC physics near the Z peak.

The present experimental bounds on physics beyond the Standard Model (SM) almost exclude the possibility to find new physics at the Born level (new particles or new couplings) at LEP. Thus, precision tests beyond the Born level will be the central theme at LEP1. The effects we want to establish are the *genuine* weak corrections, the self-interactions of gauge fields, Higgs boson and top quark interactions or similar effects from *new physics*, expected to be of the order of about 1%. Their detection requires both experimental and theoretical uncertainties to be smaller than 0.1%. Typically the expected level of accuracy for various observables at LEP are $\delta M_Z \sim 20$ MeV from the Z line-shape, $\delta \sin^2\Theta_W \sim 0.0015$ from the forward-backward asymmetry A_{FB}, $\delta \sin^2\Theta_W \sim 0.0004$ from left-right asymmetry A_{LR} and $\delta M_W \sim 70$ MeV from the W-mass measurement at LEP2.

The *weak effects* have to be clearly disentangeld from the large QED corrections (40%) which are common to any $G \otimes U(1)_{e.m.}$ theory. This requires both a precise theoretical understanding, in particular of the QED corrections (full two-loop QED, multi soft-photon emission) and a precise

experimental control of the beam properties, detector efficiencies and phase-space cuts (which requires simulation by Monte Carlo event generators). For neutral current processes up to order $O(\alpha)$ (one loop corrections), one can separate QED corrections (photonic corrections) and non-QED corrections (weak corrections) in a gauge invariant and ultraviolet finite way. QED corrections are the contributions represented by diagrams which involve one extra photon being added to the Born diagrams of a given process. The extra photon can be either a real bremsstrahlung photon or a virtual photon loop. The photon vacuum polarization is not included in this QED part of the electroweak radiative corrections . The non-QED part contains all other diagrams. These corrections depend on possible deviations from the SM but are independent of the experimental set up. For quark-loops and hadronic final states in addition QCD corrections must be taken into account.

For accurate theoretical predictions of vector boson processes, three precisely measured input parameters are needed. Since only two parameters, namely the fine structure constant α and the Fermi constant G_μ are known with high precision, one of the most important primary goals is the precise determination of the Z-mass. A systematic treatment of the radiative corrections leads to the result that *non-QED* and *non phase-space* corrections are negligible near the Z-peak, such that a model independent determination of the mass and width of the Z is possible. Existing data reveal interesting bounds on possible new-physics effects.

Besides the Z-mass measurement each additional precision experiment provides a test of electroweak theory beyond the tree level. Of particular interest are

- The detailed investigation of $e^+e^- \to f\bar{f}$ around the Z resonance which should allow us to observe small calculable deviations of the partial and total cross-sections $\sigma_f = \sigma(e^+e^- \to f\bar{f})$ and $\sigma_{tot} = \sum_f \sigma_f$ and the partial and total widths $\Gamma_f = \Gamma(Z \to f\bar{f})$ and $\Gamma_Z = \sum_f \Gamma_f$ from their lowest order predictions

$$\Gamma_{Zf\bar{f}} = \frac{\sqrt{2}G_\mu M_Z^3}{12\pi}(v_f^2 + a_f^2)N_{cf} \; ; \;\; \sigma_{peak}^{f\bar{f}} \;\; \simeq \;\; \frac{12\pi}{M_Z^2}\frac{\Gamma_e\Gamma_f}{\Gamma_Z^2}$$

  where $v_f = T_{3f} - 2Q_f \sin^2\Theta_W$ and $a_f = T_{3f}$ are, respectively, the vector and axial vector neutral current (NC) couplings for fermions with flavor f. N_{cf} is the color factor which is 1 for leptons and 3 for quarks.

- Additional information will be obtained from the on-resonance asymmetries, the forward-backward asymmetries $A_{FB}^{f\bar{f}}$ and the τ polarization-asymmetry A_{pol}^{τ}. If longitudinally polarized beams would be realized, the measurement of the left-right asymmetry A_{LR} and the polarized forward-backward asymmetries $A_{FB,pol}^{f\bar{f}}$ would substantially improve the results. All the asymmetries are functions of the specific ratios

$$A_f = \frac{2v_f a_f}{v_f^2 + a_f^2}$$

  of the NC couplings, and thus provide accurate determinations of the weak mixing angle $\sin^2\Theta_W$. At the tree level the on-resonance asymmetries are given by

$$A_{FB}^{f\bar{f}} = \frac{3}{4}A_e A_f, \quad A_{LR} = A_{pol}^{\tau} = A_e, \quad A_{FB,pol}^{f\bar{f}} = \frac{3}{4}A_f \; .$$

The "weak" (non-QED) radiative corrections reveal the asymmetries to be very interesting quantities, mainly because the different asymmetries exhibit different sensitivities to various interesting

effects. The measurement of many independent quantities, which depend in their own way on unknown physics, is important in order to be able to disentangle the origin of possible deviations from lowest order predictions.

Notice that higher order predictions depend on the unknown mass of the Higgs boson, the remnant from spontaneous symmetry breaking, and the mass of the unknown top quark, the missing member of the 3rd fermion family and other possible unknown physics. While higher order predictions of physical quantities depend substantially on the unknown top mass the dependence on the unknown Higgs mass is much weaker. As a first step, data constrain the unknown parameters of the SM. At the same time bounds on possible extensions of the SM gradually improve.

From the measurements of the Z width Γ_Z, LEP has definitely established that only the known 3 light neutrinos exist in nature. An independent *neutrino-counting* experiment will be the measurement of $e^+e^- \to \gamma\nu\bar{\nu}$ in the region above the Z peak.

2. THE STANDARD MODEL OF ELECTROWEAK INTERACTIONS

The Glashow-Weinberg-Salam model of electroweak interactions [5] together with the QCD sector of strong interactions [6] defines the standard model (SM) of elementary particle theory. The known fundamental interactions of elementary particles derive from a local gauge principle with the gauge group

$$G_{loc} = SU(3)_c \otimes SU(2)_L \otimes U(1)_Y$$

which is broken by the Higgs mechanism to $SU(3)_c \otimes U(1)_{em}$. The SM is determined essentially by specifying the transformation properties of the massless spin 1/2 matter fields. The $SU(3)_c$ distinguishes color triplets of quarks, conjugate triplets of antiquarks and leaves neutrinos and leptons as singlets. The $SU(2)_L$ distinguishes between doublets of left-handed particles and singlets of right-handed particles

$$\begin{pmatrix} \nu_e \\ e^- \end{pmatrix}_L, \begin{pmatrix} u \\ d \end{pmatrix}_L \quad ; \quad e^-_R, u_R, d_R$$

$$\begin{pmatrix} \nu_\mu \\ \mu^- \end{pmatrix}_L, \begin{pmatrix} c \\ s \end{pmatrix}_L \quad ; \quad \mu^-_R, c_R, s_R$$

$$\begin{pmatrix} \nu_\tau \\ \tau^- \end{pmatrix}_L, \begin{pmatrix} t \\ b \end{pmatrix}_L \quad ; \quad \tau^-_R, t_R, b_R$$

The $U(1)_Y$ assigns a weak hypercharge Y to the $SU(2)_L$ doublets and singlets, such that $Q = T_3 + Y/2$ is the conserved electric charge of the particles: $Q_{\nu_e} = 0$, $Q_u = 2/3$ and $Q_1 - Q_2 = 1$ for the difference between upper and lower entries of the doublets. Three families of leptons and quarks exist.

For each factor of G_{loc}, local gauge invariance requires the presence of a set of massless gauge fields, which couple minimally to the matter fields. The electroweak gauge fields are denoted by $W_{\mu i} (i = 1, 2, 3)$ and B_μ and the corresponding gauge couplings by g and g', respectively.

The physical gauge bosons are the photon $A_\mu = \cos\Theta_W B_\mu + \sin\Theta_W W_{\mu 3}$ and the neutral and charged weak bosons $Z_\mu = \cos\Theta_W W_{\mu 3} - \sin\Theta_W B_\mu$ and $W_\mu^\pm = (W_{\mu 1} \mp i W_{\mu 2})/\sqrt{2}$. These couple to the fermion currents $j_\mu^{em} = \sum_f Q_f \bar{\psi}_f \gamma_\mu \psi_f$, $J_\mu^Z = J_{3\mu} - 2\sin^2\theta_W j_{\mu em}$ and $J_\mu^\pm = J_{1\mu} \mp i J_{2\mu}$. The charged current (CC) has the form

$$J_\mu^+ = \sum_{\ell=e,\mu,\tau} \bar{\nu}_\ell \gamma_\mu (1-\gamma_5)\ell + (\bar{u},\bar{c},\bar{t})\gamma_\mu(1-\gamma_5) U_{KM} \begin{pmatrix} d \\ s \\ b \end{pmatrix} \tag{1}$$

where quarks may change flavor through the unitary Cabibbo-Kobayashi-Maskawa matrix U_{KM} [7]. The neutral current (NC) on the other hand is strictly flavor conserving (GIM mechanism) and is given by

$$J_\mu^Z = \sum_f \bar{\psi}_f \gamma_\mu (v_f - a_f \gamma_5)\psi_f \tag{2}$$

where the sum extends over the individual fermion flavors (and color). In our convention the vector- and axial-vector neutral current coefficients are given by

$$v_f = T_{3f} - 2Q_f \sin^2\Theta_W \ , \quad a_f = T_{3f} \tag{3}$$

respectively, where T_{3f} is the weak isospin ($\pm\frac{1}{2}$) of the fermion f. For three (or more) families U_{KM} exhibits CP-violating phases which are capable of "explaining" the CP-violation observed in K-decays. The leptonic CC has some very special properties, which derive from the apparent absence of right-handed neutrinos. If $\nu_{\ell R}$ does not exist the neutrinos must be massless (assuming that they are Dirac particles like the other fermions) and lepton number L_ℓ is conserved individually for $\ell = e, \mu, \tau$. Among the neutrino puzzles we mention here the following: Do the neutrinos have a mass and if so why is it so small? Do neutrinos have unusual magnetic moments? Are there neutrinos which are their own antiparticles (Majorana neutrinos)?

The matter field Lagrangian takes the form

$$\mathcal{L}_{matter} = \sum_f \bar{\psi}_f i\gamma^\mu \partial_\mu \psi_f + \frac{g}{2\sqrt{2}}(J_\mu^+ W^{\mu -} + h.c.) + \frac{g}{2\cos\theta_W} J_\mu^Z Z^\mu + e j_\mu^{em} A^\mu \tag{4}$$

where $\tan\Theta_W = g'/g$ and $e = g\sin\Theta_W$ is the charge of the positron (unification condition). The discovery of the $W^\pm$ and Z bosons at the $p\bar{p}$ collider at CERN directly confirmed these weak gauge boson couplings. On the other hand for a direct confirmation of the gauge boson self-interactions of the Yang-Mills Lagrangian

$$\mathcal{L}_{YM} = -\frac{1}{4}(\partial_\mu B_\nu - \partial_\nu B_\mu)^2 - \frac{1}{4}(\partial_\mu W_{\nu i} - \partial_\nu W_{\mu i} + ig\varepsilon_{ikl} W_{\mu k} W_{\nu l})^2 \tag{5}$$

we have to wait for W-pair production at LEP2. Phenomenologically we know that the $SU(2)_L \otimes U(1)_Y$ symmetry is broken by the mass terms

$$\mathcal{L}_{mass} = -\sum_f m_f \bar{\psi}_f \psi_f + \frac{1}{2} M_Z^2 Z_\mu Z^\mu + \frac{1}{2} M_W^2 W_\mu^+ W^{-\mu} \tag{6}$$

of the physical particles. We know that adding just these mass terms would spoil the renormalizability of the theory. The minimal renormalizable extension is obtained if the masses are generated by the Higgs mechanism. This requires the introduction of at least one complex scalar Higgs doublet field Φ which couples in a gauge invariant way to the gauge fields ($\mathcal{L}_{Higgs}$) and to the fermions ($\mathcal{L}_{Yukawa}$). The symmetry is then broken by a non-vanishing vacuum expectation value v

of the physical Higgs field H. Gauge invariance implies that three of the four fields of Φ (complex doublet) can be gauged away. As a remnant one physical Higgs scalar must exist. In the physical (unitary) gauge, where ghost particles are absent, we obtain $\mathcal{L}_{Higgs} + \mathcal{L}_{Yukawa} = \mathcal{L}_{mass} + \mathcal{L}_H$ with

$$\begin{aligned}\mathcal{L}_H &= \frac{1}{2}(\partial H)^2 - \frac{1}{2}m_H^2 H^2 - \lambda v H^3 - \frac{\lambda}{4}H^4 - \sum_f \frac{m_f}{v}\bar{\psi}_f\psi_f H + \frac{M_Z^2}{v}Z_\mu Z^\mu H \\ &+ \frac{2M_W^2}{v}W_\mu^+ W^{-\mu}H + \frac{M_Z^2}{2v^2}Z_\mu Z^\mu H^2 + \frac{M_W^2}{v^2}W_\mu^+ W^{-\mu}H^2 \ . \end{aligned} \tag{7}$$

This term is the missing piece needed to render the SM renormalizable. The Higgs sector is completely unverified so far and its confirmation is a big challenge for experimental particle physics.

The proof of renormalizability by G. 't Hooft [8] rejuvenated particle physics about 20 years ago and preceded the first phenomenological success of the SM which was the discovery of the neutral currents [9] in 1973.

A basic consequence of the Higgs mechanism is the validity of the following mass-coupling relations. The vector boson masses are given by

$$M_W = \frac{gv}{2} \ , \quad M_Z = \frac{gv}{2\cos\Theta_W} \ . \tag{8}$$

The fermion masses and the Higgs mass are given by similar relations

$$m_f = \frac{G_f}{\sqrt{2}}\, v \ , \quad m_H = \sqrt{2\lambda}\, v \ . \tag{9}$$

in terms of the Yukawa couplings G_f and of the Higgs coupling λ. In the standard model the μ-decay constant G_μ is given by

$$G_\mu = \frac{g^2}{4\sqrt{2}M_W^2} = \frac{1}{\sqrt{2}v^2} = 1.166389(22) \times 10^{-5} \ \ (\mathrm{GeV})^{-2} \tag{10}$$

and thus the Higgs vacuum expectation value

$$v = (\sqrt{2}G_\mu)^{-1/2} = 246.2186(16) \ \ GeV$$

is a very precisely known quantity, frequently called the Fermi scale, which functions as a conversion factor between couplings and masses. One important consequence is that the existence of heavy particles requires strong couplings and for too heavy particles this leads to a breakdown of perturbation theory. In other words, particles with masses much larger than the Fermi scale are unnatural in the minimal SM. The non-decoupling of heavy particles is a new feature characteristic of a spontaneously broken gauge theory. In contrast, in QED and QCD heavy particles decouple as required by the Appelquist-Carazzone theorem [10].

If we take for granted the SM, we can say that the existence of the Higgs condensate has been established. Like superconductivity the Higgs could in fact be composite. It is certainly a very interesting question, whether there is an underlying "BCS-theory" for the Standard Model. In any case, phenomenologically one expects the SM to work as a low energy effective theory at scales below 1 TeV.

At the formal level the role played by the Higgs mechanism is the following: It

- breaks $SU(2)_L \otimes U(1)_Y$ to $U(1)_{em}$,

- generates the masses of the weak gauge bosons $W^{\pm}$, Z and the fermions,
- provides a "physical cut-off" to the massive vector boson gauge theory.

The price we have to pay is that

- a neutral physical scalar particle H must exist.

The couplings of the Higgs boson are universally proportional to the fermion mass for fermions and proportional to the boson mass-squared for bosons. The extremely weak couplings to light fermions explain why the Higgs is hidden so well from experimental discovery.

Another feature of the minimal Higgs scheme is that all fermion masses and the U_{KM} mixing parameters are free parameters (13 for the 3 families). This is considered to be a serious shortcoming of the minimal SM.

Also the mass of the Higgs is a free unknown parameter. At present the limit for m_H from LEP experiments is [11]

$$m_H > 49 \text{ GeV} \ \ (95\% \text{ CL}) \ . \tag{11}$$

Possible windows for a light Higgs have been excluded all the way down to $m_H = 0$. At LEP2 the Higgs search can be extended to about $m_H \simeq M_Z$ [12]. If the Higgs should be heavier, and this is likely to be the case, a discovery is possible only at future colliders like SSC or LHC.

We should point out that the form of the weak currents is a direct consequence of the minimal Higgs assumption: Since each family is made up of fields with identical $SU(2)_L \otimes U(1)_Y$ transformation laws invariant Yukawa couplings are possible for combinations of fields from different families.

With the fields having identical $SU(2)_L \otimes U(1)_Y$ quantum numbers one can form *horizontal vectors*. For the quarks there are the 4 horizontal vectors $q_{uL}, q_{dL}, q_{uR}, q_{dR}$ where $q_u = (u, c, t)$ and $q_d = (d, s, b)$.

In order to transform the fermion mass matrix to diagonal form we must perform independent global unitary transformations of the 4 horizontal vectors. Whereas, unitary transformations of q_{uR}, q_{dR} and $(q_u, q_d)_L$, as a doublet, do *not* change the matter field Lagrangian, an independent transformation of q_{dL} leads to "mismatch" $\tilde{q}_{dL} = U_{KM} q_{dL}$ of the quark fields in the charged current. This leads us to the form of the charged current given in Eq. (1) with the unitary 3×3 matrix

$$U_{KM} = \begin{pmatrix} V_{ud} & V_{us} & V_{ub} \\ V_{cd} & V_{cs} & V_{cb} \\ V_{td} & V_{ts} & V_{tb} \end{pmatrix} \tag{12}$$

which may be parametrized in terms of 3 rotation angles and a phase.

This family mixing occurs if 4 independent unitary transformations are required to diagonalize the mass matrix, and this is the case if particles of the same charge all have different masses. This happens to be so for the quarks. If we believe that all neutrinos are massless no mixing in the leptonic current is possible. Indeed all searches for lepton number violation have yielded no signal so far.

Due to unitarity, there is no mixing effect in the neutral current, since $\overline{\tilde{q}}_{dL} \tilde{q}_{dL} \equiv \bar{q}_{dL} q_{dL}$. This is called the GIM-mechanism explaining the absence of flavor changing neutral currents (FCNC). In

fact, in order to explain the absence of FCNC's, Glashow, Iliopoulos and Maiani had to propose, in 1970, the existence of a fourth quark, the charm quark c as a doublet partner of the s quark. At that time only three quarks where known [13].

The discovery of the J/ψ [14] revealed the completeness of the 2nd family with the charm quark c. The first 3rd family member showed up in 1975 with the discovery of the τ [15]. With the observation of the Υ [16] the existence of the b quark could be established. We are still waiting for the direct observation of bottom's doublet partner, the top quark. The direct lower limit for m_t from CDF is [4]

$$m_t > 89 \ \text{GeV} \ . \tag{13}$$

In models with charged Higges, due to the possible decay $t \to H^+ b$, only the weaker limit $m_t > 45$ GeV (95% CL) can be obtained [17]. The properties of the weak currents, which essentially derive from the minimal Higgs assumption, were established in the exciting history of the weak interactions which started with the Fermi model in 1934. Here, we only mention some more recent tests of the basic structure of the weak currents: [18]

- V-A structure of the CC:
  μ-decay provides the most sensitive, clean and direct tests for right-handed currents. The best limit for the transition amplitude is

$$\frac{A_{V+A}}{A_{V-A}} < 0.029 \quad (90\% CL)$$

- absence of FCNC (at tree level):

$$\begin{array}{lcc} \Gamma(K_L \to \mu^+\mu^-)/\Gamma(K_L \to all) & = & (9.5^{+2.4}_{-1.5}) \times 10^{-9} \\ \Gamma(D^0 \to \mu^+\mu^-)/\Gamma(D^0 \to all) & < & 1.1 \times 10^{-5} \\ \Gamma(B^0 \to e^+e^-)/\Gamma(B^0 \to all) & < & 3 \times 10^{-5} \end{array}$$

  FCNC processes are allowed only through higher order transitions.

- special properties of the lepton current:
  Present limits on the neutrino masses are:

$$\begin{array}{lll} m_{\nu_e} < & 9.4 \text{ eV} & (\text{from } {}^3H \to {}^3H_e \, e^- \, \bar{\nu}_e) \\ m_{\nu_\mu} < & 250 \text{ keV} & (\text{from } \pi \to \mu \, \nu_\mu) \\ m_{\nu_\tau} < & 35 \text{ MeV} & (\text{from } \tau^- \to 3\pi \, \nu_\tau) \end{array}$$

  L_ℓ conservation is established by the branching fractions:

$$\begin{array}{lll} R < & 4.9 \times 10^{-11} & (\text{from } \mu \to e\gamma) \\ R < & 1.0 \times 10^{-13} & (\text{from } \mu \to 3e) \end{array}$$

  Neutrino mixing searches (ν-oscillations $\nu_\ell \leftrightarrow \nu_{\ell'}$) have also been negative so far.

No deviations from the SM has yet been established. Open problems are the measurements of direct CP-violation (ε') in the K-meson system and CP-violation in the B-meson system [19]. We still do not know whether CP-violation is a phenomenon which has its "origin" in the CKM-phase solely, or if it's due to a new super-weak interaction outside the SM. Still unsolved is the solar neutrino

problem [20]. The observed solar ν_e flux is too low. This could signal flavor mixing (causing conversion of ν_e into $\nu_{\mu,\tau}$ not visible to present detectors) of the neutrinos which is possible only if the neutrinos have different masses. Another possibility would be that the ν_e is unstable.

Fixing the parameters of the SM

Besides the fermion masses, the CKM-mixing parameters and the Higgs mass, the SM has 3 basic parameters g, g' and v. They are conventionally replaced by parameters which can be measured directly in a physical process. In view of the mass-coupling relations, typical for a spontaneously broken gauge theory, masses and couplings are not independent parameters and many different parametrizations may be advocated. A specific choice of experimental data points as input parameters defines a *renormalization scheme*. Like in QED a natural choice would be the fine structure constant and the physical particle masses (*on-shell scheme*):

$$\alpha, M_W, M_Z, m_f, m_H \tag{14}$$

where the universal fine structure constant $\alpha = e^2/4\pi = 1/137.0359895(61)$ may be determined in low momentum transfer Coulomb scattering. Since M_W will not be known accurately at LEP1 we must use the precisely determined Fermi constant G_μ obtained from the muon decay rate in place of M_W. Thus, we will use the parameter set

$$\alpha, G_\mu, M_Z, m_f, m_H \tag{15}$$

for accurate predictions of measurable quantities. In the pre-LEP era when M_Z was not known or known with rather limited accuracy from the $p\bar{p}$-collider, instead of M_Z the weak mixing parameter $\sin^2\Theta_W$ had to be used. This parameter has been measured first in low momentum transfer neutrino scattering. Predictions could then be made starting from the low energy parametrization

$$\alpha, G_\mu, \sin^2\Theta_{\nu N}, m_f, m_H \tag{16}$$

where we have denoted $\sin^2\Theta_W$ by $\sin^2\Theta_{\nu N}$ in order to make precise that the value has been obtained from νN-scattering. The precise definition of $\sin^2\Theta_W$ is process dependent, because the values measured in different processes differ by higher order corrections. Since $\sin^2\Theta_W$ measurements are important in the determination of the SM parameters we now briefly consider neutrino scattering.

For a low energy definition of the weak mixing angle we may use low momentum transfer neutrino electron scattering where the cross section ratio

$$R_{\nu_\mu e} = \sigma(\bar{\nu}_\mu e)/\sigma(\nu_\mu e) = (\xi^2 - \xi + 1)/(\xi^2 + \xi + 1) \tag{17}$$

is independent of the neutral current coupling G_{NC}. The latter is defined by (E_ν the incident neutrino energy)

$$G_{NC} = \left(8\pi\sigma(\nu_\mu e)/m_e E_\nu[(1+\xi)^2 + \frac{1}{3}(1-\xi)^2]\right)^{1/2} = \rho\, G_\mu \tag{18}$$

and is equivalent to a determination of the ρ-parameter, which is unity to lowest order in the Standard Model . The parameter ξ describes the relative strength of the vector coupling of the leptons

$$\xi = \frac{v_e}{a_e} = 1 - 4\sin^2\Theta_{\nu_\mu e} \tag{19}$$

where $\sin^2\Theta_{\nu_\mu e}$ stands for this particular definition of $\sin^2\Theta_W$. While the purely leptonic $\nu_\mu e$-scattering provides a clean determination of the weak mixing parameter the low event rates lead to a rather limited accuracy only. The best accuracy which should be achievable at CHARM II is $\delta\sin^2\Theta_{\nu_\mu e} \simeq 0.005$. The present value is $\sin^2\Theta_{\nu_\mu e} = 0.240 \pm 0.012$ [21].

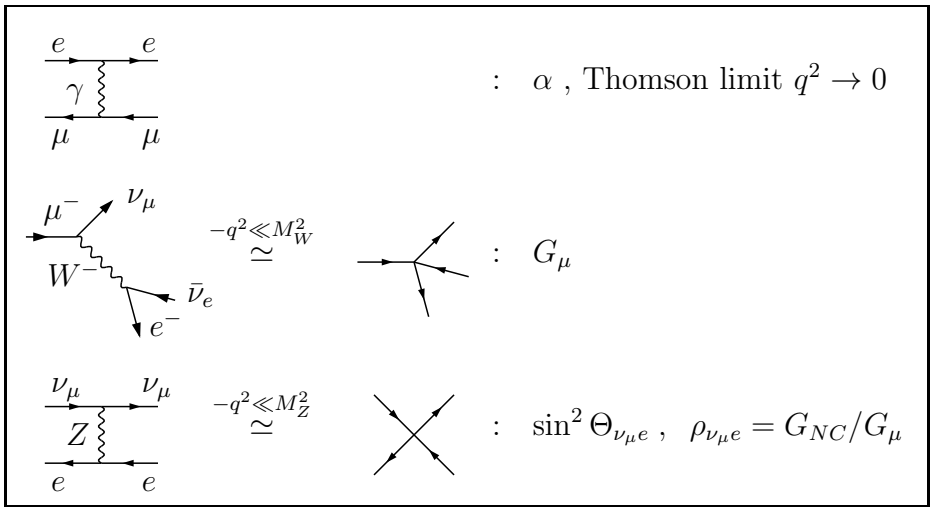

Figure 1: Processes used to define the low energy parameters

More accurate values for $\sin^2\Theta_W$ are obtained from semi-leptonic neutral current reactions. In particular the deep inelastic neutrino nucleus reactions $\nu_\mu N \to \mu^- X$ and $\nu_\mu N \to \nu_\mu X$ lead to rather precise determinations of the neutral to charged current ratios

$$R_\nu = \frac{\sigma(\nu_\mu N \to \nu_\mu X)}{\sigma(\nu_\mu N \to \mu^- X)} \ , \quad R_{\bar{\nu}} = \frac{\sigma(\bar{\nu}_\mu N \to \bar{\nu}_\mu X)}{\sigma(\bar{\nu}_\mu N \to \mu^+ X)} \ , \quad r = \frac{\sigma(\bar{\nu}_\mu N \to \mu^+ X)}{\sigma(\nu_\mu N \to \mu^- X)} \tag{20}$$

and R_ν has been measured to 1% accuracy by CDHS and CHARM [22]. In the Born approximation of the low energy effective current-current interaction, Eq. (24) below, assuming a valence quark parton model and approximately isoscalar targets N ($\frac{N_p - N_n}{N_p + N_n} = 0$, N consisting of N_p protons and N_n neutrons) one obtains the simple result

$$R_\nu = g_L^2 + g_R^2\, r \ , \quad R_{\bar{\nu}} = g_L^2 + g_R^2/r \tag{21}$$

where

$$g_L^2 = \varepsilon_{Lu}^2 + \varepsilon_{Ld}^2 \simeq \frac{1}{2} - sin^2\Theta_{\nu N} + \frac{5}{9} sin^4\Theta_{\nu N} \ , \quad g_R^2 = \varepsilon_{Ru}^2 + \varepsilon_{Rd}^2 \simeq \frac{5}{9} sin^4\Theta_{\nu N} \ . \tag{22}$$

In the SM the predictions for the couplings may be written in the form [23]

$$\begin{aligned} \varepsilon_{Lf} &= \rho_{\nu N} \left(T_{3f} - Q_f \kappa_{\nu N} \sin^2\Theta_W + \lambda_{Lf} \right) \\ \varepsilon_{Rf} &= \rho_{\nu N} \left(-Q_f \kappa_{\nu N} \sin^2\Theta_W + \lambda_{Rf} \right) \end{aligned} \tag{23}$$

where $\rho_{\nu N}$ (= 1), $\kappa_{\nu N}$ (= 1) and λ_{if} (= 0) include radiative corrections . The lowest order values are given in parentheses. One-loop effects will be discussed at the end of Section 4. For a precise comparison of $\sin^2\Theta$ measurements, a process independent definition of $\sin^2\Theta_W$ is needed. A convenient convention, proposed by Sirlin in this context, is the definition in terms of the physical vector boson masses (assuming $\rho_{tree} = 1$, see Eq. (28) below). By including process-dependent radiative corrections $\sin^2\Theta_W$ can be computed from $\sin^2\Theta_{\nu_\mu N}$ measured in a particular process.

The low energy four-fermion processes are described by the effective Fermi-type Lagrangian

$$\mathcal{L}_{eff} = -\frac{1}{\sqrt{2}}\left(G_\mu J^+_\mu J^{\mu-} + G_{NC} J^Z_\mu J^{\mu Z}\right) + e j^{em}_\mu A_\mu \tag{24}$$

which is the low energy effective form ($|q^2| \ll M_W^2, M_Z^2$) of

$$\mathcal{L}_{int} = \frac{g}{2\sqrt{2}}\left(J^+_\mu W^{\mu-} + h.c.\right) + \frac{g}{2\cos\Theta_W} J^Z_\mu Z^\mu + e j^{em}_\mu A_\mu \ . \tag{25}$$

The electroweak unification condition and the relations between the parameters appearing in (24) and (25) read

$$\begin{array}{rrcccl} i) & \sqrt{4\pi\alpha} & = & e & = & g\sin\Theta_W \\ ii) & \sqrt{2}G_\mu & = & \frac{g^2}{4M_W^2} & = & \frac{1}{v^2} \\ & \sqrt{2}G_{NC} & = & \frac{g^2}{4M_Z^2\cos^2\Theta_W} & = & \rho_0\frac{1}{v^2} \\ iii) & \rho_0 & = & \frac{G_{NC}}{G_\mu} & = & \frac{M_W^2}{M_Z^2\cos^2\Theta_W} \equiv \rho_{tree} \end{array} \tag{26}$$

For the moment we have relaxed from the assumption $\rho_0 = 1$ valid in the minimal SM.

From the parameter relations we now obtain the tree level relation

$$\begin{aligned} \pi\alpha = \frac{e^2}{4} &\overset{i)}{=} \frac{g^2\sin^2\Theta_W}{4} \\ &\overset{ii)}{=} \sqrt{2}G_\mu M_W^2\sin^2\Theta_W \\ &\overset{iii)}{=} \sqrt{2}G_\mu M_W^2\left(1 - \frac{M_W^2}{\rho_0 M_Z^2}\right). \end{aligned}$$

If radiative corrections are included, this relation is modified to [24]

$$\sqrt{2}G_\mu M_W^2\left(1 - \frac{M_W^2}{\rho_0 M_Z^2}\right) = \pi\frac{\alpha}{1-\Delta r}. \tag{27}$$

which is the defining equation for Δr (with ρ_0 kept fixed at its tree level value!). In the following we take $\rho_0 = 1$, as appropriate for Higgse doublets, such that by the last relation of Eq. (26)

$$\sin^2\Theta_W = 1 - \frac{M_W^2}{M_Z^2}. \tag{28}$$

The definition of Δr by Eq. (27) is conceptually very simple, all quantities involved have been measured and can be found in the particle data tables.

Later, we will often use α and the physical particle masses as a convenient set of independent parameters. The Fermi constant is then a calculable quantity (μ-decay amplitude). Originally, the μ life-time τ_μ has been calculated within the framework of the effective Fermi interaction.

If we include QED corrections (see Fig. 2) we obtain the result

$$\frac{1}{\tau_\mu} = \frac{G_\mu^2 m_\mu^5}{192\pi^3}\left(1 - \frac{8m_e^2}{m_\mu^2}\right)\left[1 + \frac{\alpha}{2\pi}(1 + \frac{2\alpha}{3\pi}\log\frac{m_\mu}{m_e})(\frac{25}{4} - \pi^2)\right]. \tag{29}$$

This formula is used as the defining equation for G_μ in terms of the experimental μ life-time. Present data [18] yield the value given in Eq. (10).

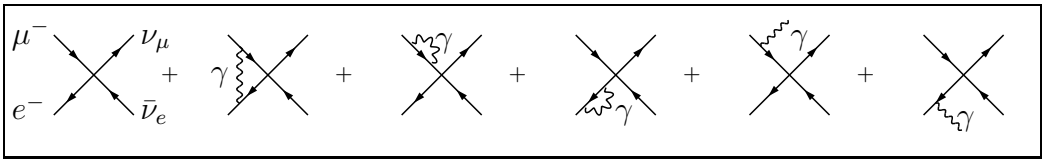

Figure 2: μ decay with QED corrections in the effective Fermi model

The Z-mass has been determined rather accurately now at LEP [1]

$$M_Z = 91.174 \pm 0.021 \ \text{GeV} \tag{30}$$

while the W mass is known from the collider experiments UA2 [2] and CDF [3]. Using their determination of the mass ratio M_W/M_Z, for which common systematic errors largely drop out, together with the Z mass from LEP1 we obtain (in brakets the absolute determination from CDF)

$$M_W = 80.19 \ \pm 0.32 \ (79.91 \ \pm 0.39) \quad \text{GeV} \ . \tag{31}$$

The value for $\sin^2\Theta_W$ obtained from the hadron colliders is

$$\sin^2\Theta_W = 0.2265 \pm 0.0062 \tag{32}$$

independent of model assumptions. The νN scattering data yield

$$\sin^2\Theta_W = 0.232 \pm 0.006 \tag{33}$$

assuming the SM with $m_t = 60$ GeV and $m_H = 100$ GeV [22].

In Table 1 and Figure 3 the status of $\sin^2\Theta_W$-measurements is summarized. The results are in good agreement with each other. By $\sin^2\Theta_e$ we have denoted $\sin^2\Theta$ measured at the Z-resonance and by $\sin^2\Theta_{\nu_\mu e}$ the one measured by $\nu_\mu e$-scattering. In Fig. 4 we show conversion factors for various definitions of $\sin^2\Theta_W$. For a discussion we refer the reader to Section 4.

Table 1. $\sin^2\Theta_W$ measurements in NC processes [4,22,18,21,1]

Measurement	$\sin^2\Theta_W$				
$\frac{M_W}{M_Z}$ $(p\bar{p})$	0.2265	$\pm$	0.0062		(ave.)
UA2	0.2202	$\pm$	0.0084	$\pm$	0.0045
CDF	0.229	$\pm$	0.016	$\pm$	0.002
$\left(\frac{\sigma_{NC}}{\sigma_{CC}}\right)_{\nu_\mu N}$	0.232	$\pm$	0.006		(ave.)
CDHS	0.2275	$\pm$	0.005	$\pm$	0.005
CHARM	0.236	$\pm$	0.005	$\pm$	0.005
P. V. in Cs	0.215	$\pm$	0.007	$\pm$	$[0.017]^{th}$
e^-D (SLAC)	0.217	$\pm$	0.015	$\pm$	$[0.013]^{th}$
$R_{\nu_\mu e} = \frac{\sigma_{\nu_\mu e}}{\sigma_{\bar{\nu}_\mu e}}$ CHARM II	0.240	$\pm$	0.009	$\pm$	0.008
assume $m_t = 140 \pm 40 \quad \rightarrow$	0.230	$\pm$	0.016		
Γ_ℓ, A_{FB}^ℓ LEP	0.2302	$\pm$	0.0025		
assume $m_t = 140 \pm 40 \quad \rightarrow$	0.220	$\pm$	0.006		

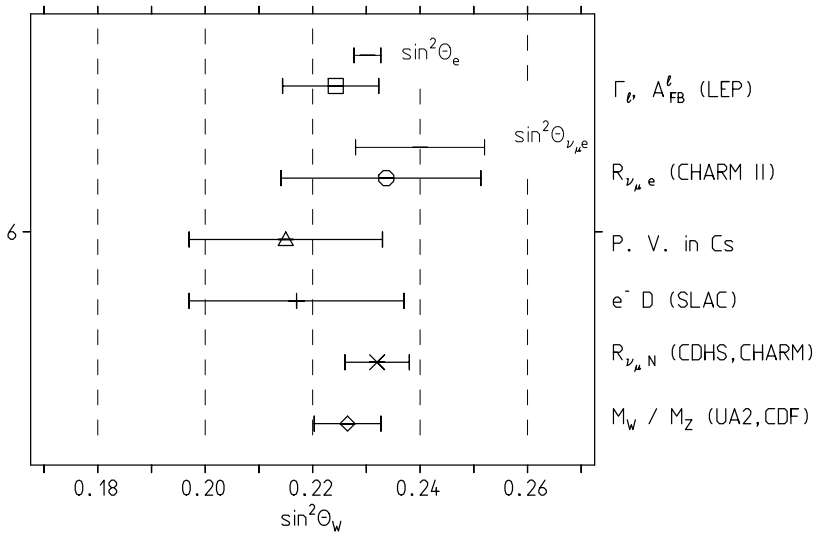

Figure 3: Comparison of various $\sin^2\Theta$ measurements.

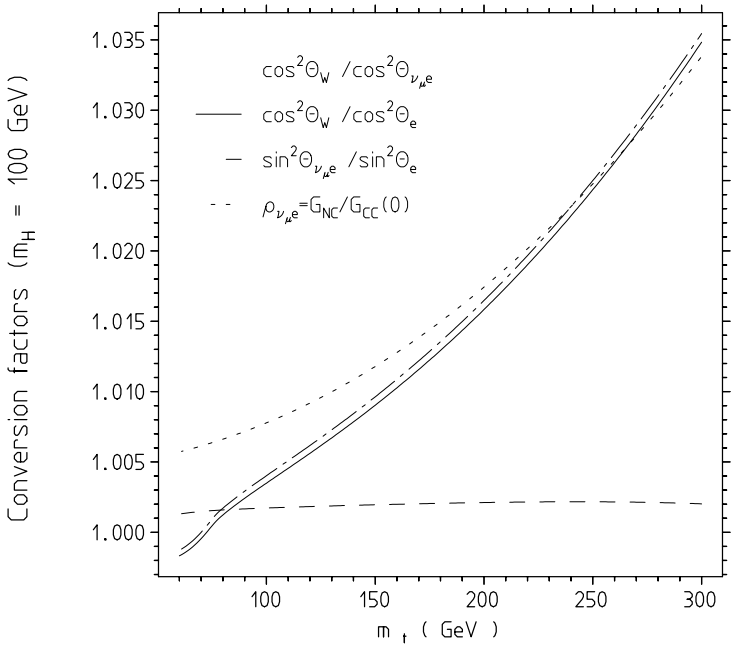

Figure 4: m_t-dependence of various $\sin^2\Theta$ conversions.

Assuming $\rho_{tree} = 1$, as required by the minimal SM, recent global fits yield for the weak mixing angle and the top mass ($68\% C.L.$)

$$\begin{array}{lllll} \sin^2\Theta_W & = 0.2273 \pm 0.0033, & m_t = 122^{+41}_{-32} & \text{GeV} & \text{Ref. 25} \\ \sin^2\Theta_W & = 0.2291 \pm 0.0040, & m_t = 124^{+28+20}_{-34-15} & \text{GeV} & \text{Ref. 26} \\ \sin^2\bar{\Theta} & = 0.2327 \pm 0.0009, & m_t = 126 \pm 30 \pm 18 & \text{GeV} & \text{Ref. 1} \end{array} \tag{34}$$

when $40\ \text{GeV} < m_H < 1\ \text{TeV}$.

A very important parameter in electroweak theory is the ρ-parameter, defined by the neutral to charged current ratio at low energy. The νN scattering data yield the most sensitive determination of the ρ-parameter.

Taking ρ and $\sin^2\Theta_W$ as independent parameters, a recent global fit to all NC-data [26] yields (the values indicated with an asterisk I have obtained by scaling with the theoretical predictions)

m_t (GeV)	100	140	180	200	
$\sin^2\Theta_W$	0.2305	0.2260*	0.2207*	0.2215	$\pm$ 0.0010
$\sin^2\Theta_W$ (SM)	0.23027	0.22580	0.22048	0.21741	
ρ_0	1.003	0.99996*	0.996*	0.994	$\pm$ 0.003
ρ (SM)	1.00776	1.01082	1.01492	1.01737	

where the theoretical values (SM) are given for $m_H = 100$ GeV. $\rho_0 = \frac{\rho^{exp}}{\rho_{SM}}$ corresponds to ρ_{tree} if we ignore possible radiative corrections from non-standard physics. Thus ρ_0 is remarkably close to the minimal standard model value $\rho_{tree} = 1$.

These experimental results are extremely important constraints for possible deviations from the SM. For example, the measured value for $\sin^2\Theta_W$ is clearly in contradiction to the simplest grand unified model, namely, minimal SU(5), which predicts $\sin^2\Theta_W \simeq 0.211 - 0.218$. Independently, this theory has been ruled out by proton decay experiments. The bounds on the ρ-parameter permit additional scalar doublets or singlets which do not affect the minimal SM value $\rho_{tree} = 1$. However, possible Higgs triplet contaminations are limited because they imply $\rho_{tree} \neq 1$ and a pure triplet $(\Delta^{++}, \Delta^{+}, \Delta^{0})$ would give $\rho_{tree} = 1/2$.

3. LEP PHYSICS, BASIC PROCESSES

3.1 Production and Decay of the Weak Vector Bosons

At lowest order, production and decay of massive vector bosons are described by the Born diagrams

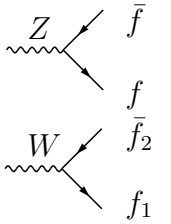

$$:= \frac{g}{2\cos\theta}\bar{f}_{\bar{c}\alpha}\left(\gamma^\mu(v_f - a_f\gamma_5)\right)_{\alpha\beta} f_{c\beta}\delta_{\bar{c}c}$$

$$:= \frac{g}{2\sqrt{2}}\bar{f}_{2_{\bar{c}\alpha}}\left(\gamma^\mu(1-\gamma_5)\right)_{\alpha\beta} f_{1_{c\beta}}\delta_{\bar{c}c} \qquad (35)$$

if we ignore Cabibbo-Kobayashi-Maskawa mixing for the quark flavors in 1st approximation. We have indicated the color and spinor indices. Both Z and $W^\pm$ production and decay may be described by a general vertex $\hat{g}\bar{f}_2\gamma^\mu(v - a\gamma_5)f_1$. The production cross section for unpolarized beams in the zero-width approximation is:

$$f_1(p_1) + \bar{f}_2(p_2) \to V(p)$$

$$\sigma(f_1 + \bar{f}_2 \to V) = \frac{1}{N_{c1}}\frac{1}{N_{c2}}\frac{1}{(2s_1+1)}\frac{1}{(2s_2+1)}\,\pi\,\delta\left((p_1+p_2)^2 - M_V^2\right)\cdot\frac{\sum|T_{12}|^2}{M_V^2} \qquad (36)$$

where T_{12} is the transition matrix element and the sum extends over color (c_i) and spin (s_i) of initial and final state particles. With respect to the initial states, the cross section is determined by the color and spin averages of $|T_{12}|^2$.

The decay width is determined by the same $\sum|T_{12}|^2$ (the processes are related by crossing) and given by

$$V(p) \to f_1(p_1) + \bar{f}_2(p_2)$$

$$\Gamma(V \to f_1 + \bar{f}_2) = \frac{1}{(2s_V+1)} \frac{M_V}{16\pi} \frac{2|\vec{p}|}{M_V} \frac{\sum |T_{12}|^2}{M_V^2} \tag{37}$$

where $\vec{p}$ is the decay momentum of a fermion in the center of mass frame.
The T-matrix element can be easily obtained

$$T_{12} = \hat{g} \bar{v}_{2_{\bar{c}\alpha}}(p_2, s_2)(\gamma^\mu(v - a\gamma_5))_{\alpha\beta} u_{1_{c\beta}}(p_1, s_1) \varepsilon^*_\mu(p, \lambda) \delta_{\bar{c}c} \; .$$

Taking $|T_{12}|^2$ and summing over color and spin one obtains

$$\begin{aligned} \frac{\sum |T_{12}|^2}{M_V^2} &= \hat{g}^2 N_{cf} \left\{ (v^2 + a^2) \left(1 - (2 - \tfrac{s}{M_V^2}) \tfrac{m_1^2 + m_2^2}{2M_V^2} - \tfrac{(m_1^2 - m_2^2)^2}{2M_V^4} \right) \right. \\ &\quad \left. + (v^2 - a^2)(4 - \tfrac{s}{M_V^2}) \tfrac{m_1 m_2}{M_V^2} \right\} \; . \end{aligned}$$

As a result the formula for the partial widths are given by

$$\begin{aligned} \Gamma_{V \to f_1 \bar{f}_2} &= \tfrac{\sqrt{2} G_\mu M_V^3}{12\pi} \tfrac{2|\vec{p}|}{M_V} N_{cf} \left\{ (v^2 + a^2) \left(1 - \tfrac{1}{2} \tfrac{(m_1^2 + m_2^2)}{M_V^2} - \tfrac{1}{2} \tfrac{(m_1^2 - m_2^2)^2}{M_V^4} \right) \right. \\ &\quad \left. + (v^2 - a^2) 3 \tfrac{m_1 m_2}{M_V^2} \right\} \end{aligned} \tag{38}$$

or, for light fermions $m_i \ll M_V$, $|\vec{p}| \simeq \frac{M_V}{2}$,

$$\Gamma_{W \to f_1 \bar{f}_2} = \tfrac{\sqrt{2} G_\mu M_W^3}{12\pi} N_{cf} |V_{12}|^2 \; ; \;\; \Gamma_{Z \to f\bar{f}} = \tfrac{\sqrt{2} G_\mu M_Z^3}{12\pi} N_{cf} (v_f^2 + a_f^2) \tag{39}$$

where we have indicated the Cabibbo-Kobayashi-Maskawa matrix element V_{12} for the charged current. Notice that for $\sin^2 \Theta_W = 0$ (i.e. $g' = 0$) $M_Z = M_W$ and

$$\Gamma_{W \to f_1 \bar{f}_2} = \Gamma_{Z \to f_1 \bar{f}_1} + \Gamma_{Z \to f_2 \bar{f}_2} \; .$$

Since $m_t > 89 \; GeV$, the decays $Z \to t\bar{t}$ and $W \to tb$ are energetically forbidden. LEP has excluded the existence of a fourth family neutrino of mass $m_\nu < 40 \; GeV$ [1]. Since the heaviest fermion, the b quark, has mass $m_b \simeq 4.8 \; GeV$ we can safely neglect all mass effects in calculating the widths.

By $\Gamma_{inv} = 3\Gamma_{Z \to \nu\bar{\nu}}$ we denote the invisible width for the decays into ν_e, ν_μ and ν_τ. Γ_{had} is the total hadronic width for the decays into u, d, s, c and b quarks or the corresponding hadronic states. The total Z-width (and similarly the W-width) is given with high accuracy by the sum over the two body decays

$$\Gamma_{tot} = \Gamma_Z \simeq \sum_f \Gamma_f \; ; \;\; \Gamma_f = \Gamma_{Z \to f\bar{f}} = \Gamma_\nu \; f_f(\sin^2 \Theta_W)$$

with $f_f(\sin^2 \Theta_W) \doteq 1 - 4|Q_f| \sin^2 \Theta_W + 8 Q_f^2 \sin^4 \Theta_W$ normalized to the ν channel. Since $m_H > 49$ GeV, the contribution $\Gamma_{Z \to Hf\bar{f}}$ which would be non-negligible for a very light Higgs also can be ignored.

Table 2. Lowest order predictions for Γ_W and Γ_Z for $\sin^2\Theta_W = 0.23$, $M_W = 80.19(32)$ GeV and $M_Z = 91.174(21)$ GeV.

$W \to f_1 f_2$			$Z \to f\bar{f}$			
$f_1 f_2$	Γ_0(MeV)	B_r(%)	$f\bar{f}$	$f(\sin^2\Theta_W)^+$	Γ_0(MeV)	B_r(%)
$\ell\bar{\nu}_\ell$	225.6	11.1	$\nu_\ell\bar{\nu}_\ell$	1	165.8	6.8
			inv		497.5	20.5
			$\ell\bar{\ell}$	0.5032	83.4	3.4
$u\bar{d}$	676.7	33.3	$u\bar{u}$	0.5748	286.0	11.8
			$d\bar{d}$	0.7404	368.3	15.2
had	1353.4	66.6	had		1676.6	69.2
tot	2030.1	100.0	tot		2424.3	100.0

We now consider $Z-$**production in** e^+e^-**collisions.** In the light fermion approximation

$$\frac{\sum |T_{12}|^2}{M_V^2} = 3 \cdot 16\pi \, \frac{\Gamma_{Z\to f\bar{f}}}{M_Z}$$

and hence, in the narrow width approximation,

$$\sigma(e^+e^- \to Z) = 12\pi \frac{\Gamma_{Z\to e^+e^-}}{M_Z} \pi\delta(s - M_Z^2)$$

with $s = (p_1 + p_2)^2 = 4E_b^2$ and E_b the beam energy.

Using the relation (the Breit-Wigner form will be "derived" below)

$$\pi\delta(s - M_Z^2) = \lim_{\Gamma_Z \to 0} \frac{M_Z \Gamma_Z}{(s - M_Z^2)^2 + \Gamma_Z^2 M_Z^2}$$

we easily obtain the cross section for (finite width) resonance production, described by a Breit-Wigner line-shape,

$$\sigma(e^+e^- \to Z) = \frac{12\pi}{M_Z^2} \frac{\Gamma_{Z\to ee}\Gamma_Z M_Z^2}{(s - M_Z^2)^2 + \Gamma_Z^2 M_Z^2} \quad .$$

Near resonance, the cross section for $e^+e^- \to Z \to f\bar{f}$ is

$$\sigma(e^+e^- \to Z \to f\bar{f}) = \sigma(e^+e^- \to Z) \cdot \frac{\Gamma_{Z\to ff}}{\Gamma_Z}$$

and hence

$$\sigma_{0Z}^f = \sigma(e^+e^- \to Z \to f\bar{f}) = \sigma_{\rm peak}^f \frac{\Gamma_Z^2 M_Z^2}{(s - M_Z^2)^2 + \Gamma_Z^2 M_Z^2} \quad . \tag{40}$$

where $\sigma_{\rm peak}^f$ is the peak cross section (at $s = M_Z^2$)

$$\sigma_{\rm peak}^f = \frac{12\pi}{M_Z^2} \frac{\Gamma_e}{\Gamma_Z} \frac{\Gamma_f}{\Gamma_Z} \quad . \tag{41}$$

Table 3. Lowest order peak cross section $\sigma^f_{\rm peak}$. M_Z and Γ_f as in Tab. 2. ($1\text{GeV}^{-2} = 0.38938 \times 10^6$ nb)

f	ν	μ	u	d	inv	had	tot
$\sigma^f_{\rm peak}$(nb)	4.16	2.09	7.17	9.23	12.47	42.03	60.77

3.2 The process $e^+e^- \to f\bar{f}, (f\bar{f}\gamma)(f \neq e)$

We now consider in detail the process

$$e^+(p_+) + e^-(p_-) \to \bar{f}(q_+) + f(q_-) + \text{“}\gamma(k)\text{”}$$

in the Born approximation given by the diagrams in Fig. 5. Real γ emission will be considered below.

In the center of mass frame in terms of the beam energy $s = (p_+ + p_-)^2 = 4E_b^2$ and $t = (p_+ - q_+)^2 = 2E_b^2(1-\cos\theta)$ with θ the angle between p_+ and q_+. By the arguments given in the previous chapter we can safely neglect the fermion masses if we assume $s \gg m_b^2$ (the bottom quark is the heaviest of the final state fermions at LEP energies). $t\bar{t}$ production is not considered.

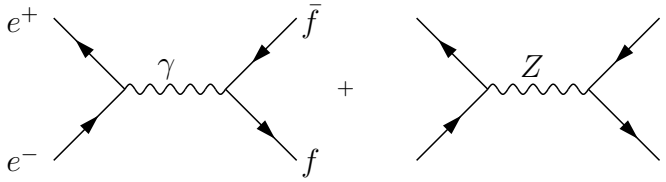

Figure 5: Born diagrams for the process $e^+e^- \to f\bar{f}$

Since we are considering beam energies E_b far above the Υ threshold the fermions are essentially massless and helicity is a good quantum number. It is therefore convenient to use left- and right-handed fields $f_L = \frac{1-\gamma_5}{2}f$ and $f_R = \frac{1+\gamma_5}{2}f$ which describe polarized fermion states: The couplings are

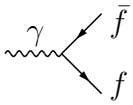

$$:= \quad eQ_f \bar{f}\gamma^\mu f \; ; \qquad$$

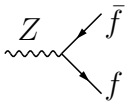

$$:= \quad \tfrac{M_Z}{v}\bar{f}\gamma^\mu(v_f - a_f\gamma_5)f \qquad (42)$$

where $\bar{f}\gamma^\mu f = \bar{f}_L\gamma^\mu f_L + \bar{f}_R\gamma^\mu f_R$ and $\bar{f}\gamma^\mu(v_f - a_f\gamma_5)f = \varepsilon_{Lf}\bar{f}_L\gamma^\mu f_L + \varepsilon_{Rf}\bar{f}_R\gamma^\mu f_R$ with $\varepsilon_{Lf} = v_f + a_f$ and $\varepsilon_{Rf} = v_f - a_f$.

We notice that for the vector-like couplings (i.e. vector or axial-vector) no $\bar{f}_R \ldots f_L$ or $\bar{f}_L \ldots f_R$ terms are present. This is a general feature of *any* gauge interaction (coupling via spin 1 vector fields). Since e^-_L describes a left-handed electron and a right-handed positron etc. there are no transitions from equal helicity e^+e^- into equal helicity $\bar{f}f$ states! Therefore there are only <u>four</u> possible transition amplitudes $T_{h_i h_f}$ for polarized states: $T_{LL}, T_{LR}, T_{RL}, T_{RR}$, where $h_i = -1$ (L), $+1$ (R) is the electron helicity and $h_f = -1$ (L), $+1$ (R) the final state helicity of the fermion f. The helicity of the antiparticle in each case is fixed to the opposite value. This is true for any gauge theory!

The differential cross section is given by

$$\frac{d\sigma}{d\cos\theta} = \frac{s}{48\pi} N_{cf} \sum |T_{h_i h_f}|^2 \qquad (43)$$

with

$$|T_{h_e h_f}|^2 = \frac{3}{8}(1 \pm \cos\theta)^2 \left| \varepsilon_{h_e e}\varepsilon_{h_f f} \frac{\sqrt{2}G_\mu M_Z^2}{s - M_Z^2 + iM_Z\Gamma_Z} + Q_e Q_f \frac{4\pi\alpha}{s} \right|^2$$

The sign +(-) is for T_{LL},T_{RR} (T_{LR}, T_{RL}).

In the cross section we distinguish three pieces, the pure QED cross section, the $\gamma - Z$ interference term and the pure Z-exchange cross section:

$$\frac{d\sigma}{d\cos\theta}(e^+e^- \to \gamma^*, Z^* \to \bar{f}f) = \frac{d\sigma^\gamma}{d\cos\theta} + \frac{d\sigma^{\gamma Z}}{d\cos\theta} + \frac{d\sigma^Z}{d\cos\theta} \ . \tag{44}$$

Of course, in general, there is no way to measure these terms individually. However, individual terms may dominate as for example the QED piece at low s or the Z-exchange term near the Z-resonance.

For unpolarized beams and final states we obtain

$$\begin{array}{lcl} \frac{d\sigma^\gamma}{d\cos\theta} & = & \frac{\pi\alpha^2 Q_f^2 N_{cf}}{2s}(1 + \cos^2\theta) \\ \frac{d\sigma^{\gamma Z}}{d\cos\theta} & = & -\frac{\alpha Q_f \sqrt{2}G_\mu M_Z^2}{4s} N_{cf} Re\chi(s) \cdot \{v_e v_f(1 + \cos^2\theta) \\ & & +2a_e a_f \cos\theta\} \\ \frac{d\sigma^Z}{d\cos\theta} & = & \frac{G_\mu^2 M_Z^4}{16\pi s} N_{cf} |\chi(s)|^2 \cdot \Big\{(v_e^2 + a_e^2)(v_f^2 + a_f^2)(1 + \cos^2\theta) \\ & & +8a_e a_f v_e v_f \cos\theta\} \end{array} \tag{45}$$

with the resonance factor

$$\chi(s) = \frac{s}{s - M_Z^2 + iM_Z\Gamma_Z} \ .$$

Near the Z-resonance, the process $e^+e^- \to f\bar{f}$ is predominantly a parity violating weak interaction transition. The axial couplings a_f lead to *asymmetries* at the tree level.

i) asymmetry in the angular distribution due to terms linear in $\cos\theta$ called forward-backward asymmetry or charge asymmetry A_{FB}, e.g. in $e^+e^- \to \mu^+\mu^-$ the μ^+ is produced with different probability in opposite directions relative to the incoming e^+. [1]

ii) asymmetry between cross sections for (polarized) L and R states, the so called left-right asymmetries A_{LR}.

Before we discuss the asymmetries in more detail, we briefly consider the total cross section.

Total cross section

The total cross section, with respect to the final state couplings, may be split into a pure vector and a pure axial-vector piece

$$\sigma_0^f = \int_{-1}^{+1} d\cos\theta \frac{d\sigma}{d\cos\theta} = \sigma_{0f}^{VV} + \sigma_{0f}^{AA} \tag{46}$$

[1] This type of asymmetry (though much smaller) is also present in pure QED (parity conserving) coming from higher order effects (box diagrams).

with

$$\begin{aligned}\sigma_{0f}^{VV} &= \frac{4\pi\alpha^2 Q_f^2 N_{cf}}{3s} - \frac{2\alpha Q_f \sqrt{2} G_\mu M_Z^2 N_{cf}}{3s} Re\chi(s) v_e v_f + \frac{G_\mu^2 M_Z^4 N_{cf}}{6\pi s} |\chi|^2 (v_e^2 + a_e^2) v_f^2 \\ \sigma_{0f}^{AA} &= \frac{G_\mu^2 M_Z^4 N_{cf}}{6\pi s} |\chi|^2 (v_e^2 + a_e^2) a_f^2 \ .\end{aligned}$$

Near the Z-resonance the pure Z-exchange term dominates and we may rewrite the cross section in the form:

$$\sigma_{0f} = \sigma_{0f}^{\gamma} + \sigma_{0f}^{\gamma Z} + \sigma_{0f}^{Z} = \sigma_{0f}^{Z} \cdot \left(1 + \frac{\sigma_{0f}^{\gamma Z}}{\sigma_{0f}^{Z}}\right) + \sigma_{0f}^{\gamma} = \sigma_{0f}^{Z} \left(1 + \mathcal{R}_f \frac{s - M_Z^2}{s}\right) + \sigma_{0f}^{\gamma} \ .$$

For $\mathcal{R}_f$ we find a $\gamma - Z$ interference correction

$$\mathcal{R}_f = \frac{8\pi\alpha Q_e Q_f}{\sqrt{2} G_\mu M_Z^2} \frac{v_e v_f}{(v_e^2 + a_e^2)(v_f^2 + a_f^2)} \ .$$

At resonance ($s = M_Z^2$) this correction does not contribute. σ_{0f}^{γ} is the QED background term

$$\sigma_{0f}^{\gamma} = \frac{4\pi\alpha^2 Q_f^2 N_{cf}}{3s}$$

which leads to a correction below 1% at resonance. Finally, using formula (39) for the width we find Eqs. (40) and (41) in agreement with our simplified derivation of the previous chapter. Closer inspection shows that the cross section formula

$$\sigma_{\rm eff}^{f}(s) = \frac{12\pi\Gamma_e\Gamma_f}{(s - M_Z^2)^2 + s^2 \frac{\Gamma_Z^2}{M_Z^2}} \left\{ \frac{s}{M_Z^2} + \mathcal{R}_f \frac{s - M_Z^2}{M_Z^2} + \mathcal{I}_f \frac{\Gamma_Z}{M_Z} + \ldots \right\} + \sigma_{0,\rm QED}^{f} \tag{47}$$

yields a model independent fit of the Z-line-shape provided Γ_e, Γ_f and Γ_Z are the physical (partial) widths, i.e. they include higher order corrections. We have included possible corrections proportional to Γ_Z/M_Z and the ellipses represent higher order terms in the expansion in $\frac{s-M_Z^2}{M_Z^2}$ and $\frac{\Gamma_Z}{M_Z}$. One important point (see below) is that $\Gamma_Z(s)$ defined in terms of the Z self-energy $\Pi_Z(s)$ by $M_Z\Gamma_Z(s) = Im\Pi_Z(s)$ is to high accuracy proportional to s:

$$\Gamma_Z(s) \simeq \frac{s}{M_Z^2}\Gamma_Z.$$

3.3 Asymmetries

A. Forward-backward asymmetry:

The differential cross section has a $\cos\theta$ even and a $\cos\theta$ odd term:

$$\frac{d\sigma}{d\cos\theta} = \sigma_{0f} \cdot \frac{3}{8}(1 + \cos^2\theta) + \Delta_{0f}\cos\theta \tag{48}$$

where σ_{0f} is the total cross section and

$$\begin{aligned}\Delta_{0f} &= \Delta_{0f}^{\gamma Z} + \Delta_{0f}^{Z} \\ \Delta_{0f}^{\gamma Z} &= -\frac{\alpha Q_f N_{cf}}{2s} \sqrt{2} G_\mu M_Z^2 Re\chi a_e a_f \\ \Delta_{0f}^{Z} &= \frac{G_\mu^2 M_Z^4}{2\pi s} N_{cf} |\chi|^2 a_e a_f v_e v_f \qquad .\end{aligned}$$

The forward-backward asymmetry is

$$A_{FB}(s,\cos\theta) = \frac{d\sigma(\theta) - d\sigma(\pi-\theta)}{d\sigma(\theta) + d\sigma(\pi-\theta)} = \frac{8}{3}\frac{\Delta_{0f}}{\sigma_{0f}}\frac{\cos\theta}{1+\cos^2\theta}$$

or in integrated form

$$A_{FB}(s) = \frac{\left(\int_0^1 - \int_{-1}^0\right) d\cos\theta \frac{d\sigma}{d\cos\theta}}{\int_{-1}^{+1} d\cos\theta \frac{d\sigma}{d\cos\theta}} = \frac{\Delta_{0f}}{\sigma_{0f}}\,. \tag{49}$$

Particular regimes of interest are the following:

i) For small $s \ll M_Z^2$ we have

$$R_{0f} = \frac{\sigma_{0f}}{\sigma_{\mu\mu}} \simeq \left\{ Q_f^2 N_{cf} + \frac{\sqrt{2}G_\mu}{2\pi\alpha} N_{cf} \frac{v_e (Q_f v_f)\, s}{1 - s/M_Z^2} \right\} \tag{50}$$

where

$$\sigma_{\mu\mu} = \sigma_0(e^+e^- \to \gamma^* \to \mu^+\mu^-) = \frac{4\pi\alpha^2}{3s}$$

is the QED "point" cross section used to normalize the hadronic cross section

$$\begin{aligned} \sigma_{\rm had} &= \sigma(e^+e^- \to \text{ hadrons }) = \sum_{\text{quark } q} \sigma_{0q} \\ R(s) &\doteq \frac{\sigma_{\rm had}}{\sigma_{\mu\mu}} = \sum_q R_q \simeq 3 \sum_{\substack{q \\ m_q \le \sqrt{s}}} Q_q^2 \end{aligned} \tag{51}$$

Notice that in this quantity the color factor 3 can be directly measured! For the asymmetry we get

$$A_{FB}^{f\bar{f}}(s) \simeq \frac{3}{8} a_e \left(\frac{a_f}{Q_f}\right) \frac{\sqrt{2}G_\mu}{\pi\alpha} \frac{s}{1 - s/M_Z^2} \tag{52}$$

an expression which vanishes for $s \to 0$.

ii) For $s \simeq M_Z$ we find

$$A_{FB}(M_Z^2) = \frac{\Delta_{0f}^Z(M_Z^2)}{\sigma_{0f}^Z(M_Z^2)} = \frac{3}{4} \cdot \frac{2v_e a_e}{v_e^2 + a_e^2} \cdot \frac{2v_f a_f}{v_f^2 + a_f^2}\,. \tag{53}$$

Asymmetries at the $Z-$resonance can all be expressed in terms of the coupling ratios

$$A_f \doteq \frac{2v_f a_f}{v_f^2 + a_f^2} = \frac{\varepsilon_{Lf}^2 - \varepsilon_{Rf}^2}{\varepsilon_{Lf}^2 + \varepsilon_{Rf}^2}\cdot \tag{54}$$

From the representation in terms of left- and right-handed couplings introduced earlier we see that A_f measures the normalized difference between left-handed and right-handed transition amplitudes. For A_{FB} we have

$$A_{FB}^{f\bar{f}}(M_Z^2) = \frac{3}{4} A_e A_f. \tag{55}$$

It is important to notice that

$$A_e = \frac{2\xi}{1+\xi^2} \text{ with } \xi = \frac{v_e}{a_e} = 1 - 4\sin^2\Theta_W$$

is a quantity which would vanish for $\sin^2\Theta_W = 0.25$. Since the experimental value for $\sin^2\Theta_W$ is about 0.23 A_e is unfortunately rather small. A small difference of large numbers is difficult to determine precisely. By universality A_e is the same for $\ell = e, \mu$ and τ and hence

$$A_{FB}^{\mu\bar{\mu}}(M_Z^2) = \frac{3}{4}A_e^2 \simeq 3\xi^2$$

Table 4. $e^+e^- \to f\bar{f}$ forward-backward asymmetry at the Z-peak for various values of $\sin^2\Theta_W$

$\sin^2\Theta_W$	0.22	0.23	0.24	0.25
ξ	0.12	0.08	0.04	0
A_e	0.237	0.159	0.0799	0
$A_{FB}^{\mu\bar{\mu}}$	0.0420	0.0190	0.0048	0
$A_{FB}^{c\bar{c}}$	0.1253	0.0802	0.0382	0
$A_{FB}^{b\bar{b}}$	0.1673	0.1117	0.0557	0

B. Final state polarization asymmetry

We only consider the integrated asymmetry

$$A_{\text{pol}}^f \doteq \frac{\sigma(e^+e^- \to f_L\bar{f}) - \sigma(e^+e^- \to f_R\bar{f})}{\sigma(e^+e^- \to f_L\bar{f}) + \sigma(e^+e^- \to f_R\bar{f})} \tag{56}$$

at the Z-resonance. Using the helicity amplitudes $|T_{h_i h_e}|^2$ we obtain:

$$A_{\text{pol}}^f(M_Z^2) = \frac{(\varepsilon_{Lf}^2 - \varepsilon_{Rf}^2)}{(\varepsilon_{Lf}^2 + \varepsilon_{Rf}^2)} = A_f \tag{57}$$

which is independent of the initial state couplings. This asymmetry cannot be measured for quarks which hadronize into hadron showers. The only case which can be investigated is the τ-polarization where it is possible to reconstruct the τ-polarization from the decays $\tau \to \pi\nu$, $\tau \to \rho\nu$ and $\tau \to a_1\nu$ with the subsequent decays $\rho \to \pi\pi$ and $a_1 \to \pi\pi\pi$. For $e^+e^- \to \tau^+\tau^-$ we have

$$A_{\text{pol}}^\tau(M_Z^2) = A_e = \frac{2\xi}{1+\xi^2} \tag{58}$$

which is linear in the vector coupling ξ. Some numerical values have been given in Table 4.

C. Polarized beams

With polarized beams one can measure a number of additional asymmetries:

a) Initial state transversal polarization asymmetry
(azimuthal asymmetry for natural polarization)

In the magnetic field of a ring collider the e^+-spins tend to line up with the magnetic field ($-y$-direction) such that a natural transverse polarization is set up. If we assume the electron to move in the z-direction we may write the e^+-polarization vector in the form

$$\vec{P}^{\pm} = \left(P_{\perp}^{\pm}\,\cos\varphi^{\pm}, P_{\perp}^{\pm}\sin\varphi^{\pm}, P_{L}^{\pm}\right)$$

where $P_{\perp}^{\pm}$ measures the transverse and $P_{L}^{\pm}$ the longitudinal degree of polarization. $\varphi^{\pm} = -\pi/2$ and $P_{L}^{\pm} = 0$ means natural polarization. If beams are transversely polarized one has an azimuthal asymmetry and one defines

$$A_{\perp} = \frac{4}{P_{\perp}^{+}P_{\perp}^{-}} \frac{\int d\Omega\,\cos 2\varphi \frac{d\sigma}{d\Omega}\left(e^{+}(P_{\perp}^{+}) + e^{-}(P_{\perp}^{-}) \to f\bar{f}\right)}{\int d\Omega \frac{d\sigma}{d\Omega}\left(e^{+}(P_{\perp}^{+}) + e^{-}(P_{\perp}^{-}) \to f\bar{f}\right)}\,. \tag{59}$$

We just give, without derivation, the result one obtains for $s = M_Z^2$:

$$A_{\perp}(M_Z^2) = \frac{v_e^2 - a_e^2}{v_e^2 + a_e^2} = -\frac{1-\xi^2}{1+\xi^2} \tag{60}$$

a quantity which is independent of the final state.

b) Initial state longitudinal polarization asymmetry

In this case, assuming longitudinally polarized beams, one measures the total cross section with left-handed and right-handed electrons separately and defines

$$A_{LR} = \frac{\sigma(e_L^- e^+ \to f\bar{f}) - \sigma(e_R^- e^+ \to f\bar{f})}{\sigma(e_L^- e^+ \to f\bar{f}) + \sigma(e_R^- e^+ \to f\bar{f})}\,. \tag{61}$$

At $s = M_Z^2$ one finds

$$A_{LR}(M_Z^2) = \frac{\varepsilon_{Le}^2 - \varepsilon_{Re}^2}{\varepsilon_{Le}^2 + \varepsilon_{Re}^2} = A_e \simeq 2\xi \tag{62}$$

for the integrated asymmetry.

The left-right asymmetry is a very important observable due to the following properties: It is

- a ratio of <u>total</u> cross sections
- independent of the final state [2]
- linear in ξ

The first property is very important since the notoriously large QED and QCD corrections are almost identical for left- and right-handed states and therefore drop out in the ratio almost completely. The second property implies that one can sum over all flavors gaining enormously in statistics. The third property tells us that A_{LR} is enhanced by a factor $2/(3\xi)$ relative to $A_{FB}^{\mu\bar{\mu}}$.

In addition the polarized forward-backward asymmetries can be measured:

$$A_{FB,\mathrm{pol}}^{f} = \frac{2}{P_L^{+} + P_L^{-}} \frac{(\int_0^1 - \int_{-1}^0) d\cos\theta \frac{d\sigma}{d\cos\theta}(P_L^{+} \neq 0) - (\int_0^1 - \int_{-1}^0) d\cos\theta \frac{d\sigma}{d\cos\theta}(P_L^{-} \neq 0)}{\int_{-1}^{+1} d\cos\theta \frac{d\sigma}{d\cos\theta}(P_L^{+} \neq 0) + \int_{-1}^{+1} d\cos\theta \frac{d\sigma}{d\cos\theta}(P_L^{-} \neq 0)} \tag{63}$$

[2] This is true only for the integrated asymmetry. The angular distributions $A_{LR}^{f}(\cos\theta)$ depend on the flavor f.

which on the Z-resonance yields:

$$A^f_{FB,\mathrm{pol}}(M_Z^2) = \frac{3}{4} A_f \tag{64}$$

3.4 Conclusions:

The measurement of asymmetries opens up the possibility to determine many independent observables. This is crucial for precision tests of the SM. Two points make asymmetries at the Z-peak very interesting. First, at the Z-peak very high rates of events are available which makes high precision tests possible. Second, at the Z-peak one is dealing almost purely with a weak NC process! No detailed clean tests of the NC were possible before LEP. The clean $\nu_\mu e$-scattering processes suffer from low rates and the deep inelastic $\nu_\mu N$-scattering data from hadronic uncertainties.

Longitudinally polarized beams are highly desired, since only in this case one has good observables that can test

$$A_f = \frac{2 v_f a_f}{v_f^2 + a_f^2}$$

for individual flavors to a good accuracy. This is an important supplement to the measurement of the partial widths which yields tests of

$$v_f^2 + a_f^2.$$

For precision tests it will be crucial to carefully analyse the following types of corrections:

i) QED corrections, bremsstrahlung;

ii) electroweak "non-QED" corrections;

iii) QCD corrections for hadronic final states;

iv) mass effects.

These corrections will be discussed in the following. Particularly interesting are the "non-QED" higher order corrections since they are the key in finding deviations from the SM at its quantum level.

4. RADIATIVE CORRECTIONS FOR PRECISION TESTS

4.1 Renormalization

For the calculation of higher order terms we must specify the renormalization procedure. We choose for the independent parameters the physical particle masses plus a coupling constant. A natural choice for the coupling is the universal (due to electromagnetic current conservation) fine structure constant α. This defines a QED-like on-shell renormalization scheme. All other couplings are then fixed (*dependent parameters*) by the mass-coupling relations:

$$\begin{aligned} \sin^2\Theta_W &= 1-\frac{M_W^2}{M_Z^2} \\ g=\frac{\sqrt{4\pi\alpha}}{\sin\Theta_W}\,, &\qquad g'=\frac{\sqrt{4\pi\alpha}}{\cos\Theta_W} \\ \sqrt{2}G_\mu &= \frac{1}{v^2}=\frac{\pi\alpha}{M_W^2\sin^2\Theta_W}. \end{aligned} \tag{65}$$

The renormalization then may be performed in two steps:

1. Parameter renormalization

The parameters in the true bare Lagrangian are the bare parameters $\alpha_b, M_{Wb}, \cdots$. We *reparametrize* the bare Lagrangian in terms of the physical parameters (experimental input) $\alpha, M_W, \cdots$ by the following parameter renormalizations:

$$\begin{aligned} M_{Vb}^2 &= M_V^2+\delta M_V^2 = M_V^2\,(1+\frac{\delta M_V^2}{M_V^2})\,; V=W,Z \\ \alpha_b &= \alpha+\delta\alpha=\alpha\,(1+\frac{\delta\alpha}{\alpha}) \end{aligned} \tag{66}$$

which have to be performed for the dependent parameters (which serve as convenient abbreviations only) correspondingly :

$$\begin{aligned} \sin^2\Theta_{Wb} &= \sin^2\Theta_W+\delta\sin^2\Theta_W=\sin^2\Theta_W\,(1+\frac{\delta\sin^2\Theta_W}{\sin^2\Theta_W}) \\ G_{\mu b} &= G_\mu+\delta G_\mu = G_\mu\,(1+\frac{\delta G_\mu}{G_\mu}) \end{aligned} \tag{67}$$

where, to *linear* order (suitable for one-loop calculations):

$$\begin{aligned} \frac{\delta\sin^2\Theta_W}{\sin^2\Theta_W} &= \cot^2\Theta_W(\frac{\delta M_Z^2}{M_Z^2}-\frac{\delta M_W^2}{M_W^2}) \\ \frac{\delta G_\mu}{G_\mu} &= 2\frac{\delta v^{-1}}{v^{-1}}=\frac{\delta\alpha}{\alpha}-\frac{\delta M_W^2}{M_W^2}-\frac{\delta\sin^2\Theta_W}{\sin^2\Theta_W}\,. \end{aligned} \tag{68}$$

It is important to notice that these parameter shifts do not alter the invariance properties of the Lagrangian. Since the bare parameters and the renormalized parameters (determined by S-matrix elements) both are gauge invariant the counterterms are gauge invariant.

2. Field renormalization (wave-function renormalization)

In order that the fields describe properly normalized scattering states we must renormalize them such that the residue of the propagator pole is *unity*.

For simplicity we ignore the *infrared problem* caused by soft photon effects. This problem has to be treated in the same way as in pure QED and we assume the reader to be familiar with it. We shall

use an infinitesimal photon mass m_γ as an infrared regulator at intermediate steps. For observable quantities the limit $m_\gamma \to 0$ must exist.

We then write for the physical fields:

$$\begin{aligned} V_{\mu\, b} &= \sqrt{Z_V} V_{\mu\, ren}\ ; \quad V = A, Z, W^\pm \\ \psi_{f\, b} &= \sqrt{Z_f}\psi_{f\, ren} \\ H_b &= \sqrt{Z_H} H_{ren} \end{aligned} \tag{69}$$

and the Z-factors are fixed by the condition that propagators of the renormalized fields have residue one at the pole. To leading order $Z_i = 1$ and we may write

$$Z_i = 1 + \delta Z_i\ ;\ \sqrt{Z_i} \simeq 1 + \frac{1}{2}\delta Z_i + \cdots\ . \tag{70}$$

The renormalization procedure for physical amplitudes may be summarized by the following simple rules: Performing the parameter shifts and the field renormalizations and expanding to linear order (appropriate for one-loop calculations), for the fermion-gauge boson vertices, we get the simple substitutions

$$\begin{aligned} eQ_f\gamma^\mu \quad &\to \quad eQ_f\gamma^\mu\left(1 + \tfrac{1}{2}\delta Z_\gamma + \delta Z_f + \tfrac{\delta e}{e}\right) \\ \tfrac{M_Z}{v}\gamma^\mu\left(T_{3f}(1-\gamma_5) - 2Q_f \sin^2\Theta_W\right) \quad &\to \quad \tfrac{M_Z}{v}\gamma^\mu\left(T_{3f}(1-\gamma_5) - 2Q_f\sin^2\Theta_W\left(1 + \tfrac{\delta\sin^2\Theta_W}{\sin^2\Theta_W}\right)\right) \\ &\qquad \left(1 + \tfrac{1}{2}\delta Z_Z + \delta Z_f + \tfrac{1}{2}\tfrac{\delta M_Z^2}{M_Z^2} + \tfrac{1}{2}\tfrac{\delta G_\mu}{G_\mu}\right) \\ \tfrac{M_W}{\sqrt{2}v}\gamma^\mu(1-\gamma_5) \quad &\to \quad \tfrac{M_W}{\sqrt{2}v}\gamma^\mu(1-\gamma_5) \\ &\qquad \left(1 + \tfrac{1}{2}\delta Z_W + \tfrac{1}{2}\delta Z_{f_1} + \tfrac{1}{2}\delta Z_{f_2} + \tfrac{1}{2}\tfrac{\delta M_W^2}{M_W^2} + \tfrac{1}{2}\tfrac{\delta G_\mu}{G_\mu}\right) \end{aligned}$$

and analogously for the other vertices.

The mass counterterms and the wave-function factors are determined by the transverse parts of the vector boson self-energies Π_V ($V = \gamma, Z, W$). In terms of the self-energies the propagators are given by

$$D_V^{\mu\nu}(k^2) = \frac{-ig^{\mu\nu}}{k^2 - M_{Vb} + \Pi_V(k^2)} + \cdots\ . \tag{71}$$

Since the $g^{\mu\nu}$-term determines the physical transverse part we need to consider this term only.

Strictly speaking, this is true for the W-propagator only. For the Z-propagator the situation is complicated by $\gamma - Z$-mixing. Due to mixing one cannot treat the Z and the γ propagators separately. They rather form a 2×2 -matrix propagator. The simplest way to treat this problem is to start from the inverse propagator given by the irreducible self-energies (sum of one-particle irreducible diagrams). Again we restrict ourselves to a discussion of the transverse part and we take out a trivial factor $-i\ g^{\mu\nu}$ in order to keep notation as simple as possible. With this convention we have for the inverse $\gamma - Z$-propagator the symmetric matrix [27]

$$\hat{D}^{-1} = \begin{pmatrix} k^2 + \Pi_{\gamma\gamma}(k^2) & \Pi_{\gamma Z}(k^2) \\ \Pi_{\gamma Z}(k^2) & k^2 - M_Z^2 + \Pi_{ZZ}(k^2) \end{pmatrix}\ .$$

Taking the inverse we obtain

$$D_{\gamma\gamma} = \frac{1}{k^2 + \Pi_{\gamma\gamma}(k^2) - \frac{\Pi_{\gamma Z}^2(k^2)}{k^2 - M_Z^2 + \Pi_{ZZ}(k^2)}} = \frac{1}{k^2 + \Pi_\gamma(k^2)}$$

$$
\begin{aligned}
D_{\gamma Z} &= \frac{-\Pi_{\gamma Z}(k^2)}{(k^2+\Pi_{\gamma\gamma}(k^2))(k^2-M_Z^2+\Pi_{ZZ}(k^2))-\Pi_{\gamma Z}^2(k^2)} \simeq \frac{-\Pi_{\gamma Z}(k^2)}{k^2\,(k^2-M_Z^2)} \\
D_{ZZ} &= \frac{1}{k^2-M_Z^2+\Pi_{ZZ}(k^2)-\frac{\Pi_{\gamma Z}^2(k^2)}{k^2+\Pi_{\gamma\gamma}(k^2)}} = \frac{1}{k^2-M_Z^2+\Pi_Z(k^2)}\ .
\end{aligned} \tag{72}
$$

These expressions sum correctly all the reducible diagrams. In the one-loop approximations we get $\Pi_V \simeq \Pi_{VV}$. The extra terms are higher order contributions. For precision physics at LEP1 they have to be taken into account. With the definition that Π_Z includes the quadratic γZ mixing term the Z propagator is renormalized in the same way as the W propagator.

Because the self-energy functions are quadratically divergent two subtractions (chosen on-shell) are needed such that the renormalized self-energy function reads

$$
\begin{aligned}
\Pi_{Vren}(k^2) &= \Pi_V(k^2)-\Pi_V(M_V^2)-(k^2-M_V^2)\,\frac{d\Pi_W}{dk^2}(M_V^2) \\
&\quad +\text{higher order terms}\ .
\end{aligned} \tag{73}
$$

The way the counterterms enter in the self-energies is determined from the transverse part of the free inverse propagator

$$
\begin{aligned}
-ig^{\mu\nu}\,(k^2-M_{Vb}^2) &\rightarrow -ig^{\mu\nu}\,Z_V\,(k^2-M_V^2-\delta M_V^2) \\
&= -ig^{\mu\nu}\,(k^2-M_V^2-\delta M_V^2+\delta Z_V\,(k^2-M_V^2)+\cdots)
\end{aligned}
$$

The renormalization conditions then imply that the transverse part of the renormalized self-energy

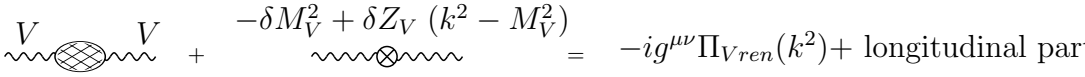

and its derivative vanish for $k^2 \rightarrow M_V^2$. This yields for the mass counterterm

$$
\delta M_V^2 = \text{Re}\ \Pi_V(M_V^2) \tag{74}
$$

(vanishes for the photon) and for the wave-function renormalization

$$
\delta Z_V = Z_V - 1 = -\text{Re}\,\frac{d\Pi_V}{dk^2}(M_V^2)\ . \tag{75}
$$

Since $V = Z, W$ are unstable particles Π_V has an imaginary part

$$
Im\ \Pi_V(k^2=M_V^2) \equiv M_V\,\Gamma_V \neq 0 \tag{76}
$$

which determines the width Γ_V.

The fermion propagators are renormalized in the same way as the electron propagator in QED. However unlike in QED the right-handed and left-handed fields are renormalized in a different way such that

$$
\delta Z_f = z_{vf} + z_{af}\gamma_5\ . \tag{77}
$$

Finally, we have to determine the counterterm for the electric charge.

The condition is that

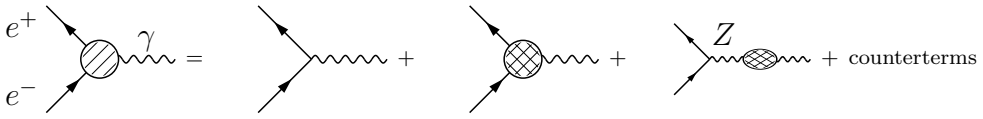

evaluated in the Thomson limit ($k^2 = 0$, $E_\gamma \to 0$) gives the renormalized charge e. Thus

$$\begin{aligned} - \quad & i\,e\left\{\gamma^\mu\left(1+\frac{\delta e}{e}+\frac{1}{2}\delta Z_\gamma + z_{ve} + A_1^{\gamma ee} - \frac{v_e}{2\sin\Theta_W\cos\Theta_W}\frac{\Pi_{\gamma Z}}{M_Z^2}\right.\right. \\ & \left.\left. +(z_{ae} + A_2^{\gamma ee} - \frac{a_e}{2\sin\Theta_W\cos\Theta_W}\frac{\Pi_{\gamma Z}}{M_Z^2})\gamma_5\right) - i\sigma^{\mu\alpha}\frac{k_\alpha}{2m_e}A_3^{\gamma ee}\right\} \\ \to \quad - \quad & ie\gamma^\mu \ \text{ in the Thomson limit} \end{aligned} \tag{78}$$

where $A_i^{\gamma ee}$ are vertex corrections and $\Pi_{\gamma Z}$ is the $\gamma - Z$ mixing term. From the electromagnetic Ward-Takahashi identity ($\partial_\mu j^\mu_{em} = 0$) some of the diagrams cancel. While in pure QED

$$\frac{\delta e}{e} = -\frac{1}{2}\delta Z_\gamma = \frac{1}{2}\Pi'_\gamma(0)\ .$$

In the Standard Model we find

$$\frac{\delta e}{e} = \frac{1}{2}\Pi'_\gamma(0) - \frac{1-4s_W^2}{4s_W c_W}\frac{\Pi_{\gamma Z}(0)}{M_Z^2} - A_1^{\gamma ee}(0) - z_{ve} = \frac{1}{2}\Pi'_\gamma(0) + 2Ks_W^2 L \tag{79}$$

where $K = \frac{\alpha}{4\pi s_W^2}$, $L = \ln\frac{M_W^2}{\mu^2}$. The last term is the non-abelian contribution from bosonic loops in the $\overline{MS}$ scheme [3] and the Feynman-'t Hooft gauge. [4] The fermionic contributions $\Pi^f_{\gamma Z}(0) = 0$ vanish at zero momentum transfer. By the e.m. Ward-Takahashi identity we have

$$A_2^{\gamma ee} + z_{ae} - \frac{1}{4s_W c_W}\frac{\Pi_{\gamma Z}(0)}{M_Z^2} = 0\ .$$

With δe, the mass counter-terms and the wave-function renormalization factors we have a complete set of counter-terms which renormalize all other divergent quantities. The Feynman diagrams for the vector boson self-energies are depicted in Fig. 6. Since the tadpoles drop out in renormalized quantities we will not consider them. The fermion self-energies are needed for the determination of the wave-function renormalization factors only. The diagrams for the fermion self-energies and the electromagnetic vertex are shown in Figs. 7 and 8, respectively.

[3] Using dimensional regularization, the bare (ultraviolet divergent) quantities exhibit poles in $\varepsilon = 4-d$ for $d \to 4$ space-time dimensions. In the $\overline{MS}$-scheme the poles are subtracted (together with some constants which accompany the pole term) such that

$$2/\varepsilon - \gamma + \ln 4\pi \to \ln\mu^2$$

with μ an arbitrary renormalization scale. γ is the Euler constant. For physical (renormalized) quantities the μ-dependent terms must cancel.

[4] In the general 't Hooft gauge the vector boson propagators have the form

$$D_V^{\mu\nu}(p,\xi) \equiv -i\left(g^{\mu\nu} - (1-\xi)\frac{p^\mu p^\nu}{p^2 - \xi M_V^2 + i\epsilon}\right)\frac{1}{p^2 - M_V^2 + i\epsilon}\ . \tag{80}$$

Physical quantities must be ξ-independent (gauge invariance). For $\xi = 1$ we have the 't Hooft-Feynman gauge where the propagators take a particularly simple form. For $\xi \to \infty$ the propagator becomes purely transverse. This is the physical (unitary) gauge, where Higgs and Faddeev-Popov ghost particles are absent.

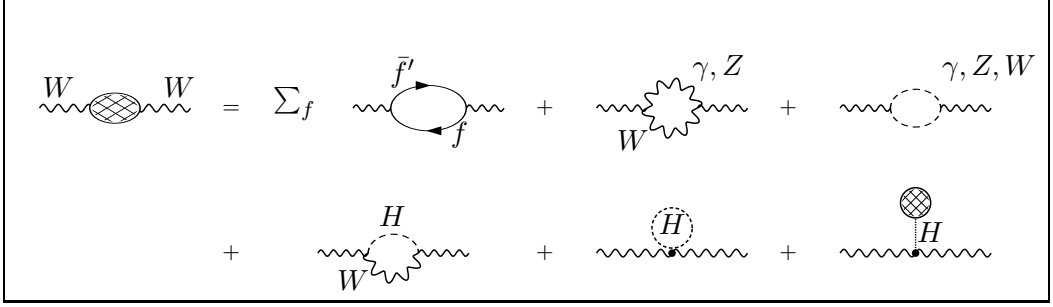

Figure 6a: W self-energy diagrams

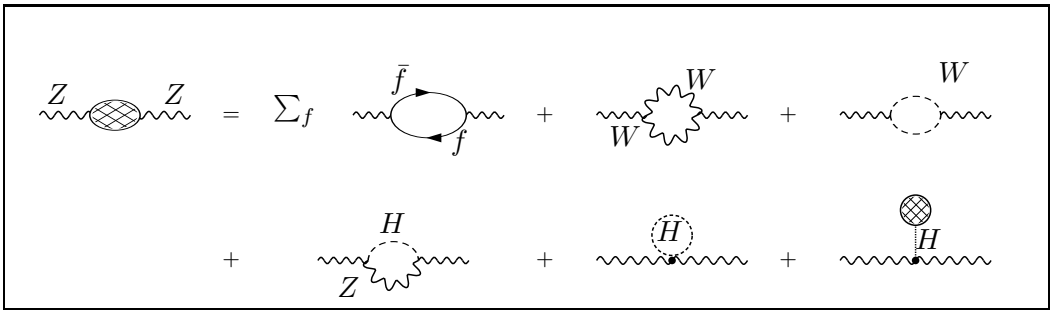

Figure 6b: Z self-energy diagrams

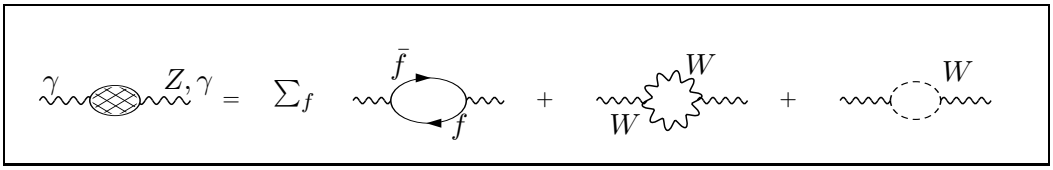

Figure 6c: γ and γZ self-energy diagrams

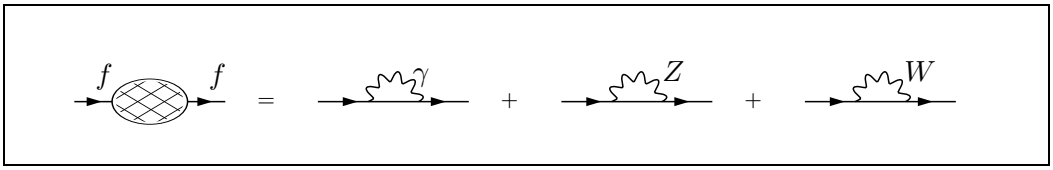

Figure 7: Fermion self-energy diagrams

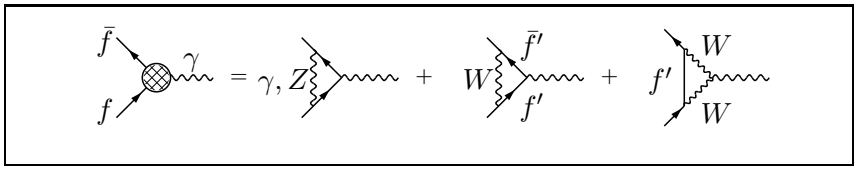

Figure 8: Electromagnetic vertex diagrams

4.2 μ-decay and the Mass-coupling Interdependence

By the relation (27) the parameters M_W, M_Z, α and G_μ are not independent. Here we calculate G_μ from α, M_W and M_Z (on-shell scheme):

$$G_\mu = \frac{\pi\alpha}{\sqrt{2}} \frac{1}{M_W^2 \ \sin^2\Theta_W} \frac{1}{1-\Delta r}$$

where $\Delta r \neq 0$ due to radiative corrections. Since the QED corrections have been included in the definition of G_μ already, we have to calculate the non-QED part of the μ decay transition amplitude

$$-4\frac{G_\mu}{\sqrt{2}} J_\mu^{(\mu)} J^{(e)\mu}$$

for $k^2 \simeq 0$. Here,

$$J_\mu^{(\mu)} = \bar{u}_{\nu_\mu} \left[\gamma_\mu \left(1-\gamma_5\right)\right] \ u_\mu, \quad J_\mu^{(e)} = \bar{u}_e \ \left[\gamma_\mu \left(1-\gamma_5\right)\right] \ v_{\nu_e}$$

denote the muon (μ) and the electron (e) charged current matrix elements where u and v are the external spinors. The different contributions are shown in Fig. 9.

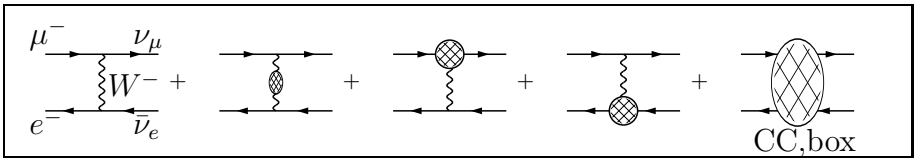

Figure 9a: Radiative corrections to μ-decay

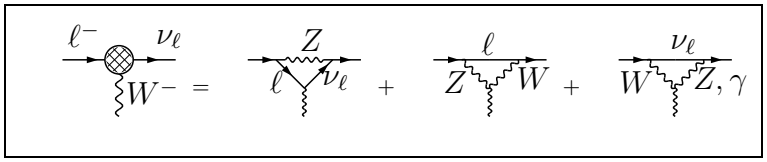

Figure 9b: CC vertex diagrams

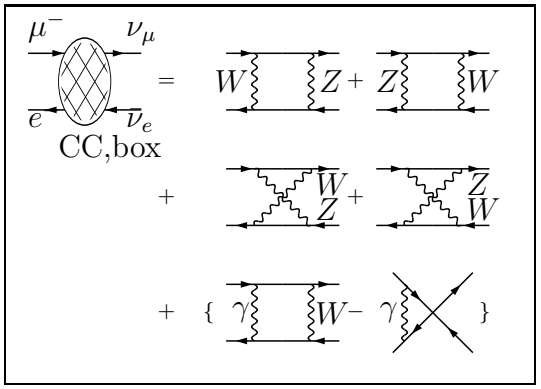

Figure 9c: CC box diagrams

At the tree level we read off

$$\frac{G_\mu}{\sqrt{2}} = \frac{e^2}{8M_W^2 \sin^2\Theta_W} = \frac{\pi\alpha}{M_W^2\left(1-\frac{M_W^2}{M_Z^2}\right)} \ .$$

Including the one-loop radiative corrections we distinguish among 1) propagator (self-energy) corrections, 2) vertex corrections and 3) box contributions. We will neglect terms proportional to the light fermion masses, since for $m_f \ll M_W$, they are numerically insignificant. This will lead to rather simple analytical expressions for the vertex and box contributions in the low energy limit.

Using the bare parameter relations (66-68) we get

$$\begin{aligned}
\frac{G_\mu}{\sqrt{2}} &= \frac{e_b^2}{8\sin^2\Theta_{Wb}M_{Wb}^2}\left\{1+\frac{\Pi_W(0)}{M_W^2}+\delta_{CC,vertex}+\delta_{CC,box}\right\} \\
&= \frac{e^2}{8\sin^2\Theta_W M_W^2}\left\{1+2\frac{\delta e}{e}-\frac{\cos^2\Theta_W}{\sin^2\Theta_W}\left(\frac{\delta M_Z^2}{M_Z^2}-\frac{\delta M_W^2}{M_W^2}\right)\right. \\
&\quad \left.-\frac{\delta M_W^2}{M_W^2}+\frac{\Pi_W(0)}{M_W^2}+\delta_{CC,vertex}+\delta_{CC,box}\right\} \\
&= \frac{\pi\alpha}{2\sin^2\Theta_W M_W^2}\{1+\Delta r\}
\end{aligned}$$

The vertex and box diagrams are depicted in Figs. 9b and 9c.

The important quantity Δr was first calculated by Sirlin [24]. We read off the formal one-loop result from the foregoing expression. Collecting the self-energy terms in Δr_{se} we may write [5]

$$\begin{aligned}
\Delta r &= \Delta r(\alpha, M_W, M_Z, m_H, m_f) \\
&= \Delta r_{se} + \Delta r_{vertex+box}\ . \qquad (81)
\end{aligned}$$

and denoting $s_W^2 = \sin^2\Theta_W$ and $c_W^2 = \cos^2\Theta_W$ we have

$$\Delta r_{vertex+box} = \frac{\alpha}{4\pi s_W^2}\left(6+\frac{7-4s_W^2}{2s_W^2}\ln c_W^2\right) \qquad (82)$$

which is the sum of the vertex, box and lepton wave-function contributions plus a γZ mixing term $2\frac{c_W}{s_W}\frac{\Pi_{\gamma Z}(0)}{M_Z^2}$, rendering the term ultraviolet-finite (in the 't Hooft-Feynman gauge) .

[5] Unlike the NC processes (at one-loop order), for the CC processes there is no natural separation into QED and "weak" part in the Standard Model. The QED corrections to μ decay are not ultraviolet finite and they do not form a gauge invariant subset . This is in contrast also to the QED corrections for this process if modeled by an effective Fermi interaction, which can be transformed into a NC form via a Fierz transformation. The only trouble is caused by the photonic box diagram. After subtraction of the photonic four-fermion vertex correction, which has been included by convention in the QED correction factor of (29), an ultraviolet divergent and gauge dependent contribution R_w, as indicated in Fig. 9c, is left over which has to be included in (82).

We then have

$$\Delta r_{vertex+box} = 2\left(\frac{\delta e}{e}\right)_{vertex} + \delta_{CC,vertex} + \delta_{CC,box} + 2\frac{c_W}{s_W}\frac{\Pi_{\gamma Z}(0)}{M_Z^2}$$

where

$$\begin{aligned}
2\left(\frac{\delta e}{e}\right)_{vertex} &= -2A_1^{\gamma ee} + \frac{4s_W^2-1}{2s_W c_W}\frac{\Pi_{\gamma Z}(0)}{M_Z^2} = K\cdot 4s_W^2 L \\
\delta_{CC,vertex} &= \left(A_L^{W\mu\nu_\mu} + A_L^{We\nu_e}\right) = -K\cdot 2\left\{\left(2+\frac{s_W^2}{2}\right)L + \left(\frac{1}{2}-\frac{3}{s_W^2}\right)c_W^2\ln c_W^2 + \left(\frac{s_W^2}{4}-3\right)\right\} \\
\delta_{CC,box} &= A_{LCC}^{box} = -K\cdot\frac{1}{2s_W^2}\left(-3+6c_W^2+2c_W^4\right)\ln c_W^2 + R_w
\end{aligned}$$

where $K = \frac{\alpha}{4\pi s_W^2}$, $L = \ln\frac{M_W^2}{\mu^2}$ and $R_w = K\cdot\frac{s_W^2}{2}\ (2L+1)$. The amplitudes $A_\cdot$ are normalized to the Born terms. We refer the reader to [28] for a more detailed discussion.

If we insert the expressions for the counter-terms and rewrite the result by splitting off the self-energies at $k^2 = 0$ as

$$\Pi(k^2) \equiv \Pi(0) + k^2\,\Pi'(k^2)$$

the self-energy contributions read:

$$\begin{aligned}
\Delta r_{se} &= \Pi'_\gamma(0) - \Pi'_\gamma(M_Z^2) \\
&\quad -\frac{\cos^2\Theta_W}{\sin^2\Theta_W}\left\{\frac{\Pi_Z(0)}{M_Z^2} - \frac{\Pi_W(0)}{M_W^2} + 2\frac{\sin\Theta_W}{\cos\Theta_W}\frac{\Pi_{\gamma Z}(0)}{M_Z^2}\right\} \\
&\quad -\Pi'_W(M_W^2) + \Pi'_\gamma(M_Z^2) + \frac{\cos\Theta_W}{\sin\Theta_W}\Pi'_{\gamma Z}(M_Z^2) \\
&\quad -\frac{\cos^2\Theta_W}{\sin^2\Theta_W}\left\{\Pi'_Z(M_Z^2) - \Pi'_W(M_W^2) + \frac{\sin\Theta_W}{\cos\Theta_W}\Pi'_{\gamma Z}(M_Z^2)\right\}
\end{aligned} \tag{83}$$

This is a representation of Δr_{se} in terms of the unrenormalized gauge boson self-energy functions. The form of this result exhibits the large (or potentially large) terms in Δr which we may write as

$$\Delta r = \Delta\alpha - \frac{\cos^2\Theta_W}{\sin^2\Theta_W}\Delta\rho + \Delta r_{rem} \tag{84}$$

where

$$\begin{aligned}
\Delta\alpha &= \Pi'_\gamma(0) - \Pi'_\gamma(M_Z^2) \\
\Delta\rho &= \frac{\Pi_Z(0)}{M_Z^2} - \frac{\Pi_W(0)}{M_W^2} + 2\frac{\sin\Theta_W}{\cos\Theta_W}\frac{\Pi_{\gamma Z}(0)}{M_Z^2}
\end{aligned} \tag{85}$$

are the large (due to fermion loop contributions) terms and Δr_{rem} is the remainder. Though the latter term is numerically smaller by one order of magnitude it is an interesting term which includes contributions from gauge boson self-couplings and Higgs-vector boson interactions. We are now going to discuss the various terms in (84) in some detail.

(i) $\Delta\alpha$

$\Delta\alpha$ is the photon vacuum polarization contribution which comes in through

$$\begin{aligned}
2\frac{\delta e}{e} &= \Pi'_\gamma(0) + \cdots \\
&= \Pi'_\gamma(0) - \Pi'_\gamma(M_Z^2) + \cdots + \Pi'_\gamma(M_Z^2) \\
&= \Delta\alpha + \cdots
\end{aligned}$$

and is large due to the large change in scale going from zero momentum (Thomson limit) to the Z-mass scale $\mu = M_Z$. Here, by zero momentum more precisely we mean the light fermion mass thresholds. The leading light fermion ($m_f \ll M_W$) contribution is given by

$$\Delta\alpha = \sum_f \quad \gamma \overset{f}{\underset{f}{\circlearrowleft}} \gamma$$

$$= \frac{\alpha}{3\pi}\sum_f Q_f^2 N_{cf}(\ln\frac{M_Z^2}{m_f^2} - \frac{5}{3}\,)$$

$$= \Delta\alpha_{\rm leptons} + \Delta\alpha^{(5)}_{\rm hadrons} + \Delta\alpha_{\rm top}\ . \tag{86}$$

Since the top quark is heavy we cannot use the light fermion approximation for it. A very heavy top in fact gives no contribution since

$$\Delta\alpha_{\rm top} \simeq -\frac{\alpha}{3\pi}\frac{4}{15}\frac{M_Z^2}{m_t^2} \to 0$$

when $m_t \gg M_Z$. A serious problem is the low energy contributions of the five light quarks u,d,s,c and b which cannot be reliably calculated using perturbative QCD. Fortunately one can evaluate this hadronic term $\Delta\alpha^{(5)}_{hadrons}$ from hadronic e^+e^-- annihilation data by using a dispersion relation. The relevant vacuum polarization amplitude satisfies the convergent dispersion relation

$$Re\Pi'_\gamma(s) - \Pi'_\gamma(0) = \frac{s}{\pi}Re\int_{s_0}^\infty ds'\frac{Im\Pi'_\gamma(s')}{s'(s'-s-i\varepsilon)}$$

and using the optical theorem (unitarity) one has

$$Im\Pi'_\gamma(s) = \frac{s}{e^2}\sigma_{tot}(e^+e^-\to\gamma^*\to{\rm hadrons})(s)\ .$$

In terms of the cross-section ratio

$$R(s) = \frac{\sigma_{tot}(e^+e^-\to\gamma^*\to{\rm hadrons})}{\sigma(e^+e^-\to\gamma^*\to\mu^+\mu^-)}\ ,$$

where $\sigma(e^+e^-\to\gamma^*\to\mu^+\mu^-) = \frac{4\pi\alpha^2}{3s}$ at tree level, we finally obtain

$$\Delta\alpha^{(5)}_{\rm hadrons}(M_Z^2) = -\frac{\alpha M_Z^2}{3\pi}Re\int_{4m_\pi^2}^\infty ds\frac{R(s)}{s(s-M_Z^2-i\varepsilon)}\ . \tag{87}$$

Using the experimental data for $R(s)$ up to $E_{cut} = 40$ GeV (for larger energies γZ mixing would complicate the analysis) and perturbative QCD for the high energy tail we get

$$\Delta\alpha^{(5)}_{\rm hadrons}(s) = 0.0282 \pm 0.0009 + 0.002980\cdot\{\ln(s/s_0) + 0.005696\cdot(s_0/s-1)\} \tag{88}$$

with $\sqrt{s_0} = 91.176$ GeV [29].

In the range 50 GeV $\le\sqrt{s}\le$ 200 GeV the above fit is "exact" as compared to the error. Alternatively, *this* result of the dispersion calculation can be reproduced by using perturbative QCD with the effective "quark masses"

$$\begin{array}{ll} m_u = 62\ {\rm MeV}, & m_d = 83\ {\rm MeV} \\ m_s = 215\ {\rm MeV}, & m_c = 1.5\ {\rm GeV} \\ m_b = 4.5\ {\rm GeV} & \end{array}$$

and a QCD correction factor $(1+\alpha_{s,eff}/\pi)$ with $\alpha_{s,eff}=0.133$. [6]

We should mention that a light fermion not only contributes to $\Delta\alpha$ but also to Δr_{rem}:

$$\Delta r^f_{rem} \simeq \frac{\alpha}{4\pi s_W^2}\,(1-\frac{c_W^2}{s_W^2})\,\frac{N_{cf}}{6}K_{QCD}\ln c_W^2.$$

This yields $\Delta r_{rem,leptons}\simeq 0.0015$ and $\Delta r^{(5)}_{rem,hadrons}\simeq 0.0040$.

Perturbative QCD corrections for light quarks (at some high energy scale) are taken care of by the factor $K_{QCD}=1+\delta_{QCD}$ given by

$$\delta_{QCD}=\frac{\alpha_s(M_Z^2)}{\pi}+1.405\,\left(\frac{\alpha_s(M_Z^2)}{\pi}\right)^2 \tag{89}$$

using [30]

$$\Lambda^{(5)}_{\overline{MS}}=200^{+200}_{-100}\ \text{MeV},\quad \text{corresponding to } \alpha_s(M_Z^2)=0.117\pm 0.01\ . \tag{90}$$

We first assume the top to be a "normal" not too heavy fermion and will discuss heavy top effects in a second step. If there would not exist heavy unknown particles, Δr would be determined by the following typical contributions ($m_t=60$ GeV, $m_H=100$ GeV):

$$\begin{aligned}
\Delta r_{leptons} &\simeq 0.0315{+}0.0015 = 0.0330\\
\Delta r_{hadrons} &\simeq 0.0282{+}0.0040 = 0.0322\pm 0.0009\\
\Delta r_{top} &\simeq 0.0025 \qquad (\text{depends on } m_t)\\
\Delta r_{bosons} &\simeq 0.0033 \qquad (\text{depends on } m_H)\ .
\end{aligned}$$

The term $\Delta r_{vertex+box}\simeq 0.0064$ is included in Δr_{bosons}. For the light fermions the individual contributions from $\Delta\alpha$ and Δr_{rem} are exhibited as a sum of two terms. The full analytic expression for a light top would be

$$\Delta r^{top}=\frac{\alpha}{3\pi}\frac{4}{3}\left(\ln\frac{M_Z^2}{m_t^2}-\frac{5}{3}\right)+\frac{\alpha}{16\pi s_W^2}\left(1-\frac{c_W^2}{s_W^2}\right)\ 2\ \ln c_W^2 \tag{91}$$

for $m_t \ll M_Z$.

Numerically the fermionic contributions dominate. The bosonic contributions are smaller by one order of magnitude but they are nevertheless non-negligible. The self-energy contributions are large and depend on unknown physics, like the top mass, the Higgs mass, on 4th family fermion masses etc. Next we consider what happens if the top is very heavy.

(ii) $\Delta\rho$

It was observed first by Veltman [31] that fermion doublets with large mass splittings give large non-decoupling contributions to $\Delta\rho$ (large weak isospin breaking effects). By now we know that the top quark is unexpectedly heavy , $m_t>89$ GeV, while $m_b\simeq 4.8$ GeV is rather light.

[6] *Warning*: Do not use these values for the quark masses for small spacelike momenta (as needed in Bhabha scattering). These would give wrong results.

The diagrams that give rise to leading doublet mass splitting effects are those which exhibit Wtb (CC) transitions and are quadratically divergent. The Ztt and Zbb (NC) vertices do not mix t and b and thus do not "feel" the mass splitting. In our case (μ decay) we are concerned only with the W self-energy diagram

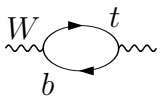

$$= \quad -\frac{\alpha}{4\pi}\frac{1}{4s_W^2}N_c\frac{m_t^2}{M_W^2}+\cdots$$

It yields a k^2-independent leading term which is (for dimensional reasons) quadratic in m_t. We thus obtain

$$\Delta\rho = \frac{\Pi_Z(0)}{M_Z^2} - \frac{\Pi_W(0)}{M_W^2} \simeq \frac{\alpha}{16\pi s_W^2}N_c\frac{m_t^2}{M_W^2}+\cdots \tag{92}$$

and this large contribution gets further *enhanced* in Δr

$$\Delta r|_{heavy} \quad = \quad -\frac{c_W^2}{s_M^2}\Delta\rho+\cdots$$

by an enhancement factor $\simeq 3.34$ for $s_W^2 = 0.23$.

The remainder also contains logarithmic terms which are not negligible numerically. A heavy top would give the contribution

$$\Delta r^{top} = -\frac{\sqrt{2}G_\mu M_W^2}{16\pi^2}\left\{3\frac{c_W^2}{s_W^2}\frac{m_t^2}{M_W^2}+2\left(\frac{c_W^2}{s_W^2}-\frac{1}{3}\right)\ln\frac{m_t^2}{M_W^2}+\frac{4}{3}\ln c_W^2+\frac{c_W^2}{s_W^2}-\frac{7}{9}\right\} . \tag{93}$$

Let us mention finally that whereas $\Delta\alpha$ will not be changed by unknown physics, $\Delta\rho$ is sensitive to all kinds of $SU(2)_L$ multiplets which directly couple to the gauge bosons and exhibit large mass-splittings.

(iii) Higgs contribution

The Higgs contributions deserve our special attention. In the light fermion approximation only the vector-boson self-energy diagrams

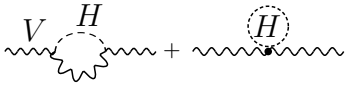

$$V = Z, W$$

contribute. At one-loop order there is no quadratic Higgs mass dependence in $\Delta\rho$ and in Δr. The leading heavy Higgs contributions

$$\begin{aligned}\Delta\rho^{Higgs} &\simeq -\frac{\sqrt{2}G_\mu M_W^2}{16\pi^2}\frac{s_W^2}{c_W^2}\left\{3\,(\ln\frac{m_H^2}{M_W^2}-\frac{5}{6}\,)\right\}\\ \Delta r^{Higgs} &\simeq \frac{\sqrt{2}G_\mu M_W^2}{16\pi^2}\left\{\frac{11}{3}(\ln\frac{m_H^2}{M_W^2}-\frac{5}{6}\,)\right\} \quad (m_H \gg M_W).\end{aligned} \tag{94}$$

are logarithmic.[7] This is due to the accidental global $SU(2)$ symmetry of the Higgs sector in the minimal Standard Model, which implies $\rho = 1$ at tree level (Veltman screening) [35]. More precisely, the theorem states that for vanishing fermion masses quadratic terms are absent. Furthermore, in $\Delta\rho$ also the logarithmic term disappears in the limit of vanishing $U(1)_Y$ coupling g'. The

[7]The two-loop contributions to $\Delta\rho$ and the mass-shifts ΔM_W and ΔM_Z have been computed in Refs. [32] and [33], respectively. The corresponding contribution to Δr can be obtained easily by using the relation (see Eq. (3.8)

logarithmic term in the low energy observable $\Delta\rho$ is a consequence of the weak isospin breaking by hypercharge. On the other hand, in Δr the coefficient of the logarithm does not depend on g'. Next we have to include the leading higher order effects.

(iv) Summation of leading higher order effects

Our one-loop calculation gave us the $O(\alpha)$ result

$$\sqrt{2}G_\mu = \frac{\pi\alpha}{\sin^2\Theta_W M_W^2}\,(1+\Delta r)\;.$$

Typically we get $\Delta r \simeq 0.07$ for M_Z=91 GeV, m_t=60 GeV and m_H=100 GeV. For the next order term we expect a contribution of the order $\Delta r^2 \simeq 0.005$. This would yield a shift in the prediction of the W mass (in terms of α, G_μ and M_Z) of $\delta M_W \simeq 190$ MeV. Since M_W will be measured with an accuracy of $\delta M_W \simeq 70$ MeV at LEP2, the $O(\alpha)$ result is insufficient for LEP experiments and we have to think about how to include the leading higher order terms.

a. Summation of leading logarithms.

The summation of leading logarithms is governed by the renormalization group. Since, in our case, the leading logs showed up in the QED vacuum polarization only, the leading log summation may be understood as the solution of the renormalization group equation for the $U(1)_{em}$ coupling constant (μ = renormalization scale)

$$\mu^2\frac{\partial}{\partial\mu^2}\alpha(\mu^2) = \frac{\beta(\alpha)}{2} = \frac{\alpha^2(\mu^2)}{3\pi}\sum_{m_f<\mu} N_{cf}Q_f^2$$

yielding the effective fine structure constant at scale M_Z

$$\alpha(M_Z) = \frac{\alpha}{1-\Delta\alpha} \tag{95}$$

where

$$\Delta r \simeq \Delta\alpha \simeq \frac{\alpha}{3\pi}\sum_{m_f<M_Z} N_{cf}Q_f^2\ln\frac{M_Z^2}{m_f^2}$$

---

of Ref. [29])

$$\Delta r = \frac{\Delta M_W^2}{M_W^2} + \frac{c_W^2}{s_W^2}\left(\frac{\Delta M_Z^2}{M_Z^2} - \frac{\Delta M_W^2}{M_W^2} - \Delta\rho\right)\;.$$

The results are

$$\begin{aligned}
\Delta\rho^{(2)Higgs} &= \left(\frac{\alpha}{4\pi s_W^2}\right)^2\frac{1}{8}\frac{s_W^2}{c_W^2}\frac{m_H^2}{c_W^2 M_Z^2}\left\{-9\sqrt{3}C\ell_2(\tfrac{\pi}{3}) - \frac{21}{8} + \frac{9\pi\sqrt{3}}{4} + \frac{3\pi^2}{4}\right\}\\
&\simeq 0.001\times\left(\frac{m_H}{4.74\ \mathrm{TeV}}\right)^2\\
\Delta r^{(2)Higgs} &= \left(\frac{\alpha}{4\pi s_W^2}\right)^2\frac{1}{8}\frac{m_H^2}{c_W^2 M_Z^2}\left\{9\sqrt{3}C\ell_2(\tfrac{\pi}{3}) + \frac{49}{72} + s_W^2 - \frac{11\pi\sqrt{3}}{4} - \frac{25\pi^2}{108}\right\}\\
&\simeq -0.001\times\left(\frac{m_H}{3.94\ \mathrm{TeV}}\right)^2
\end{aligned}$$

The result for Δr differs by the s_W^2 term from that given in Ref. [34]. Our result is smaller by roughly a factor 1.5 . $C\ell_2$ is the Clausen function and $9\sqrt{3}C\ell_2(\frac{\pi}{3})$=0.58597681. The numerical values are given for $\sin^2\Theta_W = 0.23$. Since $\Gamma_H > m_H$ for $m_H \gtrsim 1.3$ GeV [27] these perturbative results are sensible only for Higgs masses below 1.3 TeV. In this region the contributions are negligibly small.

in this approximation. Thus Eq. (27) obtained from our one-loop result by the substitution

$$1 + \Delta r \to \frac{1}{1 - \Delta r}$$

represents the resummation of all powers of $(\alpha \ln \frac{M_Z^2}{m_f^2})$. It is important to notice that the leading log summation is scheme independent. This can be seen by writing, in leading log approximation,

$$\Delta\alpha^{-1} = \frac{1}{\alpha(0)} - \frac{1}{\alpha(\mu^2)} = \frac{1}{3\pi} \sum_{m_f < \mu} N_{cf} Q_f^2 \ln \frac{\mu^2}{m_f^2} \; ; \; \mu \leq M_W$$

exhibiting that the r.h.s is independent of the electroweak couplings and hence of the parametrization used.

Including non-leading log terms we observe that the substitution

$$1 + \Delta r = 1 + \Delta\alpha + \Delta r_w \to \frac{1}{1 - \Delta\alpha - \Delta r_w} = \frac{1}{1 - \Delta r}$$

is in fact correct only if Δr_w is small, which is the case only if the top is light. As a next step we have to investigate what happens if $\Delta\rho$ is large.

b. Summation of large $\Delta\rho$ terms.

A careful analysis of the resummation of large $\Delta\rho$ terms [36] shows that Eq. (27) gets modified into

$$G_\mu = \frac{\pi\alpha}{\sqrt{2} M_W^2 \sin^2\Theta_W} \left\{ \frac{1}{1 - \Delta\alpha} \frac{1}{1 + \frac{\cos^2\Theta_W}{\sin^2\Theta_W} (\Delta\rho)_{irr}} + \Delta r_{rem} \right\} . \tag{96}$$

Here, $(\Delta\rho)_{irr}$ represents the leading irreducible contribution to the ρ parameter defined from the ratio of neutral current to charged current amplitudes at low energy, calculated in Ref. [37], i.e.

$$\frac{G_{NC}(0)}{G_{CC}(0)} = \rho = 1 + (\Delta\rho)_{irr} + (\Delta\rho)_{irr}^2 + \cdots = \frac{1}{1 - (\Delta\rho)_{irr}}. \tag{97}$$

It is important to note that, in contrast to $\Delta\alpha$, which is not significantly modified by the inclusion of two loop irreducible contributions,

$$\Delta\alpha^{(1)}_{leptons} \to (1 + \frac{3\alpha}{4\pi}) \Delta\alpha^{(1)}_{leptons}$$

where $\Delta\alpha^{(1)}_{leptons}$ is the one-loop lepton contribution to $\Delta\alpha$, ρ as defined in Eq. (97), can differ sizably from the one loop result. In fact as shown in Ref. [36], by including the two loop irreducible terms calculated in Ref. [37], one finds

$$(\Delta\rho)_{irr} = N_{cf} x_f [1 - (2\pi^2 - 19) x_f + \cdots] \tag{98}$$

with

$$x_f = \frac{\Delta m_f^2}{8\pi^2} \frac{G_\mu}{\sqrt{2}} .$$

This means that low energy physics is not sensitive to the *bare* mass splitting (Δm_f^2), but rather to the effective quantity

$$(\Delta m_f^2)_{eff} = \Delta m_f^2 \left\{ 1 - (2\pi^2 - 19) \frac{\Delta m_f^2 G_\mu}{8\pi^2 \sqrt{2}} \right\} .$$

The screening effects due to the Yukawa coupling with the scalar sector, may become large for a large mass splitting. This phenomenon, if confirmed from a closer inspection of the higher order terms in the perturbative expansion, may have far reaching consequences (possible restoration of decoupling) for our understanding of the Standard Model.

If we take the result of the full one loop calculation and include correctly the $\Delta\alpha$ and $\Delta\rho$ effects, resummed to all orders, we arrive at the final expression

$$M_W^2 = \frac{\rho M_Z^2}{2}\,(1+\sqrt{1-\frac{4A_0^2}{\rho M_Z^2}\,(\frac{1}{1-\Delta\alpha}+\Delta r_{rem})}\;). \tag{99}$$

Non-leading one-loop self-energy effects can be included by using Eq.(99) together with the replacements [36,38] (combining the 1st and 3rd line and the 2nd and 4th line of Eq. (83), respectively):

$$\begin{aligned}\Delta\alpha &\rightarrow \Delta e = \Pi'_\gamma(0) - \Pi'_W(M_W^2) + \frac{c_W}{s_W}\,\Pi'_{\gamma Z}(M_Z^2)\\ \Delta\rho &\rightarrow \Delta\hat{\rho} = \frac{\Pi_Z(M_Z^2)}{M_Z^2} - \frac{\Pi_W(M_W^2)}{M_W^2} + \frac{s_W}{c_W}\frac{\Pi_{\gamma Z}(M_Z^2)+\Pi_{\gamma Z}(0)}{M_Z^2}\,,\end{aligned} \tag{100}$$

where Π_Z includes γZ mixing terms as given in Eq. (71). Notice that Δe must be calculated in terms of α and the masses, while $\Delta\hat{\rho}$ must be calculated in terms of G_μ and the masses. We have checked that the above substitution reproduces correctly all self-energy terms up to $O(\alpha^2)$. Such a resummation could make sense for the fermion contributions, which form a gauge invariant subset. However, since terms like the irreducible contribution proportional to $\frac{\alpha}{4\pi}\sqrt{2}G_\mu m_t^2\ln(m_t^2/M_Z^2)$ are unknown, non-leading terms and the vertex and box corrections (contributing to Eq.(27)) should be added perturbatively, i.e. included in Δr_{rem}.

(v) Applications

Once Δr is given the W mass can be predicted by using the values of α, G_μ and M_Z from LEP1. According to Eqs. (27) and (28) we obtain

$$M_W^2 = \frac{M_Z^2}{2}\,(1+\sqrt{1-\frac{4A_0^2}{M_Z^2}\frac{1}{1-\Delta r}}\;) \tag{101}$$

and, equivalently,

$$\sin^2\Theta_W = \frac{1}{2}\,(1-\sqrt{1-\frac{4A_0^2}{M_Z^2}\frac{1}{1-\Delta r}}\;). \tag{102}$$

with

$$A_0 = (\frac{\pi\alpha}{\sqrt{2}G_\mu})^{1/2} = 37.2802(3)\quad GeV. \tag{103}$$

Explicit expressions for the various quantities which have been mentioned in this section can be found in Refs. [24,28]. Numerical results are given in Tab. 5. In Fig. 10 the m_t-dependence of Δr is shown for various Higgs masses. The W mass measurement is equivalent to a determination of

$$\Delta r = 1 - \frac{\pi\alpha}{\sqrt{2}G_\mu}\frac{1}{M_Z^2\frac{M_W^2}{M_Z^2}\,(1-\frac{M_W^2}{M_Z^2})}. \tag{104}$$

Using the experimental values (30-32) for M_Z and M_W, Δr is determined fairly well and since Δr is strongly dependent on the top mass we can use the results to find a direct constraint on the

top mass. Within one standard deviation we read off from Fig. 10 (the second uncertainty in m_t comes from the change of m_H)

$$\Delta r = 0.046^{+0.018}_{-0.019} \quad \Leftrightarrow \quad m_t = 136^{+47+21}_{-57-5} \ \text{GeV} \tag{105}$$

assuming $m_H \leq 1$ TeV. We notice that the direct lower limit $m_t > 89$ GeV is stronger than the indirect one obtained here.

In future one expects to be able to achieve a precision of $\delta M_W = 70$ MeV at LEP2. An accuracy $\delta M_W = 100$ MeV possibly may be achieved by combining the hadron collider results from CDF and D0 by the end of 1995 with an integrated luminosity of about $70 pb^{-1}$ [4]. This corresponds to an error in Δr of $\delta \Delta r = 0.0056$, and using $\frac{\delta m_t}{m_t} = -\frac{1}{2}\frac{\delta \Delta r}{\Delta r}$ this would determine m_t to an accuracy better than $\delta m_t = 10$ GeV. Of course we are waiting for the direct discovery of the top which should be within reach in the next few years at the Tevatron.

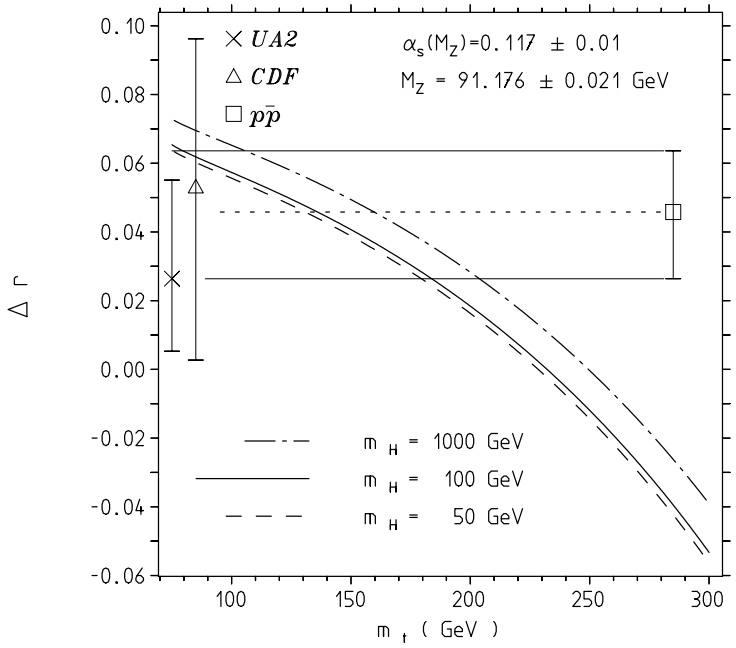

Figure 10: Δr as a function of the top mass for various m_H

Table 5. Prediction of M_W and related parameters ($M_Z = 91.176$ GeV, $\alpha_s = 0.117$). Masses in GeV. $\sin^2\Theta_e$, $\sin^2\Theta_b$ and $\sin^2\bar{\Theta}$ will be considered below.

m_t	m_H	M_W	Δr	$\sin^2\Theta_W$	$\sin^2\Theta_e$	$\sin^2\Theta_b$	$\sin^2\bar{\Theta}$
90	100	79.928	0.06032	0.2315	0.2334	0.2335	0.2326
110	100	80.037	0.05430	0.2294	0.2329	0.2333	0.2322
130	50	81.182	0.04607	0.2266	0.2321	0.2328	0.2313
130	100	80.151	0.04786	0.2272	0.2324	0.2330	0.2316
130	1000	80.002	0.05623	0.2301	0.2334	0.2341	0.2327
150	100	80.275	0.04068	0.2248	0.2318	0.2328	0.2310
200	100	80.642	0.01840	0.2177	0.2299	0.2321	0.2292
230	100	80.905	0.00133	0.2126	0.2286	0.2315	0.2278

4.3 Effective Couplings at the Z Resonance

In this section, for simplicity, we concentrate on LEP1 observables directly related to the NC process $e^+e^- \to f\bar{f}$ near the Z peak. Radiative corrections for this process have been calculated by many groups [39,40]. The diagrams for the one-loop corrections are depicted in Figure 11.

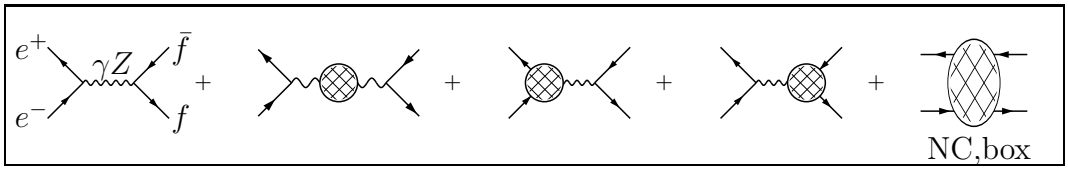

Figure 11a: Radiative corrections to $e^+e^- \to f\bar{f}$

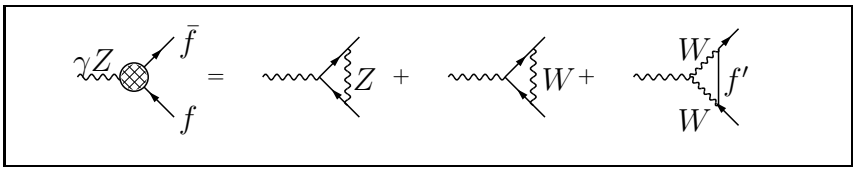

Figure 11b: NC vertex diagrams

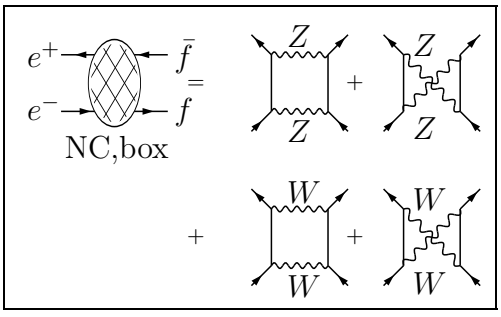

Figure 11c: NC box diagrams

Because of the factorization of the non-QED corrections at the resonance, the *weak* corrections

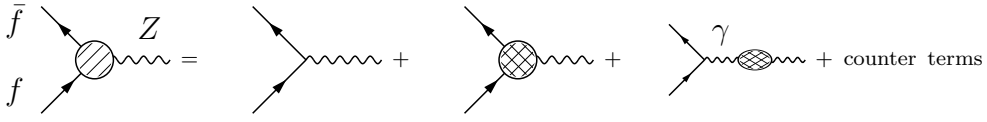

can be cast into an overall renormalization of the $Zf\bar{f}$ vertex

$$(\sqrt{2}G_\mu)^{1/2} M_Z \gamma^\mu (-2Q_f \sin^2\Theta_W + (1-\gamma_5)T_{3f})$$

by $\rho_f^{1/2}$ and a renormalization of $\sin^2\Theta_W$ in the NC vector-coupling [41]:

$$\begin{aligned} G_\mu &\rightarrow \rho_f G_\mu \\ \sin^2\Theta_W &\rightarrow \kappa_f \sin^2\Theta_W, \end{aligned} \tag{106}$$

where $\rho_f = 1 + \Delta\rho_{se} + \Delta\rho_{f,vertex}$ and $\kappa_f = 1 + \Delta\kappa_{se} + \Delta\kappa_{f,vertex}$.[8] In terms of the corrections δv_f and δa_f of the vector and axial vector couplings we have

$$\Delta\rho_f = 2\frac{\delta a_f}{a_f}, \quad \Delta\kappa_f = \frac{a_f\delta v_f - v_f \delta a_f}{a_f(v_f - a_f)} = \frac{a_f\delta v_f - v_f\delta a_f}{-2Q_f a_f \sin^2\Theta_W} \ .$$

The potentially large self-energy (se) contributions are universal. The analogues of Eq. (84) for $\Delta\rho$ and $\Delta\kappa$ read

$$\begin{aligned} \Delta\rho_{se} &= \Delta\bar{\rho} = \Delta\rho + \Delta\rho_{se,rem} \\ \Delta\kappa_{se} &= \Delta\bar{\kappa} = \frac{c_W^2}{s_W^2}\Delta\rho + \Delta\kappa_{se,rem} = \frac{c_W^2}{s_W^2}\Delta\hat{\rho} \end{aligned} \tag{108}$$

with $\Delta\rho$ and $\Delta\hat{\rho}$ defined in Eqs. (85) and (100), respectively. The self-energy terms are given by

$$\Delta\rho_{se,rem} = \Delta_Z = \frac{\Pi_Z(M_Z^2)}{M_Z^2} - \frac{\Pi_Z(0)}{M_Z^2} - \left(\frac{d\Pi_Z}{dq^2}\right)(M_Z^2) \ . \tag{109}$$

The vertex contributions are (if $f \neq b$) relatively small (but not negligible) and flavor dependent. We may define effective $\sin^2\Theta$'s by

$$\sin^2\Theta_f = \kappa_f \sin^2\Theta_W = \tilde{\kappa}_f \tilde{s}^2 \tag{110}$$

[8] The explicit expressions for the light fermion vertex corrections are [42]

$$\begin{aligned} \Delta\rho_{f,vertex} &= \frac{\sqrt{2}G_\mu M_Z^2}{16\pi^2}\left\{2(3v_f^2 + a_f^2)\Lambda_2(s,M_Z)\right. \\ &\quad \left. -4c_W^2(1-2(1-|Q_f|)s_W^2)\Lambda_2(s,M_W) + 24c_W^4\Lambda_3(s,M_W)\right\} - \Delta r_{vertex+box} \\ \Delta\kappa_{f,vertex} &= \frac{\sqrt{2}G_\mu M_Z^2}{16\pi^2}\left\{-(1-4|Q_f|s_W^2)(1-2|Q_f|s_W^2)\Lambda_2(s,M_Z)\right. \\ &\quad \left. +2c_W^2(1-2(1-|Q_f|)s_W^2)\Lambda_2(s,M_W) - 12c_W^4\Lambda_3(s,M_W)\right\} \end{aligned} \tag{107}$$

where $\Delta r_{vertex+box}$ is given by Eq. (82) and comes in through the $\alpha \rightarrow G_\mu$ replacement used here. The functions $\Lambda_i(s,M)$ are given ($y = M^2/s$ with $M = M_Z$ or M_W, $s > 0$)

$$\begin{aligned} \Lambda_2(s,M) &= -\frac{7}{2} - 2y - (2y+3)\ln(y) \\ &\quad +2(1+y)^2\left[\ln(y)\ln(\frac{1+y}{y}) - Sp(-\frac{1}{y})\right] \\ &\quad -i\pi\left[3 + 2y - 2(y+1)^2\ln\left(\frac{1+y}{y}\right)\right] \\ \Lambda_3(s,M) &= \frac{5}{6} - \frac{2y}{3} + \frac{2}{3}(2y+1)\sqrt{4y-1}\arctan\frac{1}{\sqrt{4y-1}} \\ &\quad -\frac{8}{3}y(y+2)\left(\arctan\frac{1}{\sqrt{4y-1}}\right)^2. \end{aligned}$$

where the formula for Λ_3 is valid for $s < 4M^2$ only. The Spence function is defined by $Sp(x) = -\int_0^1 \frac{dt}{t}\ln(1-xt)$. For f=b the expressions are more complicated and may be found in Ref. [43].

where

$$\tilde{s}^2 = \sin^2\tilde{\Theta} = \frac{1}{2}\,(1 - \sqrt{1 - 4A_0^2/M_Z^2}\,) = 0.2122(1) \tag{111}$$

is the lowest order $\sin^2\Theta$ in terms of α, G_μ and M_Z. We have

$$\tilde{\kappa}_f = \kappa_f + \frac{\tilde{c}^2}{\tilde{c}^2 - \tilde{s}^2}\Delta r = \frac{\tilde{c}^2}{\tilde{c}^2 - \tilde{s}^2}\Delta r_f \tag{112}$$

and, generalizing Eq. (104),

$$\sqrt{2}G_\mu M_Z^2\,\cos^2\Theta_f \sin^2\Theta_f = \frac{\pi\alpha}{(1-\Delta r_f)}\;\;;\;\;\Delta r_f \;\;=\;\; \Delta r + \frac{\tilde{c}^2 - \tilde{s}^2}{\tilde{c}^2}\Delta\kappa_f\;\;. \tag{113}$$

Using Eqs. (84) and (107) we obtain

$$\Delta r_f = \Delta\alpha - \Delta\rho + \Delta r_{f,rem}\;\;. \tag{114}$$

and we may calculate

$$\sin^2\Theta_f \;\;=\;\; \kappa_f \sin^2\Theta_W = \frac{1}{2}(1 - \sqrt{1 - \frac{4A_0^2}{M_Z^2}\frac{1}{1-\Delta r_f}}\,) \tag{115}$$

which compares to Eq. (102).

Comparing Eq. (114) with Eq. (84), we notice that the LEP1 versions Δr_f and $\sin^2\Theta_f$ of Δr and $\sin^2\Theta_W$ (obtained from the W-mass measurement) are by a factor $c_W^2/s_W^2 \simeq 3.3$ less sensitive to heavy particle effects (see Fig. 14 below). But in both cases it is the same quantity , namely $\Delta\rho$, which is measured.

Figures 14 and 15 exhibit the different behavior as a function of m_t.

Also, one finds that the sensitive to a heavy Higgs is lower by a factor $(1 + 9s_W^2)/(11c_W^2) \simeq 2.8$. This does not mean that LEP1 experiments are less suitable to get important information on heavy physics, however. Thanks to the higher statistics of LEP1 experiments, LEP1 observables are measured with higher precision. Furthermore, the relative sensitivity to the Higgs is higher at LEP1, a welcome fact, since the Higgs remains "the big unknown" in the Standard Model.

From the measured effective $\sin^2\Theta_i$'s we may evaluate

$$\Delta r_i^{exp} = 1 - \frac{\pi\alpha}{\sqrt{2}G_\mu M_Z^2}\frac{1}{\sin^2\Theta_i^{exp}\cos^2\Theta_i^{exp}}. \tag{116}$$

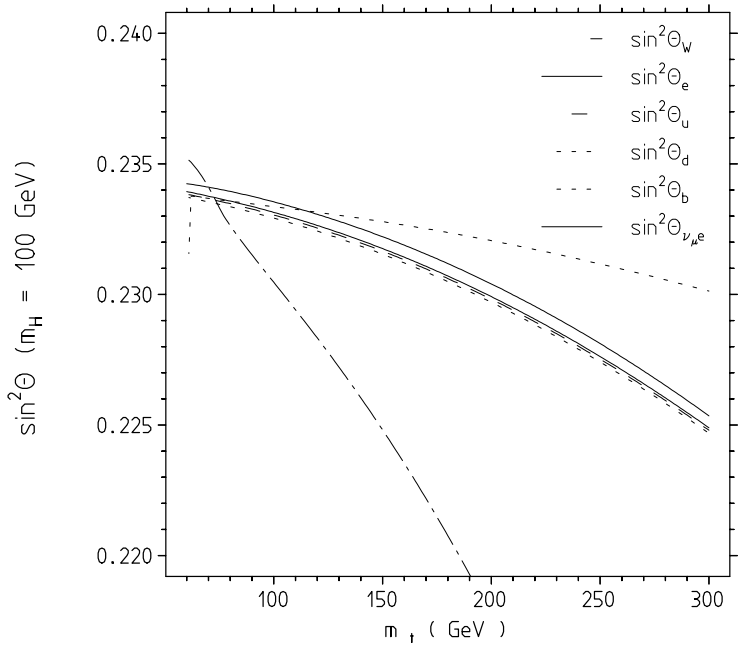

Figure 14: Flavor dependence of effective $\sin^2\Theta$'s.

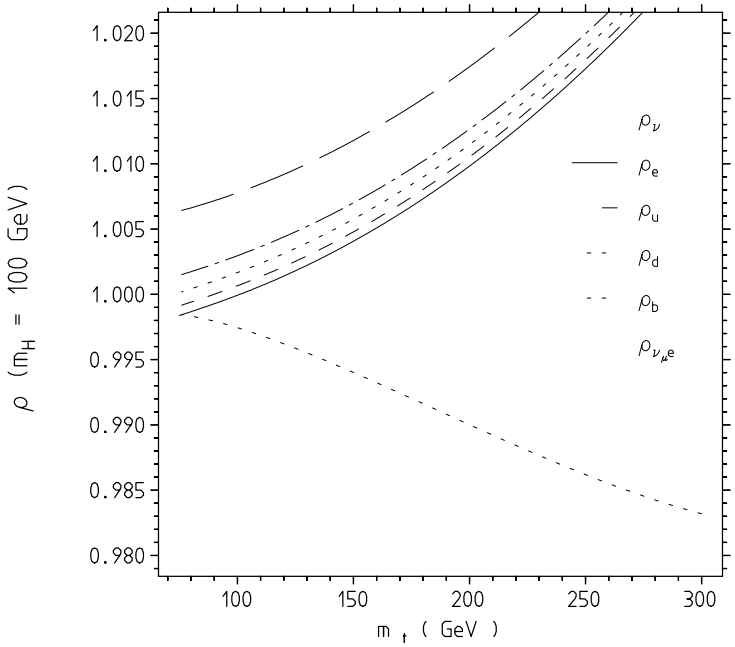

Figure 15: Flavor dependence of effective ρ's.

The values for $\sin^2\Theta_f^{exp}$ can be obtained, using the tree level formulae, from the on-resonance asymmetries which have been corrected for QED effects, experimental cuts and detector efficiencies. For example, from the experimental left-right asymmetry we get

$$\sin^2\Theta_e^{exp} = \sin^2\Theta_{LR} = \frac{A_{LR} - 1 + \sqrt{1 - A_{LR}^2}}{4A_{LR}}, \tag{117}$$

which confronts with the theoretical prediction Eq. (115). The last equation may also be used to

determine $\sin^2\Theta_e^{exp}$ from the forward-backward asymmetry $A_{FB}^{\mu^+\mu^-}$ if we identify

$$A_{LR} = \sqrt{\frac{4}{3}A_{FB}^{\mu^+\mu^-}} \ .$$

The weak mixing parameter most precisely measured at LEP is

$$\sin^2\Theta_e(M_Z^2) = 0.2302 \pm 0.0025 \quad \Leftrightarrow \quad m_t = 196^{+54+24}_{-76-16}\ \text{GeV} \ . \tag{118}$$

We see that the m_t-bound is weaker than the one obtained from the hadron collider results. The smaller error cannot yet compensate for the weaker m_t-dependence of $\sin^2\Theta_e$ in comparison to $\sin^2\Theta_W$. While this measurement does not improve the upper limit, it does improve the lower limit to $m_t > 104$ GeV. LEP has dramatically improved the precision of the leptonic Z couplings

Particle Data 90 [17]	LEP 90 [1]
g_V^e = -0.045 ± 0.022	-0.037 ± 0.005
g_A^e = -0.513 ± 0.025	-0.501 ± 0.003

Since $g_A^e = -\sqrt{\rho_e}/2$ and $g_V^e/g_A^e = 1 - 4\,(1+\Delta\tilde{\kappa}_e)\,\tilde{s}^2 = 1 - 4\sin^2\Theta_e$ we obtain

$$\Delta\rho_e = 0.002 \pm 0.006 \ , \ \ \Delta\tilde{\kappa}_e = 0.126 \pm 0.048 \ , \ \ \sin^2\Theta_e = 0.2315 \pm 0.0027 \ .$$

Due to virtual b-t transitions in the $Zb\bar{b}$ vertex

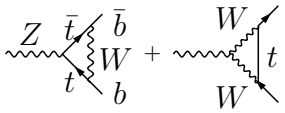

one finds large vertex corrections from a heavy top quark, given by [41]

$$\begin{aligned} \Delta\kappa_{b,vertex} &= \frac{\sqrt{2}G_\mu M_W^2}{16\pi^2}\left\{2\frac{m_t^2}{M_W^2} + \frac{1}{3}(16 + \frac{1}{c_W^2})\ln\frac{m_t^2}{M_W^2} + \cdots\right\} \\ \Delta\rho_{b,vertex} &= -2\Delta\kappa_{b,vertex}. \end{aligned} \tag{119}$$

These corrections lead to a much weaker top mass dependence of quantities (partial width, asymmetries) associated with $b\bar{b}$ final states.

Thus, in comparison with other channels the production of $b\bar{b}$ is particularly interesting since

$$\begin{aligned} \sin^2\Theta_b - \sin^2\Theta_e &= \tilde{s}^2(\Delta\kappa_{b,vertex} - \Delta\kappa_{e,vertex}) \\ g_A^b/g_A^e &= 1 + (\Delta\rho_{b,vertex} - \Delta\rho_{e,vertex}) \end{aligned}$$

measure the large top contribution of the Zbb-vertex. They are completely independent of Higgs and other heavy particle effects and hence they are ideal *heavy-top-mass-meters*. As an example, for $m_t = 200$ GeV we obtain $\sin^2\Theta_b - \sin^2\Theta_e = 0.0020$ and $g_A^b/g_A^e = 0.9821$. For $\sin^2\Theta_b$ an experimental accuracy of 0.0009 is supposed to be achievable.

We may define a flavor independent effective $\sin^2\bar{\Theta}$ by

$$\sin^2\bar{\Theta} \ = \ (1 + \Delta\kappa_{se})\sin^2\Theta_W \tag{120}$$

and include the small vertex corrections in a second step

$$\sin^2\Theta_f \;=\; (1+\Delta\kappa_{f,vertex})\sin^2\bar{\Theta} \tag{121}$$

up to negligible higher order terms. The flavor independent auxiliary quantity $\sin^2\bar{\Theta}$ is used in Ref. [40] and is very similar to s_*^2 introduced in Ref. [44]. The "barred"(or "starred")-quantities are obtained by ignoring (small) corrections different from the vector boson self-energies.

The leading heavy top and heavy Higgs dependence is given by

$$\begin{aligned}
\Delta\bar{r}^{top} &= \frac{\sqrt{2}G_\mu M_W^2}{16\pi^2}\left\{-3\frac{m_t^2}{M_W^2}+\frac{2}{3c_W^2}\ln\frac{m_t^2}{M_W^2}+\cdots\right\} \\
\Delta r_b^{top} &= \frac{\sqrt{2}G_\mu M_W^2}{16\pi^2}\left\{-\frac{1+s_W^2}{c_W^2}\frac{m_t^2}{M_W^2}+\frac{16c_W^2(c_W^2-s_W^2)-1}{3c_W^4}\ln\frac{m_t^2}{M_W^2}+\cdots\right\}
\end{aligned} \tag{122}$$

and

$$\Delta\bar{r}^{Higgs} \;\simeq\; \frac{\sqrt{2}G_\mu M_W^2}{16\pi^2}\left\{\frac{1+9s_W^2}{3c_W^2}(\ln\frac{m_H^2}{M_W^2}-\frac{5}{6}\,)\right\} \tag{123}$$

respectively. Except from extra top contributions in the case of $f=b$, all heavy particle effects are universal, i.e. $\Delta r_{f\neq b}^{top}=\Delta\bar{r}^{top}$ and $\Delta r_f^{Higgs}=\Delta\bar{r}^{Higgs}$.

What is the proper resummation of the large higher terms in case $\Delta\rho$ is large? Using Eqs. (107), (97) and (99) we have

$$\begin{aligned}
\sin^2\Theta_f &= \left(1+\frac{\cos^2\Theta_W}{\sin^2\Theta_W}\Delta\rho+\cdots\right)\sin^2\Theta_W \\
&= 1-\frac{M_W^2}{\rho M_Z^2}+\cdots \\
&= \frac{1}{2}(1-\sqrt{1-\frac{4A_0^2}{\rho M_Z^2}(\frac{1}{1-\Delta\alpha}+\cdots)}\,)+\cdots
\end{aligned}$$

where the ellipses stand for the small remainder terms. As a result we obtain

$$\frac{1}{1-\Delta r_f}=\frac{1}{1-\Delta\alpha}\,(1-(\Delta\rho)_{irr})+\Delta r_{f,rem} \tag{124}$$

for the proper resummation of the large terms in Eqs. (113) and (115). This leads to the important relation

$$\sqrt{2}G_\mu\bar{\rho}M_Z^2\,\cos^2\Theta_f\sin^2\Theta_f=\pi\bar{\alpha}(1+\Delta r_{f,vertex}) \tag{125}$$

where

$$\begin{aligned}
\bar{\rho} &= \frac{1}{1-\Delta\bar{\rho}}\simeq\frac{1}{1-\Delta\rho} \\
\bar{\alpha} &= \frac{\alpha}{1-\Delta e}\simeq\frac{\alpha}{1-\Delta\alpha}
\end{aligned} \tag{126}$$

with $\Delta\bar{\rho}$ and Δe given in Eqs. (108) and (100), respectively. Ignoring vertex corrections we obtain the universal relation

$$\sqrt{2}G_\mu\bar{\rho}M_Z^2\,\cos^2\bar{\Theta}\sin^2\bar{\Theta}=\pi\bar{\alpha}\;\;. \tag{127}$$

For completeness we mention that $\sin^2\Theta_e$ measured at the Z peak is the high energy analogue of $\sin^2\Theta_{\nu_\mu e}$ measured in low momentum transfer $\nu_\mu e - scattering$. In fact, the two versions of $\sin^2\Theta$ are related in a way which is practically independent of unknown effects (they differ by $\gamma Z\, mixing$ and $\nu_\mu\, charge\, radius$ contributions only, which, by accident, largely cancel each other numerically). Formally we have

$$\sin^2\Theta_e = (1 + \Delta_{se} + \Delta_{\nu_\mu e,vertex+box} + \Delta\kappa_{e,vertex})\sin^2\Theta_{\nu_\mu e} \tag{128}$$

where

$$\begin{aligned}
\Delta_{se} &= \frac{\cos\Theta_W}{\sin\Theta_W}\left\{\Pi'_{\gamma Z}(M_Z^2) - \frac{d\Pi_{\gamma Z}}{dq^2}(0)\right\} \qquad (129)\\
&= \Delta\alpha - \Delta\alpha_2 \\
\Delta_{\nu_\mu e,vertex+box} &= \frac{\alpha}{4\pi s_W^2}\left\{\frac{2}{3}\left(\ln\frac{M_W^2}{m_\mu^2} + 1\right) + \frac{24c_W^4 - 14c_W^2 + 9}{4c_W^2}\right\}
\end{aligned}$$

and $\Delta\kappa_{e,vertex}$ is the same as in Eq. (107). The shift $\Delta\alpha_2$ in the $SU(2)_L$ coupling $\alpha_2 = \frac{g^2}{4\pi}$ is analogous to $\Delta\alpha$ in Eq. (85)

$$\begin{aligned}
\Delta\alpha_2 &= \Pi'_{3\gamma}(0) - \Pi'_{3\gamma}(M_Z^2) \qquad (130)\\
&= \frac{\alpha_2}{12\pi}\Sigma_l|Q_l|(\ln\frac{M_Z^2}{m_l^2} - \frac{5}{3}) + \Delta\alpha^{(5)}_{2,\mathrm{hadrons}} \qquad (131)
\end{aligned}$$

where the sum extends over the light leptons and [29]

$$\begin{aligned}
\Delta\alpha^{(5)}_{2,\mathrm{hadrons}}(s) &= 0.0587 \pm 0.0018 \qquad (132)\\
&\quad +0.006184\cdot\{\ln(s/s_0) + 0.005513\cdot(s_0/s - 1)\}
\end{aligned}$$

is the hadronic contribution of the 5 known light quarks u,d,s,c,b ($\sqrt{s_0} = 91.176$ GeV).

The proper summation of the higher order effects in this case reads

$$\sin^2\Theta_e = \left\{\frac{1-\Delta\alpha_2}{1-\Delta\alpha} + \Delta_{\nu_\mu e,vertex+box} + \Delta\kappa_{e,vertex}\right\}\sin^2\Theta_{\nu_\mu e} \tag{133}$$

The ratio $\sin^2\Theta_{\nu_\mu e}/\sin^2\Theta_e$ is shown in Fig. 4 as a function of m_t. The value of this ratio is close to 1.002. This relation provides a sort of "model independent" constraint for the Standard Model . The CHARM II value for 0.240 ± 0.012 [21] is in agreement with the SM. The precise definition of the low energy ρ-parameter is (to linear order)

$$\rho_{\nu_\mu e} = \frac{G_{NC}(0)}{G_{CC}(0)} = 1 + \Delta\rho + \Delta\rho_{vertex+box} \tag{134}$$

with $\Delta\rho$ given in Eq. (85) and

$$\Delta\rho_{vertex+box} = \frac{\sqrt{2}G_\mu M_Z^2}{16\pi^2}\left\{24c_W^4 - 44c_W^2 + 15 - 2\frac{c_W^2}{s_W^2}(4c_W^2 + 3)\ln c_W^2\right\}\ .$$

Similar to the asymmetries, the corrected partial widths $\Gamma_{Zf\bar{f}} = \frac{\sqrt{2}G_\mu M_Z^3}{3\pi}(v_f^2 + a_f^2)N_{cf}K_{QCD}\,(1 + \delta_{QED})$ and the peak cross-sections $\sigma^{f\bar{f}}_{peak} \simeq \frac{12\pi}{M_Z^2}\frac{\Gamma_e\Gamma_f}{\Gamma_Z^2}$ are given by the Born formulae using the effective parameters Eq. (106). The uncertainty in α_s implies an uncertainty of 12 MeV in $\Gamma_{Z,tot}$.

The QED-correction including real photon emission is given by $\delta_{QED} = \frac{3\alpha}{4\pi} Q_f^2$. In Tab. 6 some values are given for the widths and peak cross-sections. The full QCD corrections will be discussed in subsection 4.5 below.

Table 6. Z widths and peak cross-sections for $M_Z = 91.176$ GeV and $\alpha_s = 0.117$. Masses are given in GeV, widths in MeV and cross sections in nb.

m_t	m_H	Γ_Z	Γ_h	Γ_ℓ	Γ_{inv}	Γ_c	Γ_b	R_{had}	σ_μ^{peak}	σ_{had}^{peak}
90	100	2482	1733	83.4	499	296	378	20.787	1.9927	41.423
110	100	2485	1735	83.5	499	296	378	20.782	1.9937	41.432
130	50	2490	1739	83.7	500	297	378	20.780	1.9944	41.443
130	100	2489	1738	83.7	500	297	377	20.775	1.9949	41.444
130	1000	2481	1732	83.5	499	296	376	20.755	1.9971	41.449
150	100	2494	1741	83.9	501	298	377	20.767	1.9963	41.456
200	100	2508	1751	84.4	504	301	375	20.745	2.0002	41.494
230	100	2519	1759	84.9	506	303	375	20.731	2.0028	41.521

4.4 Results from LEP at the Z Resonance

The results from LEP based on 600,000 Z decays (presented at the Aspen Conference January 1991) are collected in Tab. 5.

The central values are given for $m_t = 136$ GeV and $m_H = 100$ GeV. The uncertainties for the SM predictions include variations of the parameters within the one standard deviation bounds 89 GeV $< m_t <$ 204 GeV, from UA2 and CDF data, and 50 GeV $< m_H <$ 1 TeV. More precisely, the allowed range for m_t depends on m_H. Since, in the range of interest, all quantities are monotonic functions of m_H and m_t we may inspect the extremal cases simply: For $m_H = 50$ GeV the 1σ range for m_t is (74,180) GeV or (89,180) GeV if we take into account the direct bound (26). For $m_H = 1$ TeV we get (104,204) GeV. The bounds given in Tab. 5 are then the maximum or minimum values from the two extremal cases. Taking an upper bound 1 TeV for the Higgs mass is of course a theoretical prejudice.

The mass and the total width of the Z are determined from the line-shape. The separate analyse of the visible channels $e^+e^- \to$ hadrons and $e^+e^- \to \ell^+\ell^-$ lead to Γ_{had} and Γ_ℓ ($\ell = e, \mu, \tau$), respectively. Using these and the total Z-width

$$\Gamma_Z = \Gamma_{had} + 3\,\Gamma_\ell + \Gamma_{invisible};\quad \Gamma_{invisible} = N_\nu(\Gamma_\nu)_{SM}$$

in terms of the hadronic, leptonic and neutrinic contributions, $\Gamma_{invisible}$ can be determined. N_ν is then extracted as the effective number of SM neutrinos. The most important result established by the LEP experiments so far is that $N_\nu = 2.95 \pm 0.05$ and hence no additional light ($m_\nu \lesssim 45 GeV$) neutrino (sneutrino, Majoron etc.) exists [1]. This rules out the existence of further family replicas of the known type with (within experimental limits) massless neutrinos.

Table 7. LEP results on the Z peak

	ALEPH	DELPHI	L3	OPAL	LEP	SM	$\sin^2\bar{\Theta}$
Z decays	195,000	130,000	125,000	184,000	634,000		
M_Z (GeV)	91.182 ±0.009 ±0.020	91.175 ±0.010 ±0.020	91.180 ±0.010 ±0.020	91.160 ±0.009 ±0.020	91.174 ±0.005 ±0.020		0.2315 $^{+.0018}_{-.0019}$
Γ_Z (MeV)	2488 ±17	2454 ±21	2500 ±17	2497 ±17	2487 ±9	2490 ±22	0.2322 $^{+.0017}_{-.0024}$
σ^{peak}_{had} (nb)	41.76 ±0.39	41.98 ±0.63	40.92 ±0.47	41.23 ±0.47	41.46 ±0.29	41.45 ±0.12	0.2313
Γ_{had} (MeV)	1756 ±15	1718 ±22	1739 ±19	1747 ±19	1744 ±10	1739 ±18	0.2314 ±.0022
Γ_ℓ (MeV)	83.3 ±0.7	83.4 ±1.0	83.3 ±0.8	83.4 ±0.7	83.3 ±0.4	83.7 ±0.5	0.2326 ±.0021
R_{had}	21.07 ±0.19	21.61 ±0.33	20.88 ±0.28	20.94 ±0.24	20.94 ±0.12	20.77 ±0.12	
Γ_{inv} (MeV)	481 ±14	486 ±21	511 ±18	499 ±17	493 ±9	500 ±3	
N_ν	2.90 ±.08	2.93 ±.13	3.08 ±.10	2.99 ±.10	2.96 ±.06	3	
$A^{\mu^+\mu^-}_{FB}$	0.024 ±.008	0.008 ±.013	0.024 ±.015	0.007 ±.008	0.016 ±.005	0.0151 ±.004	0.2313 ±.0027
$(v_e/a_e)^2$	0.0082 ±.0026	0.0028 ±.0044	0.0080 ±.0048	0.0023 ±.0028	0.0054 ±.0016	0.0051 ±.0013	0.2315 ±.0027
A^b_{FB}	0.141 ±.044		0.130 ±.043		0.135 ±.031	0.0962 $^{+.012}_{-.006}$	0.2241 ±.0077

Of particular interest is the observable $R_{had} = \Gamma_{had}/\Gamma_\ell$ which is almost independent of m_t, due to an accidental cancellation of the m_t-dependence between the Zbb-vertex and the self-energies. A deviation from the SM would be a direct signal for non-standard physics. The experimental value 20.92 ± 0.13 is slightly higher than the SM prediction 20.77 ± 0.12. Also the hadronic peak cross-section σ^{peak}_{had} is weakly dependent on m_t only. The experimental value is in perfect agreement with the prediction. Before more stringent tests are possible one has to pin down further the allowed mass ranges for the top and the Higgs. We do not expect that the errors on M_Z and α_s can be substantially improved further.

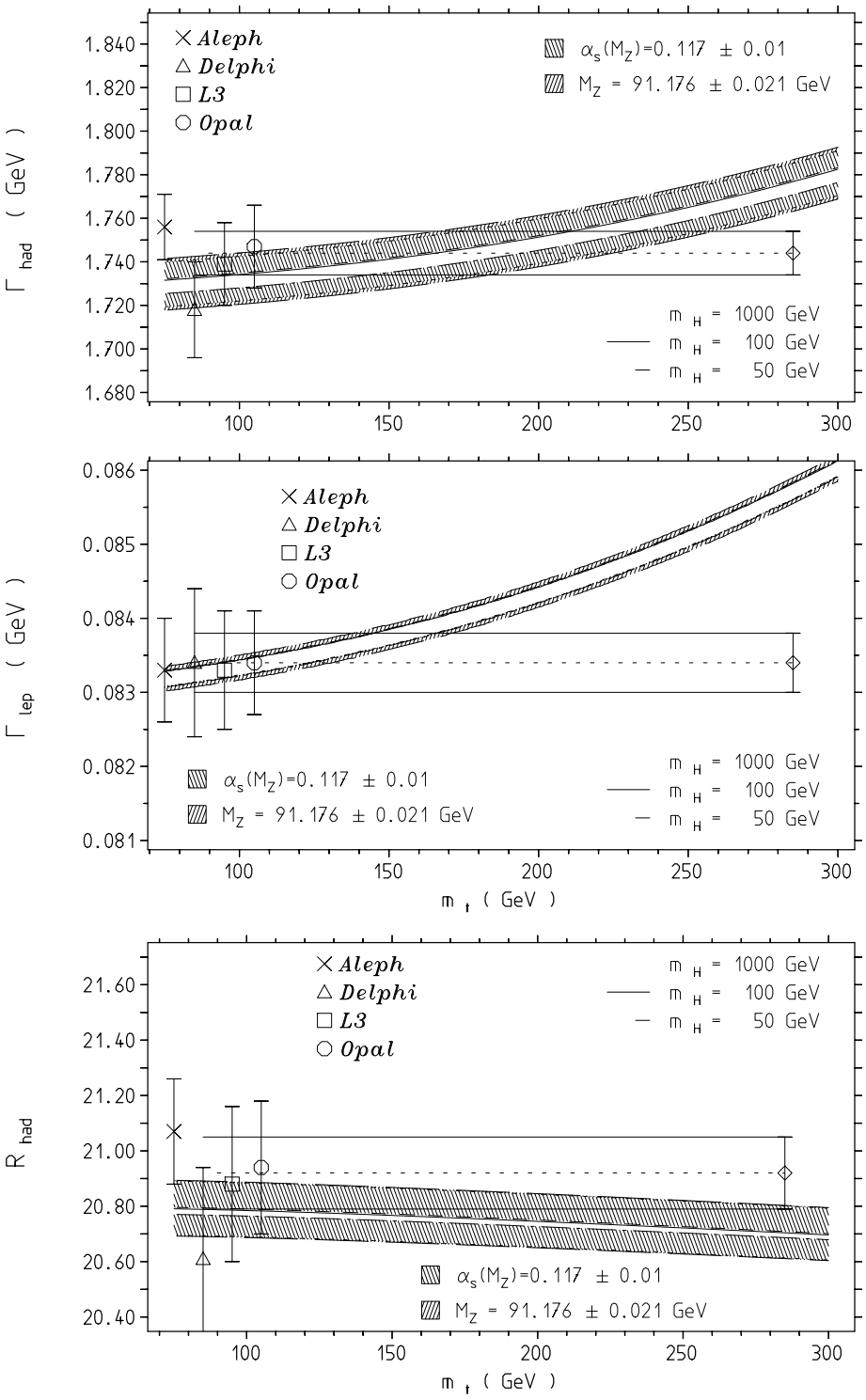

Figure 16: Results for Γ_{had}, Γ_ℓ and R_{had}.

Some major results obtained in the first year of LEP ($\sim$ 600 000 Z's) are shown together with theoretical predictions in Figures 16 and 17. All Figures show the data together with the theoretical prediction as a function of the top mass for m_H= 50, 100 and 1000 GeV. An uncertainty $\delta\alpha_s = \pm 0.01$ in the strong interaction coupling constant is shown as an inner error band whereas the outer error band shows the uncertainty in the prediction due to the experimental error $\delta M_Z = \pm 0.021$ in the Z-mass. The agreement between the experimental numbers and the theoretical predictions is impressive.

4.5 QCD Corrections

We distinguish two different kinds of QCD corrections:

i) gluonic corrections of quark loops contributing to parameter shifts.

ii) gluonic corrections to quark final states

We first discuss the QCD corrections to quark loops. Typically, we have to distinguish between two cases, the light quark contributions to $\Delta\alpha$ and the heavy quark contributions to $\Delta\rho$. In both cases there are uncertainties because strong interaction effects are not well under control by theory. The problems are due to:

(i) the ill-defined QCD parameters. The scale of α_s and the definition and scale of quark masses to be used in the calculation of a particular quantity are quite ambiguous in many cases.
(ii) the bad convergence and/or breakdown of perturbative QCD. In particular at low q^2 and in the resonance regions non-perturbative effects that are theoretically poorly known are non-negligible.

The theoretical problems with the hadronic contributions of the 5 known light quarks to $\Delta\alpha$ can be circumvented by evaluating the dispersion integral (87) using the experimental e^+e^--data as input (which include all orders in perturbation theory). The hadronic contribution of the 5 known light quarks u,d,s,c,b obtained in this way have been given in Eqs. (88) and (132). The errors $\delta(\Delta\alpha)_{\rm had} = \pm 0.0009$ and $\delta(\Delta\alpha_2)_{\rm had} = \pm 0.0018$ are dominated by the large experimental errors in the continuum contributions to $\sigma_{tot}(e^+e^- \to \gamma^* \to hadrons)$ below the Υ threshold, and can be improved only by more precise measurements of hadron production in e^+e^--annihilation in the corresponding low energy region. This uncertainty leads to an error of $\delta M_W = 17$ MeV in the W-mass prediction and $\delta \sin^2\Theta = 0.0003$ in the prediction of the weak mixing parameters.

For the high energy tail we have to apply perturbation theory. For the light quarks the perturbative QCD corrections amount to the correction factor $K_{\rm QCD} = 1 + \delta_{\rm QCD}$ given in Eqs. (89) and (90). At the Z mass scale $\delta_{\rm QCD} \simeq 0.039$ for the u,d,s and c quarks, whereas for the b quark $\delta_{\rm QCD} \simeq 0.044$ as we shall see below.

The contribution to $\Delta\rho$ from quark doublets with large mass splittings exhibits large QCD corrections in the weak current quark loops. The relevant exact analytic expressions for the vacuum polarization amplitudes have been given in Ref. [45]. The effect for a heavy top was first calculated in Ref. [46]. One finds

$$\Delta\rho = \frac{\sqrt{2}G_\mu}{16\pi^2} 3 m_t^2 K_{\rm QCD} + \cdots \tag{135}$$

with

$$K_{\rm QCD} = 1 - \frac{2\pi^2 + 6}{9}\frac{\alpha_s}{\pi} \simeq 1 - 2.860\frac{\alpha_s}{\pi} \tag{136}$$

for asymptotically large m_t, which is a large correction. Here, m_t is assumed to be the on-shell quark mass. We shall use below renormalization group (RG) improved perturbation theory using

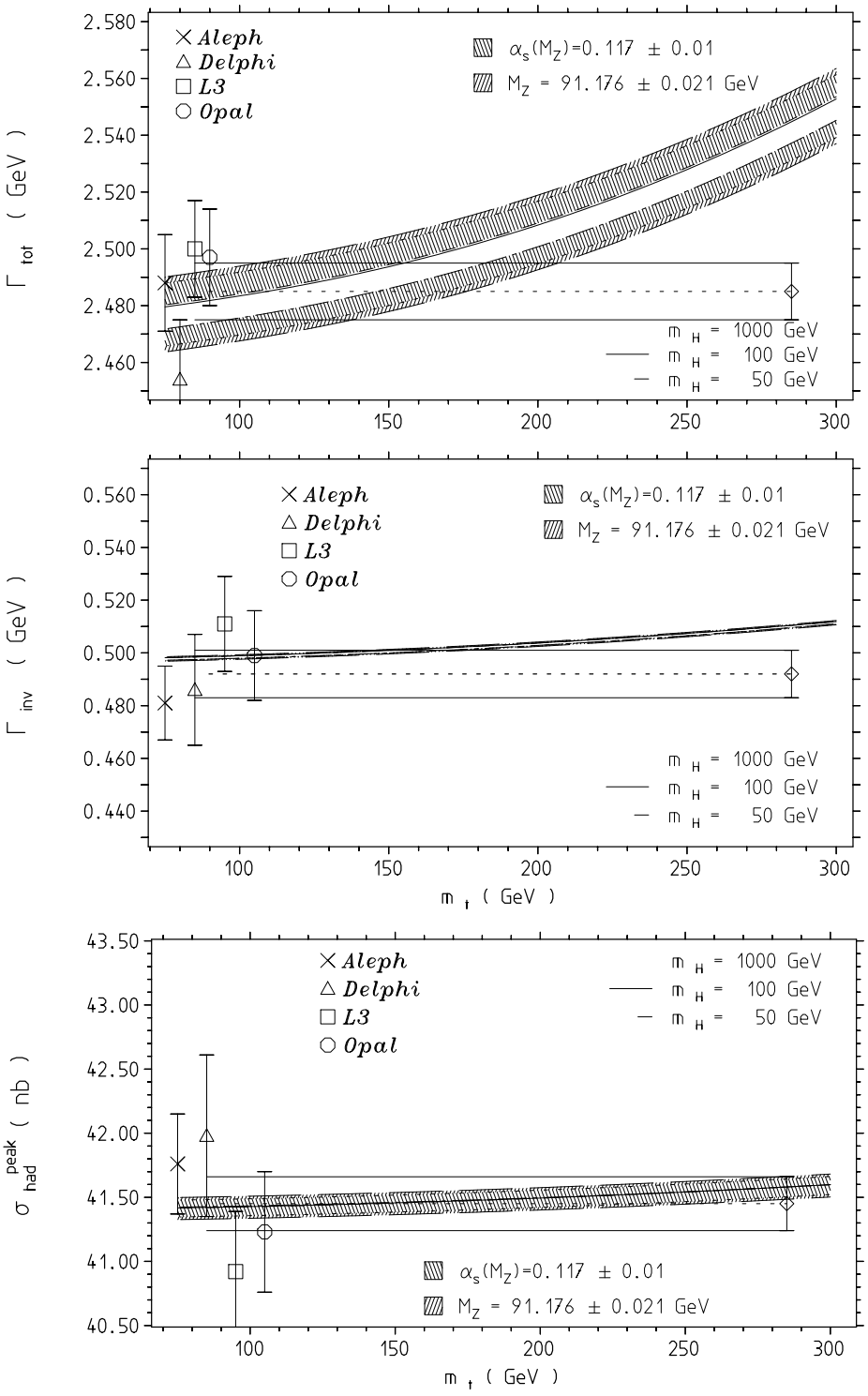

Figure 17: Results for Γ_Z, $\Gamma_{\rm inv}$ and $\sigma^{\rm peak}_{\rm had}$.

the $\overline{MS}$ scheme. The $\overline{MS}$ running mass $m_i(\mu)$ at scale μ is related to the on-shell mass at threshold by [47]

$$m_i = m_i(m_i)\left(1 + \frac{4}{3}\frac{\alpha_s(4m_i^2)}{\pi}\right) . \tag{137}$$

Thus using a running top quark mass the leading top contribution changes to

$$\Delta\rho = \frac{\sqrt{2}G_\mu}{16\pi^2} 3 m_t(m_t)^2 \bar{K}_{\rm QCD} + \cdots \tag{138}$$

with

$$\bar{K}_{\rm QCD} = 1 - \frac{2\pi^2 - 18}{9}\frac{\alpha_s}{\pi} \simeq 1 - 0.193\frac{\alpha_s}{\pi} \tag{139}$$

and yields a correction which is smaller by more than a factor 10. Recently the numerically important subleading terms have also been worked out [48,49]. At first, the corrections obtained are not well-determined numerically because it is not so evident which scale should be chosen for α_s. Also finite corrections to the quark mass can change the result drastically as we have illustrated with the above example (ambiguity in the definition of m_t). Again, the problem can be controlled better by using the representation

$$\Delta\rho^{\rm top}(0) = -\frac{\sqrt{2}G_\mu}{3\pi^2} Re \int_{4m_b^2}^{\infty} ds R_\rho(s) \tag{140}$$

as a dispersion integral [29]. For the imaginary part $R_\rho(s)$ the perturbative result, known to two-loop [50], can be used away from the resonance regions (since $\sqrt{s} \geq 2m_b \simeq 10$ GeV). If one evaluates the dispersion integral numerically, one can use running parameters for the parametrization of the absorptive part. This is precisely what one does in parametrizing the e^+e^- annihilation data for $R(s)$ where s-dependent parameters at scale $\sqrt{s}$ are used. This we do for the other currents in the same way. The resonance regions can be treated using semi-phenomenological quark potential models. Using this approach, the QCD corrected heavy top contribution to Δr has been calculated in Ref. [51]. [9]

Here we adapt the analytic approach of Refs. [45,46,48,49] and closely follow Ref. [49]. We will use however running parameters as in Ref. [29], for example.

We denote by J_μ^A the hadronic part of the electroweak currents which couple to the gauge bosons $A = \gamma, Z$ or W. Expressed in terms of the vector and axial-vector quark currents

$$V_\mu^{q_1 q_2} = \bar{q}_1 \gamma_\mu q_2 \;\; \text{and} \;\; A_\mu^{q_1 q_2} = \bar{q}_1 \gamma_\mu \gamma_5 q_2 \tag{141}$$

we have

$$\begin{aligned}
J_\mu^\gamma &= \sum_i \left(\frac{2}{3}\bar{u}_i\gamma_\mu u_i - \frac{1}{3}\bar{d}_i\gamma_\mu d_i\right) \\
J_\mu^Z &= J_\mu^3 - 2\sin^2\Theta_W J_\mu^\gamma \\
J_\mu^3 &= \frac{1}{2}\sum_i (\bar{u}_i\gamma_\mu\,(1-\gamma_5)\,u_i - \bar{d}_i\gamma_\mu\,(1-\gamma_5)\,d_i\,) \\
J_\mu^{W^-} &= \frac{J_\mu^1 + iJ_\mu^2}{\sqrt{2}} = \frac{1}{2}\sum_i \bar{u}_i\gamma_\mu(1-\gamma_5)d_i
\end{aligned} \tag{142}$$

[9] The authors of Ref. [51] use a different scale for the running coupling and treat masses as fixed on-shell quantities.

where u_i and d_i stand for the upper and lower components of the weak isodoublets, respectively (i is the family index). The self-energy functions are then given by

$$\begin{aligned}\Pi_{\mu\nu}^{AB}(q) &= ig_A g_B \int d^4x e^{iqx} < 0|T J_\mu^A\ (x)\ J_\nu^B\ (0)\ |0> \\ &= -\left(g_{\mu\nu} - \frac{q_\mu q_\nu}{q^2}\right)\ \Pi_1^{AB}\ (q^2)\ + \frac{q_\mu q_\nu}{q^2}\Pi_0^{AB}\ (q^2) \end{aligned} \tag{143}$$

with $g_\gamma = e$, $g_Z = g/(2\cos\Theta_W)$ and $g_W = g/\sqrt{2}$. In the following we need the transverse amplitudes $\Pi_1\ (q^2)$ only, which we simply denote by $\Pi\ (q^2)$. Furthermore, we introduce the subtracted amplitudes $\Pi'\ (q^2)$ by

$$\Pi\ (s) = \Pi\ (0) + s\Pi'\ (s) \tag{144}$$

and use $\Pi\ (0) = 0$ for the flavor diagonal vector currents. [10]

According to Eqs. (143) and (142) the vector boson self-energies are determined by QCD vacuum polarization functions $\Pi_{V,A}^{NC}(s, m_i)$ and $\Pi_{V,A}^{CC}(s, m_1, m_2)$ of the vector (V) and axial-vector (A) currents Eq. (141). Explicitly, we have

$$\begin{aligned}\Pi^{\gamma\gamma} &= e^2 Q_i^2 \Pi_V^{NC}\ (s, m_i) \\ \Pi^{Z\gamma} &= \left(\frac{eg}{4c_W}|Q_i| - \frac{e^2 s_W}{c_W} Q_i^2\right) \Pi_V^{NC}\ (s, m_i) \\ \Pi^{ZZ} &= \left(\frac{g^2}{16 c_W^2}\right) \left(\left(1 - 8s_W^2|Q_i| + 16 s_W^4 Q_i^2\right) \Pi_V^{NC}\ (s, m_i) + \Pi_A^{NC}\ (s, m_i)\right) \\ \Pi^{WW} &= \left(\frac{g^2}{8}\right) \left(\Pi_V^{CC}\ (s, m_1, m_2) + \Pi_A^{CC}\ (s, m_1, m_2)\right)\ . \end{aligned} \tag{145}$$

For the charged currents we restrict ourselves to consider the approximation $m_b = 0$. In this case

$$\Pi_A\ (s, m_t, 0) = \Pi_V\ (s, m_t, 0) \equiv \Pi_W\ (s, m_t, 0)\ .$$

The contributions we are considering correspond to the diagrams depicted in Fig. 18.

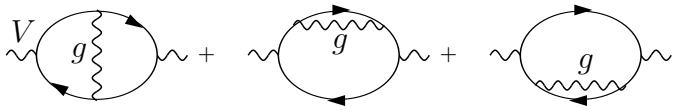

Figure 18: Gluonic corrections to quark loops.

Before we discuss the QCD corrections in detail, let us summarize the representations of the parameter renormalizations in terms of the self-energy contributions. The various quantities of interest are the following:

$$\begin{aligned}\Delta\rho &= \frac{\Pi_Z(0)}{M_Z^2} - \frac{\Pi_W(0)}{M_W^2} + 2\frac{s_W}{c_W}\frac{\Pi_{\gamma Z}(0)}{M_Z^2} \\ \Delta\hat{\rho} &= \frac{\Pi_Z(M_Z^2)}{M_Z^2} - \frac{\Pi_W(M_W^2)}{M_W^2} + \frac{s_W}{c_W}\frac{\Pi_{\gamma Z}(M_Z^2) + \Pi_{\gamma Z}(0)}{M_Z^2} = \Delta\rho - \frac{s_W^2}{c_W^2}\Delta_1 + \Delta_2 \\ \Delta\bar{\rho} &= \Delta\rho + \frac{\Pi_Z(M_Z^2)}{M_Z^2} - \frac{\Pi_Z(0)}{M_Z^2} - \left(\frac{d\Pi_Z}{dq^2}\right)(M_Z^2) = \Delta\rho + \Delta_Z \end{aligned}$$

[10] The canonical divergences of the currents Eq. (141) are $\partial^\mu V_\mu^{q_1 q_2} = i\ (m_1 - m_2)\ \bar{q}_1 q_2$ and $\partial^\mu A_\mu^{q_1 q_2} = i\ (m_1 + m_2)\ \bar{q}_1\gamma_5 q_2$.

$$
\begin{aligned}
\Delta_W &= \frac{\Pi_W(M_W^2)}{M_W^2} - \frac{\Pi_W(0)}{M_W^2} - \left(\frac{d\Pi_W}{dq^2}\right)(M_W^2) \\
\Delta\kappa &= \frac{c_W^2}{s_W^2}\Delta\hat{\rho} = \frac{c_W^2}{s_W^2}\Delta\rho - \Delta_1 + \frac{c_W^2}{s_W^2}\Delta_2 \\
\Delta e &= \Pi'_\gamma(0) - \Pi'_W(M_W^2) + \frac{c_W}{s_W}\Pi'_{\gamma Z}(M_Z^2) = \Delta\alpha + \Delta_1 + \Delta_2 \\
\bar{\Delta} &= \frac{c_W}{s_W}\left\{\frac{\Pi_{\gamma Z}(M_Z^2)}{M_Z^2} - \frac{\Pi_{\gamma Z}(0)}{M_Z^2} - \left(\frac{d\Pi_{\gamma Z}}{dq^2}\right)(0)\right\} = \Delta\alpha - \Delta\alpha_2
\end{aligned}
\tag{146}
$$

where

$$
\begin{aligned}
\Delta\rho &= g^2\left(\hat{\Pi}_{33}(0) - \hat{\Pi}_\pm(0)\right)/M_W^2 \\
\Delta_1 &= g^2\left(\hat{\Pi}'_{3\gamma}(M_Z^2) - \hat{\Pi}'_{33}(M_Z^2)\right) \\
\Delta_2 &= g^2\left(\hat{\Pi}'_{33}(M_Z^2) - \hat{\Pi}'_\pm(M_W^2)\right) \\
\Delta\alpha &= e^2\left(\hat{\Pi}'_{\gamma\gamma}(0) - \hat{\Pi}'_{\gamma\gamma}(M_Z^2)\right) \\
\Delta\alpha_2 &= g^2\left(\hat{\Pi}'_{3\gamma}(0) - \hat{\Pi}'_{3\gamma}(M_Z^2)\right)
\end{aligned}
\tag{147}
$$

in terms of vacuum matrix elements of the currents Eq. (142). Using this notation we have, for example,

$$
\begin{aligned}
\Delta r &= \Delta e - \Delta\kappa = \Delta\alpha - \frac{c_W^2}{s_W^2}\Delta\rho + 2\Delta_1 + \left(1 - \frac{c_W^2}{s_W^2}\right)\Delta_2 \\
\Delta\bar{r} &= \Delta e - \Delta\hat{\rho} = \Delta\alpha - \Delta\rho + \frac{1}{c_W^2}\Delta_1 \; .
\end{aligned}
\tag{148}
$$

The heavy quark QCD corrections to the parameter shifts are now determined by the real parts of the self-energy functions Eq. (145). For the top-bottom doublet the contributions are given by

$$
\begin{aligned}
\Delta\rho &= \frac{g^2}{4M_W^2}\frac{\alpha_s}{4\pi}\mathrm{Re}\left\{\Pi_V^{NC}(0,m_t) + \Pi_V^{NC}(0,m_b)\right. \\
&\quad \left. + \Pi_A^{NC}(0,m_t) + \Pi_A^{NC}(0,m_b) - 4\Pi_W^{CC}(0,m_t,m_b)\right\} \\
\Delta\alpha^i &= -e^2Q_i^2\frac{\alpha_s}{\pi}\mathrm{Re}\left\{\Pi_V'^{NC}(M_Z^2,m_i) - \dot{\Pi}_V^{NC}(0,m_i)\right\} \\
\Delta\alpha_2^i &= -g^2\frac{|Q_i|}{4}\frac{\alpha_s}{\pi}\mathrm{Re}\left\{\Pi_V'^{NC}(M_Z^2,m_i) - \dot{\Pi}_V^{NC}(0,m_i)\right\} \\
\Delta_1^i &= \frac{g^2}{16}\frac{\alpha_s}{\pi}\mathrm{Re}\left\{\Pi_V'^{NC}(M_Z^2,m_i) - \Pi_A'^{NC}(M_Z^2,m_i) - (2-4|Q_i|)\Pi_V'^{NC}(M_Z^2,m_i)\right\} \\
\Delta_2^{(tb)} &= \frac{g^2}{16}\frac{\alpha_s}{\pi}\mathrm{Re}\left\{\Pi_A'^{NC}(M_Z^2,m_t) + \Pi_V'^{NC}(M_Z^2,m_t)\right. \\
&\quad \left. + \Pi_A'^{NC}(M_Z^2,m_b) + \Pi_V'^{NC}(M_Z^2,m_b) - 4\Pi_W'^{CC}(M_W^2,m_t,m_b)\right\} \\
\Delta_Z^i &= \frac{g^2}{16c_W^2}\frac{\alpha_s}{\pi}\mathrm{Re}\left\{\Pi_A'^{NC}(M_Z^2,m_i) - \dot{\Pi}_A^{NC}(M_Z^2,m_i)\right. \\
&\quad \left. + (1 - 8s_W^2|Q_i| + 16s_W^4Q_i^2)\left(\Pi_V'^{NC}(M_Z^2,m_i) - \dot{\Pi}_V^{NC}(M_Z^2,m_i)\right)\right\} \\
\Delta_W^{(tb)} &= \frac{g^2}{4}\frac{\alpha_s}{\pi}\mathrm{Re}\left\{\Pi_W'^{CC}(M_W^2,m_t,m_b) - \dot{\Pi}_W^{CC}(M_W^2,m_t,m_b)\right\} \quad .
\end{aligned}
\tag{149}
$$

The explicit expressions are given in the Appendix. If applied to the process $e^+e^- \to f\bar{f}$ away from the resonance M_Z^2 should be replaced by s in these expressions.

We are considering now the QCD corrections to the $\gamma, Z \to q\bar{q}$ final states [52]. They are given by the imaginary parts of the same amplitudes. At the Z-peak this is incorporated in the QCD corrections to the hadronic partial widths. For the light flavors this is determined to $O(\alpha_s^2)$ by δ_{QCD} Eq. (89). For the b flavor mass corrections have to be included. In addition the $O(\alpha_s^2)$ term is modified by a singlet contribution to the axial amplitude which is due to large weak isospin breaking by the large mass difference in the tb-doublet [53]. This correction is given by the imaginary part of the three-loop diagram of Figure 19.

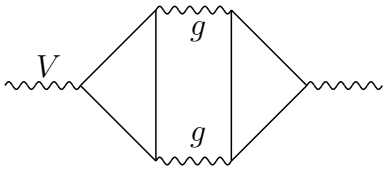

Figure 19: Diagram giving a singlet contribution to the weak axial currents

Analytically the result is given by

$$\delta\Gamma_A(b\bar{b}) = -\frac{1}{3}(\alpha_s/\pi)^2 I((M_Z/2m_t)^2)\Gamma_{0A} \tag{150}$$

where Γ_{0A} is the axial contribution to quark parton Z decay width. The function $I(x)$, for $2m_t \geq M_Z$ and $m_b = 0$, is given by

$$\begin{aligned} I(x) &= -6L - \frac{1}{2}\varphi^2 + \frac{15}{4} \\ &\quad +\sqrt{1/x-1}\,\{-2C\ell_2(\varphi) + \varphi(-2L+3) \\ &\quad + (1/x)[C\ell_2(\varphi) + \varphi(L-1)]\} \\ &\quad +(1/x)(\varphi^2+1) \\ &\quad +(1/x^2)[C\ell_3(\varphi) + \frac{\varphi}{2}C\ell_2(\varphi) - \zeta(3)] \end{aligned} \tag{151}$$

where $\varphi = 2arcsin\sqrt{x}$ and $L = \ln(\frac{M_Z}{m_t})$ and $C\ell_{2,3}$ are Clausen integrals [54]. For our purpose a perfect approximation is [53]

$$I(x) \simeq 9.250 - 1.037x - 0.632x^2 - 6L \tag{152}$$

For the $Z \to b\bar{b}$ width we get

$$\Gamma_b = 3\rho_b\Gamma_{0\nu}(v_b^2 K_{QCD,Vb} + a_b^2 K_{QCD,Ab})(1 + \frac{3Q_b^2\alpha}{4\pi}) \tag{153}$$

with

$$\begin{aligned} K_{QCD,Vb} &= 1 + \frac{\alpha_s}{\pi}(1+3y_b) + 1.405(\frac{\alpha_s}{\pi})^2 \\ K_{QCD,Ab} &= 1 - \frac{3}{2}y_b + \frac{\alpha_s}{\pi}(1 - \frac{3}{2}y_b(1 + 4\ln(\frac{m_b}{M_Z})) + (1.405 - I(x_t)/3)(\frac{\alpha_s}{\pi})^2 \end{aligned}$$

Here $y_b = 4m_b^2/M_Z^2$ and $x_t = M_Z^2/4m_t^2$.

We finally consider the forward-backward asymmetry $A_{FB} = \frac{\sigma_F - \sigma_B}{\sigma_F + \sigma_B}$. In lowest order it is given by

$$A_{FB}(s) = \frac{\Delta_{FB}(s)}{\sigma_0(s)} \tag{154}$$

with ($y_f = (1 - \frac{4m_f^2}{s})$)

$$\begin{aligned} \Delta_{FB}^{f\bar{f}}(s) &= -\frac{\alpha Q_f \sqrt{2} G_\mu M_Z^2}{2s} N_{cf} Re\chi a_e a_f \, y_f \\ &\quad + \frac{G_\mu^2 M_Z^4}{2\pi s} N_{cf} |\chi|^2 v_e v_f a_e a_f \, y_f \end{aligned} \tag{155}$$

and $\sigma_0(s)$ the total cross-section. QCD corrections can be obtained if we replace $\frac{3}{4}Q_f^2 \to 1$ in the QED final state corrections. If no cuts are applied $\Delta_{FB}(s)$ remains uncorrected in the zero mass approximation [52]. If mass effects are taken into account the correction may be approximated by [55]

$$\Delta_{FB}(s) \to \Delta_{FB}(s) \, (1 + f\frac{\alpha_s}{\pi}) \tag{156}$$

where

$$f = \frac{4\pi}{3}\frac{m_f}{\sqrt{s}} + \frac{8x}{3}\left(\frac{9}{2} + \frac{\pi^2}{8} + \frac{1}{8}\,(\ln x)^2 - \frac{3}{2}\ln x - \frac{5}{2}\ln 2\right) \tag{157}$$

with $x = m_f^2/s$. Together with the correction $(1 + \frac{\alpha_s}{\pi})$ in the total cross section one obtains

$$A_{FB}(s) \to A_{FB}(s) \, \left(1 - \frac{\alpha_s}{\pi}\,(1 - \frac{4\pi}{3}\frac{m_f}{\sqrt{s}})\right) \tag{158}$$

to a good approximation.

So far we have treated the quark masses as on-shell masses in the same way as leptons. Due to the convergence problems with perturbative QCD we have to use renormalization group improved (leading log resummed) perturbation theory. As usual, we use the convenient $\overline{MS}$-scheme. For the finite dimensionless absorptive parts $R_\rho(s)$ in the dispersion integrals the solution of the RG equation reads

$$R_\rho \, \left(\frac{m_0^2}{s}, g_0\right) = R_\rho \, \left(\frac{m^2(\mu)}{s}, g(\mu)\right); \;\; \mu = \sqrt{s} \tag{159}$$

if s_0 is a data point where $g_0 = g(\mu_0)$ and $m_0 = m(\mu_0)$ have been determined. $g(\mu)$ is the running coupling constant and $m(\mu)$ is the running mass in the $\overline{MS}$ scheme. To order $O(\alpha_s^2)$, with $\alpha_s = g^2/4\pi$, we have

$$\frac{4}{\beta_0 \alpha_s(\mu)} - \frac{\beta_1}{\beta_0^2}\ln\left(\frac{4\pi}{\beta_0 \alpha_s(\mu)} + \frac{\beta_1}{\beta_0^2}\right) = \ln(\mu^2/\Lambda^2) \tag{160}$$

where the effective RG invariant scale $\Lambda = \Lambda_{\overline{MS}}^{N_f}$ ($\leq \mu_0$) is defined in terms of the reference coupling $\alpha_s(\mu_0)$ at scale $\mu_0 = \sqrt{s_0}$. The iterative solution of Eq. (159) in terms of inverse powers of $L = \ln(\mu^2/\Lambda^2)$ ($\mu \ll \Lambda$) yields

$$\alpha_s(\mu) = \frac{4\pi}{\beta_0 L}\left(1 + \frac{\beta_1}{\beta_0^2}\frac{\ln\left(L + \frac{\beta_1}{\beta_0^2}\right)}{L} + \cdots\right)^{-1} . \tag{161}$$

The running mass is determined by

$$\begin{aligned} m_i(\mu) &= m_i(\mu_0)\frac{r(\mu)}{r(\mu_0)} \\ r(\mu) &= \exp -2\left[\frac{\gamma_0}{\beta_0}\ln\frac{4\pi}{\beta_0\alpha_s(\mu)} + \left(\frac{\gamma_0}{\beta_0} - \frac{4\gamma_1}{\beta_1}\right)\ln\left(1 + \frac{\beta_1}{\beta_0}\frac{\alpha_s(\mu)}{4\pi}\right)\right] \end{aligned} \tag{162}$$

in terms of a reference current quark mass $m_i(\mu_0)$. The RG coefficients are given by

$$\begin{array}{rclcrcl} \beta_0 & = & 11 - \frac{2}{3}N_f\,; & & \beta_1 & = & 102 - \frac{38}{3}N_f \\ \gamma_0 & = & 2\,; & & \gamma_1 & = & \frac{101}{12} - \frac{5}{18}N_f \end{array} \tag{163}$$

The integration constants Λ and $m_i(\mu_0)$ depend on the effective number of flavors N_f at a given energy. Their dependence on N_f is determined by continuity of $\alpha_s(\mu)$ and $m_i(\mu)$ at the flavor thresholds [56].

Applying the heavy quark QCD corrections to the parameter renormalizations we obtain the results of Figs. 20 and 21.

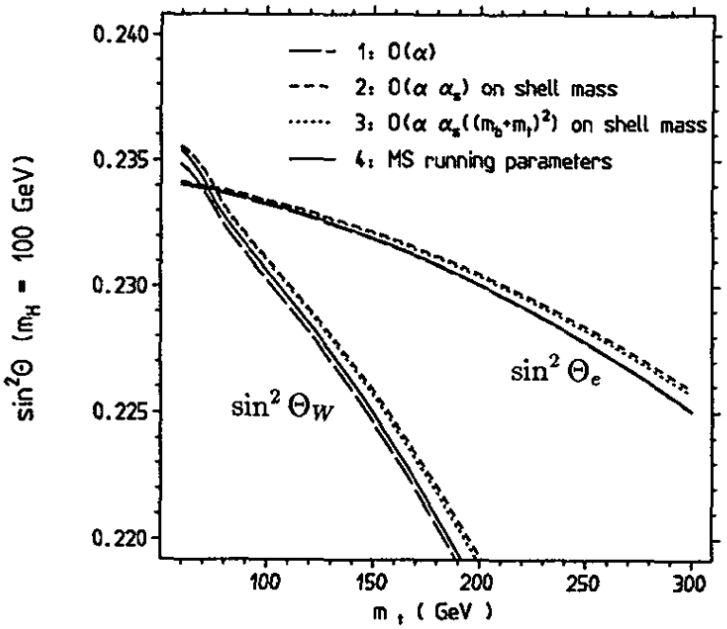

Figure 20: QCD corrections for the heavy top contribution to $\sin^2\Theta$

Using RG improved perturbation theory clearly makes the QCD corrections small and leads to much better control of the uncertainties. In particular we no longer obtain a large discrepancy between using analytic expressions or doing the dispersion integrals numerically using running parameters under the integral. In addition, corresponding QCD corrections to the Zbb vertex have not been calculated to our knowledge. Using a scheme which yields large QCD corrections we would expect additional large corrections for all quantities depending on Zbb vertex corrections. For the $\overline{MS}$ scheme we can hope that these corrections are small as well.

Appendix: Explicit Expressions

We use the following notation

$$y = (m_1 + m_2)^2/s = x^{-1}$$

where $m_1 = m_2 = m_t$ or m_b for the NC amplitudes and $m_1 = m_t$ and $m_2 = m_b$ for the CC amplitudes. We shall assume $m_b = 0$ whenever this limit exists.

In the NC case we conveniently use the variable

$$\xi = \frac{\sqrt{1-y}-1}{\sqrt{1-y}+1}$$

taking values

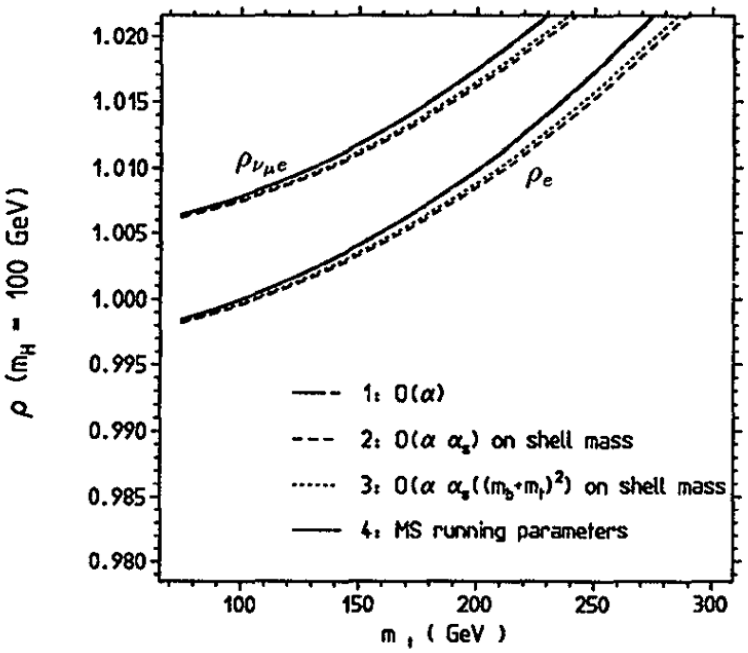

Figure 21: QCD corrections for the heavy top contribution to $\Delta\rho$

$$\begin{array}{ccc} 0 \le \xi \le 1 & \text{for} & s \le 0 \\ \xi = e^{i\varphi},\ \ 0 \le \varphi \le \pi & \text{for} & 4m^2 \ge s \ge 0 \\ -1 \le \xi \le 0 & \text{for} & 4m^2 \le s\ . \end{array}$$

Using the abbreviations

$$f = -\frac{1}{2}\ln\xi;\ \ g = \ln(1-\xi);\ \ h = \ln(1+\xi)$$

and

$$\begin{aligned} \Delta\mathrm{Li}_3 &= 2\mathrm{Li}_3(\xi) - \mathrm{Li}_3(\xi^2) \\ \Delta\mathrm{Li}_2 &= \mathrm{Li}_2(\xi) - \mathrm{Li}_2(\xi^2) \end{aligned}$$

we define

$$\begin{aligned} \mathrm{AA} &= -\frac{4}{3}(\Delta\mathrm{Li}_2 + \mathrm{Re}f\ (2h+g)) \\ \mathrm{BB} &= -\frac{8}{3}\ (2h+g+3\mathrm{Re}f) \\ \mathrm{XX} &= \Delta\mathrm{Li}_3 + \frac{8}{3}\ f\ \Delta\mathrm{Li}_2 + \frac{4}{3}\ f^2\ (2h+g) \\ \mathrm{YY} &= \frac{8}{3}\ (\Delta\mathrm{Li}_2 + 2f\ (2h+g) + 3f^2)\ . \end{aligned}$$

In terms of these functions we find the following expressions for the two-loop QCD vacuum polarization amplitudes: ($\dot{\Pi} = \frac{d\Pi}{ds}$ and $\ell \equiv \ln\frac{m^2}{\mu^2}$)

$$\begin{aligned} \frac{\pi}{m^2} Im\Pi_V^{NC} &= (4x - 1/x)\ \mathrm{AA} + \sqrt{1-1/x}\ ((x+1/2)\ \mathrm{BB} + (x+3/2)) \\ &\quad +(8x - 4/3 - 7/(6x))\ \mathrm{Re}f \quad ;\ \ x \ge 1 \\ \frac{\pi}{m^2} Im\Pi_A^{NC} &= (4x - 6 + 2/x)\ \mathrm{AA} + \sqrt{1-1/x}\ ((x-1)\ \mathrm{BB} + (x - 3 + 1/(4x))\ ) \end{aligned}$$

$$
\begin{aligned}
& +(8x-22/3+5/(6x)+1/(4x^2))\,\mathrm{Re}f \quad ; \quad x \geq 1 \\
\frac{\pi^2}{m^2} Re\Pi_V^{NC} &= (4x-1/x)\,\mathrm{XX} + \sqrt{1-1/x}\,((x+1/2)\,\mathrm{YY} - 2\,(x+3/2)\,f\,) \\
& -(8x-4/3-7/(6x))\,f^2 + 13/6 + \zeta(3)/x + x\,(55/12 - 4\zeta(3) - \ell - \frac{1}{d-4}) \\
\frac{\pi^2}{m^2} Re\Pi_A^{NC} &= (4x-6+2/x)\,\mathrm{XX} + \sqrt{1-1/x}\,((x-1)\,\mathrm{YY} - 2\,(x-3+1/(4x))\,f) \\
& -(8x-22/3+5/(6x)+1/(4x^2))\,f^2 \\
& +13/6 - 3\zeta(2) - 2\zeta(3)/x + 1/(4x) + x\,(55/12 - 4\zeta(3) - \ell - \frac{1}{d-4}) \\
& +(-11/8 + 6\zeta(3) + 3\zeta(2) - 11/2\ell + 3\ell^2 + \frac{2}{d-4}(3\ell - 11/4) + \frac{6}{(d-4)^2}) \\
4\pi^2\, Re\dot{\Pi}_V^{NC} &= (4+1/x^2)\,\mathrm{XX} + \sqrt{1-1/x}\,(-1/(2x)\,\mathrm{YY} - (2-5/(3x))\,f\,) \\
& +(16/(3x) + 13/(6x^2) + 4/(x^2(x-1)))\,f^2 \\
& -1 - 3/(2x) - \zeta(3)/x^2 + (55/12 - 4\zeta(3) - \ell - \frac{1}{d-4}) \\
4\pi^2\, Re\dot{\Pi}_A^{NC} &= (4-2/x^2)\,\mathrm{XX} + \sqrt{1-1/x}\,(1/x\,\mathrm{YY} - (2+13/(3x)-1/x^2)\,f\,) \\
& -(20/(3x) - 13/(6x^2) - 1/(2x^3))\,f^2 \\
& -1 + 3/x + 2/x^2\zeta(3) - 1/(2x^2) + (55/12 - 4\zeta(3) - \ell - \frac{1}{d-4})
\end{aligned} \tag{164}
$$

in agreement with Ref. [49]. The UV singular terms proportional to $1/(d-4)$ as well as the renormalization scale μ dependent terms cancel in the physical quantities given below. In the $\overline{\mathrm{MS}}$ scheme $\frac{1}{d-4} + \ell \equiv -1/2\ln(\mu^2/m^2)$. We have written the r.h.s as analytic functions. The imaginary parts are nonzero only for $s \geq 4m^2$. The real parts are evaluated as follows: In the physical regions $s \leq 0$ and $s \geq 4m^2$ the functions h and g and the di- and tri-logarithms ($\mathrm{Li}_2(\xi)$, $\mathrm{Li}_3(\xi)$) are real. While in the space like region f is also real, in the timelike physical region, $s \geq 4m^2$, $\ln\xi = \ln|\xi| + i\pi$ and the only changes are the replacements $f^2 \to (\mathrm{Re}f)^2 - \frac{\pi^2}{4}$ and $f \to \mathrm{Re}f$. In the unphysical region $0 \leq s \leq 4m^2$ we have to replace

$$
\begin{aligned}
\ln\xi &\to i\varphi \\
\sqrt{1-1/x} &\to -\sqrt{1/x-1} \\
\mathrm{XX} &\to \mathrm{ReXX} = \mathrm{Re}\Delta\mathrm{Li}_3 + \frac{8}{3}\frac{\varphi}{2}\mathrm{Im}\Delta\mathrm{Li}_2 + \frac{4}{3}\,(-\frac{\varphi^2}{4})\,\mathrm{Re}(2h+g) \\
\mathrm{YY} &\to \mathrm{ImYY} = \frac{8}{3}\,(\mathrm{Im}\Delta\mathrm{Li}_2 - 2\frac{\varphi}{2}\,\mathrm{Re}(2h+g)) \\
2h+g &\to \mathrm{Re}(2h+g) = 2\ln(2\sqrt{1-x}) + \ln(2\sqrt{x}) \\
f &\to \mathrm{Im}f = -\frac{\varphi}{2} \\
f^2 &\to f^2 = -\frac{\varphi^2}{4}
\end{aligned} \tag{165}
$$

where $\varphi = 2\arcsin\sqrt{x}$ and

$$
\begin{aligned}
\mathrm{Im}\Delta\mathrm{Li}_2 &= C\ell_2(\varphi) - C\ell_2(2\varphi) \\
\mathrm{Re}\Delta\mathrm{Li}_3 &= 2C\ell_3(\varphi) - C\ell_3(2\varphi)
\end{aligned}
$$

are given by differences of Clausen functions.

The two-loop contribution to the Adler function related to the QCD vector neutral current vacuum polarization amplitude it is given by

$$\dot{\Pi}_V^{'(2)} = \frac{1}{3}\left(\mathrm{Re}\Pi_V^{NC}(s)/s - \mathrm{Re}\dot{\Pi}_V^{NC}(s)\right) .$$

Explicitely:

$$\begin{aligned} 12\pi^2\,\dot{\Pi}_V^{'(2)} &= -2y^2\,\mathrm{XX} + \sqrt{1-y}\,\left((1+y)\,\mathrm{YY} - 14/3\,y\,f\,\right) \\ &\quad + \left(3y^2 - 4 - 4/(1-y)\right)\,f^2 \\ &\quad +1 + 11/3\,y + 2y^2\,\zeta(3)\ . \end{aligned}$$

For the CC amplitudes (taking $m_b = 0$), we introduce the abbreviations

$$\begin{aligned} a = \ln(-x);\ \ b = \ln(1-x) \\ \alpha = \ln(x);\ \ \beta = \ln(x-1) \end{aligned}$$

and define, in analogy to the NC case,

$$\begin{aligned} \mathrm{AA} &= \frac{1}{6}\,(-2\mathrm{Li}_2(\frac{1}{1-x}) + \alpha\beta - \beta^2) \\ \mathrm{BB} &= \frac{\alpha}{6} \\ \mathrm{XX} &= -\mathrm{Li}_3(x) - \mathrm{Li}_3(\frac{-x}{1-x}) + \frac{2}{3}\,b\,\mathrm{Li}_2(x) + \frac{b}{6}\,(b^2 - 2\zeta(2)) \\ \mathrm{YY} &= \frac{1}{6}\mathrm{Li}_2(x)\ . \end{aligned}$$

The charged current (W-propagator) two-loop QCD vacuum polarization then reads

$$\begin{aligned} \frac{\pi}{m^2} Im\Pi_W^{CC} &= (2x - 3 + 1/x^2)\ \mathrm{AA} + (2x + 1 - 1/x)\ \mathrm{BB} \\ &\quad +(4x - 3 - 6/x + 5/x^2)\ \frac{-\beta}{12} \\ &\quad +(6x - 15 + 4/x + 5/x^2)\frac{1}{24} \quad ;\ \ x \geq 1\ . \\ \frac{\pi^2}{m^2} Re\Pi_W^{CC} &= (2x - 3 + 1/x^2)\ \frac{1}{2}\mathrm{XX} + (2x + 1 - 1/x)\ \mathrm{YY} \\ &\quad +(4x - 3 - 6/x + 5/x^2)\frac{b^2}{24} \\ &\quad +(6x - 15 + 4/x + 5/x^2)\frac{-b}{24} \\ &\quad +\frac{\zeta(3)}{2}\ (2x - 3)\ + \frac{\zeta(2)}{12}\ (4x - 7 - 2/x) + 13/12 - 5/(24x) \\ &\quad +\frac{1}{4}\,x\,(55/12 - 4\zeta(3) - \ell - \frac{1}{d-4}) \\ &\quad +\frac{1}{4}\,(-11/8 + 6\zeta(3) + 3\zeta(2) - 11/2\ell + 3\ell^2 + \frac{2}{d-4}(3\ell - 11/4) + \frac{6}{(d-4)^2}) \end{aligned}$$

$$
\begin{aligned}
\pi^2\, Re\dot{\Pi}_W^{CC} &= (1-1/x^3)\ \mathrm{XX} + (1/x+2/x^2)\ \mathrm{YY} \\
&+(1+1/x-2/x^2)\ \frac{b^2}{4x} \\
&+(3+1/x+/x^2-5/x^3)\ \frac{-b}{12} \\
&+\zeta(3)+\frac{\zeta(2)}{6x}\ (1+2/x)-\frac{1}{24}\ (6-9/x-10/x^2) \\
&+\frac{1}{4}\ (55/12-4\zeta(3)-\ell-\frac{1}{d-4}) \qquad (166)
\end{aligned}
$$

in this form given in Ref. [49]. The formula for the derivative is new. The expressions for the real parts are adequate for $x \leq 1$, where all quantities on the r.h.s. are real. For $x \geq 1$ one uses

$$
\begin{array}{rcrcl}
\mathrm{XX} & \to & \mathrm{ReXX} & = & \mathrm{Li}_3(\frac{1}{1-x}) + \frac{2}{3}\beta \mathrm{Li}_2(\frac{1}{1-x}) + (\frac{\beta^2}{6} - \zeta(2))\ (\beta-\alpha) - \zeta(3) \\
\mathrm{YY} & \to & \mathrm{ReYY} & = & \frac{1}{6}\ (\mathrm{Li}_2(\frac{1}{1-x}) - \alpha\beta + \frac{1}{2}\beta^2 + 2\zeta(2)\ ) \\
b^2 & \to & \mathrm{Re}\ b^2 & = & \beta^2 - 6\zeta(2) \\
b & \to & \mathrm{Re}\ b & = & \beta\ .
\end{array} \qquad (167)
$$

amplitudes of the flavor diagonal vector current.

Addendum: General results
a) Large momentum expansion:
Using the same notation for the vacuum polarization functions as in the one–loop case, and defining the latter similarly to eq. (2.3)

$$
\Pi_{T,L}^{ij}(s) \ = \ \frac{\alpha}{\pi}\ \frac{\alpha_S}{\pi}\ \left[\ v^i v^j \Pi_{T,L}^V(s) + a^i a^j \Pi_{T,L}^A(s)\ \right]
$$

one obtains for $\Pi_{T,L}^{V,A}(s)$ in the limit $|s| \to \infty$

$$
\begin{aligned}
\Pi_T^{V,A}(|s| \to \infty) &= s\ \left[\frac{1}{\epsilon} - \frac{1}{2}(\rho_a+\rho_b) + \frac{1}{2}(\log\alpha + \log\beta) + \frac{55}{12} - 4\zeta(3)\right] \\
&+ (m_a \mp m_b)^2 \left[\frac{6}{\epsilon^2} + \frac{1}{\epsilon}\left(\frac{11}{2} - 3\rho_a - 3\rho_b\right) - \frac{11}{4}(\rho_a+\rho_b) - \frac{11}{8}\right. \\
&+ \left.\frac{3}{4}(\rho_a+\rho_b)^2 - \frac{9}{4}(\log\alpha+\log\beta) - \frac{3}{2}\log\alpha\log\beta + 6\zeta(3)\right] \\
&+ (m_a^2 - m_b^2)\log\frac{m_a^2}{m_b^2}\left[-\frac{3}{\epsilon} + \frac{3}{2}(\rho_a+\rho_b) - \frac{3}{4}(\log\alpha+\log\beta) + \frac{3}{4}\right] \\
&+ 3(m_a^2+m_b^2)(\log\alpha+\log\beta) \\
\Pi_L^{V,A}(|s| \to \infty) &= (m_a \mp m_b)^2 \left[\frac{6}{\epsilon^2} + \frac{1}{\epsilon}\left(\frac{11}{2} - 3\rho_a - 3\rho_b\right) - \frac{11}{4}(\rho_a+\rho_b) - \frac{3}{8}\right. \\
&+ \left.\frac{3}{4}(\rho_a+\rho_b)^2 - \frac{9}{4}(\log\alpha+\log\beta) - \frac{3}{2}\log\alpha\log\beta + 6\zeta(3)\right] \\
&+ (m_a^2 - m_b^2)\log\frac{m_a^2}{m_b^2}\left[-\frac{3}{\epsilon} + \frac{3}{2}(\rho_a+\rho_b) - \frac{3}{4}(\log\alpha+\log\beta) - 5\right]
\end{aligned}
$$

with $\alpha = -m_a^2/s,\ \beta = -m_b^2/s$ and $\zeta(3) = 1.202$. At this stage a few remarks are mandatory.

i) In the previous expressions the momentum transfer is defined in the space–like region, $s < 0$. The continuation to the physical region can be straightforwardly obtained by adding a small imaginary part $-i\epsilon$ to the quark masses squared. This reduces to make the substitutions $\log(m_{a,b}^2/-s) \to \log|m_{a,b}^2/-s| + i\pi$.

ii) As expected, only the transverse part of the vacuum polarization function is quadratically divergent for $|q| \to \infty$. This divergent term, the expression of which is in agreement with the one obtained in Ref. [**?**], is the same for axial and axial–vector currents as expected from chiral symmetry. Moreover, as required by the Kinoshita–Lee–Nauenberg theorem [**?**], this term does not introduce any mass singularity as $m_{a,b}$ tend to zero: $-(\rho_a+\rho_b)$ and $\log\alpha+\log\beta$ combine to give $2\log(\mu^2/-s)$.

iii) Since the vector part of the longitudinal component should vanish for $m_a = m_b$, it must be proportional to $(m_a - m_b)$ or $(m_a^2 - m_b^2)$; and since the axial–vector component can be obtained by changing the sign of one of the two masses, it must be proportional $(m_a + m_b)$ or $(m_a^2 - m_b^2)$ [$\log m_a^2/m_b^2$ alone would have introduced mass singularities]. This behavior is explicitely exhibited by the previous expression of $\Pi_L^{V,A}(s)$.

Let us now write the real parts of $\Pi_T^{V,A}(s)$, analogously to eq. (2.10),

$$\Pi_T^{V,A}(s) = s\tilde{X}_2 + (m_a \mp m_b)^2\tilde{Y}_2 + (m_a^2 - m_b^2)\log\frac{m_a^2}{m_b^2}\,\tilde{Z}_2 + F_2^{V,A}(s)$$

where the two–loop divergent constants $\tilde{X}_2$, $\tilde{Y}_2$ and $\tilde{Z}_2$ involve only the poles in ϵ and the logarithms of the scale μ of the expressions of eq. (3.3); they are given by

$$\begin{aligned}
\tilde{X}_2 &= \frac{1}{\epsilon} - \log\frac{m_a m_b}{\mu^2} \\
\tilde{Y}_2 &= \frac{6}{\epsilon^2} + \frac{2}{\epsilon}\left(\frac{11}{4} - 3\log\frac{m_a m_b}{\mu^2}\right) - \frac{11}{2}\log\frac{m_a m_b}{\mu^2} + 3\log^2\frac{m_a m_b}{\mu^2} \\
\tilde{Z}_2 &= -\frac{3}{\epsilon} + 3\log\frac{m_a m_b}{\mu^2}
\end{aligned}$$

b) Low momentum expansion:

We come now to the discussion of the zero–momentum transfer behavior of the vacuum polarization functions. In this limit, the evaluation of the two–loop diagrams Fig. 1b in the on–shell mass scheme, leads to the following expression for $\Pi_{T,L}^{V,A}(0)$

$$\begin{aligned}
\Pi_{T,L}^{V,A}(0) &= \frac{6}{\epsilon^2}(m_a^2+m_b^2) + \frac{2}{\epsilon}\left[\frac{11}{4}(m_a^2+m_b^2) - 3m_a^2\rho_a - 3m_b^2\rho_b\right] - \frac{11}{2}(m_a^2\rho_a + m_b^2\rho_b) \\
&+ 3m_a^2\rho_a^2 + 3m_b^2\rho_b^2 + \frac{35}{8}(m_a^2+m_b^2) + \frac{1}{4}(m_a^2-m_b^2)\left[G\left(\frac{m_a^2}{m_b^2}\right) - G\left(\frac{m_b^2}{m_a^2}\right)\right] \\
&+ \frac{m_a^2 m_b^2}{m_a^2-m_b^2}\log\frac{m_a^2}{m_b^2} + m_a^2 m_b^2\frac{m_a^2+m_b^2}{(m_a^2-m_b^2)^2}\log^2\frac{m_a^2}{m_b^2} \\
&\pm m_a m_b\left[-\frac{12}{\epsilon^2} + \frac{2}{\epsilon}\left(3\rho_a + 3\rho_b - \frac{11}{2}\right) - \frac{3}{2}(\rho_a+\rho_b)^2 + 4(\rho_a+\rho_b) - \frac{31}{4}\right. \\
&+ \left. 3\frac{m_a^2\rho_b - m_b^2\rho_a}{m_a^2-m_b^2} + 3\frac{m_a^2 m_b^2}{(m_a^2-m_b^2)^2}\log^2\frac{m_a^2}{m_b^2}\right]
\end{aligned}$$

where, in terms of the Spence function defined by $\mathrm{Li}_2(x) = -\int_0^1 y^{-1}\log(1-xy)\mathrm{d}y$, the function G is given by

$$G(x) = 2\mathrm{Li}_2(x) + 2\log x\log(1-x) + \frac{x}{1-x}\log^2 x$$

As one might have expected, there is no singularity in the self–energies in this limit. In addition, besides the manifest symmetry in the exchange $m_a \leftrightarrow m_b$, the previous expressions exhibit the facts that $\Pi^{V,A}_{T,L}(0)$ can be obtained from $\Pi^{A,V}_{T,L}(0)$ by simply making the substitution $m_a(m_b) \to -m_a(-m_b)$ as expected from γ_5 reflection symmetry and that the longitudinal and transverse components are equal. These features provide good checks of the calculation.

Using the previous expression, one readily obtains the QCD corrections to the contribution of a heavy quark isodoublet to the ρ parameter in the general case $m_a \neq m_b \neq 0$. Defining the contribution to the ρ parameter analogously to eq. (2.15)

$$\Delta^{(2)}\rho = \frac{\sqrt{2}G_F}{8\pi^2}\frac{\alpha_s}{\pi}\ f_2(0, m_a, m_b)$$

the function f_2 will be given by

$$\begin{aligned} f_2(0, m_a, m_b) &= -3\left\{m_a^2 + m_b^2 + \ 2\ \frac{m_a^2 m_b^2}{m_a^2 - m_b^2}\log\frac{m_a^2}{m_b^2}\left[1 + \frac{m_a^2 + m_b^2}{m_a^2 - m_b^2}\log\frac{m_b^2}{m_a^2}\right] + (m_a^2 - m_b^2)\right. \\ &\left. \times\left[2\mathrm{Li}_2\left(\frac{m_a^2}{m_b^2}\right) + 2\log\frac{m_a^2}{m_b^2}\log\left(1 - \frac{m_a^2}{m_b^2}\right) - \frac{m_a^2}{m_a^2 - m_b^2}\log^2\frac{m_a^2}{m_b^2} - \frac{\pi^2}{3}\right]\right\} \end{aligned}$$

$f_2(0, m_a, m_b)$ is free of ultraviolet divergences as it should be since $\Delta\rho$ is an observable physical quantity; furthermore it does not depend on the 't Hooft mass scale μ. Note that the symmetry in the interchange of m_a and m_b is now hidden in the term in the last line of the previous equation, but this term is simply $G(m_a^2/m_b^2) - G(m_b^2/m_a^2)$ and we have used the fact that $G(1/x) + G(x) = 2\pi^2/3$.

In the limit of large mass splitting between the two quarks, $m_a \gg m_b$, the QCD corrections to the ρ parameter reduce to the known result for $m_b = 0$ [**?**]

$$f_2(0, m_a, 0) = -\frac{2}{3}\ f_1(0, m_a, 0)\ \frac{\alpha_S}{\pi}\left(1 + \frac{\pi^2}{3}\right)$$

5. THE Z LINE-SHAPE

To lowest order, the total cross-section for $e^+e^- \to f\bar{f}$ is given by Eq. (46)

$$\begin{aligned}\sigma_0 &= \frac{4\pi}{3}\frac{\alpha^2 Q_f^2}{s} N_{cf} R_v^f \\ &\quad -2\alpha Q_f \frac{\sqrt{2}G_\mu M_Z^2}{3s} N_{cf} Re\chi v_e v_f R_v^f \\ &\quad +\frac{G_\mu^2 M_Z^4}{6\pi s} N_{cf} |\chi|^2 (v_e^2+a_e^2)(v_f^2 R_v^f + a_f^2 R_a^f)\end{aligned} \tag{168}$$

where

$$\chi(s) = \frac{s}{s - M_Z^2 + iM_Z\Gamma_Z(s)} \tag{169}$$

is the Z-resonance factor. The three terms represent the QED, the γZ -interference and the Z-exchange contributions. The functions

$$R_v^f = \sqrt{1-\frac{4m_f^2}{s}}\,(1+\frac{2m_f^2}{s}), \quad R_a^f = \sqrt{1-\frac{4m_f^2}{s}}\,(1-\frac{4m_f^2}{s})$$

describe the dependence on the mass of the final state particles. For the light fermions $R_v^f \simeq R_a^f \simeq 1$. The s-dependent "width", appearing in the Z propagator in Eq. (169), is determined by the imaginary part of the Z self-energy $M_Z\Gamma_Z(s) = Im\Pi_Z(s)$ [57]. To lowest order one has

$$\begin{aligned}\Gamma_Z(s) &= \frac{\sqrt{2}G_\mu M_Z s}{3\pi}\sum_f N_{cf}(v_f^2 R_v^f + a_f^2 R_a^f) \\ &\simeq \frac{\sqrt{2}G_\mu M_Z s}{3\pi}\sum_f N_{cf}(v_f^2+a_f^2) = \frac{s}{M_Z^2}\Gamma_Z.\end{aligned} \tag{170}$$

The s dependence of the width causes a large shift by $\Delta E = -\frac{\Gamma_Z^2}{2M_Z}$ of the maximum of the peak (see below).

Near the Z-resonance the *weak* corrections can be included using Eq. (106) and $\alpha \to \alpha(M_Z^2) \simeq (128.797(123))^{-1}$ in the Born formula. Away from the resonance this approach may be generalized by evaluating the the ρ_f's and κ_f's at $s = 4E_b^2 \neq M_Z^2$ (E_b the beam energy), thereby they are no longer gauge invariant and the box contributions must be included

$$\sigma_{tot} = \sigma_{0,eff} + \delta\sigma_{box} \tag{171}$$

in order to get a gauge invariant cross-section. However, numerically it turns out that the box contributions are negligible ($\lesssim 0.05\%$ within $M_Z \pm 10$ GeV) in the 't Hooft-Feynman gauge.

Using the effective parameters one arrives at an *improved Born approximation* which in the resonance region takes the form [57-60]

$$\sigma_{eff}(s) = \frac{12\pi\hat{\Gamma}_e\Gamma_f}{|D(s)|^2}\left\{\frac{s}{M_Z^2} + \mathcal{R}_f\frac{s-M_Z^2}{M_Z^2} + \mathcal{I}_f\frac{\Gamma_Z}{M_Z} + \cdots\right\} + \sigma_{QED}^f \tag{172}$$

where

$$D(s) = s - M_Z^2 + iM_Z\Gamma_Z(s)\ , \quad \Gamma_Z(s) = \Gamma_Z\left\{\frac{s}{M_Z^2} + \varepsilon\,\frac{s-M_Z^2}{M_Z^2} + \cdots\right\}$$

and

$$\sigma^f_{QED} = \frac{4\pi\alpha^2(M_Z^2)Q_f^2 N_{cf} K_{QCD}}{3s} \simeq \begin{cases} 0.006\ \sigma^f_{peak} & (f = \mu, \tau) \\ 0.001\ \sigma^f_{peak} & (hadrons) \end{cases} \tag{173}$$

the QED background term. Since initial state radiation will be taken into account separately we have replaced Γ_e by $\hat{\Gamma}_e = \Gamma_e/(1 + \frac{3\alpha}{4\pi})$. The expansion Eq. (172) near the peak makes use of the fact that $\frac{s-M_Z^2}{M_Z^2}$ and $\frac{\Gamma_Z}{M_Z}$ are of order $O(\alpha)$ near the resonance. The correction terms $\mathcal{R}_f$, $\mathcal{I}_f$ and ε are calculable functions within the Standard Model [60]. $\mathcal{I}_f$ and ε represent absorptive effects depending on known particles in the spectrum up to the Z mass only. The correction $\varepsilon = \sum_f \varepsilon_f$, which takes into account possible final state mass effects (according to Eq. (170) $\varepsilon_f \simeq \frac{6m_f^2}{M_Z^2}\frac{\Gamma_f}{\Gamma_Z}\frac{a_f^2}{v_f^2+a_f^2} \simeq 1.7 \times 10^{-3}$ $(f = b)$), is negligible for all the 5 known light fermions. The correction $\mathcal{I}_f$ leads to a small change of the normalization of the peak by $(1 + \mathcal{I}_f \frac{\Gamma_Z}{M_Z})$, whereas the effect of $\mathcal{R}_f$ is a slight shift to the right of the maximum of the peak. The leading (tree level) contribution to $\mathcal{R}_f$ is the γ-Z interference term (see Eq. (168))

$$\mathcal{R}_f = \frac{8Q_eQ_fv_ev_f}{(v_e^2+a_e^2)(v_f^2+a_f^2)}\frac{\pi\alpha(M_Z^2)}{\sqrt{2}G_\mu M_Z^2} + \cdots\ . \tag{174}$$

Notice that an extra neutral vector boson Z' would yield an additional interference term

$$\Delta\mathcal{R}_f = \frac{2\ (v'_ev_e + a'_ea_e)(v'_fv_f + a'_fa_f)}{(v_e^2+a_e^2)(v_f^2+a_f^2)}\frac{g'^2}{\sqrt{2}G_\mu(M_Z^2 - M_{Z'}^2)} \tag{175}$$

if we assume the coupling is given by

$$\mathcal{L}^{Z'}_{NC,int} = g'Z'_\mu \bar{f}\gamma^\mu\ (v'_f - a'_f\gamma_5)\ f\ . \tag{176}$$

All other contributions are small loop-corrections. Numerical values are given in Table 8. For $\mathcal{I}_f$ the values range from $\simeq -1.0 \times 10^{-2}$ for lower top masses to $\simeq -2.2 \times 10^{-2}$ for $m_t = 230$ GeV. Within the Standard Model the effects of the corrections $\mathcal{I}_f$and ε to the line-shape are negligible.

Since Eq. (172) models the Z-peak to high accuracy, a model-independent fit with 4 parameters, the cross-section at maximum (normalization), M_Z, Γ_Z and $\mathcal{R}_f$, is possible for each flavor f. Thus, the measurement of $\sigma(e^+e^- \to f\bar{f})$ at 5 different beam energies will fully determine the characteristics of the Z-resonance.

We ignore the corrections $\mathcal{R}_f$, $\mathcal{I}_f$, ε and σ^f_{QED}, for the moment. Then, $\sigma_{eff}(s)$ differs from a Breit-Wigner (BW) form only by the s-dependence of the width, i.e. by a substitution

$$s - M_Z^2 + iM_Z\Gamma_Z \to s - M_Z^2 + is\Gamma_Z/M_Z = (1 + i\gamma)(s - \tilde{M}_Z^2 + i\tilde{M}_Z\tilde{\Gamma}_Z)$$

with

$$\tilde{M}_Z = M_Z\ (1+\gamma^2)^{-1/2},\ \ \tilde{\Gamma}_Z = \Gamma_Z\ (1+\gamma^2)^{-1/2},\ \ \gamma = \frac{\Gamma_Z}{M_Z} = \frac{\tilde{\Gamma}_Z}{\tilde{M}_Z}. \tag{177}$$

Thus, with $\sigma_{BW}(s = M_Z^2) = \sigma_f^{peak}$, we may write

$$\sigma_{eff}(s) = \sigma_{BW}(s = M_Z^2) \cdot \frac{s\tilde{\Gamma}^2}{(s - \tilde{M}^2)^2 + \tilde{M}^2\tilde{\Gamma}^2} \tag{178}$$

as a Breit-Wigner resonance in the reduced parameters Eq. (177) [61]. By Eq. (177), the peak gets shifted by $\tilde{M}_Z - M_Z \simeq -34$ MeV and narrowed by $\tilde{\Gamma}_Z - \Gamma_Z \simeq -1$ MeV (negligible). The peak height remains unchanged.

If we ignore σ^f_{QED} in Eq. (172), the position of the peak is at

$$\sqrt{s_{max}} = \tilde{M}_Z \, (1 + \gamma^2(1 + \mathcal{R}_f))^{1/4} \tag{179}$$

with

$$\sigma_{eff,max} = \sigma_f^{peak} \frac{(1+\gamma^2)^{1/2} + 1}{2} \, (1 + \mathcal{I}_f \gamma) \tag{180}$$

and right and left half-maxima at

$$\sqrt{s_\pm} \simeq \left(\tilde{M}_Z \, (1+\gamma^2)^{1/2} \pm \frac{\tilde{\Gamma}_Z}{2} \right) / (1 + \gamma^2(1 - 4\mathcal{R}_f))^{1/8}. \tag{181}$$

The slowly varying QED background term slightly rises the peak such that the width of the peak measured between the half-maxima appears increased by $\delta(\sqrt{s_+} - \sqrt{s_-}) \simeq \Gamma_Z \cdot \frac{\sigma_{QED}}{\sigma_{peak}} \simeq 15$ MeV for $(f = \mu, \tau)$. This term will be enhanced by QED corrections to $\delta(\sqrt{s_+} - \sqrt{s_-}) \simeq \Gamma_Z \cdot \frac{\sigma^{obs}_{QED}}{\sigma^{obs}_{peak}} \simeq$ 30 MeV.

In order to obtain the observed cross-section, we have to include the QED corrections, the virtual, soft and hard photon effects. Particularly important is the initial state radiation which leads to

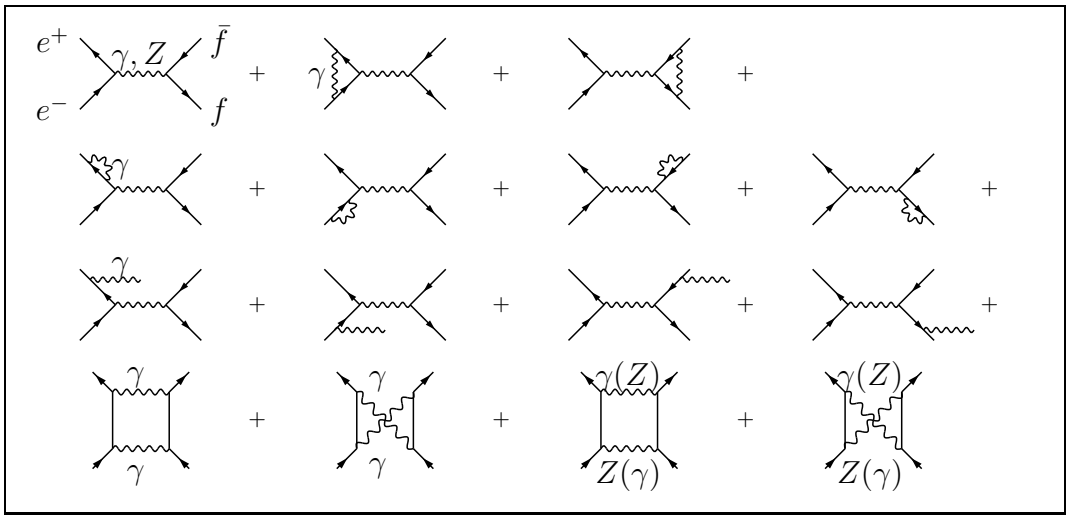

Figure 22: $O(\alpha)$ QED corrections to $e^+e^- \to f\bar{f}$

huge corrections in the line shape. Multi soft-photon emission must be taken into account in order to reach the precision needed. Due to initial-state photon emission the shape of the resonance is changed according to the convolution integral

$$\sigma^{obs}_{ini}(s) = \int_0^{k_{max}} dk \; \rho_{ini}(k) \sigma_{eff}(s(1-k)) \tag{182}$$

where $\rho_{ini}(k)$ is the photon radiation spectrum [62], which has been calculated up to two-loop order [63]. The variable $k = E_\gamma / E_b$ is the energy of the emitted photon in units of the beam energy, such that $s' = s\,(1-k)$ is the effective s available for Z-production after the photon has been emitted.

k_{max} is the maximum photon energy accepted, $k_{max} = 1 - s_0/s$ in terms of the minimum invariant mass $s_0 \geq 4m_f^2$ needed to identify the final state $f\bar{f}$ pair.

The structure of the photon distribution function is

$$\rho_{ini}(k) = \beta k^{\beta-1}(1 + \delta_1^{v+s} + \delta_2^{v+s}) + \delta_1^h + \delta_2^h \tag{183}$$

with $\beta = \frac{2\alpha}{\pi}\left(\ln\frac{s}{m_e^2} - 1\right) \simeq 0.1077$. The infrared sensitive part has been exponentiated, which takes into account multi soft photon emission [64]. Exponentiation leads to a shift of the peak by $\Delta E = 14$ MeV. The corrections are given by (v+s = virtual+soft, h = hard)

$$\begin{aligned}
\delta_1^{v+s} &= \frac{\alpha}{\pi}\left(\frac{3}{2}L + \frac{\pi^2}{3} - 2\right) \\
\delta_2^{v+s} &= \left(\frac{\alpha}{\pi}\right)^2\left((\frac{9}{8} - \frac{\pi^2}{3})L^2 + s_{21}L + s_{20}\right) \\
\delta_1^h &= \frac{\alpha}{\pi}(1-L)(2-k) \\
\delta_2^h &= \left(\frac{\alpha}{\pi}\right)^2(h_{22}L^2 + h_{21}L + h_{20})
\end{aligned} \tag{184}$$

where $L = \ln\frac{s}{m_e^2}$ ($\simeq$24.18), $h_{22} = -\frac{1+(1-k)^2}{k}\ln(1-k) + (2-k)(\frac{1}{2}\ln(1-k) - 2\ln k - \frac{3}{2}) - k$ and the other two-loop correction coefficients s_{2i} and h_{2i} are given in [63]. The main influence on the Z line-shape is a reduction of the peak height

$$\begin{aligned}
\left(\frac{\sigma^{obs}}{\sigma_{eff}}\right)_{peak} &\simeq \left(\frac{\Gamma_Z}{M_Z}\right)^\beta(1 + \delta_1^{v+s}) + \cdots + \frac{\sigma_{QED}(1 + \delta_{QED}^{NR})}{\sigma_{peak}} \\
&\simeq 0.738 + \cdots \simeq \begin{cases} 0.744 & f = \mu, \tau \\ 0.739 & hadrons \end{cases}
\end{aligned} \tag{185}$$

with an error ± 0.001, and a shift of the maximum of the peak

$$\begin{aligned}
\sqrt{s_{max}} &\simeq M_Z + \frac{\pi}{8}\beta\Gamma_Z - \frac{\Gamma_Z^2}{4M_Z}(1 - \mathcal{R}_f) + \cdots \\
&\simeq M_Z + 108.4\ MeV - 17.0\ MeV + \cdots \\
&\simeq M_Z + \begin{cases} 92\ MeV & f = \mu, \tau \\ 93\ MeV & hadrons \end{cases} .
\end{aligned} \tag{186}$$

The first correction is the QED effect the second the phase space effect which includes the effect due to the s-dependence of the width in the Z-propagator, Eq. (169). To good accuracy, the observed peak cross-section is represented by

$$\sigma_{peak}^{obs} = \left(\frac{\sigma^{obs}}{\sigma_{eff}}\right)_{peak}\frac{12\pi\Gamma_e\Gamma_f}{M_Z^2\Gamma_Z^2} + \sigma_{QED}^{obs}(M_Z^2) \tag{187}$$

where

$$\begin{aligned}
\sigma_{QED}^{obs}(M_Z^2) &= \sigma_{QED}(M_Z^2)(1 + \delta_{QED}^{NR}) \\
\delta_{QED}^{NR} &\simeq \left(\frac{\beta}{2}\ln\frac{M_Z^2}{s_{0f}} + \frac{\beta}{4} + \frac{\alpha}{\pi}(\frac{\pi^2}{3} - \frac{1}{2})\right)
\end{aligned}$$

and s_{0f} is the minimum invariant mass for the final state $f\bar{f}$ pair. If we chose $s_{0\mu} = 4m_\mu^2$ for muons and $s_{0h} = (10\ \text{GeV})^2$ for hadrons we obtain $\delta_{QED}^{NR} = 0.678$ for leptons and 0.271 for hadrons.

A very important observation is that this result is practically independent of the model dependent correction $\Delta\rho$, since the ratio $(\Gamma_e\Gamma_f)/\Gamma_Z^2$ is almost insensitive to the rescaling $\Gamma_i \to \rho_i\Gamma_i$, because the large contributions to ρ_i are universal if $i \neq b$. An exception is the top contribution from the $Zb\bar{b}$ vertex. The width can be extracted unambiguously from the location of the half-maxima

$$\begin{aligned}\sqrt{s_+} - \sqrt{s_-} &\simeq \Gamma_Z\,(1 + (\frac{\pi}{4}\beta + \frac{\beta}{2}\ln 2)\,(1 + \beta + \frac{\pi}{4}\beta) \\ &\quad - \frac{\pi}{2}\beta\gamma - \frac{5}{8}\gamma^2 + \cdots + \frac{\sigma_{QED}^{obs}}{\sigma_{peak}^{obs}}\,(1 + \beta + \frac{\pi}{4}\beta)) \\ &\simeq \Gamma_Z + \begin{cases} 396 \pm 4\text{MeV} & f = \mu, \tau \\ 360 \pm 3\text{MeV} & hadrons \end{cases} .\end{aligned} \tag{188}$$

For a more detailed discussion we refer to Ref. [65].

The important observation is that, to high accuracy, these effects only depend on M_Z and Γ_Z and universal QED corrections and phase space terms. This makes possible an unambiguous (model independent) extraction of M_Z and Γ_Z from the line-shape. For numerical results see Tab. 8.

Table 8a. The Z line-shape for $e^+e^- \to \mu^+\mu^-$ ($M_Z = 91.176 \pm 0.021$ GeV, $\alpha_s = 0.117 \pm 0.01$). Masses and energies are in GeV. Results in the upper (lower) part are before (after) QED corrections are taken into account.

m_t	m_H	σ_{max} (nb)	$\sqrt{s_{max}}$	$\sqrt{s_-}$	$\sqrt{s_+}$	$\mathcal{R}_f \cdot 10^2$
90	100	2.001	91.159	89.920	92.416	2.50
110	100	2.003	91.159	89.919	92.418	2.64
130	50	2.003	91.159	89.916	92.420	2.89
130	100	2.004	91.159	89.917	92.420	2.80
130	1000	2.006	91.159	89.921	92.416	2.48
150	100	2.005	91.159	89.914	92.422	2.99
200	100	2.009	91.159	89.907	92.429	3.61
230	100	2.011	91.159	89.902	92.435	4.09
90	100	1.491	91.267	89.969	92.845	
110	100	1.492	91.267	89.968	92.847	
130	50	1.493	91.267	89.965	92.850	
130	100	1.493	91.267	89.966	92.850	
130	1000	1.494	91.267	89.969	92.844	
150	100	1.495	91.268	89.964	92.853	
200	100	1.498	91.268	89.957	92.863	
230	100	1.501	91.269	89.951	92.870	

Table 8b. The Z line-shape for $e^+e^- \to hadrons$

m_t	m_H	σ_{max} (nb)	$\sqrt{s_{max}}$	$\sqrt{s_-}$	$\sqrt{s_+}$	$\mathcal{R}_f \cdot 10^2$
90	100	41.403	91.160	89.928	92.411	6.70
110	100	41.416	91.160	89.926	92.413	6.89
130	50	41.425	91.160	89.924	92.416	7.23
130	100	41.423	91.160	89.925	92.415	7.11
130	1000	41.430	91.160	89.928	92.411	6.67
150	100	41.439	91.160	89.922	92.418	7.35
200	100	41.474	91.160	89.915	92.425	8.08
230	100	41.501	91.160	89.910	92.431	8.61
90	100	30.635	91.268	89.986	92.826	
110	100	30.649	91.268	89.985	92.828	
130	50	30.661	91.268	89.983	92.831	
130	100	30.659	91.268	89.983	92.831	
130	1000	30.655	91.268	89.986	92.825	
150	100	30.676	91.269	89.981	92.834	
200	100	30.720	91.269	89.974	92.844	
230	100	30.753	91.270	89.969	92.851	

So far we have not discussed the QED corrections from initial-final state interference and from final state radiation. Both are small if no tight cuts to the photon spectrum are applied. In any case an $O(\alpha)$ calculation is sufficient for these corrections which are to be added to σ_{ini}^{obs} in Eq. (182).

For the interference term we have

$$\begin{aligned}\delta\sigma_{int}^{obs}(s) &= \frac{1}{2}(\delta_{int}^{\gamma\gamma}(k_0) + \delta_{int}^{\gamma Z}(k_0)\,)\,\Delta_{0f}^{\gamma Z}(s) + \delta_{int}^{\gamma Z}(k_0)\,\Delta_{0f}^{Z}(s) \\ &\quad + \int_{k_0}^{k_{max}} dk\;\rho_{int}(k)\;\Delta_{FB}^{f\bar{f}}(s, s(1-k)) \end{aligned} \tag{189}$$

where, denoting $z = (M_Z^2 - iM_Z\Gamma_Z)/s$, [66]

$$\begin{aligned}\delta_{int}^{\gamma\gamma}(k_0) &= \frac{4\alpha Q_f}{\pi}\{2\ln k_0 - k_0 - \frac{1}{2}\} \\ \delta_{int}^{\gamma Z}(k_0) &= \frac{4\alpha Q_f}{\pi}\{2\ln k_0 + \ln|z| - Re[z(z+1)\ln\frac{k_0+z-1}{z} + (z-1)(1-k_0)]\}\end{aligned} \tag{190}$$

are the virtual contributions from the $\gamma\gamma$-boxes and the γZ-boxes, respectively, plus the real photon contribution ($E_\gamma/E_b \le k_0 \le k_{max}$). $\Delta_{0f}^{\gamma Z}$ and Δ_{0f}^{Z} have been given in Eq. (48) and

$$\rho_{int} = \frac{4\alpha Q_f}{\pi}\frac{2-k}{k} \tag{191}$$

is the photon radiation spectrum.

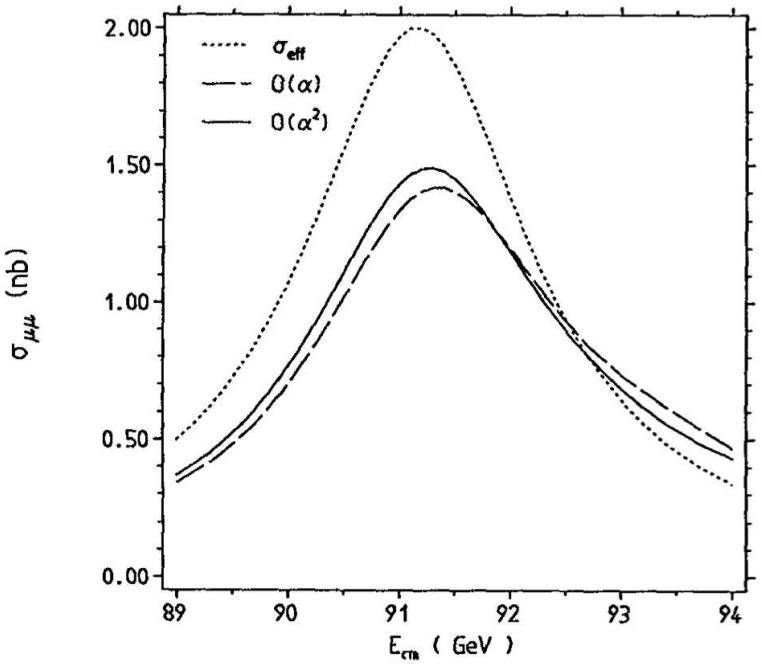

Figure 23: QED corrections to the Z line shape.

The kernel $\Delta_{FB}^{f\bar{f}}(s,s')$ follows from the C-odd function $\Delta_{FB}^{f\bar{f}}(s)$ given in Eq. (198) below by substituting

$$\begin{aligned} Re\chi(s) &\rightarrow \frac{1}{2}Re(\chi(s)+\chi^*(s')) \\ |\chi|^2(s) &\rightarrow Re(\chi(s)\chi^*(s')) \end{aligned} \tag{192}$$

such that $\Delta_{FB}^{f\bar{f}}(s,s) = \Delta_{FB}^{f\bar{f}}(s)$. Near resonance, where the γZ interference term in $\Delta_{FB}(s)$ (first term in Eq. (198)) is negligible, we have

$$\begin{aligned} \delta\sigma_{obs}^{int}(s) \simeq\ & \frac{4\alpha Q_f}{\pi}\{2\ln k_{max} + \ln|z| \\ & -Re[z(z+1)\ln\frac{k_{max}+z-1}{z} + (z-1)(1-k_{max})]\}\cdot A_{FB}(s)\,\sigma_0(s). \end{aligned}$$

For $s \simeq M_Z^2$ and loose cuts ($k_{max} \simeq 0.1-1$) the bracket reduces to $\frac{1}{2}(\Gamma_Z/M_Z)^2$, which indeed leads to a negligibly small contribution. For tight cuts the leading term in the bracket is $2\ln(k_0\frac{M_Z}{\Gamma_Z})$ which again is small compared to the term $2\ln k_0(\ln\frac{s}{m_e^2}-1)$ sensitive to cuts from the initial state bremsstrahlung and a similar term from final state radiation.

The final state radiation factors out, yielding

$$\delta\sigma_{fin}^{obs}(s) = \left(\delta_{fin}(k_0) + \int_{k_0}^{k_{max}} dk\rho_{fin}(k)\right)\ \sigma_0(s) \tag{193}$$

with

$$\delta_{fin}(k_0) = \frac{\alpha Q_f^2}{\pi}\left(2(L_f-1)\ln k_0 + \frac{3}{2}L_f + \frac{\pi^2}{3} - 2\right) \tag{194}$$

the virtual plus soft photon contribution and

$$\rho_{fin} = \frac{\alpha Q_f^2}{\pi}\frac{1+(1-k)^2}{k}\ (L_f - 1 + \ln(1-k)) \tag{195}$$

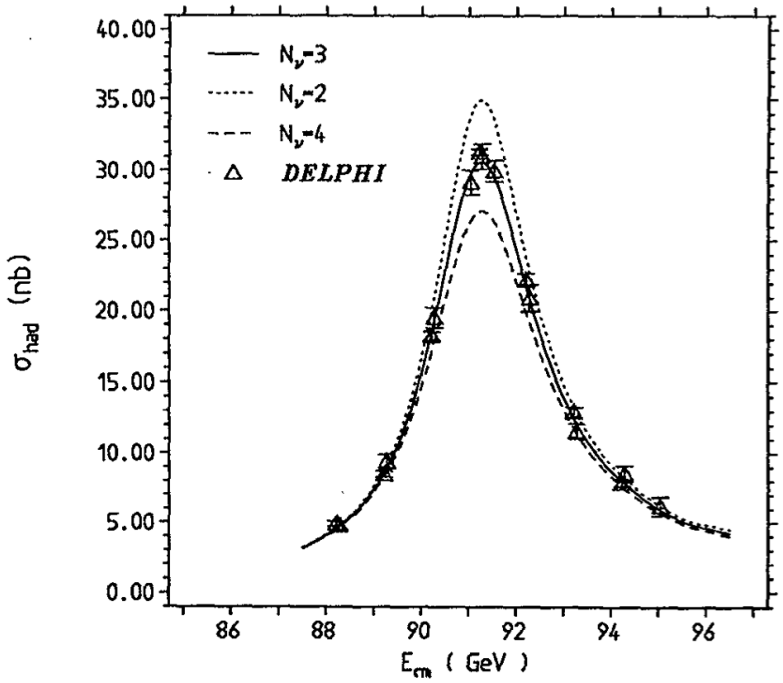

Figure 24: Example for the observed hadronic cross-section.

the hard photon radiation spectrum. If no cut is applied ($k_{max} = 1 - \frac{4m_f^2}{s} \simeq 1$) we get the small contribution

$$\delta\sigma_{obs}^{fin}(s)/\sigma_0(s) = \frac{3\alpha Q_f^2}{4\pi} \simeq 0.00174\ Q_f^2 \tag{196}$$

which already has been included in the Γ_f's (Tab. 6) and which are used in the calculation of the effective cross-section Eq. (172).

In Figure 23 we illustrate the QED corrections to the Z line-shape. Figure 24 shows some experimental data points together with the SM prediction.

6. THE FORWARD BACKWARD ASYMMERTY

In Section 3 we have discussed the various definitions and properties of asymmetries at the Born level. We have mentioned that the precision measurements of asymmetries, predominantly caused by the parity-violation of the weak interactions, belong to the most important tasks for LEP1. Of particular interest is the investigation of the asymmetries at the Z-resonance, where $e^+e^- \to f\bar{f}$ is practically a *pure weak neutral current process*, a fact which provides clean and precise tests of the NC couplings of the different flavors (see Eq. (2-4) and Section 2). Here, we shall concentrate on the discussion radiative corrections for the forward-backward asymmetry [67] $A_{FB} = \frac{\sigma_F - \sigma_B}{\sigma_F + \sigma_B}$ ($\sigma_{F(B)}$ = cross-section integrated over the forward (backward) hemisphere) which in lowest order is given by Eq. (49)

$$A_{FB}(s) = \frac{\Delta_{FB}(s)}{\sigma_0(s)} \tag{197}$$

with ($y_f = (1 - \frac{4m_f^2}{s})$)

$$\Delta_{FB}^{f\bar{f}}(s) \;=\; -\frac{\alpha Q_f\,\sqrt{2}G_\mu M_Z^2}{2s} N_{cf} Re\chi a_e a_f\, y_f \tag{198}$$

$$+\frac{G_\mu^2 M_Z^4}{2\pi s} N_{cf} |\chi|^2 v_e v_f a_e a_f \, y_f$$

and $\sigma_0(s)$ the total cross-section given in Eqs. (46),(168). In Eq. (198) the first term is the γZ-interference and the second the Z-resonance term.

At the resonance we have

$$A_{FB}^{f\bar{f}}(s = M_Z^2) = \frac{3}{4} \frac{2 v_e a_e \; 2 v_f a_f \; y_f}{(v_e^2 + a_e^2)(v_f^2 R_v^f + a_f^2 R_a^f) + (\frac{\Gamma_Z}{M_Z})^2 (16 Q_f^2 \sin^4 \Theta_f \cos^4 \Theta_f R_v^f)} \tag{199}$$

where the second term in the denominator is due to the QED background term in the total cross-section.

The finite mass effects can be ignored if $f \neq b$. For the b-quark asymmetry Eq. (158) is a good approximation.

If we neglect the small contribution $\sigma_{0,QED}$ (see Eq. (172)) to $\sigma_0(s)$, for $s = M_Z^2$ we obtain the simple expression

$$A_{FB}^{f\bar{f}} = A_{FB}^{f\bar{f}}(s = M_Z^2) = \frac{3}{4} A_e A_f \tag{200}$$

with A_f defined in Eq. (54) depending on $\sin^2 \Theta_f$ only. The *improved Born approximation* again follows by using the effective weak mixing parameter $\sin^2 \Theta_f = \kappa_f \sin^2 \Theta_W$ as discussed extensively in Section 4.3

The expected accuracies for $A_{FB}^{f\bar{f}}$ (or, equivalently, $\sin^2 \Theta_f$) are 0.0035 (0.0017) ($f = \mu$), 0.007 (0.0012) (f=s), 0.007 (0.0015) (f=c) and 0.005 (0.0009) (f=b). For A_{pol}^{τ} 0.011 (0.0014). An integrated luminosity of at least 100 pb^{-1} is assumed here.

Notice that A_{FB} is largely insensitive to the normalization of the cross-section and the s-dependence of the width, which are important for the line-shape.

Away from the resonance the correction factors ρ_f and κ_f must be evaluated at $s \neq M_Z^2$ (they are no longer gauge invariant) and the box contributions must be included

$$A_{FB}^{f\bar{f}} = (A_{FB}^{f\bar{f}})_{0,eff} + \delta(A_{FB}^{f\bar{f}})_{box} \tag{201}$$

in order to get a gauge invariant cross-section. Again, numerically the box contributions are negligible ($\lesssim 0.02\%$ within $M_Z \pm 10$ GeV) for the 't Hooft-Feynman gauge.

Due to the high precision required, leading higher order effects (beyond the one loop level) cannot be neglected. For the real parts of the effective $\sin^2 \Theta_f$, Eq. (115) together with Eq. (124) provide the correct summation of large higher order terms. The imaginary parts must be included as well since they give rise to non-negligible a $O(\alpha^2)$-contribution $\Delta A_{FB}^{f\bar{f}} = 0.002$. In Figures 25 and 26 we compare the expermental results for A_{FB}^{μ} and A_{FB}^{b}, respectively, with the theoretical prediction as a function of the top mass. In Table 9 some numerical results are presented.

Table 9. Results for $A_{FB}^{f\bar{f}}$. ($M_Z = 91.17$ GeV, $\alpha_s = 0.12$, from Ref. [69]).

m_t	m_H	A_{FB}^{ℓ}	A_{FB}^{c}	A_{FB}^{s}	A_{FB}^{b}	$A_e = A_{LR}$
90	100	0.0135	0.0687	0.0868	0.0840	0.1258
100	100	0.0138	0.0627	0.0881	0.0853	0.1277
120	100	0.0147	0.0649	0.0910	0.0881	0.1318
120	500	0.0134	0.0614	0.0864	0.0836	0.1251
120	1000	0.0128	0.0598	0.0842	0.0815	0.1220
150	100	0.0162	0.0687	0.0960	0.0929	0.1391
200	100	0.0195	0.0766	0.1062	0.1027	0.1541
250	100	0.0241	0.0866	0.1190	0.1150	0.1725

The QED corrections, including soft and hard photon emission, can be calculated in a way similar to the one outlined in the previous section for the total cross-section. The observed asymmetry is

$$A_{FB,obs}(s) = \Delta_{FB,obs}(s)/\sigma_{obs}(s)$$

where $\sigma_{obs}(s)$ is given by Eq. (182) and

$$\Delta_{FB,obs}(s) = \int_0^{k_{max}} dk\ \rho_{FB,ini}(k)(\Delta_{FB})_{0,eff}(s(1-k)). \tag{202}$$

In order to keep as close a relation to the C-even case of Eq. (182) as is possible we split off a regular kinematical factor by writing [68]

$$\rho_{FB,ini}(k) = \frac{1-k}{(1-k/2)^2}\tilde{\rho}_{ini}. \tag{203}$$

The "reduced" radiation spectrum $\tilde{\rho}_{ini}$ is then given by ρ_{ini} of Eqs. (183) and (184) with the replacements

$$\begin{aligned}
\delta_1^h &\rightarrow \delta_1^h - \frac{\alpha}{\pi}\frac{1+(1-k)^2}{k}\ln\frac{1-k}{(1-k/2)^2} \\
h_{22} &\rightarrow h_{22} + [\frac{(1-x)^3}{2x} + \frac{(1-x)^2}{\sqrt{x}}(\arctan\frac{1}{\sqrt{x}} - \arctan\sqrt{x}) \\
&\quad -(1+x)\ln x + 2(1-x)]/4
\end{aligned}$$

with $x = 1-k$. Of course the subleading terms h_{21} and h_{20} of Eq. (184) also change.

Because $A_{FB}(s)$ is a strongly increasing function in the resonance region, the effect from the initial state bremsstrahlung is very large and negative, typically $\delta A_{FB} = -0.025$, which is in modulus as large as the asymmetry itself. Certainly, a full two-loop calculation (determination of h_{21} and h_{20}) for the initial state QED corrections is the most urgent missing piece necessary to make

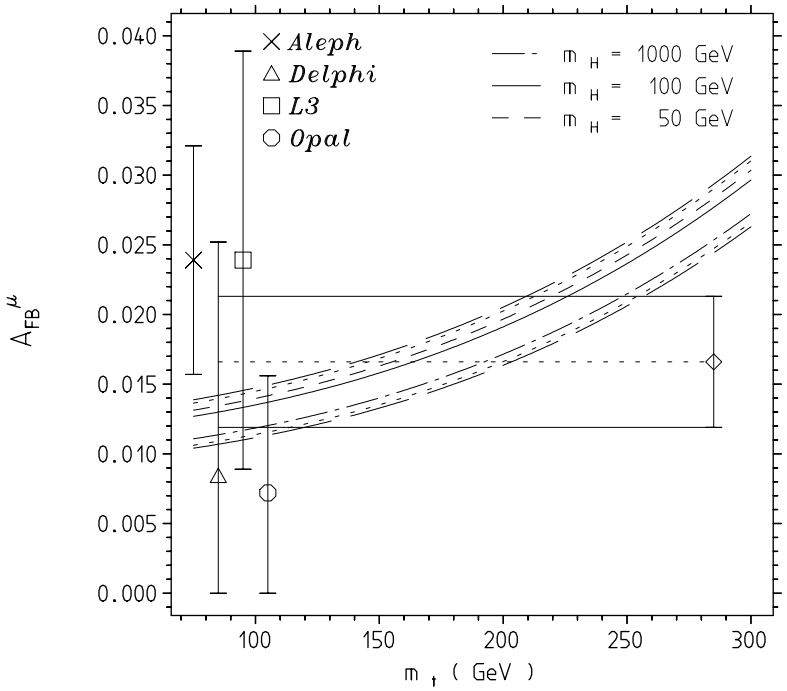

Figure 25: LEP measurement of A^{μ}_{FB}.

well established predictions for the observed asymmetry. The other $O(\alpha)$ QED-effects are the initial-final state interference and the final state corrections.

The interference term is given by

$$\begin{aligned}\delta\Delta^{int}_{FB,obs}(s) &= \delta^{\gamma\gamma}_{FB,int}(k_0)\,\sigma^{\gamma}_{0f}(s) + \frac{1}{2}\left(\delta^{\gamma\gamma}_{FB,int}(k_0) + \delta^{\gamma Z}_{FB,int}(k_0)\right)\sigma^{\gamma Z}_{0f}(s) \\ &+ \delta^{\gamma Z}_{FB,int}(k_0)\,\sigma^{Z}_{0f}(s) + \int_{k_0}^{k_{max}} dk\rho_{FB,int}(k)\;\sigma_0(s,s(1-k)) \qquad (204)\end{aligned}$$

where [68]

$$\begin{aligned}\delta^{\gamma\gamma}_{FB,int}(k_0) &= \frac{3\alpha Q_e Q_f}{4\pi}\left\{-(1+8\ln 2)\ln k_0 + \frac{13}{4}\ln^2 2 - \frac{7}{2}\ln 2 - \frac{1}{4} + \frac{\pi^2}{3}\right\} \\ \delta^{\gamma Z}_{FB,int}(k_0) &= \frac{3\alpha Q_e Q_f}{4\pi}\left\{-(1+8\ln 2)\ln k_0 + \frac{127}{32}\ln^2 2 - \frac{5}{4}\ln 2 + \frac{1}{8} + \frac{\pi^2}{3}\right. \\ &+4z(1+z)\ln 2 + z - 2z^3\frac{\pi^2}{3} + (2z-5/2)\ln z \\ &+\left((5-3z+6z^2)\ln 2 - 2 + \frac{9}{2}z - \frac{3}{2}z^2\right)\ln\frac{z-1}{z} \\ &\left.(1-3z+6z^2+8z^3)\left[Sp(1-\frac{1}{z}) - Sp(1-\frac{1}{2z})\right] + 4z^3 Sp(1-\frac{1}{z})\right\} \qquad (205)\end{aligned}$$

are the virtual contributions from the $\gamma\gamma$-boxes and the γZ-boxes, respectively, plus the soft photon contribution ($E_\gamma/E_b \le k_0 \ll k_{max}$). The σ^i_{0f}'s have been given after Eq. (46) and $Sp(x) = Li_2(x)$ is the Spence function [54]. By z we denoted $z = M_R^2/s$ with $M_R^2 = M_Z^2 - iM_Z\Gamma_Z$.

$$\begin{aligned}\rho_{FB,int} &= \frac{3\alpha Q_e Q_f}{4\pi k}\left\{-(1-k-k^2/2) + (4-5k+5k^2/2)\ln(1-k)\right. \qquad (206) \\ &\left.-(8-12k+9k^2-5k^3/2)\frac{\ln(2-k)}{1-k}\right\}\end{aligned}$$

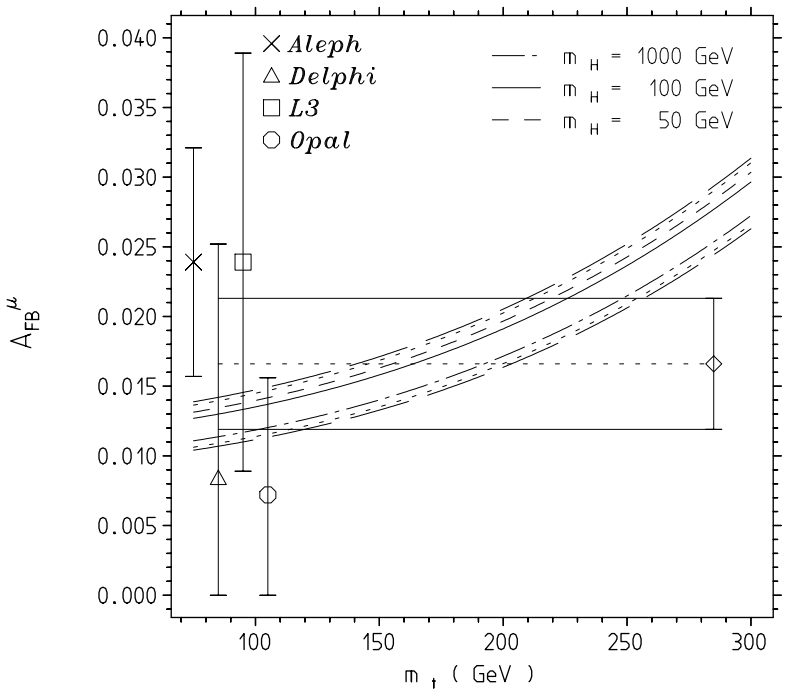

Figure 26: LEP measurement of A_{FB}^b.

describes the photon radiation spectrum [68]. The kernel $\sigma_0(s,s')$ follows from the C-even total cross-section Eq. (168) by the substitution Eq. (192) such that $\sigma_0(s,s) = \sigma_0(s)$.

For $s \simeq M_Z^2$ and no cuts ($k_{max} \simeq 1$) the interference contribution is proportional to $(\alpha/\pi)(\Gamma_Z/M_Z)$ and hence negligibly small (5×10^{-4}). For $M_Z \leq \sqrt{s} \leq M_Z + 2$ GeV and $k_{max} \leq 0.2$, i. e., for $E_\gamma \leq 10$ GeV the contribution is smaller than 10^{-3} [67]. For tight cuts ($k_{max} = k_0 \simeq 0.01$ or smaller), but still near resonance, the leading correction in the angular distribution coming from soft plus virtual photons is given by

$$1 + \frac{4Q_eQ_f\alpha}{\pi} \ln\frac{1-\cos\theta}{1+\cos\theta} \ln\left|\frac{k_0}{z-1+k_0}\right| + O(\frac{\alpha}{\pi}\frac{\Gamma_Z}{M_Z}) \quad .$$

Integration yields

$$\delta\Delta_{FB,obs}^{int}(s) \quad \simeq \quad \frac{3\alpha Q_eQ_f}{4\pi}\{(1+8\ln 2)\ \ln\left|\frac{M_R^2/s-1+k_0}{k_0}\right|\} \cdot \sigma_0(s). \tag{207}$$

These corrections are positive and of the order of a few percent. Away from the resonance corrections from the initial-final state interference are at the percent level.

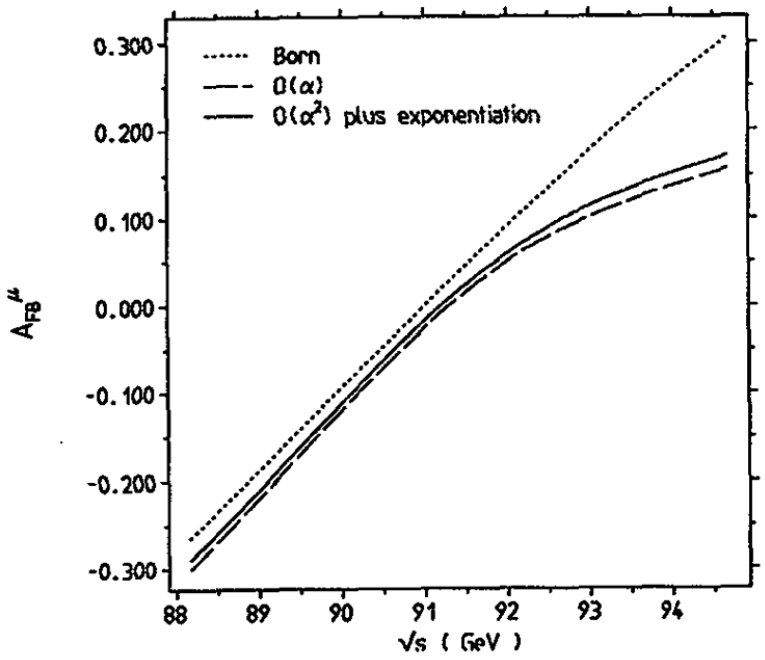

Figure 27: QED corrections of A^{μ}_{FB}.

The final state QED corrections are the simplests and least important ones. Since the photon is emitted from the final state the convolution Eq. (201) we had in case of initial state radiation turns into a simple product

$$\delta\Delta^{fin}_{FB,obs}(s) = \left(\delta_{fin}(k_0) + \int_{k_0}^{k_{max}} dk\ \rho_{fin}(k)\right)\ \ (\Delta_{FB})_{0,eff}(s) \tag{208}$$

where the virtual plus soft photon contribution $\delta_{fin}(k_0)$ is given again by Eq. (194) and

$$\rho_{fin}(k) = \frac{\alpha Q_f^2}{\pi}\left\{\frac{1+(1-k)^2}{k}(L_f-1) + 2\,\frac{\ln(1-k)}{k} + k\right\}$$

is the hard photon spectrum. If no cuts are applied ($k_{max} \simeq 1$) this correction is zero:

$$\delta\Delta^{fin}_{FB,obs}(s) = 0\,. \tag{209}$$

On the other hand σ_0 gets corrected according to Eq. (196). Therefore, a small negative correction

$$\delta A^{f\bar{f}}_{FB}/A^{f\bar{f}}_{FB} = -\frac{3\alpha}{4\pi}\,Q_f^2 \simeq -\,0.00174\,Q_f^2 \tag{210}$$

is obtained. The soft photon effects (tight cuts) are the same for C-odd and C-even functions and therefore do not affect the asymmetry, $\delta(A_{FB})^{fin} = 0$, independently of soft photon resummation.

The results given above for the final state photon radiation follow immediately from the classical calculation of the QCD corrections [52] by the substitution $\frac{3}{4}Q_f^2 \to 1$. With the latter replacement all we said about the final state QED corrections applies to QCD corrections as well. The QCD corrections have been discussed in more detail in Section 4.5.

At present, asymmetry measurements are not yet very precise. The reasons for the difficulties are obvious. The leptonic channels have a relatively low cross-section and the asymmetry $A_{FB}^{\mu^+\mu^-}$ is numerically small. For the hadronic channels flavor tagging is necessary, which is difficult and leads to a substantial efficiency loss.

In future, with increasing statistics, the asymmetry measurements will become more and more important to disentangle possible new physics from standard model effects.

said on the final state QED corrections applies to QCD corrections as well. The QCD corrections have been discussed in more detail in Section 4.5.

At present, asymmetry measurements are not yet very precise. The reasons for the difficulties are obvious. The leptonic channels have a relatively low cross-section and the asymmetry $A_{FB}^{\mu^+\mu^-}$ is numerically small. For the hadronic channels flavor tagging is necessary, which is difficult and leads to a substantial efficiency loss.

In future, with increasing statistics, the asymmetry measurements will become more and more important to disentangle possible new physics from standard model effects.

7. TESTING PHYSICS BEYOND THE STANDARD MODEL

Many authors have considered all kinds of extensions to the standard model. Here some of the simplest possibilities of new physics effects are discussed. General introductions to this subject can be found e.g. in [70-73] and in the "New Physics" sections of Ref. [74].

7.1 Additional Fermion Doublets

An almost standard extension of the SM is to allow for additional lepton and quark doublets. It should be remembered here that the existence of new light neutrinos, leptons or quarks with standard couplings is ruled out in particular by the LEP results [1]. Most limits are given by the kinematical limit for pair production. Thus, typically, $m_f > 45$ GeV for Dirac particles $f = \nu_D, \ell', b'$ etc.. For Majorana neutrinos the limits are slightly lower, $\nu_M > 36$ GeV, due to the different threshold behaviour.

We thus focus our discussion on virtual fermion effects. At one-loop order, additional fermions only contribute to the vector boson self-energies. Hence, the additional contributions are obvious from the general form of the self-energy contributions to various parameter shifts as listed in Eq. (146). It is convenient to represent them in terms of the quantities introduced in Eq. (147):

Observable	correction	defining Eq.
$\rho_{\nu_\mu N(e)}$	$\Delta\rho$	$(85, 134)$
	$\Delta\hat{\rho} = \Delta\rho - \frac{s_W^2}{c_W^2}\Delta_1 + \Delta_2$	(100)
$\sin^2\Theta_f$	$\Delta\kappa = \frac{c_W^2}{s_W^2}\Delta\hat{\rho} = \frac{c_W^2}{s_W^2}\Delta\rho - \Delta_1 + \frac{c_W^2}{s_W^2}\Delta_2$	(107)
$\Gamma_{Zf\bar{f}}$	$\Delta\bar{\rho} = \Delta\rho + \Delta_Z$	(108)
	$\Delta e = \Delta\alpha + \Delta_1 + \Delta_2$	(100)
M_W	$\Delta r = \Delta e - \Delta\kappa = \Delta\alpha - \frac{c_W^2}{s_W^2}\Delta\rho + 2\Delta_1 - \left(\frac{c_W^2}{s_W^2} - 1\right)\Delta_2$	$(27, 104)$
$\Gamma_{Zf\bar{f}}, A_{FB}^{f\bar{f}}$	$\Delta\bar{r} = \Delta e - \Delta\hat{\rho} = \Delta\alpha - \Delta\rho + \left(1 + \frac{s_W^2}{c_W^2}\right)\Delta_1$	(120)
$\sin^2\Theta_{\nu_\mu N(e)}$	$\bar{\Delta} = \Delta\alpha - \Delta\alpha_2$	$(128, 129)$

(211)

For a fermion doublet the different terms are given by

$$
\begin{aligned}
\Delta\alpha &= 4s_W^2 Q_f \Delta\alpha_2 = \frac{\alpha}{3\pi} Q_f^2 N_{cf} \left\{ \left(1 + \frac{y_f}{2}\right) G(y_f) - y_f - 5/3 \right\} \\
\Delta_1 &= \frac{\alpha}{16\pi s_W^2} \frac{N_{cf}}{3} \left\{ \left[2\left(1 - \frac{y_f}{4}\right) - 4|Q_f| \left(1 + \frac{y_f}{2}\right) \right] G(y_f) \right. \\
&\quad \left. + (4|Q_f| + 1)\, y_f - (4|Q_f| - 2) \ln \frac{m_f^2}{M_Z^2} \right\} \\
\Delta\rho &= \frac{\sqrt{2} G_\mu N_{cf}}{16\pi^2} \left\{ m_1^2 + m_2^2 - 2 \frac{m_1^2 m_2^2}{m_1^2 - m_2^2} \ln \frac{m_1^2}{m_2^2} \right\} \\
\Delta_2 &= \frac{\sqrt{2} G_\mu M_W^2}{16\pi^2} \frac{N_{cf}}{3} \left\{ a + 2b^2 + \frac{3a^2 + 3b^2 - 2b^4}{2b} \ln \frac{m_1^2}{m_2^2} + (2 - a - b^2) F(a,b) \right. \\
&\quad \left. - y_1 - 2\left(1 - \frac{y_1}{4}\right) G(y_1) - y_2 - 2\left(1 - \frac{y_2}{4}\right) G(y_2) \right\} \\
\Delta_Z &= \frac{\sqrt{2} G_\mu M_Z^2 N_{cf}}{12\pi^2} \left\{ v_f^2 \ (1 + 3/2 y_f \ (1 + y_f G(y_f))) \right. \\
&\quad \left. + a_f^2 \ (1 - 3 y_f \ (1 - (1 - y_f) \ G(y_f))) \right\}
\end{aligned}
\tag{212}
$$

where $y_i = \frac{4m_i^2}{M_Z^2}$, $a = \frac{m_1^2 + m_2^2}{M_W^2}$, $b = \frac{m_1^2 - m_2^2}{M_W^2}$ and

$$
G(y) = \begin{cases} \sqrt{1-y} \ln \frac{1+\sqrt{1-y}}{1-\sqrt{1-y}}; & 0 < y < 1 \\ 2\sqrt{y-1} \arctan \frac{1}{\sqrt{y-1}}; & y > 1 \end{cases}
$$

$$
F(a,b) = \begin{cases} \sqrt{\lambda} \ln \frac{1-a+\sqrt{\lambda}}{1-a-\sqrt{\lambda}}; & 0 < s < (m_1 - m_2)^2 \ \ or \ \ (m_1 + m_2)^2 < s \\ 2\sqrt{-\lambda} \arctan \frac{\sqrt{-\lambda}}{a-1}; & (m_1 - m_2)^2 < s < (m_1 + m_2)^2 \end{cases}
$$

with $\lambda = 1 - 2a + b^2$, $s = M_W^2$.

If one or both members are light (ℓ) or heavy (h), we get the following simple formulae

$$
\Delta\alpha = \begin{cases} \frac{\alpha}{3\pi} Q_f^2 N_{cf} \left(\ln \frac{M_Z^2}{m_f^2} - \frac{5}{3} \right) & ; \ (\ell) \\ 0 & ; \ (h) \end{cases}
$$

$$
\Delta_1 = \begin{cases} 0 & ; \ (\ell) \\ \frac{\alpha}{16\pi s_W^2} \frac{N_{cf}}{3} \left\{ 1 - (2 - 4|Q_h|) \left(\ln \frac{M_Z^2}{m_h^2} - \frac{5}{3} \right) \right\} & ; \ (h) \end{cases}
$$

$$
\Delta_Z = \begin{cases} \frac{\sqrt{2} G_\mu M_Z^2 N_{cf}}{12\pi^2} (v_f^2 + a_f^2) & ; \ (\ell) \\ 0 & ; \ (h) \end{cases}
$$

$$
\Delta\rho = \begin{cases} \frac{\sqrt{2} G_\mu N_{cf}}{16\pi^2} \left\{ m_1^2 + m_2^2 - 2 \frac{m_1^2 m_2^2}{m_1^2 - m_2^2} \ln \frac{m_1^2}{m_2^2} \right\}; \ 0 \text{ if } m_1 = m_2 & ; \ (\ell\ell) \\ \frac{\sqrt{2} G_\mu N_{cf}}{16\pi^2} \left\{ m_h^2 + m_\ell^2 + 2\, m_\ell^2 \ln \frac{m_\ell^2}{m_h^2} + \cdots \right\} & ; \ (h\ell) \\ \frac{\sqrt{2} G_\mu N_{cf}}{16\pi^2} \left\{ \frac{2\,(m_1^2 - m_2^2)^2}{3\,(m_1^2 + m2^2)} + \cdots \right\} & ; \ (hh) \end{cases}
$$

$$\Delta_2 = \frac{\sqrt{2}G_\mu M_W^2}{16\pi^2}\frac{N_{cf}}{3}\begin{cases} 4\ln c_W^2 & ; \ (\ell\ell) \\ 2\ln\frac{m_h^2}{M_Z^2}+1 & ; \ (h\ell) \\ 0 & ; \ (hh) \end{cases} .$$

In these approximations terms of order $O(\alpha\frac{m_\ell^2}{M_W^2})$ and $O(\alpha\frac{M_W^2}{m_h^2})$ (up to log's) have been neglected.

It is interesting to notice that due to chiral symmetry breaking by masses there is a non-decoupling effect also for a mass degenerate doublet

$$\begin{aligned} \Delta r^{(hh)} &= \frac{\alpha}{4\pi s_W^2}\frac{N_{cf}}{3} \\ \Delta\bar{r}^{(hh)} &= \frac{\alpha}{8\pi s_W^2}\frac{N_{cf}}{3}\left(1+\frac{s_W^2}{c_W^2}\right) . \end{aligned} \tag{213}$$

This is very interesting because heavy degenerate doublets give a kind of model independent contributions, since $\Delta\alpha$, $\Delta\alpha_2$, $\Delta\rho$, Δ_2 , $\Delta_Z = 0$ while only $\Delta_1 = \frac{\alpha}{24\pi s_W^2}N_d \neq 0$ counting directly the number N_d of degenerate doublets.

Given the present accuracy we easily estimate the number N_d of mass degenerate doublets needed to give a one standard deviation effect (we assume $\sin^2\Theta_W = 0.23$):

Measurement	$\delta\Delta r$ per doublet	accuracy	N_d
M_W	$\Delta r^{(hh)}= 8.42 \times 10^{-4}$	$\delta\Delta r^{exp}= 0.0180\ (0.0040)$	$> 21(4)$
$\sin^2\bar{\Theta}\ (A_{LR}, A_{FB}^{\mu^+\mu^-})$	$\Delta\bar{r}^{(hh)}= 5.46 \times 10^{-4}$	$\delta\Delta\bar{r}^{exp}= 0.0078\ (0.0043)$	$> 14(7)$

in parentheses are given the values which can be reached at LEP in future.

Notice that the "weak isospin conserving" contribution Δ_2 gives a *positive* contribution to Δr. A fourth family can contribute at most

$$\Delta r^{(4)} \simeq 3.4 \times 10^{-3} \qquad (Dirac\ \ \nu_4) \ . \tag{214}$$

Such a contribution would weaken the upper bound for the top mass Eq. (105) by at most 8 GeV. In contrast all "weak isospin violating" effects give *negative* contributions to Δr.

If, besides the (t,b)-doublet, additional split doublets exist, the sum of the quadratic heavy particle effects is constraint by the "m_t-bounds", which then are bounds on $m_{t\,\mathrm{eff}}$ defined by

$$\Delta\rho = \frac{N_c\sqrt{2}G_\mu m_{t\,\mathrm{eff}}^2}{16\pi^2} = \frac{N_c\sqrt{2}G_\mu m_t^2}{16\pi^2} + \sum_d \frac{N_c\sqrt{2}G_\mu}{16\pi^2}\left(m_1^2+m_2^2-\frac{2m_1^2m_2^2}{m_1^2-m_2^2}\ln\frac{m_1^2}{m_2^2}\right) \tag{215}$$

if we assume that there are no other contributions to $\Delta\rho$ (see below). Such split heavy doublets ($m_1, m_2 \gg M_Z$) also modify Δ_1 to

$$\Delta_1 = \frac{\alpha}{24\pi s_W^2}\left(1-4\bar{Q}\ln\frac{m_1}{m_2}\right) , \ \ \bar{Q} = \frac{1}{2}\left(Q_1+Q_2\right) . \tag{216}$$

Recently, by treating $\Delta\rho$, Δ_1 and Δ_2 as free parameters, a number of bounds have been derived for these quantities. The results have been obtained by assuming that new physics shows up in the vector-boson self-energies only. Before we discuss the results we give a translation for the notation used by various authors.

Comparison of notations			
$\Delta\rho$	Δ_1	Δ_2	Burgers-Jegerlehner [24]
$4\sqrt{2}G_\mu\Delta_\rho(0)$	$-4\sqrt{2}G_\mu c_W^2\Delta_3(M_Z^2)$	$-4\sqrt{2}G_\mu\left(\Delta_\pm(M_W^2)-c_W^2\Delta_3(M_Z^2)\right)$	Kennedy-Lynn [44]
αT	$\frac{\alpha S}{4s_W^2}$	$\simeq 0$	Peskin-Takeuchi [75]
αT	$\frac{\alpha S_Z}{4s_W^2}$	$\frac{\alpha\,(S_W-S_Z)}{4s_W^2}$	Marciano-Rosner [76]
αh_V	$\frac{\sqrt{2}G_\mu M_W^2}{4\pi}h_{AZ}$	$\frac{\sqrt{2}G_\mu M_W^2}{4\pi}\,(h_{AW}-h_{AZ})$	Langacker-Kennedy [77]
ϵ_1	ϵ_3	$-\epsilon_2$	Altarelli-Barbieri [78]

Notice that for additional heavy fermions one has $\Delta\rho\ (T)\ > 0$, $\Delta_1\ (S)\ > 0$ and $\Delta_2 \simeq 0$ ($S_W \simeq S_Z$) and one may perform two-parameter fits in terms of T ($\simeq h_V$) and S ($= S_Z \simeq h_{AZ}$), for example. Since the $\Delta\rho\ (T)$ bounds are equivalent to the familiar m_t-bounds, here, we focus on $\Delta_1\ (S)$ (equivalent to $\Delta r^{(hh)}$ considered above). Bounds on S not only restrict the number of additional heavy mass degenerate fermion families but any extension of the SM which exhibits a large number of additional fermions. An example of this kind are the technicolor (TC) models (for which $m_H = O(1\text{ TeV})$) [75]. Using "scaled up QCD" arguments, TC models with N_{TC} technicolors and N_{TD} doublets of technifermions are estimated to yield [75]

$$S^{technicolor} \simeq (0.05-0.1)\,N_{TC}N_{TD} + 0.12\,. \tag{217}$$

For example, one finds $S \simeq 2$ for $N_{TC} = 4$ and one technifermion family. As we shall see such a contribution is almost excluded by the present experimental data. Constraints on S are obtained from

- LEP data on Γ_Z, Γ_ℓ and $A_{FB}^{\mu^+\mu^-}$
- $p\bar{p}$ collider data on $\sin^2\Theta_W$ (or M_W)
- νN scattering data
- data from measurements of parity violation in atoms.

An important observation has been made by Marciano and Rosner [76], namely, that the weak charge which determines parity violation in Cesium is almost independent of T ($\Delta\rho$) and hence of the top mass. They obtain

$$Q_w^{the}\left({}^{133}_{55}C_s\right) = -73.20 \pm 0.13 - 0.8S - 0.006T \tag{218}$$

for the theoretical prediction. This result is normalized to S=T=0 when $m_t = 140$ GeV and $m_H = 100$ GeV and no physics beyond the SM is present. The small coefficient of T is due to an accidental cancellation of terms for the stable C_s isotope. Using a new atomic calculation [79] the experimental result obtained by the Boulder group [80] is

$$Q_w^{exp}\left({}^{133}_{55}C_s\right) = -71.04 \pm 1.58(\text{exp}) \pm 0.88(\text{the}) \tag{219}$$

where the first error is mostly statistical and the second is the theoretical uncertainty of the atomic theory. Assuming S=T=0 we have

$$\delta Q_w = Q_w^{exp} - Q_w^{the} = 2.16 \pm 1.81 \ \text{ or } \ -1.38 \leq \delta Q_w \leq 5.70 \ \text{ at } 95\% \ CL \ . \tag{220}$$

Setting $Q_w^{exp} = Q_w^{the}$ S is determined to be

$$S = -2.7 \pm 2.0 \pm 1.1 \pm 0.16 \ .$$

From a global fit to all data Kennedy and Langacker [77] obtain (consistent with "no new physics")

$$S = -1.1 \pm 1.7 \ \text{ or } \ S < 0.7(1.2) \ \text{ at } 90\% \ (95\%) \ \text{CL} \ . \tag{221}$$

Thus no more than four extra families of heavy degenerate fermions can exist in this scenario.

We close this subsection with a remark on Majorana neutrinos. In models with isosinglet *right handed neutrinos* ν_{Rj} [81] the neutrinos are expected to be massive and to mix like the quarks. Since the right handed neutrinos have trivial quantum numbers they can be either Dirac or Majorana particles. In general, additional heavy singlet neutrinos are expected to lower the invisible widths of the Z. This follows from unitary mixing and the assumption that the ν_R is too heavy to be produced. The effective number of ν's then would be $N_\nu^{eff} \leq 3$. A "natural" scenario for a heavy additional neutrino which does not contribute to Γ_Z has been proposed by Hill and Paschos [82]. The fourth family ν_R is assumed to have a Majorana mass $M = O(v)$ besides a Dirac mass $m_D = O(m_{\ell'})$, where v is the vacuum expectation value of the Higgs field and $m_{\ell'}$ the fourth family lepton mass. Mixing of the fourth family with the first three is assumed to be negligible. Diagonalizing the neutrino mass matrix one has two Majorana neutrinos of mass m_1 and $m_2 = m_D^2/m_1$. Bertolini and Sirlin [83] found that in this case masses can be chosen such that the leptonic contribution to $\Delta r(\Delta\rho)$ are similar to the "isospin violating" large doublet mass splitting effects but with the *opposite* sign! For arbitrary m_D a maximum value

$$\Delta r_{max}^{leptons} \simeq \frac{\alpha}{4\pi s_W^4} \left(\frac{m_D}{M_Z}\right)^2 \frac{1}{9.49} \tag{222}$$

is obtained for $m_{\ell'} = m_1 = m_D/3.08$. Assuming $m_D \leq 300$ GeV, a fourth family could contribute at most

$$\Delta r_{max}^{(4)} \simeq 1.7 \times 10^{-2} \qquad (Majorana \ \ \nu_4) \tag{223}$$

and a compensating increase of $(m_t)_{max}$ of at most 36 GeV would follow.

7.2 Additional Higgs multiplets

7.2.1 General considerations

We first discuss the possibility of having $\rho_0 = \rho_{tree} \neq 1$. Doing so, we have to remember the phenomenological bound

$$\rho_0 = 0.992 \pm 0.011 \qquad \text{Ref. [26]} \ . \tag{224}$$

If several Higgs multiplets couple to the gauge bosons the mass formulae Eq. (26) are modified to

$$\begin{aligned} M_W^2 &= \frac{g^2}{2} \sum_i v_i^2 \left(I_i(I_i+1) - I_{3i}^2 \right) \\ M_Z^2 &= \frac{g^2}{2\cos^2\Theta_g} \sum_i v_i^2 2 I_{3i}^2 \end{aligned}$$

such that

$$\rho_0 = \frac{\sum_i v_i^2 \left(I_i(I_i+1) - I_{3i}^2\right)}{\sum_i v_i^2 2 I_{3i}^2} \ .$$

Here $v_i =< H_i >_0$ is the vacuum expectation value (VEV) of the charge zero component of the multiplet i with weak isospin I_i with 3rd component I_{3i}. For a mixture of doublets ($I_i = 1/2$, $|I_{3i}| = 1/2$) and Y=2 triplets $\Delta = (\Delta^{++}, \Delta^{+}, \Delta^{0})$ ($I_i = 1$, $|I_{3i}| = 1$) ρ_0 is bounded by

$$\begin{array}{ccccccc} 1 & & \geq & \rho_0 & = & \frac{v_d^2+v_t^2}{v_d^2+2v_t^2} & \geq & \frac{1}{2} \\ \text{doublets} & & & & & \text{mixed} & & \text{triplets} \\ \text{only} & & & & & & & \text{only} \end{array}$$

with $v_d^2 = \sum_i v_{i,doublets}^2$, $v_t^2 = \sum_i v_{i,triplets}^2$. Notice that Y=2 triplet contaminations change the value of ρ_0 below 1. On the other hand Y=0 triplets $\Delta = (\Delta^{+}, \Delta^{0}, \Delta^{-})$, yield a positive contribution

$$\Delta\rho_0 = 4\frac{v_t^2}{v_d^2} \ > \ 0 \tag{225}$$

to the ρ-parameter. At 68% CL, the bound Eq. (224) restricts the triplet VEV's by

$$v_t < 34\,(7) \ \text{GeV} \ \text{ for } Y = 2\,(0) \ .$$

It is important to notice that since both v_d and v_t are free parameters, we need two measurable quantities as input parameters now. One still has the definition

$$v^2 = \sum_i v_i^2 \left(I_i(I_i+1) - I_{3i}^2\right) = \left(\sqrt{2}G_\mu\right)^{-1}$$

which fixes a certain combination of the VEV's, however unlike to the case when $\rho_0 = \rho_{tree} = 1$, now, ρ_0 must be considered as an additional free parameter. The consequences for the renormalization procedure have been pointed out by Lynn and Nardi [84] and will be discussed in an Appendix to this Section.

Here we mention that if $\rho_0 = \rho_{tree} \neq 1$ one should consequently replace

$$\begin{aligned} \sin^2\Theta_W \ &\rightarrow \ \sin^2\Theta_g = (e/g)^2 = 1 - \frac{M_W^2}{\rho_0 M_Z^2} \\ \Delta r \ &\rightarrow \ \Delta r_g = 1 - \frac{\pi\alpha}{\sqrt{2}G_\mu M_W^2}\frac{1}{\sin^2\Theta_g} \end{aligned} \tag{226}$$

in all formulae. If we define $\Delta\rho_0$ in analogy to Eq. (97) by

$$\rho_0 = \frac{1}{1-\Delta\rho_0}$$

we have

$$\sin^2\Theta_g = \sin^2\Theta_W \ (1 + \frac{\cos^2\Theta_W}{\sin^2\Theta_W}\Delta\rho_0)$$

and hence the *exact* relation

$$\frac{1}{1-\Delta r} = \frac{1}{1-\Delta r_g} \ (1 + \frac{\cos^2\Theta_W}{\sin^2\Theta_W}\Delta\rho_0) \tag{227}$$

holds. The experimental bounds mentioned before suggest that deviations from $\rho_0 = 1$ can be treated as perturbations. In the standard approach such "tree level" perturbations may be included by using

$$(\Delta\rho)_{irr} \to (\Delta\rho)_{irr} + (1 - \rho_0^{-1}) \tag{228}$$

or, in linear approximation, simply by adding

$$\delta\Delta r = -\frac{\cos^2\Theta_W}{\sin^2\Theta_W}\Delta\rho_0, \;\; \Delta\rho_0 \simeq -\frac{v_t^2}{v_d^2}; \; (v_t^2 \ll v_d^2) \;\; . \tag{229}$$

Notice that a 0.6% Y=2 triplet contamination ($v_t \simeq 19$ GeV) yields a +2% effect in Δr, a contribution which could cancel heavy particle effects! The sensitivity to Y=0 triplets is by a factor of four larger and of opposite sign.

Besides the tree level effects additional Higgs fields would contribute to Δr through loops

$$\Delta r = \Delta r^{SM} + \Delta r^{extraHiggses}.$$

For triplets these terms have not been worked out in full detail [84,85]. We expect them to be small (large) for triplets with small (large) mass-splitting.

7.2.2 Two Higgs doublet model

From a theoretical point of view the case with two Higgs doublets is very attractive. Two Higgs doublets are obtained in minimal supersymmetric (SUSY) extensions of the SM. Such models also have been considered as a possible "explanation" for the appearance of very different mass scales which could be set by the very different VEV's. For example, if the vector-bosons and fermions acquire their masses from vastly different VEV's this could be the reason why $m_f \ll M_W$. Since now we know that the top is heavier than the intermediate vector bosons this is not a plausible argument any longer. On the other hand one easily may get $m_t \gg m_b$ without having vastly different Yukawa couplings because upper and lower entries of the fermion doublets must get their masses from different VEV's ($m_t \sim v_2$, $m_b \sim v_1$) in order to prevent FCNC's. Notice, however, that the experimental bounds on Δr Eq. (105) seems to require a top with a large Yukawa coupling, not just a large top mass. Anyway, the possibility of two Higgs doublets is not ruled out phenomenologically and therefore must be studied.

The model is identical to the SM except that two independent doublets

$$\Phi_i = \begin{pmatrix} \phi_i^+ \\ (v_i + \eta_i + i\chi_i)/\sqrt{2} \end{pmatrix}$$

of hypercharge 1 are present. Both doublets in general couple to the fermions. If only one doublet couples to the fermions the diagonalization of the fermion mass matrix simultaneously diagonalizes the Yukawa couplings (see Eqs. (6) and (7)) and no FCNC's mediated by scalars is possible. Obviously, if more than one Higgs field couples to the fermions this is no longer the case. In order to ensure the absence of FCNC's mediated by scalars, fermions of a given charge must be required to couple to one Higgs field only [86]. We assume Φ_1 to couple to the $T_{3f} = -\frac{1}{2}$ and Φ_2 to the $T_{3f} = +\frac{1}{2}$ fermions. This can be achieved by imposing a discrete symmetry $\Phi_2 \to -\Phi_2$ and $u_{Rj} \to -u_{Rj}$ for the up-type quark fields. The scalar potential must share the symmetry $\Phi_2 \to -\Phi_2$. The most general renormalizable Higgs potential is then given by

$$\begin{aligned} V &= -\mu_1^2(\Phi_1^+\Phi_1) - \mu_2^2(\Phi_2^+\Phi_2) + \lambda_1(\Phi_1^+\Phi_1)^2 + \lambda_2(\Phi_2^+\Phi_2)^2 \\ &+ \lambda_3(\Phi_1^+\Phi_1)(\Phi_2^+\Phi_2) + \lambda_4(\Phi_1^+\Phi_2)(\Phi_2^+\Phi_1) + \frac{\lambda_5}{2}\left[(\Phi_1^+\Phi_2)^2 + (\Phi_2^+\Phi_1)^2\right] \end{aligned}$$

The physical states result from mixing of the fields of the two doublets with vacuum expectation values v_1 and v_2. By a rotation with rotation angle β determined by

$$\tan\beta = \frac{v_2}{v_1} \equiv \frac{v_{top}}{v_{bottom}} \ , \ 0 \le \beta \le \frac{\pi}{2} \ , \tag{230}$$

we obtain doublets Φ'_i, where Φ'_1 may be identified with the SM Higgs field with vacuum expectation value $v = \sqrt{v_1^2 + v_2^2}$. The fields $\phi_1^{'\pm}$ and χ'_1 can be gauged away and hence represent the Higgs ghosts $\varphi^\pm$ and φ.

The new physical scalars are the charged Higgses $H^\pm$ and a pseudoscalar A:

$$\begin{aligned} H^\pm &= -\sin\beta\ \phi_1^\pm + \cos\beta\ \phi_2^\pm \\ A &= -\sin\beta\ \chi_1 + \cos\beta\ \chi_2 \end{aligned}$$

while the two physical scalars H and h are given by mixing of η'_1 and η'_2 with mixing angle $\alpha - \beta$ such that

$$\begin{aligned} H &= \cos\alpha\ \eta_1 + \sin\alpha\ \eta_2 \\ h &= -\sin\alpha\ \eta_1 + \cos\alpha\ \eta_2 \ . \end{aligned}$$

Noticing that the fields

$$\begin{aligned} \eta'_1 &= \cos(\alpha-\beta)\ H - \sin(\alpha-\beta)\ h \\ \eta'_2 &= \sin(\alpha-\beta)\ H + \cos(\alpha-\beta)\ h \end{aligned}$$

couple to the gauge bosons identical as the Higgs in the SM, i.e. $Z\varphi H \to Z\varphi\eta'_1$, $ZA\eta'_2$ and $W^+\varphi^- H \to W^+\varphi^-\eta'_1$, $W^+H^-\eta'_2$, we easily find the couplings for H and h, which simply pick factors $\cos(\alpha-\beta)$ and $\pm\sin(\alpha-\beta)$. Similarly, $VVH \to VVH\ \cos(\alpha-\beta) - VVh\ \sin(\alpha-\beta)$ $(V = W, Z)$.

Whereas β only depends on the ratio of the vacuum expectation values α depends on all the parameters of the Higgs potential, $\tan 2\alpha = \frac{v_1 v_2(\lambda_3+\lambda_4+\lambda_5)}{\lambda_2 v_2^2 - \lambda_1 v_1^2}$ $(-\frac{\pi}{2} \le \alpha \le 0)$.

In a two Higgs model the Yukawa couplings may be enhanced by large factors v_2/v_1 or v_1/v_2. This is important for the heavier fermions. The relevant couplings read

$$\begin{array}{lll} Hf\bar{f}, & f = b,t & -\frac{g}{2}\left(\ \frac{m_b}{M_W}\frac{\cos\alpha}{\cos\beta},\ \ \frac{m_t}{M_W}\frac{\sin\alpha}{\sin\beta}\right) \\ hf\bar{f}, & f = b,t & -\frac{g}{2}\left(-\frac{m_b}{M_W}\frac{\sin\alpha}{\cos\beta},\ \ \frac{m_t}{M_W}\frac{\cos\alpha}{\sin\beta}\right) \\ Af\bar{f}, & f = b,t & -\gamma_5\frac{g}{2}\left(\ \frac{m_b}{M_W}\tan\beta,\ \ \frac{m_t}{M_W}\cot\beta\right) \\ H^+b\bar{t} & & \frac{g}{\sqrt{2}}\left(\ \frac{m_b}{M_W}\tan\beta\,\frac{1+\gamma_5}{2} + \frac{m_t}{M_W}\cot\beta\,\frac{1-\gamma_5}{2}\right)\ V_{tb} \ . \end{array} \tag{231}$$

The couplings for the other fermions are given by analogous expressions. For example, the coupling for the τ may be obtained by substituting $m_t \to 0$, $m_b \to m_\tau$.

In the minimal SUSY model the masses of the extra Higgses at tree level are severely constrained by the following mass- and coupling-relationships:

$$\begin{aligned} m_\pm^2 &= M_W^2 + m_A^2 \\ m_{H,h}^2 &= \frac{1}{2}\left(M_Z^2 + m_A^2 \pm \sqrt{(M_Z^2 - m_A^2)^2 + 4M_Z^2 m_A^2 \sin^2 2\beta}\right) \\ \tan(2\alpha) &= \tan(2\beta)\ \frac{m_A^2 + M_Z^2}{m_A^2 - M_Z^2} \end{aligned}$$

$$\sin^2(\alpha-\beta) = \frac{m_H^2}{m_A^2}\frac{M_Z^2-m_H^2}{M_Z^2+m_A^2-2m_H^2}$$
$$\cos^2(\alpha-\beta) = \frac{m_h^2}{m_A^2}\frac{M_Z^2-m_h^2}{M_Z^2+m_A^2-2m_h^2} \ . \qquad (232)$$

Only two independent parameters are left, which we may choose to be $\tan\beta$ and m_A. In Fig. 28 we plot the dependent parameters as a function of m_A for various $\tan\beta$.

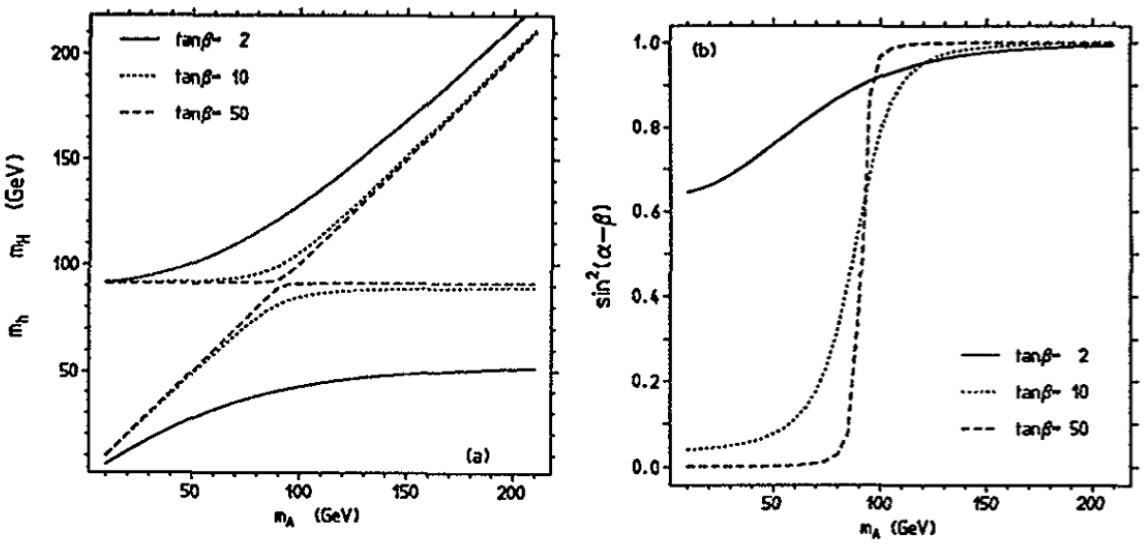

Figure 28: a) the scalar masses m_h, m_H and b) $\sin^2(\alpha-\beta)$ as a function of the pseudoscalar mass m_A for various values of $\tan\beta$.

In this model one scalar is always lighter than $\mathrm{Min}(M_Z, m_A)$, the other is always heavier than $\mathrm{Max}(M_Z, m_A)$. The charged Higgs must be heavier than M_W. Notice that the solutions for m_h, m_H and $\sin^2(\alpha-\beta)$ are symmetric under the replacement $\tan\beta \leftrightarrow \cot\beta$. The angles α and β and the Yukawa couplings Eq. (231) do not share this symmetry. Large mass-splittings between the $I_3 = +1/2$ and $I_3 = -1/2$ states are forbidden such that no large contributions to the radiative corrections are obtained in this case (see below).

7.2.3 Present bounds on scalar masses

Experimental bounds on scalars masses [1] depend on the parameters of the two doublet model. The bound on the lightest scalar (corresponding to the SM Higgs) gets weaker due to the suppression of the production rate by

$$\frac{\Gamma(Z\to hf\bar{f})}{\Gamma^{SM}(Z\to Hf\bar{f})} = \sin^2(\alpha-\beta) \ .$$

Thus one may loose the bound Eq. (11) for the lightest Higgs denoted by h here. In the minimal SUSY model the constraints Eq. (232) imply $\sin^2(\alpha-\beta) \geq 0.5$ for $m_A \geq M_Z$ and the bound essentially remains valid. The reason is that most of the mass bounds are primarily a matter of kinematical accessibility, rather than a problem of rate. Notice that a corresponding bounds on the pseudoscalar mass m_A cannot be obtained via $Z \to Af\bar{f}$ since this decay is not allowed by the absence of a ZZA coupling at tree level.

Fortunately there is a complementary Z decay mode $Z \to Ah$ available if $m_A + m_h < M_Z$. This

decay has a branching fraction

$$\frac{\Gamma(Z \to hA)}{\Gamma^{SM}(Z \to \nu\bar{\nu})} = \frac{1}{2}\cos^2(\alpha-\beta)\lambda^{3/2}$$

where $\lambda = \lambda(1, m_h^2/M_Z^2, m_A^2/M_Z^2)$ is the two body phase space function $\lambda(x,y,z) = x^2+y^2+z^2-2xy-2xz-2yz$). Notice that the couplings for the decays of the scalars into fermion pairs depend on the mixing angles α and β, according to Eq. (231). Bounds therefore are not symmetric under $\tan\beta \leftrightarrow \cot\beta$.

Present bounds usually are given for the minimal SUSY scenario, assuming that the mass-coupling relations Eq. (232) hold. If $m_A > M_Z$ the SM bound Eq. (11) applies for the light scalar. For $m_A < M_Z$ we have $m_h < m_A$ and $\cos^2(\alpha-\beta) > 0.5$. Notice that $m_A \simeq m_h$ requires $\tan\beta \gg 1$ or $\tan\beta \ll 1$ which implies $\cos^2(\alpha-\beta) \simeq 1$. The resulting mass bounds obtained from a study of the decay $Z \to hA$ are the following:

$$\begin{array}{rrl} m_h > 28 \text{ GeV},\ m_A > 30 \text{ GeV} & \text{for} & \tan\beta < 1 \\ m_h > 34 \text{ GeV},\ m_A > 43 \text{ GeV} & \text{for} & \tan\beta > 1 \\ m_h \simeq m_A > 40 \text{ GeV} & \text{for} & \tan\beta < 1 \\ m_h \simeq m_A > 42 \text{ GeV} & \text{for} & \tan\beta > 1 \quad . \end{array} \tag{233}$$

We finally consider the charged Higgs. At LEP a charged Higgs cannot be singly produced by $t \to H^+b$, because, given the bound $m_t > 89$ GeV, a top quark connot be produced. Pair production by $Z \to H^+H^-$ is possible, however. The partial with for this Z decay channel is

$$\Gamma(Z \to H^+H^-) = \frac{\sqrt{2}G_\mu M_Z^3}{48\pi}(1-2s_W^2)^2\left(1-\frac{4m_\pm^2}{M_Z^2}\right)^{3/2} \quad .$$

Since the Z rates are no limiting factor the charged Higgs search is possible right to the kinematical limit ~ 45 GeV. The partial decay widths are

$$\begin{aligned} \Gamma(H^+ \to \ell^+\nu_\ell) &= \frac{\sqrt{2}G_\mu m_H}{8\pi}\tan^2\beta m_\ell^2 \\ \Gamma(H^+ \to u_i\bar{d}_j) &= \frac{3\sqrt{2}G_\mu m_H}{8\pi}(|V_{ij}|\,(\cot^2\beta m_i^2 + \tan^2\beta m_j^2) \end{aligned}$$

for leptonic and hadronic decays, respectively. The experimental limit slightly depends on the branching fraction $Br(H \to \tau\nu_\tau) \simeq \frac{\Gamma(H\to\tau\nu_\tau)}{\Gamma(H\to c\bar{s})} \simeq \frac{m_\tau^2}{3m_c^2}\tan^4\beta$:

$$m_\pm > \begin{cases} 40 \text{ GeV} & Br(H \to \tau\nu) = 0 \\ 45 \text{ GeV} & Br(H \to \tau\nu) = 1 \quad . \end{cases} \tag{234}$$

These limits will slightly improve towards $M_Z/2$ during the LEP1 run time. For substantial improvements we have to wait for LEP2.

7.2.4 Virtual effects

The case of an additional Higgs doublet has been analysed in detail in Refs. [87,88]. The leading heavy particle contributions as usual show up in the ρ-parameter Eq. (85). A Higgs-gauge boson loops yields

$$\Delta\rho^H = \frac{3\sqrt{2}G_\mu M_W^2|d|^2}{16\pi^2} f_H(\frac{m_H^2}{M_Z^2}, c_W^2)$$

with

$$f_H(x,y) = x\left(\frac{\ln(y/x)}{y-x} + \frac{\ln x}{y\,(1-x)}\right)$$

when the coupling is d times the SM HVV coupling.

For a scalar loop (masses m_1 and m_2) with coupling $iaV_\mu\varphi_1^* \overset{\leftrightarrow}{\partial^\mu} \varphi_2$ the contribution is

$$\Pi_V^S(0) = \frac{a^2}{16\pi^2} f_S(m_1^2, m_2^2) \tag{235}$$

with

$$f_S(m_1^2, m_2^2) = \frac{1}{2}(m_1^2 + m_2^2) - \frac{m_1^2 m_2^2}{m_1^2 - m_2^2}\ln\frac{m_1^2}{m_2^2} \quad .$$

The total Higgs contribution is then given by

$$\begin{aligned}\Delta\rho^{Higgs} = \frac{\sqrt{2}G_\mu}{16\pi^2}\Big\{ & 3M_W^2\left[\sin^2(\alpha-\beta)\, f_H(\frac{m_h^2}{M_Z^2}, c_W^2) + \cos^2(\alpha-\beta)\, f_H(\frac{m_H^2}{M_Z^2}, c_W^2)\right] \\ & + \cos^2(\alpha-\beta)\,\left(f_S(m_\pm^2, m_h^2) + f_S(m_\pm^2, m_A^2) - f_S(m_A^2, m_h^2)\right) \\ & + \sin^2(\alpha-\beta)\,\left(f_S(m_\pm^2, m_H^2) + f_S(m_\pm^2, m_A^2) - f_S(m_A^2, m_H^2)\right)\Big\}\end{aligned} \tag{236}$$

Without loss of generality we may assume that $m_h \le m_H$. Thus h corresponds to the minimal SM Higgs. Different observables are affected as follows from Eqs. (211). Typically, for large weak isospin splitting (excluded in SUSY models) the change in ρ is given by [88]

$$\Delta\rho^{Higgs} \simeq \begin{cases} \frac{\sqrt{2}G_\mu}{16\pi^2} m_\pm^2 & \text{for} \quad m_\pm \gg m_{neutrals} \\ \frac{\sqrt{2}G_\mu}{16\pi^2} m_{neutrals}^2 & \text{for} \quad m_{neutrals} \gg m_\pm \quad . \end{cases} \tag{237}$$

Assuming $m_\pm$= 200 GeV ($\gg m_{neutrals}$), for example, we would obtain a shift $\delta\Delta r \simeq -1.4\times10^{-2}$ which would tighten the upper bound for m_t Eq. (105) by 36 GeV.

In Ref. [89] it has been found that there exist windows $m_{H,h} < m_\pm < m_A$ and $m_A < m_\pm < m_{H,h}$ (which are excluded in SUSY scenarios) in which the scalars give a large negative contribution to $\Delta\rho$. The maximum value is attained at the minimum $c \simeq 0.562$ of the function $f(c^2) = c^2 + \frac{c^2}{1-c^2}\ln c^2$ where $f_{min} \simeq -0.216$. The result

$$\Delta\rho_{min}^{Higgs} = \frac{\sqrt{2}G_\mu}{16\pi^2}\,\frac{f_{min}}{c^2}\, m_\pm^2 \simeq -7.14\times10^{-8}\ \text{GeV}^{-2}\, m_\pm^2 \tag{238}$$

is obtained for the cases

- $m_h = m_H = 0$, $\sin^2(\alpha-\beta)$ arbitrary and $m_\pm = c\, m_A$
- $m_h = m_H$, $m_A = 0$, $\sin^2(\alpha-\beta)$ arbitrary and $m_\pm = c\, m_H$
- $m_h = 0$, m_H arbitrary, $\sin^2(\alpha-\beta) = 0$ and $m_\pm = c\, m_A$
- $m_A = 0$, m_h arbitrary, $\sin^2(\alpha-\beta) = 1$ and $m_\pm = c\, m_H$.

As an example, choosing $m_\pm = 200$ GeV and $m_A = 356$ GeV ($\gg m_{H,h}$) yields $\delta\Delta r \simeq 9.6 \times 10^{-3}$ which would weaken the upper top mass bound by 21 GeV.

Large effects are expected from extra vertex corrections to the $Zb\bar{b}$ vertex, and the $Z\tau^-\tau^+$ vertex also should be inspected. From Eq. (231) we learn that if $\tan\beta = O(1)$ only the couplings proportional to m_t are important. If $\tan\beta \gg 1$ the m_b (m_τ) Yukawa couplings are enhanced and may give rise to large non-standard effects. We distinguish the two cases:

i) $\tan\beta \sim 1$ (disfavored by minimal SUSY)

Only the $H^+b\bar{t}$ vertex is of importance here. It yields a negative contribution

$$\Delta\rho^{(H^+)} \simeq -\frac{4}{3}\cot^2\beta\,\frac{\alpha}{\pi}\left(\frac{m_t}{M_Z}\right)^2 \tag{239}$$

and affects the Z-width, $\Delta\Gamma(Z \to b\bar{b}) < 0$, according to

$$\sqrt{2}G_\mu M_Z^2\,\left(1+\Delta\rho^{(H^+)}\right)\,T_{3b}\gamma_\mu\,(1-\gamma_5)\ . \tag{240}$$

ii) $\tan\beta \gg 1$

Here besides the H^+ also heavy neutrals can give large effects of either sign. Lepton universality may be violated in Γ_τ/Γ_μ by effects proportional to m_τ^2. These are below 1% and may be positive ($m_\pm$ large) or negative (m_A large).

7.3 Extra Z Bosons

The existence of additional neutral gauge-bosons is predicted by most extensions of the standard model gauge group. For a general investigation of effects from extra neutral gauge-bosons we refer to [70-74,90]. Here we only consider the simplest case of one extra Z-boson Z'^0 which mixes with the standard model Z denoted by Z^0. It is supposed that the particles of the Standard Model with 3 families have the normal $SU(2)_L \otimes U(1)_Y$ transformation properties such that

$$\begin{aligned}\mathcal{L}_{em} &= e j_\mu^{em} A^\mu \\ \mathcal{L}_{NC} &= \frac{g}{\cos\Theta_g}(J_{3L\mu} - \sin^2\Theta_g j_\mu^{em})Z^{0\mu} + \tilde{g}\tilde{J}_\mu Z'^{0\mu}\end{aligned} \tag{241}$$

with

$$A_\mu = \sin^2\Theta_g W_{3L\mu} + \cos^2\Theta_g B_\mu\ ;\quad Z_{0\mu} = \cos^2\Theta_g W_{3L\mu} - \sin^2\Theta_g B_\mu$$

and ($\Pi_\pm = \frac{1\pm\gamma_5}{2}$)

$$\begin{aligned} j_\mu^{em} &= J_{3L\mu} + J_Y \\ \tilde{J}_\mu &= \bar{f}\gamma_\mu(\Pi_-\tilde{Y}_L + \Pi_+\tilde{Y}_R)f \end{aligned} \tag{242}$$

depending on the specific extension. $SU(2)_L$ symmetry requires $\tilde{Y}_{\nu_e L} = \tilde{Y}_{eL}$, $\tilde{Y}_{uL} = \tilde{Y}_{dL}$ and we shall assume generation universality $\tilde{Y}_{\mu L} = \tilde{Y}_{eL}$, $\tilde{Y}_{sL} = \tilde{Y}_{dL}$ etc. Below, we shall restrict to the case of an extra $\tilde{U}(1)_{Y'}$ of most general E_6 origin where the symmetry is broken according to $E_6 \to G \otimes U_{1\beta}, G \supset SU(3)_c \otimes SU(2)_L \otimes U(1)_Y$ with $Z'^0 = \cos\beta Z_\chi + \sin\beta Z_\psi$. Then

$$\tilde{Y}_{L,R} = \cos\beta Q^\chi_{L,R} + \sin\beta Q^\psi_{L,R} \tag{243}$$

with

$$\begin{array}{rcrl} Q_L^\chi & = & \sqrt{\frac{3}{8}} & for \qquad (\nu_e, e^-, \bar{d})_L \\ Q_L^\chi & = & -\frac{1}{3}\sqrt{\frac{3}{8}} & for \qquad (e^+, u, \bar{u}, d)_L \\ Q_L^\psi & = & \frac{1}{3}\sqrt{\frac{5}{8}} & for \quad (\nu_e, e^-, e^+, u, \bar{u}, d, \bar{d})_L \end{array}$$

and $Q(f_R) = -Q(\bar{f}_L)$.[11]

Due to mixing the mass matrix is of the form

$$\mathcal{L}_{mass} = M_W^2 W^+ W^- + \frac{1}{2}\left(Z^0, Z'^0\right)\begin{pmatrix} M_{Z^0}^2 & \Delta^2 \\ \Delta^2 & M_{Z'^0}^2 \end{pmatrix}\begin{pmatrix} Z^0 \\ Z'^0 \end{pmatrix} \tag{244}$$

and can be diagonalized by

$$\begin{pmatrix} Z \\ Z' \end{pmatrix} = \begin{pmatrix} \cos\theta & \sin\theta \\ -\sin\theta & \cos\theta \end{pmatrix}\begin{pmatrix} Z^0 \\ Z'^0 \end{pmatrix} . \tag{245}$$

As a consequence the following effects are obtained

- a reduction of the Z mass by mixing (see below)

$$\begin{array}{rcl} M_Z^2\cos^2\theta + M_{Z'}^2\sin^2\theta & = & M_{Z^0}^2 \\ M_Z^2\sin^2\theta + M_{Z'}^2\cos^2\theta & = & M_{Z'^0}^2 \\ (M_{Z'}^2 - M_Z^2)\,\sin\theta\cos\theta & = & -\Delta^2 \end{array} \tag{246}$$

- a modification of the Z-couplings by mixing:

$$\begin{aligned} J_{Z\mu} &= \cos\theta J_{Z^0\mu} + \sin\theta\,\frac{\tilde{g}\cos\Theta_g}{g} J_{Z'^0\mu} \\ J_{Z'\mu} &= \cos\theta J_{Z'^0\mu} - \sin\theta\,\frac{g}{\tilde{g}\cos\Theta_g} J_{Z^0\mu} \end{aligned} \tag{247}$$

- Z'-exchange effects, for example, through the mixing amplitude

$$\frac{ig\tilde{g}}{\cos\Theta_g}\sin\theta J_Z^\mu J_{Z'\mu}\left(\frac{1}{s - M_Z^2} - \frac{1}{s - M_{Z'}^2}\right).$$

In general the parameters e, M_W, M_Z, $\sin\Theta_g = e/g$, $M_{Z'}$ $\tilde{g}$ and $\sin\theta$ are free. More interesting is the *constrained Higgs* case where all Higgses are in doublets and singlets. Generically we consider a model with two doublets (ϕ_1^0, ϕ_1^-) and (ϕ_2^+, ϕ_2^0) and two singlets ϕ_3^0 and ϕ_4^0 with vacuum expectation values $<\phi_i>= v_i/\sqrt{2}$. The mixing angle is then fixed by

$$\begin{aligned} \Delta^2 &= 2M_{Z^0}^2\sin^2\Theta_g\left(\tilde{Y}_1 v_1^2 - \tilde{Y}_2 v_2^2\right)/v^2 = \pm\sqrt{(M_{Z'}^2 - M_{Z^0}^2)(M_{Z^0}^2 - M_Z^2)} \\ M_{Z'^0}^2 &= 4M_{Z^0}^2\sin^2\Theta_g\sum_i\left(\tilde{Y}_i v_i\right)^2/v^2 \end{aligned} \tag{248}$$

[11] Special cases are the symmetry breaking patterns

$$\begin{array}{rcl} Z_\chi: & E_6 \to SO(10) \to SU(5)\otimes U(1)_\chi & for\ \ \beta = 0 \\ Z_\psi: & E_6 \to SO(10)\otimes U(1)_\psi & for\ \ \beta = \pi/2 \\ -Z_\eta: & E_6 \to SU(3)_c \otimes SU(2)_L \otimes U(1)_Y \otimes U(1)_\eta & for\ \ \beta = \pi - \arctan\sqrt{\frac{5}{3}} \end{array}$$

where $v^2 = v_1^2 + v_2^2$ and $M_W = gv/2$ and we have

$$\tan^2\theta = \frac{M_{Z^0}^2 - M_Z^2}{M_{Z'}^2 - M_{Z^0}^2};\;\; \sin\theta = \mp\sqrt{(M_{Z^0}^2 - M_Z^2)/(M_{Z'}^2 - M_Z^2)} \tag{249}$$

and

$$M_{Z^0}^2 = \frac{M_W^2}{\cos^2\Theta_g}\ . \tag{250}$$

due to standard model mixing with $\sin\Theta_g = e/g$. This implies

$$M_Z < M_{Z^0} < M_{Z'}$$

and hence

$$\rho_0 \;\; = \;\; \frac{M_W^2}{M_Z^2\cos^2\Theta_g} = \frac{M_{Z^0}^2}{M_Z^2} = 1 + \sin^2\theta\left(\frac{M_{Z'}^2}{M_Z^2} - 1\right) \geq 1\ . \tag{251}$$

This tree level modification mimics heavy particle effects.[12] Since the Higgs doublets have some given hypercharge, in our generic example,

$$\tilde{Y}_1 = -\frac{2}{3}\left(\cos\beta\sqrt{\frac{3}{8}} + \sin\beta\sqrt{\frac{5}{8}}\right);\;\; \tilde{Y}_2 = \frac{2}{3}\left(\cos\beta\sqrt{\frac{3}{8}} - \sin\beta\sqrt{\frac{5}{8}}\right)$$

The quantity

$$x = \tilde{Y}_1\xi - \tilde{Y}_2\,(1-\xi) = \pm\frac{1}{2\sin^2\Theta_g}\frac{\Delta\rho_0}{\rho_0};\;\; 0 \leq \xi = \frac{v_1^2}{v_1^2 + v_2^2} \leq 1$$

is fixed for a given model. This is called the *Higgs constraint* and determines $M_{Z'}$ in terms of $\sin\theta$ for given ξ and $\sin^2\Theta_g$. Notice the bound $min\,(\tilde{Y}_1, -\tilde{Y}_2)\ \leq x \leq max\,(\tilde{Y}_1, -\tilde{Y}_2)$. Since v_2 is the VEV that gives rise to the top mass, it is assumed that $0 \leq \xi \leq 0.5$ in the Higgs constraint.

In cases of interest, mentioned above, there is a second constraint coming from the unification condition if the group factors merge into a simple Lie group at some higher energy scale. Then $\tilde{g}$ is related to g by

$$\tilde{g} = g\tan\Theta_g\sqrt{\lambda};\;\; \lambda = O(1). \tag{252}$$

The constraint holds with $\lambda = 1$ if G breaks directly to $G_{SM}\otimes\tilde{U}(1)$. The effects from an extra $\tilde{U}(1)$ boson in Δr has been investigated in Ref. [91]. Since $\rho_0 \neq 1$ at tree level a natural renormalization scheme is the one using $\sin^2\Theta_g$ Eq. (74) which allows for a smooth limit

$$\lim_{\theta\to 0}\ \cos\Theta_g = \frac{M_W^2}{M_Z^2}$$

[12]The analysis applies also to the left-right symmetric model (LR), which is characterized by the gauge group $SU(2)_R\otimes SU(2)_L\otimes U(1)_{B-L}$. In this case

$$J_{Z'^0} = J_{LR} = c\,J_{3R} - \frac{1}{2c}\,J_{B-L};\;\; c = \left(\left(\frac{g_R}{g_L}\right)^2\frac{c_g^2}{s_g^2} - 1\right)^{1/2}$$

and $\tilde{g} = g\tan\Theta_g$. Mixing between the charged gauge bosons $W_L^\pm$ and $W_R^\pm$ (mixing angle $\theta^\pm$) may change the physical W mass, the Fermi constant $\sqrt{2}G_\mu = \frac{g^2}{4M_W^2}\cos^2\theta^\pm$ and ρ_0, which becomes $\rho_0/\rho^\pm$ where ρ_0 is given by Eq. (251) and $\rho^\pm = 1 + \sin^2\theta_\pm\,(M_{W'}^2/M_W^2 - 1)$. We assume the right-handed neutrino to be heavy and mixing in the charged sector to be negligible such that the charged sector for our purpose looks the same as in the SM. In the minimal LR model with $g_R = g_L$ we further have $\sin\theta \sim \sqrt{c_g^2 - s_g^2}\,(M_Z/M_{Z'})^2$.

and such that Eq. (27) holds true with the replacement

$$\Delta r \to \Delta\tilde{r}_g = \Delta r_g + (B)_{Z'} \tag{253}$$

where $(B)_{Z'}$ is the contribution from the $W-Z'$ box diagrams contributing to μ-decay. [13] Explicitly

$$\begin{aligned}(B)_{Z'} &= -\frac{3\tilde{g}^2}{8\pi^2}(\tilde{Y})^2_\ell \frac{\ln x}{x-1} \\ &= -\frac{9\alpha\lambda}{16\pi\cos^2\Theta_W}\left(\cos\beta + \sin\beta\sqrt{\frac{5}{27}}\right)^2 \frac{\ln x}{x-1}\end{aligned} \tag{254}$$

where $x = \frac{M^2_{Z'}}{M^2_W}$. With the general constraint $(\cos\beta + \sin\beta\sqrt{5/27})^2 \leq 1.185$ one obtains $|(B)_{Z'}| \leq 1.6\times10^{-3},\ \ 1.0\times10^{-3},\ \ 0.7\times10^{-3}$ for $\lambda = 1$ and $M_{Z'} = 100,\ 150,\ 200$ GeV. For the Z_η boson from $E_6 \to S_{SM}\otimes U(1)_\eta$ one has $\cos\beta = \sqrt{3/8}$, $\sin\beta = -\sqrt{5/8}$ and hence for the same values of λ and $M_{Z'}$:$|(B)_{Z'}| \leq -1.0\times10^{-4},\ \ -0.6\times10^{-4},\ \ -0.4\times10^{-4}$.

In view of the expected experimental precision of LEP experiments, $\delta\Delta r \simeq 0.004$, these contributions to Δr are likely to be negligible. As a result

$$\sin^2\Theta_g = \frac{A_0^2}{M_W^2}\frac{1}{1-\Delta\tilde{r}_g}\ \ ;\ \ \Delta\tilde{r}_g \simeq \Delta r^{SM} \tag{255}$$

such that $sin^2\Theta_g \simeq \sin^2\Theta_W^{SM}$ when calculated in terms of α, G_μ and M_W.

However, since $\rho_0 > 1$, the prediction of the W-mass is affected as follows from Eqs. (101) and (227). In linear approximation we get

$$\delta\Delta r = -\frac{\cos^2\Theta_W}{\sin^2\Theta_W}\Delta\rho_0,\ \ \Delta\rho_0 = \sin^2\theta\left(\frac{M^2_{Z'}}{M^2_Z} - 1\right). \tag{256}$$

When calculated in terms of α, G_μ and M_Z the weak mixing parameter changes according to

$$\sin^2\Theta'_g = \frac{1}{2}\left\{1 - \sqrt{1 - \frac{4A_0^2}{\rho_0 M_Z^2}\frac{1}{1-\Delta\tilde{r}_g}}\right\} \simeq \sin^2\Theta_g - \frac{s_g^2 c_g^2}{c_g^2 - s_g^2}\frac{\Delta\rho_0}{\rho_0} \tag{257}$$

where we used the notation $\sin^2\Theta_g = s_g^2, c_g^2 = 1-s_g^2$. The W mass is given by $M_W^2 = \rho_0 M_Z^2\cos^2\Theta'_g$.

Also the tree level modifications of the Z-couplings through mixing can be tested at LEP. Mixing affects the Z-width and the interference term as indicated in Eqs. (175) and (176). The widths now read

$$\Gamma_f = \frac{\sqrt{2}G_\mu M_Z^3\rho_0\rho_f N_{cf}}{12\pi}\ \frac{\left\{\cos^2\theta(v_f^2+a_f^2) + 2\cos\theta\sin\theta'(v_f v'_f + a_f a'_f) + \sin^2\theta'(v'^2_f + a'^2_f)\right\}}{(1+\delta_{QED})\,(1+\delta_{QCD})} \tag{258}$$

where $\sin\theta' = \sin\theta\ \sin\Theta_g\ \sqrt{\lambda}$. Here we have used Eqs. (247) and (252). The new couplings are parametrized by

$$\begin{array}{lcclcc} a'_\nu &=& \cos\beta\ \sqrt{\frac{3}{8}} + \sin\beta\frac{1}{3}\sqrt{\frac{5}{8}} & & v'_\nu &=& a'_\nu \\ a'_e &=& \cos\beta\frac{2}{3}\sqrt{\frac{3}{8}} + \sin\beta\frac{2}{3}\sqrt{\frac{5}{8}} & & v'_e &=& \cos\beta\frac{4}{3}\sqrt{\frac{3}{8}} \\ a'_u &=& \cos\beta\frac{2}{3}\sqrt{\frac{3}{8}} + \sin\beta\frac{2}{3}\sqrt{\frac{5}{8}} & & v'_u &=& 0 \\ a'_d &=& a'_e & & v'_d &=& -v'_e \end{array} \tag{259}$$

[13] Contributions like the extra vertex corrections which vanish for $\theta \to 0$ have been neglected. Also neglected are the contributions to the vector-boson self-energies of the extra particles present in such models

Treating the Z' effects as perturbations we obtain

$$\Delta\Gamma'_f = \Gamma'_f - \Gamma_f = \Delta\Gamma^\rho_f + \Delta\Gamma^\theta_f \tag{260}$$

with

$$\begin{aligned}
\Delta\Gamma^\rho_f &= \Delta\rho_0\,\Gamma^{SM}_f\,\left(1+\frac{4Q_f v_f}{v_f^2+a_f^2}\frac{s_g^2c_g^2}{c_g^2-s_g^2}\right)\\
\Delta\Gamma^\theta_f &= \sin\theta\,\sin^2\Theta_g\sqrt{\lambda}\,\Gamma^{SM}_f\frac{2\,(v_f v'_f + a_f a'_f)}{v_f^2+a_f^2}
\end{aligned} \tag{261}$$

The second term contributing to $\Delta\Gamma^\rho_f$ is $\frac{d\Gamma^{SM}}{ds_g^2}\,\Delta s_g^2$ coming from the change in $\sin^2\Theta_g$ as given by Eq. (257).

Given the "corrected" witdhs, which also determine other quantities like Γ_Z, σ^{peak} and R_{had}, one may directly derive bounds on the additional contributions using the results presented in Tab. 7. It shoud be noted, however, that the effective cross-section Eq. (172) is also directly affected through the mixing term Eq. (175) which shifts the Z-peak according to Eqs. (179) and (181).

New Z''s also modify low energy NC quantities. For example, in $\nu_\mu e$ scattering additional contributions may be absorbed into effective Zee couplings $v^{\nu e} = (\varepsilon^{\nu e}_L + \varepsilon^{\nu e}_R)/2$, $a^{\nu e} = (\varepsilon^{\nu e}_L - \varepsilon^{\nu e}_R)/2$ for which one finds

$$\begin{aligned}
\Delta\varepsilon^{\nu e}_{L,R} &= \varepsilon^{'}_{L,R} - \varepsilon^{SM}_{L,R}\\
&= \Delta\rho_0\,\left(\varepsilon^{SM}_{L,R} + 2\frac{s_g^2c_g^2}{c_g^2-s_g^2}\right)\\
&+ \sin\theta\sin^2\Theta_g\sqrt{\lambda}\,((v_e\pm a_e)(v'_\nu+a'_\nu)+(v'_e\pm a'_e)(v_\nu+a_\nu))\\
&+ \sin^2\Theta_g\lambda\frac{M_Z^2}{M_{Z'}^2}(v'_e\pm a'_e)(v'_\nu+a'_\nu)\ .
\end{aligned} \tag{262}$$

Similay formulae are obtained for νN scattering.

At present there in no phenomenological evidence for new Z''s. The direct bound on the Z' mass

$$M_{Z'} > 300 \quad \text{GeV} \tag{263}$$

coming from the $p\bar{p}$ colliders (CDF in particular) is quite model-independent [92]. On the other hand, signals which could be seen at LEP and in low energy NC processes are rather model-dependent. Fortunately, LEP and NC data provide complementary bounds on the mixing angle θ. The Z resonance observations are mainly sensitive to mixing. Typical (90% CL) allowed regions for $\xi_0 = -\theta\sqrt{\lambda}$ and lower bounds for $M_{Z'}$ are the following [90,92,93,94]:

model	β	$\xi_0\,(\theta)$ (radians)	$M_{Z'}$ (GeV)	
			CDF	electroweak data
χ	0	$-0.015 \le \xi_0 \le 0.005$	340	290(600)
ψ	$\pi/2$	$-0.004 \le \xi_0 \le 0.021$	350	250(550)
η	$-\arctan\sqrt{\frac{5}{3}}$	$-0.024 \le \xi_0 \le 0.075$	320	110(330)
LR	0	$-0.004 \le \theta \le 0.020$	360	270(800)

(264)

In parantheses are given the lower bounds for $M_{Z'}$ when the Higgs constraint is applied. Very little room remains for ξ_0 outside the "central" range $|\beta + \arctan\sqrt{\frac{5}{3}}| \le 30^\circ$. The best place to

put model-independent bounds on the Z' mass are the future hadron colliders by looking for direct production. If such gauge bosons would be found they would be a strong indication for unified gauge models.

Finally, we mention Z' contributions to parity violation in atoms. For an atom with Z protons and N neutrons, the weak charge is defined by

$$Q_w = -4a_e \ \{v_u \, (2Z + N) + v_d \, (Z + 2N)\} \tag{265}$$

It is shifted due to $\rho_0 \neq 1$ by

$$\Delta Q_w^\rho = \Delta\rho_0 \ \left(Q_w^{SM} + 4Z \frac{s_g^2 c_g^2}{c_g^2 - s_g^2} \right) \tag{266}$$

where the second term is due to the change of $\sin^2 \Theta_g$. The change of the Z couplings due to mixing (to linear order in $\sin\theta$) yields

$$\Delta Q_w^\theta = \sin\theta \sin^2 \Theta_g \sqrt{\lambda} \left(a'_e/a_e Q_w^{SM} - 4a_e \, \{v'_u \, (2Z + N) + v'_d \, (Z + 2N)\} \right) \quad . \tag{267}$$

Finally, the contribution from direct Z' exchange is given by

$$\Delta Q_w^{Z'} = -4a'_e \sin^2 \Theta_g \lambda \frac{M_Z^2}{M_{Z'}^2} \ \{v'_u \, (2Z + N) + v'_d \, (Z + 2N)\} \tag{268}$$

where we have used Eqs. (247) and (252). Altogether, we have

$$\Delta Q'_w = Q'_w - Q_w^{SM} = \Delta Q_w^\rho + \Delta Q_w^\theta + \Delta Q_w^{Z'} \tag{269}$$

which is constrained, for Z=55 and N=78, by Eq. (220). Again the bounds are very model dependent and will not be reported here [95,96]. Notice that the two terms contributing to ΔQ_w^ρ essentially cancel for Cesium: We find $\Delta Q_w^\rho \simeq 0.1 \, \Delta\rho_0$ for $\sin^2 \Theta_g = 0.23$. This result agrees with the observation of Ref. [76] that the weak charge of C_s is largely independent of $\Delta\rho$. However, we neither agree with Ref. [95], where the second contribution to ΔQ_w^ρ is not taken into account, nor with Ref. [96] where the second term has a different coefficient of opposite sign.

7.4 SUSY particles

Supersymmetric extensions of the Standard Model require the existence of new superpartners for all known leptons, quarks, gauge and Higgs bosons. They are called sleptons, squarks, gauginos and higgsinos, respectively. In addition there must be at least one extra Higgs doublet which also has its SUSY partners. We restrict ourselves to a discussion of the minimal supersymmetric SM (MSSM) which usually is thought as a renormalizable low energy effective theory emerging from a supergravity (SUGRA) model [97]. The Lagrangian exhibits global supersymmetry softly broken at a scale M_{SUSY} commonly taken to coincide with the "new physics scale" $\Lambda_{NP} \simeq 1$ TeV, where the SM is expected to loose its validity. If one assumes the SUSY particles (sparticles) all to have masses below M_{SUSY}, then light sparticles of a few tens of GeV are expected in the spectrum. The MSSM scenario is characterized by the following features:

- the gauge group is the SM gauge group and no new heavy gauge bosons besides the W and Z exist;
- there are no new matter fields besides the quarks and leptons and two Higgs doublets which are needed to provide supersymmetric masses to quarks and leptons;
- it follows that gauge- and Yukawa-couplings of the sparticles are all fixed by supersymmetry;
- in spite of some constraints, masses and mixings of the sparticles remain quite arbitrary.

In addition one assumes that

- flavor- and CP-violation is as in the SM, namely coming from the (now supersymmetrized) Yukawa couplings only.

This implies that at some grand unification scale M_X there is a universal mass term for all scalars as well as a universal gaugino mass term, i. e. the SUSY-breaking Majorana masses of the gauginos are equal at M_X. A further assumption is that

- R-parity, even for particles, odd for sparticles, is conserved.

This is a strong assumption implying that sparticles must be produced in pairs and that there exists a absolutely stable *lightest supersymmetric particle* (LSP).

Although local gauge symmetry and supersymmetry constrain the structure of the models there are many additional free parameters like the sfermion masses and mixing parameters and the gaugino-higgsino masses and mixing parameters. The MSSM parameter space is the following:

7.4.1 MSSM parameters

i) Higgs sector

The parameters of the MSSM Higgs sector are the same as the ones for the two doublet Higgs model considered in Sec. 7.2 with the SUSY constraints Eq. (237). The tree level mass constraints imply $m_h \leq M_Z \, |\cos 2\beta| \leq M_Z$ and the upper bound is saturated at $\beta = \pi/2$. If the two Higgs

VEV's are equal, $v_1 = v_2$ and thus $\tan\beta = 1$, then $m_h = 0$. The CP-odd scalar mass m_A is a key parameter. The limiting cases are

$$\begin{array}{lllll} 1) & m_A & \to & \infty : \\ & m_\pm & \to & m_A \\ & m_H & \to & m_A \\ & m_h & \to & M_Z \,|\cos 2\beta| \\ & \sin^2(\alpha-\beta) & \to & 1 \end{array} \tag{270}$$

and the light Higgs h couples as in the minimal SM.

$$\begin{array}{lllll} 2) & m_A & \to & 0 : \\ & m_\pm & \to & M_W \\ & m_H & \to & M_Z \\ & m_h & \to & 0 \\ & \sin^2(\alpha-\beta) & \to & \sin^2 2\beta \ . \end{array} \tag{271}$$

From the tree level constraints we would conclude that $\tan\beta \simeq 1$ is excluded by the Higgs mass bound $m_h > 49$ GeV from LEP. Using Eq. (237), and *assuming* that the solution with $\tan\beta = v_{top}/v_{bottom} > 1$ is realized we obtain

$$\tan\beta > 2.38\,(1.82) \text{ if } m_A \leq 1 \text{ TeV}(\infty) \ . \tag{272}$$

The assumption made is suggested by the fact that $m_t \gg m_b$ which lets look $v_{top}/v_{bottom} < 1$ unnatural. For this solution we have

$$\cos 2\beta = \frac{1-\tan^2\beta}{1+\tan^2\beta} < 0 \ . \tag{273}$$

Another consequence of the Eq. (237) is the following. Since at LEP2 one should be able to detect a Higgs up th $m_h \simeq M_Z$ the MSSM could be ruled out if no Higgs is found. Recently, it has been discovered [98] that radiative corrections to the mass relations Eq. (237) may be huge if the top is heavy.[14] The conclusions thus must be modified accordingly. The major impact is that the bound $m_h \leq M_Z$ gets changed to the much *weaker* bound $m_h \leq 1.2\,(1.6)\,M_Z$ if $m_t = 150\,(200)$ GeV. For $m_t \simeq 100$ GeV the shift is about 2 GeV. $M_{\tilde{Q}} = 1$ TeV has been taken here.

[14]Haber and Hempfling [98] derived an expression for

$$\Delta m_h^2 \equiv m_{h^0}^2 - M_Z^2$$

by calculating the shift for $\tan\beta = \infty$ ($\beta = \pi/2$) where the bound $m_{h^0} = M_Z$ is saturated, and correcting for finite β at tree level:

$$\Delta m_h^2 = \left(\Delta m_h^2\right)_{\beta=\pi/2} - \frac{1}{2}\left(\sqrt{(m_A^2 - M_Z^2)^2 + 4m_A^2 M_Z^2 \sin^2 2\beta} - \ (m_A^2 - M_Z^2)\right) \ .$$

The shift is given by the difference of the h and Z self-energy functions (with tadpoles omited) minus a tadpole contribution

$$\left(\Delta m_h^2\right)_{\beta=\pi/2} = Re\left\{\Pi_{hh}(M_Z^2) - \Pi_{ZZ}(M_Z^2)\right\} - \frac{g}{2M_W} T_h(0) \ .$$

This correction turns out to be large if $M_Z < m_t \ll M_{\tilde{Q}}$. If one neglects $\tilde{t}_L - \tilde{t}_R$ mixing the leading term is given by

$$\Delta m_h^2 \simeq \frac{3g^2 m_t^4}{8\pi^2 M_W^2} \ln\left(\frac{M_{\tilde{Q}}^2}{m_t^2}\right) + \cdots$$

The same leading behavior is obtained for $\tan\beta = 1$ ($\beta = 0$) where $m_{h^0} = 0$, so that this kind of shift looks to be universal.

ii) Sleptons and squarks sector

The diagonal masses of the sfermioms are given by

$$\begin{aligned} m^2_{\tilde{f}_L} &= M^2_{\tilde{F}_L} + m^2_f + M^2_Z \cos 2\beta \, (T_{3f} - Q_f s^2_W) \\ m^2_{\tilde{f}_R} &= M^2_{\tilde{F}} + m^2_f + M^2_Z \cos 2\beta \, Q_f s^2_W \end{aligned} \tag{274}$$

where

$$M_{\tilde{F}_L} = \left\{ \begin{array}{lcl} M_{\tilde{L}} & ; & f = \nu, e \\ M_{\tilde{Q}} & ; & f = u, d \end{array} \right. \quad M_{\tilde{F}} = M_{\tilde{E}}, M_{\tilde{U}}, M_{\tilde{D}} \, ; f = e, u, d$$

are the soft SUSY-breaking masses. In particular, this mass interdependence implies the constraints (setting $m^2_e, m^2_d - m^2_u \simeq 0$)

$$m^2_{\tilde{e}_L} - m^2_{\tilde{\nu}_L} = m^2_{\tilde{d}_L} - m^2_{\tilde{u}_L} = -M^2_W \cos 2\beta \tag{275}$$

for the mass splittings of the SUSY partners of the light fermions. In addition L-R mixing terms $A^{(f)}_{mix} \, (\tilde{f}^*_L \tilde{f}_R + \tilde{f}^*_R \tilde{f}_L)$ are present where the mixing parameters are of the form

$$A^{(f)}_{mix} = m_f \, (A_f - \mu \cot \beta) \tag{276}$$

and A_t is another model dependent soft SUSY breaking parameter. For the stop sector neglecting the bottom mass ($m_b = 0$) the mass matrix is of the form

$$(\tilde{t}^*_L, \tilde{t}^c_R) \left(\begin{array}{cc} m^2_{\tilde{b}_L} + m^2_t + M^2_W \cos 2\beta & m_t A_t \\ m_t A_t & m^2_{\tilde{t}_R} \end{array} \right) \left(\begin{array}{c} \tilde{t}_L \\ \tilde{t}^{*c}_R \end{array} \right)$$

such that the physical masses are given by

$$\begin{aligned} m^2_{\tilde{t}_{1,2}} = \frac{1}{2} \Big\{ & m^2_{\tilde{b}_L} + M^2_{\tilde{U}} + 2m^2_t + M^2_W \cos 2\beta \, (1 + \frac{2}{3} \tan^2 \Theta_W) \\ & \mp \sqrt{(m^2_{\tilde{b}_L} - M^2_{\tilde{U}} + M^2_W \cos 2\beta \, (1 - \frac{2}{3} \tan^2 \Theta_W))^2 + 4 m^2_t A^2_t} \Big\} \end{aligned} \tag{277}$$

with $m_{\tilde{t}_1} \leq m_{\tilde{t}_2}$ and the mixing angle is given by

$$\tan \phi_t = \frac{m^2_{\tilde{t}_1} - m^2_{\tilde{b}_L} - m^2_t - M^2_W \cos 2\beta}{m_t A_t} \tag{278}$$

where $m^2_{\tilde{b}_L}$ is the physical mass of the left-handed sbottom. Notice that in the limit $m_b = 0$, considered here, the $\tilde{b}_L$ does not mix with the $\tilde{b}_R$.

For simplicity we will assume $M_{\tilde{Q}} = M_{\tilde{U}} = M_{\tilde{D}} \simeq m_{\tilde{q}}$ where $m_{\tilde{q}}$ represents an *average* squark mass.

Family mixing will be neglected here.

ii) Chargino-neutralino (gaugino-higgsino) sector

The chargino-neutralino sector is given by the SUSY partners of the gauge bosons and the Higgs scalars. The mixing of the states depends on the following parameters:

- $\tan\beta$
- μ the supersymmetric higgsino mass
- M the $SU(2)_L$ gaugino mass
- M' the $U(1)_Y$ gaugino mass
- $m_{\tilde{g}}$ the $SU(3)_c$ gluino mass .

The two chargino mass eigenstates $\tilde{\chi}_1^\pm$ and $\tilde{\chi}_2^\pm$ (charged Dirac fermions) are mixtures of winos $\tilde{W}^\pm$ and higgsinos $\tilde{\phi}^\pm$ and $\tilde{H}^\pm$. The mixing is described by the 2×2 matrix (in the $(\tilde{W}^+, \tilde{H}^+)$ basis)

$$\begin{pmatrix} M & \sqrt{2}M_W \sin\beta \\ \sqrt{2}M_W \cos\beta & \mu \end{pmatrix} . \tag{279}$$

The neutralinos $\tilde{\chi}_i^0$ $(i = 1, 2, 3, 4)$ (neutral Majorana fermions), labeled in order of increasing mass, are obtained by diagonalizing the 4×4 mixing matrix (in the $(\tilde{B}, \tilde{W}_3, \tilde{h}, \tilde{H})$ basis)

$$\begin{pmatrix} M' & 0 & -M_Z\cos\beta\sin\Theta_W & M_Z\sin\beta\sin\Theta_W \\ 0 & M & M_Z\cos\beta\cos\Theta_W & -M_Z\sin\beta\cos\Theta_W \\ -M_Z\cos\beta\sin\Theta_W & M_Z\cos\beta\cos\Theta_W & 0 & -\mu \\ M_Z\sin\beta\sin\Theta_W & -M_Z\sin\beta\cos\Theta_W & -\mu & 0 \end{pmatrix} . \tag{280}$$

Usually a grand-unification assumption

$$M' = \frac{5}{3}\tan^2\Theta_W\, M = \frac{5}{3}\frac{\alpha}{\cos^2\Theta_W \alpha_s} m_{\tilde{g}} \tag{281}$$

is made which holds in supergravity (SUGRA) scenarios.

7.4.2 Mass limits for sparticles

The fact that no SUSY particles have been seen until now may be expressed more quantitatively in term of lower bounds for sparticle masses [4,99,100]. These limits usually refer to the MSSM and the assumption of R-parity conservation. Part of the limits are direct search bounds, some derive from the fact that the partial Z widths are rather close to the SM prediction and finally there are limits which derive from the mass relations Eqs. (237) and (272-281).

An important bound was obtained at CDF for the *gluino* mass [4]

$$m_{\tilde{g}} > 150 \text{ GeV} \tag{282}$$

which implies bounds on M and M' through the unification condition Eq. (281). Bounds from UA2 and CDF [4] for the *squark* masses are given by

$$m_{\tilde{q}} > 90 \text{ GeV} . \tag{283}$$

The *sneutrino* mass is constrained by the absence a the corresponding contribution ($\Gamma_{\tilde{\nu}} = 1/2\Gamma_\nu^{SM}$ if $m_{\tilde{\nu}} < M_Z/2$) to the Z width, yielding

$$m_{\tilde{\nu}} > 29\,(39) \text{ GeV if only one light } \tilde{\nu} \text{ (if three light } \tilde{\nu}'s) \tag{284}$$

is (are) assumed. For *left-handed sleptons* direct LEP searches [99] yield the limit $m_{\tilde{\ell}_L} > 43$ GeV . Here, using Eq. (275), a stronger bound follows from the sneutrion mass bound

$$m_{\tilde{\ell}_L} > 73\,(65) \text{ GeV if } m_A \leq 1 \text{ TeV } (\infty) . \tag{285}$$

Since the *right-handed sleptons* are not related to sneutrino masses and a massless $m_{\tilde{\ell}_R}$ would contribute 17.3 MeV only to the Z width only direct search limits can be given. LEP searches give

$$m_{\tilde{\ell}_R} > 41 \text{ GeV} \quad \ell = e, \mu, \tau \ . \tag{286}$$

Finally, bounds on *chargino* and *neutralino* are as follows: For the lightest chargino Z width bounds imply

$$m_{\tilde{\chi}^\pm} > 45 \text{ GeV} \ . \tag{287}$$

Within the MSSM such a limit yields a bound

$$m_{\tilde{\chi_1}^\pm} - m_{\tilde{\chi_1}^0} > 13 \ (5) \text{ GeV} \tag{288}$$

if we assume $m_{\tilde{q}} \leq 1$ TeV (5 TeV). Bounds on the neutralinos are more difficult to obtain. For the lightest neutralinos only bounds deriving from the MSSM assumptions, the unification condition, in particular, give restrictions. They are very weak $m_{\tilde{\chi_1}^0}, m_{\tilde{\chi_2}^0} >$ a few GeV, however. A bound

$$m_{\tilde{\chi_3}^0} > 61 \text{ GeV} \tag{289}$$

follows from the Z width [100].

7.4.3 Virtual effects from sparticles

For the minimal supersymmetric extension of the Standard Model one-loop radiative corrections have been calculated by several authors [101-108]. We concentrate our discussion to the contributions of SUSY particles to the ρ-parameter. The contributions from the Higgs scalars, the sfermion scalars and the gaugino-higgsino fermions may be considered separately

$$\Delta\rho^{SUSY} = \Delta\rho^H + \Delta\rho^{SF} + \Delta\rho^{GH} \ . \tag{290}$$

(a) Higgs contributions

The two doublet Higgs contribution Eq. (236) to the ρ parameter is now constrained by the mass relationships Eq. (232). From the limiting cases Eqs. (270) and (271) one finds

$$\Delta\rho^H \simeq \frac{\sqrt{2}G_\mu M_Z^2 c_W^2}{16\pi^2} \left\{ 3\cos^2 2\beta \ \left(\frac{\ln c_W^2}{c_W^2 - 1} - \frac{1}{c_W^2} \right) - \sin^2 2\beta \ \frac{\ln c_W^2}{c_W^2 - 1} + 1 \right\} \ ; \ m_A \to 0 \tag{291}$$

which maximizes $\Delta\rho^H$ for $\cos^2 2\beta = 1$. On the other hand

$$\Delta\rho^H \simeq \frac{\sqrt{2}G_\mu M_Z^2 c_W^2}{16\pi^2} \ 3 \ f_H(\cos^2 2\beta, c_W^2) \ ; \ m_A \to \infty \tag{292}$$

minimizes $\Delta\rho^H$ for $\cos^2 2\beta = 1$. As a result the total contribution from the Higgs sector is bound by (for $s_W^2 = 0.22$)

$$-3.1 \times 10^{-4} \leq \Delta\rho^H \leq 3.6 \times 10^{-4} \tag{293}$$

beyond observability at LEP experiments. This is much smaller than the SM Higgs contribution

$$\Delta\rho_{SM}^H \simeq -2.2 \times 10^{-3} \text{ for } m_H \simeq 1 \text{ TeV} \tag{294}$$

and also is in contrast to the large effects Eqs. (237) and (238) possible in two doublet models of non-SUSY type.

(b) SUSY partners of the light fermions.

We first should mention that SUSY partners of fermions occur in pairs, one sfermion for each helicity. The contributions of the scalar sleptons and squarks to the vector boson self-energies are given by Eq. (235). Notice that $f_S(m_1^2, m_2^2)$ vanishes for equal masses. Hence only pairs of fermions with different masses contribute. Two fermion doublet partners yield a ρ-parameter contribution

$$\Delta\rho^{sfermion\ doublet} = \frac{\sqrt{2}G_\mu N_{cf}}{16\pi^2} f_S(\tilde{m}_1^2, \tilde{m}_2^2) \tag{295}$$

which is half of a corresponding fermion doublet contribution.

The SUSY partners of zero mass fermions cannot give large contributions. The spartners of the right-handed fermions do not contribute, since (in the zero fermion mass limit) they do not couple to $W^\pm$ and W_3. For the left-handed fermion spartners gauge symmetry requires the SUSY-breaking masses to be equal such that mass differences can only be due to the gauge symmetry breaking which leads to the mass differences Eq. (275). We consider the sleptons first. The largest contribution can be obtained if all sneutrino masses vanish and the slepton masses are equal to the W mass and if we assume, unrealistically, that right- and left-scalars give equal contributions. Then

$$\Delta\rho^{sleptons} \leq \frac{\sqrt{2}G_\mu N_f}{16\pi^2} \simeq 2.1 \times 10^{-3} \quad (N_f = 3)\ . \tag{296}$$

Taking into account the actual mass limit for the sneutrino mass Eq. (284) this bound improves to

$$\Delta\rho^{sleptons} \leq 1.1 \times 10^{-3} \quad (N_f = 3, m_{\tilde{\nu}} > 39\ \text{GeV})\ . \tag{297}$$

For the squarks a similar result is obtained

$$\Delta\rho^{\tilde{u},\tilde{d},\tilde{s},\tilde{c}} \leq 0.8 \times 10^{-3} \quad (m_{\tilde{q}} > 90\ \text{GeV})\ . \tag{298}$$

(c) SUSY partners of t and b.

Taking into account the $\tilde{t}_L - \tilde{t}_R$ mixing one obtains [105]

$$\Delta\rho^{\tilde{t},\tilde{b}} = \frac{\sqrt{2}G_\mu}{16\pi^2}\left\{\cos^2\phi_t f_S(m_{\tilde{t}_1}^2, m_{\tilde{b}_L}^2) + \sin^2\phi_t f_S(m_{\tilde{t}_2}^2, m_{\tilde{b}_L}^2) - \cos^2\phi_t \sin^2\phi_t f_S(m_{\tilde{t}_1}^2, m_{\tilde{t}_2}^2)\right\} \tag{299}$$

where the masses and the mixing angle are given by Eqs. (277) and (278). Again some limiting cases best illustrate the kind of contributions one may obtain. The key parameter is the soft SUSY breaking parameter $m = M_{\tilde{F}}$ of Eqs. (274) and (277). Barbieri and Maiani [101] have summarized the result as follows:

- Squarks give a significant only if the associated fermion doublet splitting is greater than m. For the tb-doublet one finds ($m_b = 0$)

$$\Delta\rho^{stop} = \frac{\sqrt{2}G_\mu N_{cf}}{16\pi^2} m_t^2 \quad ;\ (m_t \gg m)\ . \tag{300}$$

  This contribution is equal in size with the top contribution itself and thus the top mass bound would be scaled to smaller values by a factor $\sqrt{2}$ if m is small. Again, for simplicity, we have assumed the right- and left-scalars to be degenerate and give equal contributions.

- The other limiting case we have for m large (assuming $\tan\beta = 1$ for simplicity) yielding

$$\Delta\rho^{stop} = \frac{\sqrt{2}G_\mu N_{cf}}{16\pi^2 3}\frac{m_t^4}{m^2}\,(1 - 2a + \frac{8}{5}a^2) \quad ;\ (m_t \ll m) \tag{301}$$

  where $a = A_t/2m_t$ is taken to be of order $O(1)$. The truth lies somewhere between the two cases. One may identify m with the average squark mass $m_{\tilde{q}}$ obeying the bound Eq. (283).

A global analysis by Bilal et al. [109] yields the top mass bound

$$m_t = 131^{+24}_{-28}\ \text{GeV}, \quad \sin^2\Theta_W = 0.2272^{+0.0035}_{-0.0032} \tag{302}$$

for $m_{\tilde{q}} = 150$ GeV and $\tan\beta = 1.3$ which compares with the SM value

$$m_t = 135^{+27}_{-31}\ \text{GeV}, \quad \sin^2\Theta_W = 0.2271^{+0.0035}_{-0.0032}\ . \tag{303}$$

For lower values of $m_{\tilde{q}}$ the changes of the upper bound is more significant. For $m_{\tilde{q}} = 80$ GeV the upper bound decreases to 143 GeV while the lower bound remains essentially unaffected.

(d) Gaugino-higgsino contributions.

Charginos and neutralinos are fermions. Their contribution to the ρ-parameter may be evaluated using the following functions. A fermion loop with masses m_1 and m_2 and couplings $\bar{\psi}_1\,(v - a\gamma_5)\,\gamma_\mu\psi_2\,V^\mu$ yields the contribution [101]

$$\Pi_V^f(0) = \frac{1}{16\pi^2}\left\{|v|^2 f_f(m_1, m_2) + |a|^2 f_f(-m_1, m_2)\right\} \tag{304}$$

with

$$f_f(m_1, m_2) = (m_1 - m_2)^2 \ln\frac{\Lambda^4}{m_1^2 m_2^2} - 2m_1 m_2 - \frac{m_1^4 + m_2^4 - 2m_1 m_2\,(m_1^2 + m_2^2)}{m_1^2 - m_2^2}\ln\frac{m_1^2}{m_2^2}\ .$$

Here Λ is a cut-off which cancels in physical quantities. In principle, it is straight forward to write down the general expression for $\Delta\rho = \Pi_W(0)/M_W^2 - \Pi_Z(0)/M_Z^2$ in terms of the chargino and neutralino masses and the $W^\pm\tilde{\chi}_i^{\mp}\tilde{\chi}_j^{\,0}$ the $Z\tilde{\chi}_i^{\pm}\tilde{\chi}_j^{\mp}$ and the $Z\tilde{\chi}_i^{\,0}\tilde{\chi}_j^{\,0}$ couplings. While it is easy to diagonalize the 2×2 chargino mass matrix analytically the diagonalization of the 4×4 neutralino mass matrix is easier to do numerically.

The largest contribution to the ρ-parameter from this sector is obtained if the soft SUSY breaking parameters vanish. In this limit a fairly simple result follows [105]

$$\begin{aligned}\Delta\rho_{max}^{GH} \;=\; & \frac{\sqrt{2}G_\mu M_W^2}{16\pi^2}\left\{-6 + \frac{\cos^2 2\beta}{c_W^2}\right. \\ & + \frac{8\cos^2\beta c_W^2 - 1 + 4s_W^2 - \cos 2\beta}{c_W^2 - 1/(2\cos^2\beta)}\ln(2\cos^2\beta c_W^2) \\ & \left. + \frac{8\sin^2\beta c_W^2 - 1 + 4s_W^2 + \cos 2\beta}{c_W^2 - 1/(2\sin^2\beta)}\ln(2\sin^2\beta c_W^2)\right\}\end{aligned} \tag{305}$$

which for $m_{\tilde{\chi}_1^\pm} > 45$ GeV leads to the bound

$$\Delta\rho^{GH} < 1.4\times 10^{-3}\ . \tag{306}$$

So far we only considered the universal vector-boson self-energy contributions. There are additional process-dependent vertex and fermion self-energy corrections coming from the gaugino-higgsino

sector. These may be of the same size and of either sign as the universal corrections. In Ref. [106] these effects have been investigated using the renormalization scheme with α, G_μ and $\sin^2\Theta_{\nu_\mu e}$ as input parameters. For the range $0 \leq M \leq 250$ GeV and $0 \leq |\mu| \leq 200$ GeV in the gaugino-higgsino parameter space, taking into account the phenomenological constraints for the SUSY masses, the following results have been found for $\tan\beta = 2\,(8)$:

$$\begin{aligned} \Delta\rho^{SUSY} &= +2\times 10^{-3} \text{ to } -2.5\times 10^{-3} \\ \delta M_W^{SUSY} &= -100 \text{ MeV to } -150 \text{ MeV} \\ \delta M_Z^{SUSY} &= -150 \text{ MeV to } -250 \text{ MeV} \end{aligned} \tag{307}$$

and for most of the above (M,μ)-window. By a factor 1.5 larger values are obtained near to the rim of the allowed regions. The shift in M_W for fixed α, G_μ and M_Z may be obtained using the relation

$$\Delta r = \frac{\Delta M_W^2}{M_W^2} + \frac{c_W^2}{s_W^2}\left(\frac{\Delta M_Z^2}{M_Z^2} - \frac{\Delta M_W^2}{M_W^2} - \Delta\rho\right) \tag{308}$$

and Eq. (101). One typically obtains (estimated from the Figures of Ref. [106])

$(M,\mu,\tan\beta)$	δM_W^{SUSY}	δM_W^{SUSY}	$\delta\rho^{SUSY}$	$\delta\Delta r^{SUSY}$	$\delta M_W^{SUSY}(M_Z$ fixed)
$(100,-100,2)$	-135	-200	0.00015	-0.011	-191
$(100,-100,8)$	-145	-220	0.00020	-0.008	-142
$(100,+100,8)$	-180	-225	0.00000	-0.006	-102
$(\ 20,-\ 20,2)$	-190	-300	0.00160	-0.016	-277

where M and μ are given in GeV and the mass shifts in MeV. All these contributions (for allowed *low* values of the soft SUSY breaking parameters) have the same sign as the top contribution and thus would strengthen the upper bound for m_t.

We may summarize the results as follows:

Virtual effects of supersymmetry may be observable in precision measurements at LEP if the masses of SUSY particles are close to the present experimental mass bounds. In this case the soft SUSY-breaking parameters (scale M_{SUSY}) must be rather small. Under reasonable assumptions for the parameter ranges $|\Delta\rho^{SUSY}| <\sim 3\times 10^{-3}$ and 100 MeV $\leq -\delta M_W^{SUSY} \leq 300$ MeV.

On the other hand, in the limit where M_{SUSY} gets large all SUSY effects decouple and no heavy physics is left over.

Finally, I should mention that the now precise knowledge of the gauge couplings allows to test grand unification scenarios. Recent studies [110] show that SUSY models are the best candidates compatible with grand unification ideas. While the running couplings within the SM do not merge in a unification point, supersymmetric theories with a grand desert between the SUSY and the grand unification scale ($\sim 10^{16}$ GeV), for M^{SUSY} in the range $M_Z - 1$ TeV, are in agreement with present data.

Appendix: Renormalization of models with $\rho_{tree} \neq 1$

One of the crucial features of the SM is the validity of the relationship

$$\rho = \frac{G_{NC}}{G_{CC}} = \frac{M_W^2}{M_Z^2 \cos^2\Theta_g} = 1\ , \quad \cos^2\Theta_g = \frac{g^2}{g^2+g'^2} \tag{309}$$

at the tree level. Many extensions of the minimal SM share this property with the SM. Examples are models with additional fermion families, additional scalar doublets, ν_R singlets, massive neutrinos which might exhibit ν-mixing and minimal supersymmetric extensions of the SM. For all these models

$$\frac{G_{NC}}{G_{CC}}(0) = \rho = 1 + \Delta\rho \tag{310}$$

is a calculable quantity which is sensitive to weak hypercharge breaking and weak isospin breaking due to mass splittings of multiplets. In particular, for a fermion doublet

$$\begin{aligned}
\Delta\rho^f &= \frac{\Pi_Z^f(0)}{M_Z^2} - \frac{\Pi_W^f(0)}{M_W^2} \\
&= \frac{g^2}{\cos^2\Theta_g M_Z^2}\hat{\Pi}_{33}^f(0) - \frac{g^2}{M_W^2}\hat{\Pi}_{\pm}^f(0) \\
&= \frac{g^2}{M_W^2}\left(\hat{\Pi}_{33}^f(0) - \hat{\Pi}_{\pm}^f(0)\right) \\
&= \frac{\sqrt{2}G_\mu N_{cf}}{16\pi^2}\left(m_1^2 + m_2^2 + 2\frac{m_1^2 m_2^2}{m_1^2 - m_2^2}\ln\frac{m_1^2}{m_2^2}\right) \\
&\simeq \frac{\sqrt{2}G_\mu N_{cf}}{16\pi^2} m_1^2, \quad m_1^2 \gg m_2^2
\end{aligned} \tag{311}$$

is finite and exhibits large non-decoupling heavy particle effects.

Extensions of the SM which do not respect the condition $\rho_{tree} = 1$, in a way, are fundamentally different, since now

$$\frac{\Pi_Z^f(0)}{M_Z^2} - \frac{\Pi_W^f(0)}{M_W^2} = \frac{g^2}{M_W^2}\left(\rho\hat{\Pi}_{33}^f(0) - \hat{\Pi}_{\pm}^f(0)\right) \tag{312}$$

is not finite any longer. Such models, for example, are models with triplet Higgs contaminations [84], models with an extra $U(1)_{Y'}$ etc. ρ or equivalently $G_{NC} = \rho G_\mu$, now, is a new free parameter which requires independent renormalization. This has far reaching consequences because the quantity $\frac{\Pi_Z(0)}{M_Z^2} - \frac{\Pi_W(0)}{M_W^2}$ exhibiting the leading heavy particle effects is not observable any more and most of the sensitivity to heavy particle effects is lost as we shall see in the following.

At tree level the following identities hold for the bare parameters:

$$\begin{aligned}
&i) \quad \sqrt{2}G_{NCb} = \frac{\pi\alpha_b}{M_{Zb}^2\cos^2\Theta_{gb}\sin^2\Theta_{gb}} \\
&ii) \quad \sqrt{2}G_{\mu b} = \frac{\pi\alpha_b}{M_{Wb}^2\sin^2\Theta_{gb}} \\
&iii) \quad \rho_b = \frac{M_{Wb}^2}{M_{Zb}^2\cos^2\Theta_{gb}} = \frac{G_{NCb}}{G_{\mu b}}
\end{aligned} \tag{313}$$

where *four* parameters are independent. For the independent parameters we may choose α, M_W, M_Z and $\sin^2\Theta_g = \sin^2\Theta_e$ where α, M_W and M_Z have the usual definition and $\sin^2\Theta_e$ may be defined from the left-right asymmetry at the Z-resonance.

The implications of a four parameter renormalization are considered now:

i) NC-processes

may be parametrized conveniently by α, M_Z, $G_{NC}(0)$ and $s_e^2 = \sin^2\Theta_e$. From the bare parameter relation Eq. (313i) we obtain

$$\sqrt{2}G_{NC} = \frac{\pi\alpha}{M_Z^2\cos^2\Theta_e\sin^2\Theta_e}\,(1+\delta_{NC}) \tag{314}$$

with

$$\delta_{NC} = \frac{\delta\alpha}{\alpha} - \frac{\delta M_Z^2}{M_Z^2} - \frac{\delta G_{NC}}{G_{NC}} - \frac{c_e^2 - s_e^2}{c_e^2}\frac{\delta s_e^2}{s_e^2}\ . \tag{315}$$

By the above definition of the parameters $\frac{\delta\alpha}{\alpha}$ and $\frac{\delta M_Z^2}{M_Z^2}$ are given by the usual expressions. Fixing $\frac{\delta s_e^2}{s_e^2}$ from $A_{LR}(s=M_Z^2)$ (requiring the Born formula to be exact) we obtain

$$\begin{aligned}\frac{\delta s_e^2}{s_e^2} &= -\left(\frac{c_e}{s_e}\frac{\Pi_{\gamma Z}(M_Z^2)+\Pi_{\gamma Z}(0)}{M_Z^2} + A_\kappa^{Zee}(M_Z^2) - \frac{c_e}{s_e}\frac{\Pi_{\gamma Z}(0)}{M_Z^2}\right)\\ &= -\frac{c_e}{s_e}\Pi'_{\gamma Z}(M_Z^2) - 2\frac{c_e}{s_e}\frac{\Pi_{\gamma Z}(0)}{M_Z^2} - \Delta\kappa_{e,vertex}(M_Z^2)\ .\end{aligned} \tag{316}$$

Defining $G_{NC}(0) = G_{NC}$ in low-momentum-transfer $\nu_\mu e$-scattering we have

$$\frac{\delta G_{NC}}{G_{NC}} = -\frac{\Pi_Z(0)}{M_Z^2} + R_{LNC} \tag{317}$$

with

$$\begin{aligned}R_{LNC} &= -\left(A_L^{Zee}(0) + A_L^{Z\nu\nu}(0) + A_{LNC}^{box}(0)\right)\\ &= K\left\{4c_W^2 L - \frac{24c_W^4 - 20c_W^2 + 15}{4c_W^2}\right\}\ .\end{aligned} \tag{318}$$

Thus

$$\begin{aligned}\delta_{NC} &= \Pi'_\gamma(0) - \Pi'_Z(M_Z^2) + \frac{c_W^2 - s_W^2}{c_W^2}\frac{c_W}{s_W}\Pi'_{\gamma Z}(M_Z^2) + \delta_{NC}^{vertex+box}\\ &= \Delta\alpha + \frac{1}{c_W^2}\Delta_1 + \delta_{NC}^{vertex+box}\\ \delta_{NC}^{vertex+box} &= K\left\{\frac{24c_W^4 - 20c_W^2 + 15}{4c_W^2}\right\} + \frac{c_W^2 - s_W^2}{c_W^2}\Delta\kappa_{e,vertex}\ .\end{aligned} \tag{319}$$

Since G_{NC} is an independent parameter here, and hence appears subtracted independently of G_μ, no term $\frac{\Pi_Z(0)}{M_Z^2} - \frac{\Pi_W(0)}{M_W^2}$ is left over.

For the leading heavy particle effects we obtain

$$\begin{aligned}\delta_{NC}^{top} &= -K\frac{2}{3c_W^2}\ln\frac{m_t^2}{M_Z^2}\\ \delta_{NC}^{Higgs} &= K\frac{1}{3c_W^2}\left(\ln\frac{m_H^2}{M_Z^2} - \frac{5}{3}\right)\ .\end{aligned} \tag{320}$$

ii) CC-processes

may be parametrized in terms of α, M_W, G_μ and $\sin^2\Theta_e$. From the bare parameter relation Eq. (313ii) we get

$$\sqrt{2}G_\mu = \frac{\pi\alpha}{M_W^2 \sin^2\Theta_e}(1+\delta_{CC}) \tag{321}$$

where α and M_W are renormalized as usual and $\sin^2\Theta_e$ as in the NC case. With G_μ fixed from the μ decay rate we have

$$\frac{\delta G_\mu}{G_\mu} = -\frac{\Pi_W(0)}{M_Z^2} + R_{LCC} \tag{322}$$

with

$$\begin{aligned} R_{LCC} &= -\left(A_L^{W\mu\nu}(0) + A_L^{We\nu}(0) + A_{LCC}^{box}(0)\right) \\ &= K\left\{4L - \frac{4c_W^2+3}{2s_W^2}\ln c_W^2 - 6\right\} \quad . \end{aligned} \tag{323}$$

Thus

$$\begin{aligned} \delta_{CC} &= \frac{\delta\alpha}{\alpha} - \frac{\delta M_W^2}{M_W^2} - \frac{\delta G_\mu}{G_\mu} - \frac{\delta s_e^2}{s_e^2} \\ &= \Pi'_\gamma(0) - \Pi'_W(M_W^2) + \frac{c_W}{s_W}\Pi'_{\gamma Z}(M_Z^2) + \delta_{CC}^{vertex+box} \\ &= \Delta\alpha + \Delta_1 + \Delta_2 + \delta_{CC}^{vertex+box} \\ \delta_{CC}^{vertex+box} &= K\left\{\frac{4c_W^2+3}{2s_W^2}\ln c_W^2 + 6\right\} + \Delta\kappa_{e,vertex} \quad . \end{aligned} \tag{324}$$

The leading heavy particle effects in this case are

$$\begin{aligned} \delta_{CC}^{top} &= K\frac{4}{3}\ln\frac{m_t^2}{M_W^2} \\ \delta_{CC}^{Higgs} &= K\frac{1}{3}\left(\ln\frac{m_H^2}{M_W^2} - \frac{5}{3}\right) \quad . \end{aligned} \tag{325}$$

The relation obtained may be used to predict M_W from α, M_Z and $\sin^2\Theta_e$

$$M_W^2 = \frac{\pi\alpha}{\sqrt{2}G_\mu \sin^2\Theta_e}(1+\delta_{CC}) \tag{326}$$

which replaces the SM prediction of M_W from α, G_μ and M_Z .

As a third relation we now consider the bare parameter relation Eq. (313iii).

iii) NC versus CC

For the renormalized quantities this reads

$$\rho = \frac{G_{NC}}{G_\mu} = \frac{M_W^2}{M_Z^2 \sin^2\Theta_e}(1-\Delta\hat{\rho}') \tag{327}$$

where $\Delta\hat{\rho}' = \delta_{CC} - \delta_{NC}$. Thus

$$\begin{aligned} \Delta\hat{\rho}' &= -\frac{s_W^2}{c_W^2}\Delta_1 + \Delta_2 + \Delta\hat{\rho}^{'vertex+box} \\ \Delta\hat{\rho}^{'vertex+box} &= K\left\{\frac{4c_W^2+3}{2s_W^2}\ln c_W^2 + 6 - \frac{24c_W^4 - 20c_W^2 + 15}{4c_W^2}\right\} + \frac{s_W^2}{c_W^2}\Delta\kappa_{e,vertex} \ . \end{aligned} \tag{328}$$

Here the leading heavy particle terms read

$$\begin{aligned} \Delta\hat{\rho}^{'top} &= K(\frac{4}{3} + \frac{2}{3c_W^2})\ln\frac{m_t^2}{M_W^2} \\ \Delta\hat{\rho}^{'Higgs} &= -K\frac{1}{3}\frac{s_W^2}{c_W^2}\left(\ln\frac{m_H^2}{M_W^2} - \frac{5}{3}\right) \ . \end{aligned} \tag{329}$$

Obviously no terms proportional to m_t^2 have survived and the leading heavy Higgs terms are reduced by roughly a factor 10! relative to the minimal SM.

Additional parameter relations:

The relationship $\sin^2\Theta_e$ versus $\sin^2\Theta_{\nu_\mu e}$ remains the same as in the minimal SM. Considering the on-shell $Zf\bar{f}$ vertex

$$\left(\sqrt{2}G_{NC}\right)^{1/2} M_Z\gamma_\mu\left(-2Q_f\sin^2\Theta_e + (1-\gamma_5)\,T_{3f}\right)$$

the mixing parameter $\sin^2\Theta_e$ is exact for $f = e, \mu, \tau$. The renormalized on-shell vertex is given by

$$\left(\sqrt{2}G_{NCf}\right)^{1/2} M_Z\gamma_\mu\left(-2Q_f\sin^2\Theta_f + (1-\gamma_5)\,T_{3f}\right)$$

where

$$G_{NCf} = \rho_{Zf}G_{NC}\ , \ \ \sin^2\Theta_f = (1+\Delta\kappa_{ef})\ \sin^2\Theta_e \tag{330}$$

with

$$\Delta\kappa_{ef} = \Delta\kappa_f - \Delta\kappa_e = \Delta\kappa_{f,vertex} - \Delta\kappa_{e,vertex}$$

$$G_{NCf}(M_Z^2)/G_{NC}(0) = \rho_{Zf} = 1 + \Delta_Z + \Delta\rho_{f,vertex} - K\left\{\frac{24c_W^4 - 20c_W^2 + 15}{4c_W^2}\right\}$$

where Δ_Z is defined in Eq. (146) and $\Delta_Z^{top} = 0$ and $\Delta_Z^{Higgs} = 0$ for the heavy top and Higgs limit. As a result we conclude: LEP experiments alone cannot test heavy particle effects besides the heavy top effects from the $Zb\bar{b}$ vertex which yields the result (119).

In the relations between low-energy NC and Z-peak NC processes terms proportional to $\ln m_t^2$ and $\ln m_H^2$ may be tested. Since these terms are small and the low-energy NC data have only limited precision the prospects to get limits on m_t and m_H are rather bad in such a scenario.

How to recover the SM relations:

Using the experimental fact that $\rho = G_{NC}/G_\mu$ is close to unity we may write

$$\begin{aligned} \rho = \frac{G_{NC}}{G_\mu} = 1 + \Delta\rho &= \frac{M_W^2}{M_Z^2\cos^2\Theta_e}\ (1 - \Delta\hat{\rho}') \\ \hat{\rho} = \frac{M_W^2}{M_Z^2\cos^2\Theta_e} &= \frac{\cos^2\Theta_W}{\cos^2\Theta_e} = \frac{1}{1-\Delta\rho-\Delta\hat{\rho}'} = \frac{1}{1-\Delta\hat{\rho}} \ . \end{aligned} \tag{331}$$

Thus for the prediction of $\sin^2\Theta_e$ from α, G_μ and M_Z

$$\begin{aligned}\sqrt{2}G_\mu\rho M_Z^2\cos^2\Theta_e\sin^2\Theta_e &= \pi\alpha\,(1+\delta_{NC})\\ \sqrt{2}G_\mu M_Z^2\cos^2\Theta_e\sin^2\Theta_e &= \frac{\pi\alpha}{1-\Delta r_e}\end{aligned} \tag{332}$$

where

$$\Delta r_e = \delta_{NC} - \Delta\rho = \Delta\alpha - \Delta\rho + \frac{1}{c_W^2}\Delta_1 + \Delta r_{e,vertex+box}$$

which is identical with the SM form, however, with the *replacement*

$$\Delta\rho = \frac{\Pi_Z(0)}{M_Z^2} - \frac{\Pi_W(0)}{M_W^2} \to \Delta\rho = \frac{G_{NC}-G_\mu}{G_\mu}\ . \tag{333}$$

Eliminating $\sin^2\Theta_e$ from $\sqrt{2}G_\mu M_W^2\sin^2\Theta_e = \pi\alpha\,(1+\delta_{CC})$ using $\hat\rho = \cos^2\Theta_W/\cos^2\Theta_e$ we obtain the relation for the prediction of M_W in terms of α, G_μ and M_Z:

$$\begin{aligned}\sqrt{2}G_\mu M_W^2\left(1-\frac{M_W^2}{M_Z^2}\,(1-\Delta\hat\rho)\right) &= \pi\alpha(1+\delta_{CC})\\ \sqrt{2}G_\mu M_W^2\left(1-\frac{M_W^2}{M_Z^2}\right) = \pi\alpha\,\left(1+\delta_{CC}-\frac{c_W^2}{s_W^2}\Delta\hat\rho\right) &= \pi\alpha\,(1+\Delta r)\end{aligned} \tag{334}$$

with Δr given by Eqs. (84,148) with the replacement (333).

This is a very puzzling situation. The interpretation of measurements looks extremely different for theories with $\rho_{tree}=1$ from those with $\rho_{tree}\neq 1$. In the second case one does not have an "explanation" why $G_{NC}\simeq G_\mu$. Only models with $\rho_{tree}=1$ seem to be natural in reality.

8. SUMMARY AND CONCLUSIONS

In the first year of LEP the four collaborations ALEPH, DELPHI, L3 and OPAL have determined the main properties of the Z boson with high accuracy under optimum experimental conditions.

Radiative corrections play a crucial role in understanding electroweak precision measurements in particular the ones which appear at the Z resonance. First of all the radiative corrections calculated in the SM are needed to pin down limits for the missing SM parameters like the top and the Higgs mass. Since these particles are too heavy to be produced at present one has to resort to a precise measurement of higher order effects. In a further step the electroweak radiative corrections play an important role as sensors for *new physics*. Before the interesting physics can be extracted from the experimental data these have to be disentangled from detector cuts and efficiencies and from the large universal but cut-dependent QED-corrections. Much emphasis has been put therefore on a precise understanding of QED-effects and on their implementation in Monte Carlo event generators which provide the bridge between the raw data and the detector independent "bare" observables of actual physical interest. The calculation of radiative corrections is well established theoretically for: the Z line-shape (including full $O(\alpha^2)$ QED-corrections), the partial and total Z-widths and the asymmetries, (excluded subleading $O(\alpha^2)$ QED-corrections to A_{FB}) and the prediction of the W-mass (equivalently Δr and $\sin^2\Theta_W$). There is complete agreement for the analytic expressions at the one-loop level and on the treatment of the leading higher order terms. The theoretical uncertainties: $\delta(\Delta r)^{hadrons}=0.0009$, $\delta(\Delta r)^{top}=0.0005$ $(m_t<150\ GeV)$

and $\delta(\Delta r)^{higher-order} = 0.001$ are small enough and will not obscure the meaning of precision measurements.

I focussed on discussing implications of the LEP results for precision tests of the Standard Model. The main results may be summarized as follows:

- The Z mass measurement provides the third very accurately known parameter $M_Z = 91.174 \pm 0.005 \pm 0.020$ GeV, such that precise predictions are possible using α, G_μ and M_Z as input parameters. The total Z width has been determined to $\Gamma_Z = 2.487 \pm 0.009$ GeV.
- The neutrino counting yields $N_\nu = 2.96 \pm 0.06$. Hence, only the 3 known light neutrinos exist. This result proves that ν_τ is different from ν_e and ν_μ.
- The weak mixing parameter has been determined very precisely. The value $\sin^2 \bar{\Theta} = 0.02315 \pm 0.0027$ improves the lower bound for the top mass slightly.

The best direct upper bound on m_t is obtained by combining the hadron collider results from the UA2 and CDF collaborations with the Z mass measurement of LEP.

- The measurement of the mass ratio yields $\sin^2 \Theta_W = 0.2265 \pm 0.0062$, which together with M_Z determines the mass $M_W = 80.14 \pm 0.32$ GeV and implies the bound $m_t < 202$ GeV. Bounds on m_t from global fits including all NC-data have been given in Eqs. (34) and (302). The total W-width $\Gamma_W = 2.17 \pm 0.12$ GeV has been obtained as an average from the UA1, UA2 and CDF results.

It should be kept in mind that the top mass bounds refer to the SM. In models which respect $\rho_{tree} = 1$ these bounds are still pretty save. In extensions of the SM with $\rho_{tree} \neq 1$ the upper bounds for the top mass are substantially weaker. A global fit [26] in this case yields

- $\sin^2 \bar{\Theta}(M_Z) = 0.2333 \pm 0.0008$, $\rho_{tree} = 0.992 \pm 0.011$, and $m_t < 294\,(310)$ GeV at 90% (95%) CL. The corresponding value for $\sin^2 \Theta_W$ is 0.2290 ± 0.0034. The uncertainties include the m_t and m_H dependence.

The most important direct new physics bounds are

- $m_H > 49.5$ GeV (95% C. L.) (LEP)
- $m_t > 89$ GeV (95% C. L.) (CDF).
- All searches for new particles have been negative. Many lower mass bounds have been improved. Most of the possible new particles must have masses $m_{new} > M_Z/2$.

So far the agreement between experimental data and standard model predictions is almost perfect. All data are compatible with "no new physics". A main obstacle for discoveries is the still incomplete knowledge of the parameters of the SM (m_t and m_H). To establish deviations we have to wait for the next step in accuracy. It will be achieved during the next year with about 10^6 Z's per experiment.

From the large number of interesting results testing QCD at the Z mass scale I only mention the determination of the strong coupling constant [30]

- $\alpha_s(M_Z^2) = 0.116 \pm 0.007$.

This is an important input parameter for calculations of radiative corrections.

For future precision measurements the electroweak radiative corrections will play an important role as they provide a window to *new physics*. Laking any experimental hints for "where to go" we have discussed a selection of possibilities for "new physics". In principle all kind of effects are possible. On one hand they are severely constrained by the electroweak data on the other hand one cannot exclude "new physics" to be right "around the corner". So, there is good hope for surprises.

So far the agreement between experimental data and standard model predictions is almost perfect. All data are compatible with "no new physics". A main obstacle for discoveries is the still incomplete knowledge of the parameters of the SM (m_t and m_H). To establish deviations we have to wait for the next step in accuracy. It will be achieved during the next year with about 10^6 Z's per experiment.

From the large number of interesting results testing QCD at the Z mass scale I only mention the determination of the strong coupling constant [30]

- $\alpha_s(M_Z^2) = 0.116 \pm 0.007$.

This is an important input parameter for calculations of radiative corrections.

For future precision measurements the electroweak radiative corrections will play an important role as they provide a window to *new physics*. Laking any experimental hints for "where to go" we have discussed a selection of possibilities for "new physics". In principle all kind of effects are possible. On one hand they are severely constrained by the electroweak data on the other hand one cannot exclude "new physics" to be right "around the corner". So, there is good hope for surprises.

Acknowledgements

I would like to thank M. Consoli and W. Hollik for stimulating discussions. I am very grateful to G. W. Hou for discussions and for reading the manuscript.

References:

1. D. Decamp et al., ALEPH Collaboration, Phys. Lett. **231** (1989) 519, **235** (1990) 399;
   B. Adeva et al., L3 Collaboration, Phys. Lett. **231** (1989) 509, **237** (1990) 136;
   M. Z. Akrawy et al., OPAL Collaboration, Phys. Lett. **231** (1989) 530, **240** (1990) 497;
   P. Abreu et al., DELPHI Collaboration, Phys. Lett. **231** (1989) 539, **241** (1990) 435;
   F. Dydak, in *Proceedings of the 25th International Conference on High Energy Physics*, Singapore, 1990, eds. K. Phua, Y. Yamaguchi, World Scientific, Singapore, 1991;
   J. Steinberger, CERN Preprint, CERN-PPE/90-149 (1990);
   E. Fernández, CERN Preprint, CERN-PPE/90-151 (1990);
   H. Burkhardt, J. Steinberger, CERN Preprint, CERN-PPE/91-50 (1991).

2. G. Arnison et al., (UA1 Collaboration), Phys. Lett. **126** (1983) 398 ; **166** (1986) 484;
   P. Bagnaia et al., (UA2 Collaboration), Phys. Lett. **129** (1983) 130; R. Ansari et al., Phys. Lett. **186** (1987) 440; J. Alitti et al., Phys. Lett. **241** (1990) 160.

3. F. Abe et al., (CDF Collaboration), Phys. Rev. Lett. **62** (1988) 613; **65** (1990) 2243.

4. L. Pondrom, in *Proceedings of the 25th International Conference on High Energy Physics*, Singapore, 1990, eds. K. Phua, Y. Yamaguchi, World Scientific, Singapore, 1991;
H. Plothow-Besch, in *Proc. of the XX. International Symposium on Multiparticle Dynamics 1990*, eds. R. Baier, D. Wegener, World Scientific, Singapore (1991);
D. Amidei, FERMILAB-CONF-91/26-E, in *Proceedings of the Xth International Conference on Physics in Collision*, Duke Univ., 1990.

5. S. L. Glashow, Nucl. Phys. B **22** (1961) 579;
S. Weinberg, Phys. Rev. Lett. **19** (1967) 1264;
A. Salam, in *Elementary Particle Theory*, ed., N. Svartholm, Almquist and Wiksells, Stockholm (1968), p. 367.

6. H. Fritzsch, M. Gell-Mann, H. Leutwyler, Phys. Lett. **47** (1973) 365;
H. D. Politzer, Phys. Rev. Lett. **30** (1973) 1346;
D. Gross, F. Wilczek, Phys. Rev. Lett. **30** (1973) 1343;
S. Weinberg, Phys. Rev. Lett. **31** (1973) 494;

7. N. Cabiobbo, Phys. Lett. **10** (1963) 513;
M. Kobayashi, K. Maskawa, Prog. Theor. Phys. **49** (1973) 652.

8. G. 't Hooft, Nucl. Phys. B **33** (1971) 173; **35** (1971) 167;
G. 't Hooft, M. Veltman, Nucl. Phys. B **50** (1972) 318.

9. F. J. Hasert et al. (Gargamelle Collaboration), Phys. Lett. **46** (1973) 121, 138;
A. Benvenuti et al. (HPW Collaboration), Phys. Rev. Lett. **32** (1974) 800, 1454, 1457.

10. T. Appelquist, J. Carazzone, Phys. Rev. D **11** (1975) 2856.

11. D. Decamp et al., ALEPH Collab., Phys. Lett. **236** (1990) 233; Phys. Lett. **241** (1990) 141; Phys. Lett. **245** (1990) 289; Phys. Lett. **246** (1990) 306;
M. Z. Akrawy et al., OPAL Collab., Phys. Lett. **236** (1990) 224; Phys. Lett. **251** (1990) 211; CERN-EP-90-100 (1990);
P. Abreu et al., DELPHI Collab., Nucl. Phys. B **342** (1990) 1; Phys. Lett. **245** (1990) 276; CERN-PPE-90-193 (1990);
B. Adeva et al., L3 Collab., Phys. Lett. **248** (1990) 203; Phys. Lett. **252** (1990) 518.

12. Z. Kunszt, W. J. Stirling, Phys. Lett. **242** (1990) 507;
S. L. Wu et al., ECFA Workshop on LEP 200, CERN/ECFA 87-08 (1987) Vol. II, eds. A. Böhm and W. Hoogland.

13. S. L. Glashow, J. Illiopoulos, L. Maiani, Phys. Rev. D **2** (1970) 1285.

14. J. J. Aubert et al., Phys. Rev. Lett. **33** (1974) 1404;
J. E. Augustin et al., Phys. Rev. Lett. **33** (1974) 1406.

15. M. L. Perl et al., Phys. Rev. Lett. **35** (1975) 1489.

16. S. W. Herb et al., Phys. Rev. Lett. **39** (1977) 252.

17. L. Mapelli, in *Proceedings of the 25th International Conference on High Energy Physics*, Singapore, 1990, eds. K. Phua, Y. Yamaguchi, World Scientific, Singapore, 1991;
for bounds on $m_{H^\pm}$ see:

M. Z. Akrawy et al., OPAL Collab., Phys. Lett. **236** (1990) 364; Phys. Lett. **242** (1990) 299;
D. Decamp et al., ALEPH Collab., Phys. Lett. **236** (1990) 511; Phys. Lett. **241** (1990) 623;
P. Abreu et al., DELPHI Collab., Phys. Lett. **241** (1990) 449; Phys. Lett. **242** (1990) 536.

18. Particle Data Group, J. J. Hernández et al., Phys. Lett. **239** (1990) 1.

19. H. Nelson, in *Proceedings of the 25th International Conference on High Energy Physics*, Singapore, 1990, eds. K. Phua, Y. Yamaguchi, World Scientific, Singapore, 1991.

20. K. Nakamura, in *Proceedings of the 25th International Conference on High Energy Physics*, Singapore, 1990, eds. K. Phua, Y. Yamaguchi, World Scientific, Singapore, 1991;
D. C. Kennedy, in *Proceedings of TASI-90*,
eds. M. Cvetič, P. Langacker, World Scientific Publ., Singapore, 1991;
University of Pennsylvania Report No. UPR-0442T, 1990.

21. D. Geiregat et al., (CHARM II), Phys. Lett. **232** (1989) 539;
J. Dorenbosch et al., (CHARM I), Z. Phys. C **41** (1989) 567;
K. Abe et al., (BNL E734), Phys. Rev. Lett. **62** (1989) 1709;
P. Vilain, in *Proceedings of the Neutrino-90 Conference*, Geneva, (1990)

22. H. Abramowicz et al., (CDHS), Phys. Rev. Lett. **57** (1986) 298,
A. Blondel et al., Z. Phys. C **45** (1990) 361;
J. V. Allaby et al., (CHARM), Phys. Lett. **177** (1986) 446, Z. Phys. C **36** (1987) 611;
M. Shaevitz, in *Proceedings of the Neutrino-90 Conference*, Geneva, (1990).

23. A. Sirlin, W. J. Marciano, Nucl. Phys. B **189** (1981) 442.

24. A. Sirlin, Phys. Rev. D **22** (1980) 971; for a review see e.g.
G. Burgers, F. Jegerlehner, in *Z Physics at LEP1*, eds. G. Altarelli et al., CERN 89-08 (1989).

25. J. Ellis, G. L. Fogli, Phys. Lett. **249** (1990) 543; see also:
F. Halzen, D. A. Morris, Phys. Lett. **237** (1990) 107;
V. Barger, J. L. Hewett, T. G. Rizzo, Phys. Rev. Lett. **65** (1990) 1313;
Z. Hioki, Phys. Rev. Lett. **65** (1990) 683; Preprints TOKUSHIMA 91-01/02 (1991).

26. P. Langacker, Phys. Rev. Lett. **63** (1989) 1920;
P. Langacker, in *Proceedings of PASCOS-90*, Northeastern, 1990;
P. Langacker, M. X. Luo, University of Pennsylvania Report No. UPR-0466T, 1991.

27. J. Fleischer, F. Jegerlehner, Phys. Rev. D **23** (1981) 2001;
F. Jegerlehner, in "Radiative Corrections in $SU(2)_L \times U(1)$",
eds. B. W. Lynn, J. F. Wheater, World Scientific Publ., Singapore, 1984.

28. F. Jegerlehner, in "Testing the Standard Model ",
eds. M. Zraj/ek,R. Mańka, World Scientific Publ., Singapore, 1988;
W. Hollik, Fortsch. Phys. **38** (1990) 165.

29. F. Jegerlehner, Z. Phys. C **32** (1986) 195, 425;
H. Burkhardt, F. Jegerlehner, G. Penso, C. Verzegnassi, Z. Phys. C **43** (1989) 497;
F. Jegerlehner, *Renormalizing the Standard Model*, in *Proceedings of TASI-90*,
eds. M. Cvetič, P. Langacker, World Scientific Publ., Singapore, 1991;
PSI preprint, PSI-PR-91-08.

30. T. Hebbeker, in *Proc. of the XX. International Symposium on Multiparticle Dynamics 1990*, eds. R. Baier, D. Wegener, World Scientific, Singapore (1991).

31. M. Veltman, Nucl. Phys. B **123** (1977) 89;
M. S. Chanowitz et al., Phys. Lett. **78** (1978) 1;
M. B. Einhorn, D. R. T. Jones, M. Veltman, Nucl. Phys. B **191** (1981) 146;
M. Consoli, S. Lo Presti, L. Maiani, Nucl. Phys. B **223** (1983) 474;
J. Fleischer, F. Jegerlehner, Nucl. Phys. B **228** (1983) 1.

32. J. J. van der Bij, M. Veltman, Nucl. Phys. B **231** (1984) 205.

33. J. J. van der Bij, Nucl. Phys. B **248** (1984) 141.

34. F. Halzen, B. A. Kniehl, Nucl. Phys. B **353** (1991) 567.

35. M. Veltman, *Acta Phys. Pol.* **B8** (1977) 475;
M. B. Einhorn, J. Wudka, Phys. Rev. D **39** (1989) 2758.

36. M. Consoli, W. Hollik, F. Jegerlehner, Phys. Lett. **227** (1989) 167.

37. J. J. van der Bij, F. Hoogeveen, Nucl. Phys. B **283** (1987) 477.

38. G. Degrassi, S. Fanchiotti, A. Sirlin, NYU preprint, 1990

39. G. Passarino, M. Veltman, Nucl. Phys. B **160** (1979) 151;
W. Wetzel, Nucl. Phys. B **227** (1983) 1;
M. Böhm, W. Hollik, Phys. Lett. **139** (1984) 213;
R. W. Brown, R. Decker, E. A. Paschos, Phys. Rev. Lett. **52** (1984) 1192;
B. W. Lynn, R. Stuart, Nucl. Phys. B **253** (1985) 216;
W. Hollik, Phys. Lett. **152** (1985) 121;
M. Igarashi, N. Nakazawa, Nucl. Phys. B **288** (1987) 301.

40. M. Consoli, W. Hollik, F. Jegerlehner, in *Z Physics at LEP1*,
eds. G. Altarelli et al., CERN 89-08 (1989);
D. Yu. Bardin, T. Riemann, in Proc. of the Nato Advanced Research Workshop *Radiative corrections: Results and Perspectives*, eds. N. Dombey, F. Boudjema, Plenum Press, New York 1990.

41. A. A. Akhundov, D. Yu. Bardin, T. Riemann, Nucl. Phys. B **276** (1986) 1.

42. M. Böhm, W. Hollik, H. Spiesberger, Fortschr. Phys. **34** (1986) 687.

43. W. Beenakker, W. Hollik, Z. Phys. C **40** (1988) 141.

44. D. C. Kennedy, B. W. Lynn, Nucl. Phys. B **322** (1989) 1.

45. D. J. Broadhurst, Phys. Lett. **101** (1981) 423;
S. Generalis, Open University preprint OUT-4102-13.

46. A. Djouadi and C. Verzegnassi, Phys. Lett. **195** (1987) 265 ;
A. Djouadi, Nuovo Cimento **100A** (1988) 357.

47. R. Coquereaux, Ann. of Phys. **125** (1980) 401.

48. D. Yu. Bardin, A. V. Chizov, Dubna preprint E2-89-525 (1989).

49. B. A. Kniehl, Nucl. Phys. B **347** (1990) 86;
S. Fanchiotti, B. A. Kniehl and A. Sirlin, Phys. Rev. D **48** (1993) 307; for the small mass approximation see:
E. G. Floratos, S. Narison and E. de Rafael, Nucl. Phys. B **155** (1979) 115;
A. Djouadi and P. Gambino, Phys. Rev. D **49** (1994) 4705.

50. T. H. Chang, K. J. F. Gaemers, W. L. van Neerven, Nucl. Phys. B **202** (1982) 407;
L. J. Reinders, H. R. Rubinstein, S. Yazaki, Phys. Rep. **127** (1985) 1.

51. B. A. Kniehl, J.H. Kühn and R.G. Stuart, Phys. Lett. **214** (1988) 621;
B. A. Kniehl, Computer Phys. Commun. **58** (1990) 293.

52. J. Jersak, E. Laermann, P. M. Zerwas, Phys. Lett. **98** (1981) 363; Phys. Rev. D **25** (1982) 1218.

53. B. A. Kniehl, J. H. Kühn, Phys. Lett. **224** (1989) 229, Nucl. Phys. B **329** (1990) 547.

54. R. Lewin, Dilogarithms and Associated Functions, Mac Millan, London (1958)

55. A. Djouadi, J. H. Kühn, P. M. Zerwas, Z. Phys. C **46** (1990) 411;
H. J. Kühn, P. M. Zerwas, in *Z Physics at LEP1*, eds. G. Altarelli et al., CERN 89-08 (1989).

56. W. Bernreuther, W. Wetzel, Nucl. Phys. B **197** (1983) 228;
W. J. Marciano, Phys. Rev. D **29** (1984) 580.

57. W. Wetzel, Nucl. Phys. B **227** (1983) 1.

58. M. Consoli, A. Sirlin, in [59];
B. W. Lynn, M. Peskin, R. G. Stuart, in [59];
D. C. Kennedy, B. W. Lynn, SLAC-PUB 4039 (1986), Nucl. Phys. B **322** (1989) 1;
G. Burgers, in *Polarization at LEP*, eds. G. Alexander et al., CERN 88-06 (1988).

59. "Physics with LEP", CERN 86-02 (1986), eds. J. Ellis and R. Peccei;
"ECFA Workshop on LEP 200", CERN/ECFA 87-08 (1987),
eds. A. Böhm and W. Hoogland.

60. A. Borrelli, M. Consoli, L. Maiani, R. Sisto, Nucl. Phys. B **333** (1990) 357;
A. Borrelli, L. Maiani, R. Sisto, Phys. Lett. **244** (1990) 117.

61. D. Yu. Bardin et al., Phys. Lett. **206** (1988) 539.

62. G. Bonneau, F. Martin, Nucl. Phys. B **27** (1971) 381;
M. Greco, G. Pancheri, Y. Srivastava, Nucl. Phys. B **171** (1980) 118;
F.A. Berends, R. Kleiss, S. Jadach, Nucl. Phys. B **202** (1982) 63;
M. Böhm, W. Hollik, Nucl. Phys. B **204** (1982) 45;
E.A. Kuraev, V.S. Fadin, Sov. J. Nucl. Phys. **41** (1985) 466;
G. Altarelli, G. Martinelli, in [59];
O. Nicrosini, L. Trentadue, Phys. Lett. **196** (1987) 551; Z. Phys. C **39** (1988) 479;
V.S. Fadin, V.A. Khoze, Yad. Fyz. **47** (1988) 1693.

63. F. A. Berends, G. Burgers, W. L. van Neerven, Phys. Lett. **185** (1987) 395;
Nucl. Phys. B **297** (1988) 429; E: Nucl. Phys. B **304** (1988) 921;
F. A. Berends, G. Burgers, W. Hollik, W. L. van Neerven, Phys. Lett. **203** (1988) 177;
F. A. Berends, in "Radiative Corrections for e^+e^--Colliders", ed. J. H. Kühn,

Springer, Berlin 1989;
F. A. Berends et al., in *Z Physics at LEP1*, eds. G. Altarelli et al., CERN 89-08 (1989).

64. D. R. Yennie, S. C. Frautschi, H.Suura, Annals of Phys. **13** (1961) 379;
D. R. Yennie, Phys. Lett. **34** (1975) 239;
J. D. Jackson, D. L. Scharre, Nucl. Instr. **128** (1975) 13;
M. Greco, G. Pancheri, Y. Srivastava, Nucl. Phys. B **101** (1975) 234.

65. W. Beenacker, F. A. Berends, S. C. van der Marck, Z. Phys. C **46** (1990) 687.

66. R.W. Brown, R. Decker, E.A. Paschos, Phys. Rev. Lett. **52** (1984) 1192;
D. Bardin et al., JINR Dubna E2-87-663 (1987), E2-88-324 (1988);
J. H. Kühn, R. G. Stuart, Phys. Lett. **200** (1988) 360;
S. Jadach, J. H. Kühn, R. G. Stuart, Z. Was, Z. Phys. C **38** (1988) 609.

67. S. Jadach, B. F. L. Ward, Phys. Rev. D **38** (1988) 2897, **42** (1990) 1404;
J. E. Campagne, R. Zituon, Z. Phys. C **43** (1989) 469; Phys. Lett. **222** (1989) 497;
Z. Wąs, S. Jadach, Phys. Rev. D **41** (1990) 1425;
G. Montagna, O. Nicrosini, L. Trentadue, Phys. Lett. **231** (1989) 492;
W. Beenakker, F. A. Berends, S. C. van der Marck, Phys. Lett. **251** (1990) 299;
S. Jadach, B. F. L. Ward, Z. Wąs, Phys. Lett. **257** (1991) 213;
M. Bilenky, M. Sachwitz, in Proc. of the Nato Advanced Research Workshop
Radiative corrections: Results and Perspectives, eds. N. Dombey, F. Boudjema,
Plenum Press, New York 1990.

68. D. Bardin, M. Bilenky, A. Chizov, A. Sazonov, Yu. Sedykh, T. Rieman, M. Sachwitz,
Phys. Lett. **229** (1989) 405;
D. Bardin et al., JINR Dubna E2-87-663 (1987), E2-88-324 (1988).

69. M. Böhm, W. Hollik, in *Z Physics at LEP1*, eds. G. Altarelli et al., CERN 89-08 (1989);
G. Degrassi, A. Sirlin, Max-Planck-Institut preprint MPI-PAE/PTh 48/90 (1990).

70. B. W. Lynn, M. Peskin, R. G. Stuart, in [59].

71. L. S. Durkin, P. Langacker, Phys. Lett. **166** (1986) 436;
D. London, J. L. Rosner, Phys. Rev. D **34** (1986) 1530.

72. M. Cvetič, B. W. Lynn, Phys. Rev. D **35** (1987) 51.

73. F. Boudjema, F. M. Renard, C. Verzegnassi, Phys. Rev. D **314** (1989) 301.

74. *Z Physics at LEP1*, eds. G. Altarelli et al., CERN 89-08 (1989) Vol.2; see also Ref. [91].

75. R. Renken, M. E. Peskin, Nucl. Phys. B **211** (1983) 93;
M. E. Peskin, T. Takeuchi, Phys. Rev. Lett. **65** (1990) 964;
B. Holdom, J. Terning, Phys. Lett. **247** (1990) 88;
M. Golden, L. Randall, FERMILAB-PUB-90/83-T (1990);
C. Roiesnel, T. N. Truong, Phys. Lett. **253** (1991) 439.

76. W. Marciano, J. Rosner, Phys. Rev. Lett. **65** (1990) 2963; see also:
P. Langacker, Phys. Lett. **256** (1991) 277.

77. D. C. Kennedy, P. Langacker, Phys. Rev. Lett. **65** (1990) 2967;
Univ. of Pennsylvania preprint UPR-0467T 1991.

78. G. Altarelli, R. Barbieri, Phys. Lett. **253** (1991) 161.

79. S. A. Blundell, W. R. Johnson, J. Sapirstein, Phys. Rev. Lett. **65** (1990) 1411;
V. A. Dzuba et al., Phys. Lett. **A 141** (1989) 147.

80. M. C. Noecker et al., Phys. Rev. Lett. **61** (1988) 310.

81. M. Gell-Mann, P. Ramond, R. Slansky, in *Supergravity*,
eds. P. van Nieuwenhuizan, D. Freedman, North Holland Amsterdam, 1979, p.315;
T. Yanagida, Prog. Theor. Phys. **64** (1980) 1103;
M. J. Duncan, P. Langacker, Nucl. Phys. B **277** (1986) 285;
J. W. F. Valle, "Gauge Theories and the Physics of Neutrino Mass", in *Progress in Particle and Nuclear Physics* **26**, ed. A. Faessler, Pergamon Press, 1991, and references therein.

82. C. T. Hill, E. A. Paschos, Phys. Lett. **241** (1990) 96.

83. S. Bertolini, A. Sirlin, Phys. Lett. **257** (1991) 179.

84. B. W. Lynn, S. Nardi, CERN-TH. 5876/90 (1990).

85. G. Passarino, Phys. Lett. **231** (1990) 458; Phys. Lett. **247** (1990) 587.

86. S. Weinberg, S. L. Glashow, Phys. Rev. D **15** (1977) 1958;
E. A. Paschos, Phys. Rev. D **15** (1977) 1966.

87. D. Toussaint, Phys. Rev. D **18** (1978) 1626;
S. Bertolini, Nucl. Phys. B **272** (1986) 77.

88. W. Hollik, Z. Phys. C **32** (1986) 291, **37** (1988) 569;
in *Polarization at LEP*, eds. G. Alexander et al., CERN 88-06 (1988).

89. A. Denner, R. J. Guth, J. H. Kühn, Phys. Lett. **240** (1990) 438.

90. C. Verzegnassi, in "Radiative Corrections for e^+e^--Colliders",
ed. J. H. Kühn, Springer Berlin 1989;
F. del Aguila, J. M. Moreno, M. Quiros, Phys. Rev. D **40** (1989) 2481;
Phys. Rev. D **41** (1990) 134; Phys. Lett. **254** (1991) 497;
G. Altarelli et al., Mod. Phys. Lett. **A5** (1989) 495; Nucl. Phys. B **342** (1990) 15;
Phys. Lett. **245** (1990) 669;
M. C. Gonzalez-Garcia, J. W. F. Valle, Phys. Lett. **236** (1990) 360; Phys. Lett. **259** (1991) 365.

91. G. Degrassi, A. Sirlin, Phys. Rev. D **40** (1989) 3066.

92. V. Barger, J. L. Hewett, T. G. Rizzo, Phys. Rev. D **42** (1990) 152.

93. U. Amaldi et al., Phys. Rev. D **36** (1987) 1385;
G. Costa et al., Nucl. Phys. B **297** (1988) 244.

94. P. Langacker, Phys. Lett. **256** (1991) 277.

95. K. T. Mahanthappa, P. K. Mohapatra, Phys. Rev. D **43** (1991) 3093.

96. T. G. Rizzo, Univ. of Wisconsin preprint, MAD/PH/604 (1990).

97. For reviews and references see:
H. P. Nilles, Phys. Rep. **110** (1984) 1;
P. Nath, R. Arnowitt, A. Chamseddine, "Applied N=1 Supergravity",
ICTP Series in Theoretical Physics, Vol. 1, World Scientific, Singapore, 1984;
H. E. Haber, G. L. Kane, Phys. Rep. **117** (1985) 75;
R. Barbieri, Riv. Nuovo Cimento **11** (1988) 1.

98. J. Ellis, G. Ridolfi, F. Zwirner, Phys. Lett. bf 257 (1991) 83;
R. Barbieri, M. Figerini, F. Cravaglios, Phys. Lett. **258** (1991) 167;
H. E. Haber, R. Hempfling, Phys. Rev. Lett. **66** (1991) 1815.

99. D. Decamp et al., ALEPH Collaboration, Phys. Lett. **236** (1990) 86; **237** (1990) 291; **244** (1990) 541;
B. Adeva et al., L3 Collaboration, Phys. Lett. **233** (1989) 530; **251** (1990) 311;
M. Z. Akrawy et al., OPAL Collaboration, Phys. Lett. **240** (1990) 261; **248** (1990) 211 ;
P. Abreu et al., DELPHI Collaboration, Phys. Lett. **247** (1990) 148,157.

100. M. Drees, X. Tata, Phys. Rev. D **43** (1991) 2971.

101. R. Barbieri, L. Maiani, Nucl. Phys. B 224 (1983) 32.

102. L. Alvarez-Gaumé, J. Polchinski, M. Wise, Nucl. Phys. B 221 (1983) 495.

103. E. Eliasson, Phys. Lett. 147 B (1984) 65.

104. J. A. Grifols, J. Sola, Phys. Lett. **137** (1984) 257; Nucl. Phys. B **253** (1985) 47;
Z. Hioki, Prog. Theor. Phys. **73** (1985) 1283.

105. C. S. Lim, T. Inami, N. Sakai, Phys. Rev. D **29** (1984) 1488.

106. R. Barbieri, M. Frigeni, F. Giuliani, H. E. Haber,Nucl. Phys. B **341** (1990) 309.

107. P. Gosdzinsky, J. Sola, Phys. Lett. **254** (1991) 139;
Univ. of Barcelona preprint, UAB-FT-253 (1990).

108. M. Drees, K. Hagiwara, Phys. Rev. D **42** (1990) 1709.

109. A. Bilal, J. Ellis, G. L. Fogli, Phys. Lett. **246** (1990) 459.

110. J. Ellis, S. Kelley, D. V. Nanopoulos, Phys. Lett. **260** (1991) 131;
U. Amaldi, W. de Boer, H. Fürstenau, Phys. Lett. **260** (1991) 447;
P. Langacker, M. X. Luo, Ref. [26].